

**MSC-E Technical Report 1/2004**

**June 2004**

# **POP Model Intercomparison Study**

## **Stage I. Comparison of descriptions of main processes determining POP behaviour in various environmental compartments**

Viktor Shatalov, Elena Mantseva, Arthur Baart, Paul Bartlett, Knut Breivik, Jesper Christensen, Sergey Dutchak, Dagmar Kallweit, Régis Farret, Mikhail Fedyunin, Sunling Gong, Kaj Mantzius Hansen, Ivan Holoubek, Ping Huang, Kevin Jones, Michael Matthies, Gerhard Petersen, Konstantinos Prevedouros, Janusz Pudykiewicz, Michael Roemer, Michael Salzmann, Martin Sheringer, Judith Stocker, Boris Strukov, Noriyuki Suzuki, Andrew Sweetman, Dirk van de Meent, Fabio Wegmann

Edited by MSC-E

### **METEOROLOGICAL SYNTHESIZING CENTRE - EAST**

Ul. Arhitektor Vlasov, 51, Moscow 117393 Russia

tel.: +7 095 128 90 98

fax: +7 095 125 24 09

e-mail: [msce@msceast.org](mailto:msce@msceast.org)

[www.msceast.org](http://www.msceast.org)



## The authors (participants):

### Arthur BAART

Delft Hydraulics  
Rotterdamseweg 185  
2629HD Delft  
The NETHERLANDS  
tel: 31 15 2858585  
fax: 31 15 2858582  
e-mail: Arthur.Baart@wldelft.nl

### Knut BREIVIK

Norwegian Institute for Air Research (NILU)  
Center for Ecological Economics, Norway  
P.O. Box 100, N-2027 Kjeller,  
NORWAY  
tel.: + 47 63 89 80 88  
fax: + 47 63 89 80 50  
e-mail: knut.breivik@nilu.no  
www.nilu.no

### Sergey DUTCHAK

Meteorological Synthesizing Centre - EAST  
Ul.Arhitektor Vlasov, 51  
117394 Moscow  
RUSSIA  
tel: 7 095 120 02 41  
fax: 7 095 125 24 09  
e-mail: sergey.dutchak@msceast.org

### Régis FARRET

Direction des Risques Chroniques  
INERIS  
Park Technologique ALATA BP no 2  
65 550 Verneuil en Halatte  
FRANCE  
tel: 33 3 44 55 61 27  
fax: 33 3 44 55 68 99  
e-mail: regis.farret@ineris.fr

### Sunling GONG

Air Quality Research Branch, Meteorological Service of  
Canada  
4905 Dufferin Street, Downsview  
Ontario, M3H 5T4  
CANADA  
tel: 416 739 5749  
fax: 416 739 5704  
e-mail: Sunling.Gong@ec.gc.ca

### Ivan HOLOUBEK

RECETOX - TOCOEN & Associates,  
Kamenice 126/3, 625 00 Brno,  
CZECH REPUBLIC  
tel: +420 5 47 121 401  
mobil: +420 602 753 138  
fax: +420 5 47 121 431  
e-mail: holoubek@recetox.muni.cz / tocoen@tocoen.cz  
<http://recetox.muni.cz/>; <http://www.tocoen.cz/>

### Kevin JONES

Lancaster University  
Environmental Science Department  
Institute of Environmental and Natural Sciences  
Lancaster LA1 4YQ  
UNITED KINGDOM  
tel: 44 1524 59 39 72  
fax: 44 1524 59 39 85  
e-mail: k.c.jones@lancaster.ac.uk

### Paul BARTLETT

CBNS, Queens College  
City University of New York  
Flushing, NY 11367  
USA  
tel.: 718 670 41 83  
fax: 718 670 41 89  
e-mail: paulwoodsbartlett@hotmail.com

### Jesper CHRISTENSEN

National Environmental Research Institute  
Department of Atmospheric Environment  
P.O.Box 358, Frederiksborgvej 399  
DK-4000 Roskilde  
DENMARK  
tel: +45 46 30 11 75  
fax: +45 46 30 12 14  
e-mail: jc@dmu.dk

### Dagmar KALLWEIT

Federal Environmental Agency  
II 6.2- Air Quality  
POB 33 00 22, D - 14191 Berlin  
GERMANY  
tel.: 49 30 8903 2839  
fax: 49 30 8903 2285  
e-mail: dagmar.Kallweit@uba.de  
<http://www.umweltbundesamt.de>

### Mikhail FEDYUNIN

Meteorological Synthesizing Center "East"  
Ul. Arhitektor Vlasov, 51,  
Moscow 117393  
RUSSIA  
tel.: +7 095 128 96 21  
fax: +7 095 125 24 09  
e-mail: msce@msceast.org

### Kaj Mantzius HANSEN

National Environmental Research Institute  
Department of Atmospheric Environment  
P.O.Box 358, Frederiksborgvej 399  
DK-4000 Roskilde  
DENMARK  
tel: +45 46 30 18 72  
fax: +45 46 30 12 14  
e-mail: kmh@dmu.dk

### Ping HUANG

Air Quality Research Branch, Meteorological  
Service of Canada  
4905 Dufferin Street, Downsview  
Ontario, M3H 5T4  
CANADA  
tel: 416 739 5749  
fax: 416 739 5704  
e-mail: Ping.Huang@ec.gc.ca

### Elena MANTSEVA

Meteorological Synthesizing Center "East"  
Ul. Arhitektor Vlasov, 51,  
Moscow 117393  
RUSSIA  
tel.: +7 095 128 96 21  
fax: +7 095 125 24 09  
e-mail: elena.mantseva@msceast.org

**Michael MATTHIES**

Institute of Environmental Systems Research  
University of Osnabrueck  
Artilleriestr. 34, D-49069 Osnabrueck  
GERMANY  
tel: 49 541 969 2576  
fax: +49 541 969 2599  
e-mail: matthies@usf.Uni-Osnabrueck.de

**Konstantinos PREVEDOUROS**

Lancaster University  
Environmental Science Department  
LA1 4YQ Lancaster,  
UNITED KINGDOM  
tel: 0044 1524 593974  
e-mail: c.prevedouros@lancaster.ac.uk

**Michael ROEMER**

TNO-MEP  
Laan van Westenenk 501  
Postbus 342  
7300 AH Apeldoorn  
The NETHERLANDS  
tel: 31 55 5493787  
fax: 31 55 5493252  
e-mail: M.G.M.Roemer@mep.tno.nl

**Martin SCHERINGER**

Swiss Federal Institute of Technology  
ETH Hönggerberg  
CH-8093 Zuerich  
SWITZERLAND  
fax: +41 1 632 11 89  
e-mail: scheringer@tech.chem.ethz.ch

**Judith STOCKER**

Swiss Federal Institute of Technology  
ETH Hönggerberg  
CH-8093 Zuerich  
SWITZERLAND  
fax: +41 1 632 11 89  
e-mail: judith.stocker@tech.chem.ethz.ch

**Noriyuki SUZUKI**

National Institute for Environmental Studies  
16-2 Onogawa, Tsukuba, Ibaragi 305-8506  
JAPAN  
tel: +81-298-50-2331  
fax: +81-298-50-2880  
e-mail: nsuzuki@nies.go.jp

**Dirk van de MEENT**

RIVM Laboratory for Ecological Risk Assessment,  
Postbus 1, 3720BA Bilthoven,  
THE NETHERLANDS  
tel: +31 30 274 3130 (3015);  
fax: +31 30 274 4413  
e-mail: D.van.de.Meent@rivm.nl

**Gerhard PETERSEN**

GKSS - Research Centre, Institute of Hydrophysics  
Max-Planck-Strasse 1, D-21502 Geesthacht  
GERMANY  
tel: 49 41 52 87 18 47  
fax: 49 41 52 87 18 88  
e-mail :  
petersen@gkss.de/Gerhard.Petersen@gkss.de

**Janusz PUDYKIEWICZ**

AES, Environment Canada Service  
2121 trans-Canada Highway  
Dorval, Quebec, H9P 1J3  
CANADA  
tel. 514 421 72 12  
fax 514 421 21 06  
e-mail Janusz.Pudykiewicz@ec.gc.ca

**Michael SALZMANN**

Swiss Federal Institute of Technology  
ETH Hönggerberg  
CH-8093 Zuerich  
SWITZERLAND  
fax: +41 1 632 11 89  
e-mail: msalz@student.ethz.ch

**Victor SHATALOV**

Meteorological Synthesizing Center "East"  
Ul. Arhitektor Vlasov, 51, Moscow 117393  
RUSSIA  
tel.: +7 095 128 96 21  
fax: +7 095 125 24 09  
e-mail: Victor.Shatalov@msceast.org

**Boris STRUKOV**

Meteorological Synthesizing Centre - EAST  
Ul. Arhitektor Vlasov, 51, 117394 Moscow  
RUSSIA  
tel: 7 095 128 96 21  
fax: 7 095 125 24 09  
e-mail: msce@msceast.org

**Andrew SWEETMAN**

Environmental Science Department  
Lancaster University  
Lancaster, LA1 4YQ  
UNITED KINGDOM  
tel: 44 1524 59 33 00  
fax: 44 1524 59 39 85  
e-mail: a.sweetman@lancaster.ac.uk

**Fabio WEGMANN**

Swiss Federal Institute of Technology  
ETH Hönggerberg  
CH-8093 Zuerich  
SWITZERLAND  
fax: +41 1 632 11 89  
e-mail: fwegmann@tech.chem.ethz.ch

# CONTENTS

|   |     |
|---|-----|
| Introduction  | 7   |
| <i>Chapter 1.</i> Overview of participating models  | 11  |
| <i>Chapter 2.</i> Intercomparison programme   | 15  |
| <i>Chapter 3.</i> Comparison of physical-chemical properties and degradation rates of PCB-153 between individual models | 19  |
| 3.1. The Henry's law constant and the air-water partition coefficient   | 21  |
| 3.2. The subcooled liquid vapour pressure   | 24  |
| 3.3. The octanol/water partition coefficient  | 26  |
| 3.4. The octanol/air partition coefficient  | 29  |
| 3.5. The organic carbon/water partition coefficient   | 31  |
| 3.6. Water solubility   | 32  |
| 3.7. Degradation rate constants of PCBs in the environmental media  | 33  |
| <i>Chapter 4.</i> Comparison of process parameterizations and results of computational experiments for PCB-153          | 37  |
| 4.1. Gas/particle partitioning  | 37  |
| 4.2. Dry deposition of the particulate phase  | 42  |
| 4.3. Wet deposition   | 45  |
| 4.4. Gaseous exchange between atmosphere and soil   | 50  |
| 4.5. Gaseous exchange between atmosphere and water  | 58  |
| 4.6. Gaseous exchange between atmosphere and vegetation   | 63  |
| Conclusions   | 67  |
| References  | 72  |
| <i>Annex A.</i> Descriptions of the models  | 77  |
| <i>Annex B.</i> Comparison of physical-chemical properties of PCB-28 and PCB-180 between individual models              | 89  |
| <i>Annex C.</i> Descriptions of main processes  | 111 |
| <i>Annex D.</i> Comparison of results of computational experiments for PCB-28   | 147 |
| <i>Annex E.</i> Comparison of results of computational experiments for PCB-180  | 157 |



## INTRODUCTION

Environmental pollution by Persistent Organic Pollutants (POPs) (or Persistent Bio-accumulative and Toxic Substances (PBTs)) is one of the global problems to be resolved by the international community. Wide interest to problems of environmental contamination by POPs can be explained by the fact that these pollutants possess high toxicity for living organisms, persistence in the environment, and ability to be built up in food chains to levels that are harmful to human health and ecosystems. Moreover, these substances can be transported over long distances from emission sources and be distributed between different environmental compartments - air, water, soil and vegetation.

The problem of environmental pollution by POPs is in the spotlight of the Convention on Long-range Transboundary Air Pollution of 1979 and the Stockholm Convention on POPs of 2001. This problem attracts attention of numerous international programmes and organisations: the United Nations Environment Programme (UNEP), the Organisation for Economic Co-operation and Development (OECD), the World Health Organisation (WHO), the World Meteorological Organisation (WMO), the Arctic Monitoring and Assessment Programme (AMAP), the Baltic Marine Environment Protection Commission (HELCOM), the Oslo-Paris Commission for the Protection of the Marine Environment of the North-East Atlantic (OSPAR) and others.

Within the framework of the Convention on Long-range Transboundary Air Pollution of 1979 (hereinafter Convention), the Protocol on Persistent Organic Pollutants (hereinafter the Protocol on POPs) is ratified by sixteen Parties to the Convention and has entered into force in October 2003. In addition to the fulfilment of their basic obligations, Parties to the Protocol shall encourage research, development, monitoring and co-operation related, in particular, to the long-range transport and deposition levels and their modelling. In compliance with the Protocol "in good time before each annual session of the Executive Body, the Co-operative Programme for Monitoring and Evaluation of the Long-range Transmission of Air Pollutants in Europe (hereinafter EMEP) shall provide information on the long-range transport and deposition of persistent organic pollutants" (Article 9) [ECE/EB.AIR/66, 1999].

For the assessment of environmental pollution, for the risk assessment, for the evaluation of new pollutants as potential candidates to be implemented in the regulatory control activity, a number of different model approaches are under development. To review different model approaches and improve our understanding of POP behaviour in various environmental compartments, POP model intercomparison study was initiated by EMEP.

A certain experience in model intercomparison for different types of pollutants is accumulated in the Meteorological Synthesizing Centre - East of EMEP (hereinafter EMEP/MSC-E). In particular, intercomparison of transport models for heavy metals was carried out in 1996 (for lead) [Sofiev *et al.*, 1996] and in 1998 (for cadmium) [Gusev *et al.*, 2000]. Intercomparison of mercury transport models was initiated in 1999 and is now in progress with participation of many scientists from various countries [Ryaboshapko *et al.*, 2002; Ryaboshapko *et al.*, 2003]. The recommendations to carry out the comparison of different POP multicompartment models were drawn by the Executive Body for the Convention [ECE/EB.AIR/75, 2002]. Later, the necessity of performing such intercomparison was stressed at the OECD/UNEP Workshop on the Use of Multimedia Models for Estimating Overall Environmental Persistence and Long-Range Transport held in Ottawa in 2001 [ENV/JM/MONO(2002)15, 2002]. Several POP model comparisons concerning particular question of estimating overall persistence and atmospheric travel distances of some POPs were accomplished [Wania and Mackay, 2000; Wania and Dugani, 2003]. In 2002, EMEP/MSC-E initiated the intercomparison study of POP multicompartment models aimed at comparing different approaches to POP modelling both in general and in detail.

The draft programme of the intercomparison study was prepared on the basis of the discussion on POP model intercomparison issues during the third EMEP/TFMM meeting in Geneva, March 2002 [EB.AIR/GE.1/2002/4]. The first meeting on the model intercomparison with participation of national experts (both in modelling and measurements) from Canada, the Czech Republic, France, Germany, Japan, Norway, Switzerland, the United Kingdom, the USA and representatives of the OECD was organised by EMEP/MSC-E (Moscow, November 2002). Presentations of the participating models, acceptance of the Programme on intercomparison study of POP models, in-depth discussion of the goals of Stage I and elaboration of its time-schedule were the main topics at this meeting. Since that time, modellers from Denmark and the Netherlands have joined this activity.

Table 1 displays a list of the participating models together with brief descriptions of model type and resolution. The study concerns a wide spectrum of models designed for the simulation of POP behaviour in the environment. It should be mentioned that both generic and spatially resolved dynamic models are involved in this study.

**Table 1.** The list of participating models

|    | Model name                   | Type/ resolution  | Experts  | Institution   |
|----|------------------------------|---|--|---|
| 1  | HYSPLIT 4                    | Lagrangian, regional  | P. Bartlett  | CBNS, Queens College, USA   |
| 2  | EVN-BETR<br>(European scale) | Dynamic box/5x5°, regional  | K. Jones,<br>A. Sweetman,<br>C. Prevedouros                                | Lancaster University, UK  |
| 3  | UK-MODEL (UK<br>scale)       | Dynamic, box model, regional (UK)   |  |   |
| 4  | ELPOS                        | Box model, regional, parameterization close to EUSES 1.0  | M. Matthies  | Univ. Osnabrück, Germany  |
| 5  | ChemRange                    | one-dimensional, steady-state box model   | M. Scheringer,<br>F. Wegmann,<br>M. Salzmann<br>J. Stocker                 | ETH Zürich, Switzerland   |
| 6  | CliMoChem                    | two-dimensional box model with temporal resolution  |  |   |
| 7  | CAM/POPs                     | Gridded, regional/global  | S. Gong,<br>P. Huang   | Air Quality Research Branch,<br>Canada                                |
| 8  | G-CIEMS                      | multi-box with geo-referenced geographical resolution (10x10 km <sup>2</sup> ), regional  | N. Suzuki  | National Institute for<br>Environmental Studies,<br>Japan             |
| 9  | INERIS                       | Box model, regional, parameterization close to EUSES and ChemCan  | R. Farret  | Chronic Risks Division,<br>INERIS, France                             |
| 10 | GLOBO-POP                    | zonally averaged non-steady state global multimedia fate and transport model  | K. Breivik   | NILU, Norway  |
| 11 | POPCYCLING-<br>Baltic        | regional multimedia fate and transport model  |  |   |
| 12 | MEDIA                        | gridded (2x2°), global  | J. Pudykiewicz   | Meteorological Service of<br>Canada                                   |
| 13 | ADOM-POP                     | 3D-Eulerian atmospheric transport and chemistry model 50x50 km  | G. Petersen  | GKSS, Germany   |
| 14 | DEHM-POP                     | 3D-Eulerian atmospheric transport and chemistry model,<br>northern hemisphere: 150x150 km, EMEP:<br>50x50 km  | J. Christensen,<br>K.M. Hansen   | National Environmental<br>Research Institute, Denmark                 |
| 15 | SimpleBox                    | nested multimedia environmental fate model,<br>generic,<br>five spatial scales: regional, continental and<br>global (arctic, moderate and tropic geographic<br>zones) | D. van de Meent  | RIVM Laboratory for<br>Ecological Risk Assessment,<br>the Netherlands |
| 16 | The LOTOS<br>model           | European domain, lowest 2 km of atmosphere;<br>resolution: about 30x30 km, every hour   | M.G.M. Roemer ,<br>A.C. Baart  | TNO-MEP, the Netherlands  |
| 17 | ADEPT                        | 3D atmospheric transport model for Europe   |  | Delft Hydraulics, the<br>Netherlands                                  |
| 18 | MSCE-POP                     | EMEP: 50x50 km or 150x150km, hemispheric:<br>2.5x2.5°   | S. Dutchak,<br>V. Shatalov ,<br>M. Fedyunin,<br>E. Mantseva,<br>B. Strukov | EMEP/MSC-E  |

This report presents the results of Stage I of the POP model intercomparison study.

Chapter 1 is devoted to a brief overview of the participating models. More detailed descriptions of the models submitted by research groups involved into the intercomparison study are contained in Annex A.

Chapter 2 is devoted to the description of model intercomparison programme. Both the general programme and the programme of Stage I of the intercomparison study are presented.

Chapter 3 provides information on physical-chemical properties of PCB-153 used for calculation experiments in participating models and on “reference data set”. The tables with physical-chemical parameters used in participating models and in “reference data set” for PCB-28 and PCB-180 are presented in Annex B.

Chapter 4 comprises descriptions of main processes determining PCBs behaviour in the environment as submitted by the participants, input data and the analysis of the results of calculation experiments for PCB-153. Descriptions of main processes determining POP behaviour in the environment are summarised in Annex C. Tables with input data for calculation experiments and results of model intercomparison on PCB-28 and PCB-180 are given in Annexes D and E, respectively.

Main conclusions are drawn in the end of the Technical Report.

More detailed information on the POP model intercomparison study can be found at the MSC-E website: [www.msceast.org](http://www.msceast.org).



## OVERVIEW OF PARTICIPATING MODELS

This chapter is devoted to a brief analysis of similarities and distinctions between models participating in the intercomparison study. This analysis is used for the determination of the intercomparison procedure. A more detailed description of individual models is presented in Annex A.

Table 2 contains the list of participating models together with their main characteristics: model type and/or spatial resolution, chemicals included in modelling, list of media considered, processes taken into account, input information needed for simulations and output of the models.

It is seen that the diversity of the models taking part in the intercomparison study is very large. These models differ by their type (box models or spatially resolved models), resolution and scope (from global to regional scales). These differences are mostly explained by the diversity of main purposes for which each individual model was designed (last column of Table 2).

However, the considered models have much in common. The majority of the models take into account POP behaviour in several environmental compartments (except for four purely atmospheric models – HYSPLIT 4, ADOM-POP, ADEPT and the LOTOS model). The main environmental compartments included in all these models are the atmosphere, soil and water. Some models take into account vegetation (EVN-BETR, ELPOS, G-CIEMS, POPCYCLING-BALTIC, MSCE-POP) and sediments (EVN-BETR and UK-MODEL, ELPOS, GLOBO-POP, POPCYCLING-BALTIC, MSCE-POP). Two models (MEDIA and MSCE-POP) consider the exchange between the atmosphere and the cryosphere (sea ice and snow). Most of the models describe the same processes: gas/aerosol partitioning, deposition processes, exchange between different environmental compartments, and POP degradation in various environmental media. However, the participating models can differ substantially from one another in the degree of detail of the descriptions of these processes. To evaluate the compatibility of the results obtained by models of different types, it is important to compare model descriptions of the above processes.

Most of the models are able to simulate the environmental behaviour of a large diversity of POPs. Such substances as PCBs, PAHs, HCHs, PCDD/Fs and HCB are included in the list of chemicals for most of the participating models. Among these substances, PCBs (in particular, PCB-153) are the most investigated chemicals for which a lot of information on physical-chemical properties and environmental pollution levels is available. This group of pollutants may be a good basis for the comparison of model descriptions of POP behaviour in the environment.

All the models use similar sets of input information. The most important input parameters common for all the models are data on physical-chemical properties of the considered POPs and on their emissions. Maximum differences in the input parameters of different models are related to meteorological and geophysical information. It should be noted that, at least at the beginning of the intercomparison study, only the information on physical-chemical properties of substances is essential, since the comparison between the models can be performed for some conventional environmental conditions. At the next steps of the intercomparison study, the information on emissions and on measured environmental levels of POPs becomes necessary.

In spite of considerable differences between output parameters of compared models, some of them can be obtained with the use of almost all of the models. These are deposition/exchange fluxes between environmental compartments, contents of POPs masses in these compartments (mass

balance calculations) and overall persistence and long-range transport potential for considered POPs. The comparison between these output parameters produced by different models under the same conventional environmental conditions is a useful exercise for harmonising outputs of different models used in the study.

Below we present the program of the intercomparison study as a whole with a detailed description of its first stage (Chapter 2), an analysis of physical-chemical properties of PCB-153 used in different POP multicompartiment models (Chapter 3) and a discussion on the results of computational experiments carried out at Stage I of the study (Chapter 4). The comparison between mass balances, environmental levels, overall persistence and long-range transport potentials of POPs as predicted by the participating models will be performed at subsequent stages of the intercomparison study.

**Table 2. Summary of model properties**

| Model                     | Type/ resolution   | Chemicals  | Media   | Processes   | Input   | Output   |
|---------------------------|--|--|---|---|---|--|
| HYSPLIT 4                 | Lagrangian, regional   | HCB, dioxin, PCBs and atrazine                                   | Atmosphere  | dispersion in the atmosphere, deposition, destruction   | phys-chem properties, emissions,  | depositions, source-to-receptor relationships  |
| EVN-BETR (European scale) | dynamic box/5°x5°, regional  | PCBs, PCDD/Fs, PAHs, Ocs, PBDEs                                  | air, veg., soil, water, sed.                        | atmospheric transport, exchange   | phys-chem properties, emissions, air flow balances                            | persistence, transport potential,  |
| UK-MODEL (UK scale)       | dynamic, box model, regional (UK)  | PCBs, PCDD/Fs, PAHs, Ocs, PBDEs                                  | air, soil, water, sed.                              | dynamic intermedia mass transfer (deposition, volatilization), gas-particle partitioning, degradation,  | phys-chem properties, dynamic emissions                                       | concentrations, mass flows, persistence  |
| ELPOS                     | box model, regional, parameterization close to EUSES 1.0                                 | 109 substances (PCBs, PCDD/Fs, pesticides, industrial chemicals) | Air, water, soil, sediments, vegetation             | intermedia mass transfer (deposition, volatilization), gas-particle partitioning (2 models), degradation, substance specific soil penetration depth | phys-chem properties, emissions, environmental parameters                     | overall persistence, CTD in air, CTD in water, mass percentages, stickiness                              |
| ChemRange                 | one-dimensional, steady-state box model  | non-polar organic chemicals                                      | air, soil, water.                                   | degradation, transport in water and air, exchange between compartment, wet and dry deposition, partitioning, runoff from soil, leaf fall            | phys-chem properties, emissions, environmental parameters                     | concentrations, mass fractions and mass flows, overall persistence, spatial range                        |
| CliMoChem                 | two-dimensional box model with temporal resolution                                       | non-polar organic chemicals                                      | air, soil, water.                                   | degradation, transport in water and air, exchange between compartment, wet and dry deposition, partitioning, runoff from soil, leaf fall            | phys-chem properties, emissions, environmental parameters                     | concentrations, mass fractions and mass flows, persistence, spatial ranges, cold condensation potentials |
| CAM/POPs                  | gridded, regional/global   | PCBs   | air, soil, water                                    | gas/aerosol partitioning, transport exchange, deposition, degradation   | phys-chem properties, emissions, environmental parameters                     | air concentrations and depositions   |
| G-CIEMS                   | multi-box with geo-referenced geographical resolution (10x10 km <sup>2</sup> ), regional | PCDD/Fs  | air, soil, rivers, coastal sea, vegetation          | transport, partitioning, deposition, degradations, runoff   | phys-chem properties, emissions, geographic/hydrological/ meteorological data | gross input and output between target area and outer boundary for each transport pathway                 |
| INERIS                    | box model, regional, parameterization close to EUSES and ChemCan                         |  |   |   |   |  |
| GLOBO-POP                 | zonally averaged non-steady state global multimedia fate and transport model             | HCHs, PCBs   | air, two soils, fresh and ocean water and sediments | degradation, transport in water and air, exchange between compartment, wet and dry deposition, partitioning   | phys-chem properties, emissions, monthly averaged environmental parameters    | assessment of the long range transport behaviour of persistent organic chemicals                         |

|                   |  |                                  |   |   |   |  |
|-------------------|--|----------------------------------|---|---|---|--|
| POPCYCLING-Baltic | regional multimedia fate and transport model   | HCHs                             | air, two soils, fresh and sea water and sediments, vegetation | degradation, transport in water and air, exchange between compartment, wet and dry deposition, partitioning         | phys-chem properties, emissions, monthly averaged environmental parameters    | a quantitative understanding of the historical behavior of HCHs in Baltic region   |
| MEDIA             | gridded (2x2°), global   | HCHs                             | air, soil, ocean, cryosphere                                  | transport in air and sea, deposition, exchange, degradation   | phys-chem properties, emissions, meteorological data                          | fields of air concentrations   |
| ADOM-POP          | 3D-Eulerian atmospheric transport and chemistry model 50x50 km   | PAHs (B[a]P)                     | air   | atmospheric transport and diffusion, cloud processes, physico-chemical transformations, deposition                  | phys-chem properties, meteorology, geophys. information, emissions            | deposition and concentration fields  |
| DEHM-POP          | 3D-Eulerian atmospheric transport and chemistry model, northern hemisphere: 150x150 km, EMEP: 50x50 km   | α-HCH                            | air, soil, water  | atmospheric advection and diffusion, deposition, air/surface gas exchange, degradation                              | phys-chem properties, meteorological data, geophysical information, emissions | deposition and concentration fields  |
| SimpleBox         | nested multimedia environmental fate model generic, five spatial scales: regional, continental and global (arctic, moderate and tropic geographic zones) | more than 100 organic substances | air, fresh and sea water, sediment, soil, vegetation          | partitioning, wet and dry deposition, intermedia transfer processes, degradation, advective and diffusive transport | phys-chem properties, emissions, environmental parameters                     | Overall persistence in the environment: <ul style="list-style-type: none"> <li>residence time at steady state ratio of inventory and input (or output)</li> <li>clearance time (dynamic)</li> </ul> Long-range transport potential: <ul style="list-style-type: none"> <li>transport out of regional scale as fraction of input (or output) at steady state</li> </ul> |
| ADEPT             | 3D atmospheric transport model for Europe  | organic pollutants               | atmosphere  | partitioning; transport; wet and dry deposition   | phys-chem properties, emissions   | concentrations, deposition fluxes  |
| The LOTOS model   | European domain, lowest 2 km of atmosphere; chemistry based on ozone and aerosols; resolution: about 30x30 km, every hour                                | lindane                          | atmosphere  | partitioning; transport; wet and dry deposition;  | phys-chem properties; analysed meteorological fields; emissions,              | deposition and concentration fields  |
| MSCE-POP          | EMEP: 50x50 km or 150x150km, hemispheric 2.5x2.5°  | PAHs, PCBs, PCDD/Fs, γ-HCH, HCB  | air, soil, water, veg., sed., cryosphere                      | gas/aerosol partitioning, exchange, deposition, degradation   | phys-chem properties, meteorology, geophysical information, emissions         | deposition and concentration fields, media distribution, long-term trends  |

## INTERCOMPARISON PROGRAMME

The description of the programme on the intercomparison study of POP models is presented in this Chapter. Its first section contains a brief overview of the intercomparison programme in general. The second section is devoted to a more detailed description of the programme of Stage I of the intercomparison study.

The study concerns a wide spectrum of models designed for simulating POP behaviour in the environment. These models can be spatially resolved or generic. Below, they are referred to as *POP models*.

**Objectives.** The main objectives of the intercomparison study are:

- to strengthen the exchange of scientific expertise between different groups working in the field of POP modelling;
- to increase the transparency of existing POP models and their results: model concept, parameterisations, temporal and spatial resolution and output and uncertainties;
- to harmonise the output parameters of POP models of different types and complexity for obtaining comparable results at different levels of regulatory activities;
- to consider model approaches to the evaluation of new substances.

**Stages of the intercomparison.** The model intercomparison study is performed in the following stages:

- Stage I.** Comparison of descriptions of main processes determining POP behaviour in various environmental compartments.
- Stage II.** Comparison of mass balance estimates and calculated deposition and concentration fields of POPs in different environmental compartments. Sensitivity study with respect to physical-chemical parameter values used in basic process descriptions and mass balance estimates.
- Stage III.** Comparison of calculated overall environmental persistence and long-range transport potential for evaluation of new substances.

At Stage I, model descriptions of the main processes determining POP fate in the environment (scavenging, partitioning, degradation etc.) are compared. This implies the comparison between the approaches to parameterisation of these processes by the models and between the models' operation. The latter is performed via relevant computational experiments. Details of Stage I are given below.

At Stage II, the balance values are compared (PCB masses in different environmental compartments: atmosphere, soil, water, vegetation; masses of PCB degraded in these compartments; mass fluxes of PCB transported in/out of the specified domain; mass fluxes of PCB transported from one compartment to another; and PCB concentrations at each interface). The comparison is carried out on agreed conditions (e.g., land cover data, leaf area index, organic matter content in the soil, environmental temperature regime etc.) and with the use of input data on emissions with zero initial concentrations of PCBs in environmental media and, as optional, with initial concentrations for the

specified calculation domain (35°N – 70°N; 10°W – 30°E). Additionally, the comparison between spatial distribution patterns of depositions and PCBs concentrations in various environmental compartments as predicted by different models is performed; these characteristics can be also compared with monitoring data (optional). Sensitivity studies with respect to physical-chemical parameter values used in the process descriptions and mass balance estimates are carried out. The second intermediate report can be an output of this stage.

At Stage III, model estimates of the long-range transport potential and the overall environmental persistence data on POPs are compared. Such a comparison can be performed for chemicals proposed below. The results of the study should be published in the final report including the results of all stages, conclusions and recommendations.

***Pollutants selected for the intercomparison:*** First priority: PCB-153. Second priority: B[a]P, lindane, PCB-28, PCB-180, as a new pollutant - PBDE (proposed by R. Farret ).

Computational experiments with PCB-153 are agreed to be the subject of this intercomparison study. For other selected pollutants, it is proposed to carry out computational experiments on the voluntary basis.

***“Reference data set”:*** Taking into account recommendations of the first meeting, the internally consistent data sets of key physical-chemical properties and degradation rates of PCBs hereinafter referred to as “reference data sets” were proposed for model testing. Calculations within the sensitivity study with respect to physical-chemical parameters should be performed at Stage II with the help of these data sets. For models using “reference data sets” as own physical-chemical properties, alternative data sets based on individual data of some other participating models are proposed for this sensitivity study.

***Emission data:*** Officially reported emission data on PCBs are still incomplete in terms of their spatial and temporal coverage to satisfy the data requirements for the calculation experiments to be performed at Stage II. Therefore, consistent global atmospheric emission estimates presented by [Breivik *et al.* 2002] (see also [www.nilu.no/projects/globalpcb/](http://www.nilu.no/projects/globalpcb/)) have been chosen. The higher (or worst-case) emission estimate is to be applied, as this particular scenario appears to be more reasonable on the global scale [Wania and Daly, 2002; Meijer *et al.* 2003].

***Time-schedule:***

***Table 3. Time-table of the intercomparison study***

| Stage   | Time period                   |
|---|-------------------------------|
| I. Process descriptions   | November 2002 – February 2004 |
| II. Mass balance estimates and calculated deposition and concentration fields | March 2004 –December 2004     |
| III. Overall environmental persistence and long-range transport potential     | December 2004 – August 2005   |

## Stage I

Stage I is aimed at the comparison of descriptions of basic processes affecting POPs fate in the environment (listed below). This comparison is based on the analysis of process descriptions (approach and parameterisation) used in different POP models coupled with the analysis of the results of computational experiments carried out by the participating POP models.

**Basic processes.** The following processes are considered:

- Gas/particle partitioning of POPs in the atmosphere.
- POP deposition from the atmosphere (wet deposition for gaseous and particulate phases and dry deposition of particulate phase onto forest, grass, bare soil, and water surfaces).
- Gas exchange processes between the atmosphere and different types of underlying surface (soil, water, vegetation).
- POP degradation in various environmental compartments (the atmosphere, soil, vegetation, water).

**Physical-chemical properties.** Within the framework of Stage I, it was agreed to carry out computational experiments for the considered PCB congeners on the basis of physical-chemical data sets applied by the individual models. Physical-chemical parameters used in the description of the above processes were submitted by the participating models. This information is analysed in Chapter 3 and Annex B.

**Computational experiments.** The following computational experiments have been performed:

- Calculations of POP gas/particle partitioning in the atmosphere (particulate fraction for a range of temperatures).
- Calculations of dry deposition fluxes to agreed types of underlying surfaces (forest, grass, bare soil, seawater).
- Calculations of wet deposition fluxes both for gaseous and particulate phases and total POP concentrations in precipitation.
- Calculations of POP concentrations in different environmental media and/or gaseous fluxes from and to underlying surfaces (soil, water, vegetation) at given atmospheric concentrations.
- Calculations of temporal trends characterising POP concentrations in the soil at the stages of their accumulation and clearance (optional additional experiment).

The input data for modelling include several sets of given PCB air concentrations in different phases (if needed) and environmental conditions (averaged ambient temperatures, organic content in the atmospheric aerosol, TSP, precipitation intensity, mean wind velocity, etc.) relevant for each of the experiments.

A more detailed description of the input data for computational experiments and the analysis of their results are presented in Chapter 4.



## COMPARISON OF PHYSICAL-CHEMICAL PROPERTIES AND DEGRADATION RATES OF PCB-153 BETWEEN INDIVIDUAL MODELS

This Chapter provides an overview of physical-chemical properties and degradation rates used in the participating models and in the “reference data set” of PCB-153. The latter is an agreed set of physical-chemical properties for model testing. Appropriate data on PCB-28 and PCB-180 are given in Annex B. Individual data sets have been presented by the following models: CAM/POPs (Canada), DEHM-POP (Denmark), G-CIEMS (Japan), EVN-BETR and UK-MODEL (UK), CliMoChem (Switzerland), and MSCE-POP (EMEP).

Model parameterization of the basic environmental processes (degradation in various media, partitioning between different phases, removal from the atmosphere, and gaseous exchange with underlying surfaces) considered at Stage I can be described with the help of the following physical-chemical properties of PCBs:

- Henry’s law constant (or air/water partition coefficient);
- subcooled liquid vapour pressure;
- octanol/water partition coefficient;
- octanol/air partition coefficient;
- organic carbon/water partition coefficient;
- water solubility;
- degradation rate constants in the environmental media.

The comparison of these parameters base values and coefficients of their temperature dependencies for PCB-153 is made in the appropriate subsections (Similar comparison on PCB-28 and PCB-180 can be found in Annex B). One can see that base values of some physical-chemical properties and/or coefficients of temperature dependencies) vary substantially between different models. The scattering of the values reported by the participants for each parameter can to some extent characterize its uncertainty. To evaluate the uncertainty, a number of statistical parameters (the maximum, the minimum, the arithmetic mean, the median and the geometric mean) are calculated. The plots comparing temperature dependencies of the considered parameters for PCB-153 are presented in Figs. 1-6 (for PCB-28 and PCB-180 – in Figs. B.1-B.12. in Annex B).

The POP Model Intercomparison Study involves models that are fundamentally different in terms of overall modelling approach and objectives. This includes differences in process descriptions as well as variability in their spatial and temporal resolutions. Comparisons of the model results are therefore considered difficult without some sort of harmonisation of input parameters. In order to make the comparison of model outputs more easily to comprehend, it has therefore been decided to standardise certain common input parameters in Stage II of the model intercomparison. The data to be harmonised at follow-up stage include the information on physical-chemical properties (including degradation rates) as well as the emission estimates as these are input parameters that are common to all models. This Chapter contains information on reference data set of PCB-153 physical-chemical properties selected for the calculations within this intercomparison study.

Many studies report data on experimentally determined or theoretically derived physical-chemical properties of individual POPs, but it is difficult to judge which data in the literature that are the more reliable or accurate. However, vapour pressure, Henry's law constant, water solubility, octanol/water and octanol/air partition coefficients should preferably adhere to thermodynamic constraints and be internally consistent [Beyer *et al.*, 2002]. As reference sets for the calculation experiments at Stage II to be carried out for PCBs (153 with 28 and 180 as optional) we have chosen to rely on information presented by Li *et al.* [2003] as this comprehensive data set and compilation fulfill the criteria of internally consistency. For the recalculation of organic carbon/water partition coefficient from octanol/water coefficient, the values of coefficients of regression relation most frequently used by the models are proposed for the "reference data sets". For the sake of simplicity, degradation rate constants in various environmental media are assumed seasonally independent. These values were taken from [Mackay *et al.* 1992].

The "reference data sets" are prepared for the three PCB congeners. Proposed "reference data set" for PCB-153 is presented in Table 4 (data on other PCBs - see Table B.1. in Annex B).

**Table 4.** "Reference data set" of physical-chemical properties and degradation rates of PCB-153\*

| Description  | Numerical values                       |          | Comments   | Ref.                          |
|--|--|----------|--|-------------------------------|
| <i>Air/water Henry's law constant, H (Pa·m<sup>3</sup>/mol)</i>  |  |          |  |                               |
| Temperature dependent:<br>$H = H_0 \exp(-a_H(1/T - 1/T_0))$<br>where $T$ - temperature (K), $H_0$ is the value at the reference temperature $T_0$ , and $a_H$ is a parameter of temperature dependence.                        | $H_0(T_0)$ ,<br>Pa·m <sup>3</sup> /mol | 4.91E+00 | Coefficients are recalculated from the following temperature dependence:<br>$\log H = \log H(25^\circ\text{C}) - (\Delta U_{aw} + R \cdot 298.15) / (\ln(10) \cdot R) \cdot (1/T - 1/298.15)$<br>where: $T$ - temperature; $R$ - Universal Gas Constant;<br>$\Delta U_{aw}$ - internal energy of phase transfer, kJ/mol (for PCB-153: 62.8).<br>$H(25^\circ\text{C})$ - Henry 's law constant at 25°C, Pa·m <sup>3</sup> /mol (PCB-153: 19.8).   | Li<br><i>et al.</i> ,<br>2003 |
|  | $a_H$                                  | 7851.7   |  |                               |
| <i>Air/water partition coefficient, K<sub>aw</sub> (dimensionless)</i>   |  |          |  |                               |
| Temperature dependent:<br>$K_{aw} = K_{aw}^0 \exp(-a_{Kaw}(1/T - 1/T_0))$<br>where $T$ - temperature (K), $K_{aw}^0$ is the value at the reference temperature $T_0$ , and $a_{Kaw}$ is a parameter of temperature dependence. | $K_{aw}^0(T_0)$ ,<br>dimensionless     | 2.09E-03 | Coefficients are recalculated from the following temperature dependence:<br>$\log K_{aw} = \log K_{aw}(25^\circ\text{C}) - \Delta U_{aw} / (\ln(10) \cdot R) \cdot (1/T - 1/298.15)$<br>where: $T$ - temperature; $R$ - Universal Gas Constant;<br>$\Delta U_{aw}$ - internal energy of phase transfer, kJ/mol (for PCB-153: 62.8).<br>$K_{aw}(25^\circ\text{C})$ - dimensionless air/water partition coefficient at 25°C, estimated from: $K_{aw}(25^\circ\text{C}) = H(25^\circ\text{C}) / (R \cdot 298.15)$ | Li<br><i>et al.</i> ,<br>2003 |
|  | $a_{Kaw}$                              | 7553.5   |  |                               |
| <i>Subcooled liquid vapour pressure, p<sub>ol</sub> (Pa)</i>   |  |          |  |                               |
| Temperature dependent:<br>$p_{ol} = p_{ol}^0 \exp(-a_p(1/T - 1/T_0))$<br>where $T$ - temperature (K), $p_{ol}^0$ is the value at the reference temperature $T_0$ , and $a_p$ is a parameter of temperature dependence.         | $p_{ol}^0(T_0)$ ,<br>Pa                | 8.82E-05 | Coefficients are recalculated from the following temperature dependence:<br>$\log p_{ol} = \log p_{ol}(25^\circ\text{C}) - (\Delta U_s + R \cdot 298.15) / (\ln(10) \cdot R) \cdot (1/T - 1/298.15)$<br>where: $T$ - temperature; $R$ - Universal Gas Constant;<br>$\Delta U_s$ - internal energy of phase transfer, kJ/mol (for PCB-153: 87.7).<br>$p_{ol}(25^\circ\text{C})$ - vapour pressure at 25°C, Pa (for PCB-153: 6.06E-4)  | Li<br><i>et al.</i> ,<br>2003 |
|  | $a_p$                                  | 10846.6  |  |                               |
| <i>Octanol/water partition coefficient, K<sub>ow</sub> (dimensionless)</i>   |  |          |  |                               |
| Temperature dependent:<br>$K_{ow} = K_{ow}^0 \exp(a_{Kow}(1/T - 1/T_0))$<br>where $T$ - temperature (K), $K_{ow}^0$ is the value at the reference temperature $T_0$ , and $a_{Kow}$ is a parameter of temperature dependence.  | $K_{ow}^0(T_0)$ ,<br>dimensionless     | 1.45E+07 | Coefficients are recalculated from the following temperature dependence:<br>$\log K_{ow} = \log K_{ow}(25^\circ\text{C}) - \Delta U_{ow} / (\ln(10) \cdot R) \cdot (1/T - 1/298.15)$<br>where: $T$ - temperature; $R$ - Universal Gas Constant;<br>$\Delta U_{ow}$ - internal energy of phase transfer, kJ/mol (for PCB-153: -31.1).<br>$K_{ow}(25^\circ\text{C})$ - octanol/water partition coefficient at 25°C, dimensionless (for PCB-153: 7.44E+6)   | Li<br><i>et al.</i> ,<br>2003 |
|  | $a_{Kow}$                              | 3740.7   |  |                               |
| <i>Octanol/air partition coefficient, K<sub>oa</sub> (dimensionless)</i>   |  |          |  |                               |
| Temperature dependent:<br>$K_{oa} = K_{oa}^0 \exp(a_{Koa}(1/T - 1/T_0))$<br>where $T$ - temperature (K), $K_{oa}^0$ is the value at the reference temperature $T_0$ , and $a_{Koa}$ is a parameter of temperature dependence.  | $K_{oa}^0(T_0)$ ,<br>dimensionless     | 2.05E+10 | Coefficients are recalculated from the following temperature dependence:<br>$\log K_{oa} = \log K_{oa}(25^\circ\text{C}) - \Delta U_{oa} / (\ln(10) \cdot R) \cdot (1/T - 1/298.15)$<br>where: $T$ - temperature; $R$ - Universal Gas Constant;<br>$\Delta U_{oa}$ - internal energy of phase transfer, kJ/mol (for PCB-153: -93.9).<br>$K_{oa}(25^\circ\text{C})$ - octanol/air partition coefficient at 25°C, dimensionless (for PCB-153: 2.76E+9);  | Li<br><i>et al.</i> ,<br>2003 |
|  | $a_{Koa}$                              | 11294.2  |  |                               |

| Description  | Numerical values                 |          | Comments  | Ref.                |
|--|----------------------------------|----------|---|---------------------|
| <i>Organic carbon/water partition coefficient, <math>K_{oc}</math> (dimensionless)</i>                         |                                  |          |   |                     |
| Regression relation:<br>$K_{oc} = regc K_{ow}^b$<br>where <i>regc</i> and <i>b</i> are regression coefficients | <i>regc</i>                      | 0.41     | $K_{oc}$ is calculated from $K_{ow}$ , where $K_{ow}$ is the temperature dependent octanol-water partitioning coefficient   | Karickhoff, 1981    |
|  | <i>b</i>                         | 1        |   |                     |
| <i>Water solubility, <math>S_{WL}</math> (mol/m<sup>3</sup>)</i>   |                                  |          |   |                     |
| Temperature independent  | $S_{WL}(T)$ , mol/m <sup>3</sup> | 1.80E-05 | Values are calculated for T = 283.15 with the help of the following temperature dependence:<br>$\log S_{WL} = \log S_{WL}(25^{\circ}C) - \Delta U_{Wl}/(\ln(10) \cdot R) \cdot (1/T - 1/298.15)$<br>where: R - Universal Gas Constant; $\Delta U_{Wl}$ - internal energy of phase transfer, kJ/mol (for PCB-153: 25.0).<br>$S_{WL}(25^{\circ}C)$ - water solubility, mol/m <sup>3</sup> at 25°C (PCB-153: 3.07E-5); | Li et al., 2003     |
| <i>Degradation rate constants, <math>k_d</math> (1/s)</i>  |                                  |          |   |                     |
| Degradation in atmosphere:<br>Temperature independent  | $k_{air}$ , 1/s                  | 3.50E-08 | Degradation rate constant in the air is converted from half-life values, $t_{1/2}$ (PCB-153: 5500): $k_d = 0.693/t_{1/2}$ where $k_d$ is the first-order rate constant (s <sup>-1</sup> ) and $t_{1/2}$ is the half-life (s).   | Mackay et al., 1992 |
| Degradation in soil:<br>Temperature independent  | $k_{soil}$ , 1/s                 | 3.50E-09 | Degradation rate constant in soil is converted from half-life values (PCB-153: 55000): $k_d = 0.693/t_{1/2}$ where $k_d$ is the first-order rate constant (s <sup>-1</sup> ) and $t_{1/2}$ is the half-life (s).  |                     |
| Degradation in water:<br>Temperature independent   | $k_{water}$ , 1/s                | 3.50E-09 | Degradation rate constant in water is converted from half-life values (PCB-153: 55000): $k_d = 0.693/t_{1/2}$ where $k_d$ is the first-order rate constant (s <sup>-1</sup> ) and $t_{1/2}$ is the half-life (s).   |                     |
| Degradation in sediment:<br>Temperature independent  | $k_{sed}$ , 1/s                  | 3.50E-09 | Degradation rate constant in sediment is converted from half-life values (PCB-153: 55000): $k_d = 0.693/t_{1/2}$ where $k_d$ is the first-order rate constant (s <sup>-1</sup> ) and $t_{1/2}$ is the half-life (s).  |                     |

\* - for the sake of comparability, the base values and coefficients of temperature dependences of the considered parameters are given here at the temperature 283.15 K ( $T_0$ ) and the way they were recalculated from original dependencies is specified in the field "Comments".

The comparison of values of physical-chemical properties and degradation rates of PCB-153 used in data sets of the participating models and "reference data set" is also performed in this Chapter (for PCB-28 and PCB-180 similar comparison is presented in Annex B). Temperature dependencies of the considered parameters from "reference data set" are given in red in Figs. 1-6. Of note that G-CIEMS and SimpleBox models have done the calculations of Stage I with the help of mentioned physical-chemical properties from "reference data sets". The exception is in the selection of  $K_{oc}$  -  $K_{ow}$  relationship by G-CIEMS. Besides individual/own data sets of EVN-BETR and UK-MODEL are extremely close to the "reference data sets".

### 3.1. The Henry's law constant and the air/water partition coefficient

Relation between the air-water Henry's law constant, ( $H$  or  $K_H$ , Pa·m<sup>3</sup>/mol) and the air/water partition coefficient ( $K_{aw}$ , dimensionless) is as follows:

$$K_{aw} = \frac{H}{RT}, \quad (1)$$

where  $T$  - temperature, K;

$R = 8.314$  J/(mol·K) - universal gas constant.

Coefficients  $K_{aw}$  and  $H$  are mainly used in the description of the gaseous exchange process between the atmosphere and soil, and between the atmosphere and water, as well as of wet deposition of the POP gaseous phase. Besides, EVN-BETR and UK-MODEL and CliMoChem models also use  $K_{aw}$  for the evaluation the octanol/air partition coefficient ( $K_{oa}$ ):

$$K_{oa} = K_{ow}/K_{aw}. \quad (2)$$

Temperature dependence of  $K_{aw}$  and  $H$  is included practically in all participating models (except  $H$  value of EVN-BETR and UK-MODEL) (Table 5). Comparison of these dependencies for PCB-153 (used in calculations at Stage I by the participating POP models and in "reference data set") is given in Figs.1a and 1b.

**Table 5.** The Henry's law constant and the air/water partition coefficient of PCB-153 (data sets of the participating POP models)\*

| Model                 | Description  | Numerical values                                 |          | Comments  | Reference  |
|-----------------------|--|--|----------|---|--|
| CAM/POPs              | Temperature dependent:<br>$H = H_0 \exp(-a_H(1/T - 1/T_0))$<br>where $T$ - temperature ( $^{\circ}\text{K}$ ), $H_0$ is the value at the reference temperature $T_0$ , and $a$ is a parameter of temperature dependence.<br>Temperature dependent:<br>$K_{aw} = H / (R \cdot T)$ | $H_0$ ,<br>$\text{Pa}\cdot\text{m}^3/\text{mol}$ | 6.09E-01 | Coefficient $a_H$ of the exponential equation are recalculated from the coefficient of the following temperature dependence:<br>$H = H_0 \cdot 10^{(-3416(1/T - 1/T_0))}$<br>with the help of the following formula:<br>$a_H = \ln(10) \cdot 3416$ ,<br>It was obtained from the following temperature dependence: $\log(H/H(25^{\circ}\text{C})) = \text{slop}(1/T - 1/298)$<br>$H(25^{\circ}\text{C})$ - Henry's law constant at $25^{\circ}\text{C}$ ,<br>$\text{Pa}\cdot\text{m}^3/\text{mol}$ (PCB-153: 2.43)  | Achman<br>et al., 1993                                 |
|                       |  | $a_H$  | 7865.6   |   |  |
|                       |  | $T_0$ , $^{\circ}\text{K}$                       | 283.15   |   |  |
| G-CIEMS               | Temperature dependent:<br>$H = H_0 \exp(-a_H(1/T - 1/T_0))$<br>where $T$ - temperature ( $\text{K}$ ), $H_0$ is the value at the reference temperature $T_0$ , and $a_H$ is a parameter of temperature dependence.   | $H_0$ ,<br>$\text{Pa}\cdot\text{m}^3/\text{mol}$ | 4.91E+00 | Same to the "reference data set"<br>The value $a_H$ can be put directly as input data.<br>When the input data is not given, temperature dependence of vapour pressure is used as surrogate, assuming the temperature-independent water solubility   | Li et al., 2003  |
|                       |  | $a_H$  | 7851.7   |   |  |
|                       |  | $T_0$ , $^{\circ}\text{K}$                       | 283.15   |   |  |
| SimpleBox             | Temperature dependent:<br>$H = H_0 \exp(-a_H(1/T - 1/T_0))$<br>where $T$ - temperature ( $\text{K}$ ), $H_0$ is the value at the reference temperature $T_0$ , and $a_H$ is a parameter of temperature dependence.   | $H_0$ ,<br>$\text{Pa}\cdot\text{m}^3/\text{mol}$ | 4.91E+00 | Same to the "reference data set"  | Li et al., 2003  |
|                       |  | $a_H$  | 7851.7   |   |  |
|                       |  | $T_0$ , $^{\circ}\text{K}$                       | 283.15   |   |  |
| EVN-BETR and UK-MODEL | Temperature independent:   | $H$ ,<br>$\text{Pa}\cdot\text{m}^3/\text{mol}$   | 19.8     | Calculated as $H = \text{Vapour Pressure (Pa)} / \text{Water Solubility (mol/m}^3)$ at $25^{\circ}\text{C}$<br>At $10^{\circ}\text{C}$ , calculated as<br>$K_{aw}(T_0) = 10^{\log K_{aw}} \cdot a$ ,<br>$a = \exp[(\Delta H_{vap} / R) \cdot (1/T_0 - 1/T)]$ .<br>$\Delta H_{vap} = 62.8 \text{ kJ/mol}$ : Enthalpy of vaporisation (from water to air)<br>here: $a_{Kaw} = \Delta H_{vap} / R$   | Li et al., 2003  |
|                       | Temperature dependent:<br>$K_{aw} = K_{aw}^0 \exp(-a_{Kaw}(1/T - 1/T_0))$<br>where $T$ - temperature ( $\text{K}$ ), $K_{aw}^0$ is the value at the reference temperature $T_0$ , and $a_{Kaw}$ is a parameter of temperature dependence.  | $K_{aw}^0$ ,<br>dimensionless                    | 2.08E-03 |   |  |
|                       |  | $a_{Kaw}$  | 7553.5   |   |  |
|                       |  | $T_0$ , $^{\circ}\text{K}$                       | 283.15   |   |  |
| CiiMoChem             | Temperature dependent:<br>$K_{aw} = K_{aw}^0 \exp(-a_{Kaw}(1/T - 1/T_0))$<br>where $T$ - temperature ( $\text{K}$ ), $K_{aw}^0$ is the value at the reference temperature $T_0$ , and $a_{Kaw}$ is a parameter of temperature dependence.  | $K_{aw}^0$ ,<br>dimensionless                    | 2.01E-03 | $K_{aw}(T) = K_{aw}(T_{ref}) \exp(dH_{Kaw}/R(1/T_{ref} - 1/T))$<br>(dimensionless)<br>$T$ = temperature (283.15 K);<br>$T_{ref}$ = reference temperature (298.15 K)<br>$K_{aw}(T_{ref})$ =Henry's law constant at $T_{ref}$<br>(dimensionless): PCB 153: 9.18E-3<br>$dH_{Kaw}$ = phase transfer enthalpy (J/mol): PCB 153: 71000<br>$R$ = universal gas constant (8.3145 J/molK)  | Beyer et al., 2002                                     |
|                       |  | $a_{Kaw}$  | 8540     |   |  |
|                       |  | $T_0$ , $^{\circ}\text{K}$                       | 283.15   |   |  |
| DEHM-POP              | Temperature dependent:<br>$K_{aw} = K_{aw}^0 \exp(-a_{Kaw}(1/T - 1/T_0))$<br>where $T$ - temperature ( $\text{K}$ ), $K_{aw}^0$ is the value at the reference temperature $T_0$ , and $a_{Kaw}$ is a parameter of temperature dependence.  | $K_{aw}^0$ ,<br>dimensionless                    | 2.01E-03 | $K_{aw}(283.15) = K_{aw}^0(298.15) \exp(-a_{Kaw}(1/T - 1/T_0))$ ,<br>where $K_{aw}^0(298.15) = 9.18\text{E-}3$ for PCB 153  | Beyer et al., 2002                                     |
|                       |  | $a_{Kaw}$  | 8536     |   |  |
|                       |  | $T_0$ , $^{\circ}\text{K}$                       | 283.15   |   |  |
| MSCE-POP              | Temperature dependent:<br>$H = H_0 \exp(-a_H(1/T - 1/T_0))$<br>where $T$ - temperature ( $\text{K}$ ), $H_0$ is the value at the reference temperature $T_0$ , and $a_H$ is a parameter of temperature dependence.<br>Temperature dependent:<br>$K_{aw} = H / (R \cdot T)$       | $H_0$ ,<br>$\text{Pa}\cdot\text{m}^3/\text{mol}$ | 3.781    | Coefficients of the exponential equation are recalculated from the standard form of temperature dependence:<br>$\log H = -A/T(\text{K}) + B$<br>with the help of the following formulas:<br>$a_H = \ln(10) \cdot A$ , $H_0 = 10^{(-A/T_0 + B)}$ ,<br>where $A = \Delta H_W / 2.303R$ ;<br>$B = \log H_{298} + \Delta H_W / 2.303R(298)$ .<br>$H_{298}$ is Henry's law constant ( $\text{Pa}\cdot\text{m}^3/\text{mol}$ ) at $25^{\circ}\text{C}$ (for PCB-153: 16.48);<br>$\Delta H_W$ is the enthalpy of volatilization from water, kJ/mol (for PCB-153: 69.4) | Burkhard<br>et al., 1985;<br>Dunnivant<br>et al., 1992 |
|                       |  | $a_H$ , $\text{K}$                               | 8347     |   |  |
|                       |  | $T_0$ , $\text{K}$                               | 283.15   |   |  |

\* - for the sake of comparability, the base values and coefficients of temperature dependences of the considered parameters are given here at the temperature 283.15 K ( $T_0$ ) and the way they were recalculated from original dependencies is specified in the field "Comments".

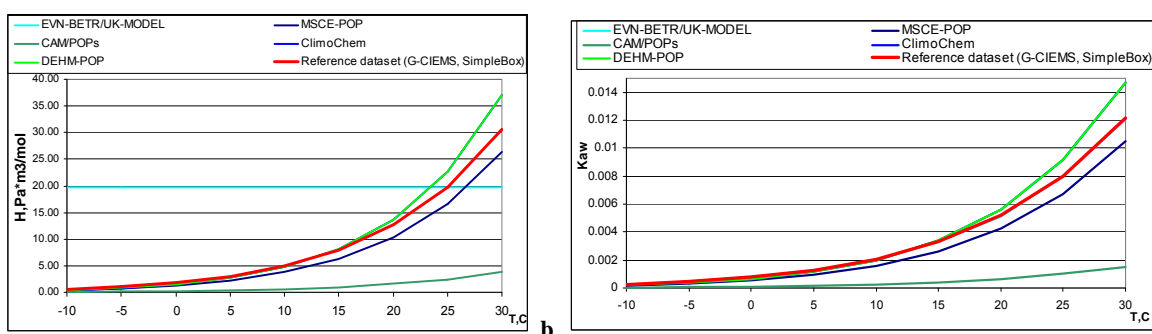


**Fig. 1.** Comparison of temperature dependencies of Henry's law constant ( $H$ ,  $\text{Pa}\cdot\text{m}^3/\text{mol}$ ) and air/water partition coefficient ( $K_{aw}$ , dimensionless) of PCB-153.

For the computations at Stage I, G-CIEMS and SimpleBox exploit temperature dependencies of Henry's law constant and air/water partition coefficient of PCB-153 presented in "reference data set". EVN-BETR and UK-MODEL also use one and the same temperature dependence of  $K_{aw}$  with "reference data set" and the constant value of  $H$  calculated for 25 °C with the help of data from [Li et al., 2003]. CliMoChem and DEHM-POP models have performed calculation experiments with equal values of these parameters from [Beyer et al., 2002]. These models present maximum values of  $K_{aw}$  among all the models. According to the data reported, there is similarity in temperature dependencies used in CliMoChem, DEHM-POP, MSCE-POP and "reference data set". CAM/POPs uses lower values of these parameters than other participating models. The difference in absolute values of  $H$  and  $K_{aw}$  calculated from various types of temperature dependencies, used by the participants in Stage I calculations, is rather large. To illustrate this statement, statistical parameters characterizing the scattering of the values of Henry's law constant and air/water partition coefficient between all models are given in Table 6 for three arbitrary temperatures (-10°C, 10°C and 25°C) and for coefficients of temperature dependencies.

**Table 6.** Absolute values and statistical parameters of Henry's law constant ( $H$ ,  $\text{Pa}\cdot\text{m}^3/\text{mol}$ ) and air/water partition coefficient ( $K_{aw}$ , dimensionless) of PCB-153 for three arbitrary temperatures (-10 °C, 10 °C and 25 °C) and coefficients of temperature dependencies

|                       | $H$ , $\text{Pa}\cdot\text{m}^3/\text{mol}$ |           |          |        | $K_{aw}$ , dimensionless |            |            |           |
|-----------------------|---|-----------|----------|--------|--------------------------|------------|------------|-----------|
|                       | -10°C                                       | 10°C      | 25°C     | $a_H$  | -10°C                    | 10°C       | 25°C       | $a_{Kaw}$ |
| CAM/POPs              | 7.37E-02                                    | 6.09E-01  | 2.46E+00 | 7865.6 | 3.37E-05                 | 2.59E-04   | 9.94E-04   | -         |
| G-CIEMS               | 5.97E-01                                    | 4.91E+00  | 1.98E+01 | 7851.7 | 2.75E-04**               | 2.09E-03** | 8.00E-03** | 7553.5    |
| SimpleBox             | 5.97E-01                                    | 4.91E+00  | 1.98E+01 | 7851.7 | 2.75E-04**               | 2.09E-03** | 8.00E-03** | 7553.5    |
| EVN-BETR and UK-MODEL | 19.8  | 19.8      | 19.8     | -      | 2.74E-04**               | 2.08E-03** | 7.96E-03** | 7553.5    |
| CliMoChem             | 4.44E-01*                                   | 4.73E+00  | 2.27E+01 | -      | 2.03E-04                 | 2.01E-03   | 9.17E-03*  | 8540*     |
| DEHM-POP              | 4.45E-01*                                   | 4.73E+00  | 2.27E+01 | -      | 2.03E-04                 | 2.01E-03   | 9.16E-03*  | 8536*     |
| MSCE-POP              | 4.02E-01                                    | 3.78E+00  | 1.67E+01 | 8347   | 1.84E-04                 | 1.61E-03   | 6.72E-03   | -         |
| "Reference data set"  | 5.97E-01                                    | 4.91E+00  | 1.98E+01 | 7851.7 | 2.75E-04**               | 2.09E-03** | 8.00E-03** | 7553.5    |
| <i>min</i>            | 7.37E-02                                    | 6.09E-01  | 2.46E+00 | 7851.7 | 3.37E-05                 | 2.59E-04   | 9.94E-04   | 7553.5    |
| <i>max</i>            | 1.98E+01                                    | 1.98E+01  | 2.27E+01 | 8347.0 | 2.75E-04                 | 2.09E-03   | 9.17E-03   | 8540.0    |
| <i>arith. mean</i>    | 2.87E+00                                    | 6.05E+00  | 1.80E+01 | 7953.5 | 2.15E-04                 | 1.78E-03   | 7.25E-03   | 7881.7    |
| <i>median</i>         | 5.21E-01                                    | 4.82E+00  | 1.98E+01 | 7851.7 | 2.39E-04                 | 2.05E-03   | 8.00E-03   | 7553.5    |
| <i>geom. mean</i>     | 6.30E-01                                    | 4.32E+00  | 1.55E+01 | 7951.2 | 1.86E-04                 | 1.54E-03   | 6.24E-03   | 7868.4    |
| <i>max/min</i>        | 8 / 269***                                  | 8 / 33*** | 9        | 1.1    | 8                        | 8          | 9          | 1.1       |

\*. \*\* - difference in absolute values obtained from identical temperature dependencies can be explained by accuracy of coefficient recalculation.

\*\*\* - the first value is calculated without the temperature independent value of  $H$  (EVN-BETR and UK-MODEL), the second value is calculated taking it into account.

There is a substantial difference between highest and lowest absolute values of  $H$  (CAM/POPs and EVN-BETR and UK-MODEL) both at -10°C and 10°C. These values differ from each other more than an order of magnitude. It can be explained by the fact that EVN-BETR and UK-MODEL use the

constant value of  $H$  calculated for 25 °C. That is why scattering of  $H$  values is going down with temperature increase. If not take into account this temperature independent value, max/min ratio for this parameter is equal to 8-9. Differences in absolute values of  $K_{aw}$  between G-CIEMS, SimpleBox, CliMoChem, DEHM-POP, MSCE-POP and “reference data set” are also not high. In this case scattering of both parameters values is slightly increasing with temperature. It is seen that median values of Henry’s law constant and air-water partition coefficient used in models is very close to those used in “reference data set”.

Comparison of Henry’s law constant and air/water partition coefficient of PCB-28 and PCB-180 used in the participating models and “reference data sets” are presented in Fig. B.1 and B.2. in Annex B. There is also statistical evaluation of absolute values and coefficients of temperature dependencies in Table B.3 and B.4.

It is seen that the difference in highest and lowest absolute values of  $H$  between all models is also very large for PCB-180. Similar to that for PCB-153, scattering is going down with temperature increase. But if not take into account temperature independent  $H$  value of PCB-180, max/min ratio for this parameter and for  $K_{aw}$  lies within factor 12-22. At that scattering of both parameters values is growing with temperature increase more substantial.

Henry’s law constant and air/water partition coefficient values of PCB-28 used by all models are closer than those data on above two congeners. Difference in  $H$  values between all models for PCB-28 is much less than for other congeners. Scattering is going down with temperature. If not take into account temperature independent  $H$  value of PCB-28, max/min ratio for this parameter and for  $K_{aw}$  lies within factor 2. Scattering of both parameters values is going down with temperature increase.

### 3.2. The subcooled liquid vapour pressure

The value of subcooled liquid-vapour pressure ( $p_{oL}$ , Pa) is used in the modelling of the process of POP partitioning between its particulate and gaseous phase in the atmosphere in accordance with the Junge-Pankow adsorption model [Junge, 1977; Pankow, 1987]. Thus, in this cases the value of  $p_{oL}$  determining the particle-bound fraction of a pollutant in air strongly influences such subsequent important processes as dry and wet particle deposition and degradation in air.

CliMoChem and DEHM-POP models do not use subcooled liquid vapour pressure for model calculations. EVN-BETR and UK-MODEL assumes this parameter temperature-independent. Other models use temperature dependence of this parameter. The coefficients of temperature dependencies for PCB-153 are presented in Table 7.

As seen from the Table, the participating models use two types of temperature dependence coefficients of  $p_{oi}$  which do not differ from each other very much. The first type of this dependence is taken from “reference data set” and it is also used by G-CIEMS and SimpleBox. The second one is utilised by CAM/POPs and MSCE-POP. Comparison of these temperature dependencies of  $p_{oi}$  is presented in Fig. 2. The “reference data set” shows slightly less values of this parameter.

**Table 7.** The subcooled liquid vapour pressure of PCB-153 (data sets of the participating POP models)\*

| Model                 | Description  | Numerical values |          | Comments  | Reference                                     |
|-----------------------|--|------------------|----------|---|---|
| CAM/POPs              | Temperature dependent:<br>$p_{ol} = p_{ol}^0 \exp(-a_p(1/T - 1/T_0))$<br>where $T$ - temperature (K), $p_{ol}^0$ is the value at the reference temperature $T_0$ , and $a_p$ is a parameter of temperature dependence. | $p_{ol}^0$ , Pa  | 9.69E-05 | Coefficients of the exponential equation are recalculated from the standard form of temperature dependence:<br>$p_{ol} = 10^{(m/T + b)}$ ,<br>where $T$ - temperature ( $^{\circ}$ K); $m = -4775$ : parameter of temperature dependence, and $b = 12.85$ : parameter depended on molecular weight.<br>It was obtained from the following original equation:<br>$\log(p_{ol}) = -Q / (2.303 RT) + b$<br>where: $T$ - temperature; $R$ - Universal Gas Constant<br>$Q$ - the heat of vaporisation (KJ/mol) | Harner et al., 1996;<br>Falconer et al., 1995 |
|                       |  | $a_p$            | 10995    |   |   |
|                       |  | $T_0$ , K        | 283.15   |   |   |
| SimpleBox             | Temperature dependent:<br>$p_{ol} = p_{ol}^0 \exp(-a_p(1/T - 1/T_0))$<br>where $T$ - temperature (K), $p_{ol}^0$ is the value at the reference temperature $T_0$ , and $a_p$ is a parameter of temperature dependence. | $p_{ol}^0$ , Pa  | 8.82E-05 | Same to the "reference data set"  | Li et al., 2003                               |
|                       |  | $a_p$            | 10846.6  |   |   |
|                       |  | $T_0$ , K        | 283.15   |   |   |
| G-CIEMS               | Temperature dependent:<br>$p_{ol} = p_{ol}^0 \exp(-a_p(1/T - 1/T_0))$<br>where $T$ - temperature (K), $p_{ol}^0$ is the value at the reference temperature $T_0$ , and $a_p$ is a parameter of temperature dependence. | $p_{ol}^0$ , Pa  | 8.82E-05 | Same to the "reference data set"  | Li et al., 2003                               |
|                       |  | $a_p$            | 10846.6  |   |   |
|                       |  | $T_0$ , K        | 283.15   |   |   |
| EVN-BETR and UK-MODEL | Temperature independent:   | $p_{ol}$ , Pa    | 6.60E-04 | $T = 25^{\circ}\text{C}$  | Li et al., 2003                               |
| MSCE-POP              | Temperature dependent:<br>$p_{ol} = p_{ol}^0 \exp(-a_p(1/T - 1/T_0))$<br>where $T$ - temperature (K), $p_{ol}^0$ is the value at the reference temperature $T_0$ , and $a_p$ is a parameter of temperature dependence. | $p_{ol}^0$ , Pa  | 9.69E-05 | Coefficients of the exponential equation are recalculated from the standard form of temperature dependence: $\log p_{ol} \text{ (Pa)} = -4775/T(\text{K}) + 12.85$ with the help of the following formulas:<br>$a_p = \ln(10) \cdot 4775$ ,<br>$p_{ol}^0 = 10^{(-4775/T_0 + 12.85)}$  | Falconer and Bidleman, 1994                   |
|                       |  | $a_p$            | 10995    |   |   |
|                       |  | $T_0$ , K        | 283.15   |   |   |

\* - for the sake of comparability, the base values and coefficients of temperature dependences of the considered parameters are given here at the temperature 283.15 K ( $T_0$ ) and the way they were recalculated from original dependencies is specified in the field "Comments".

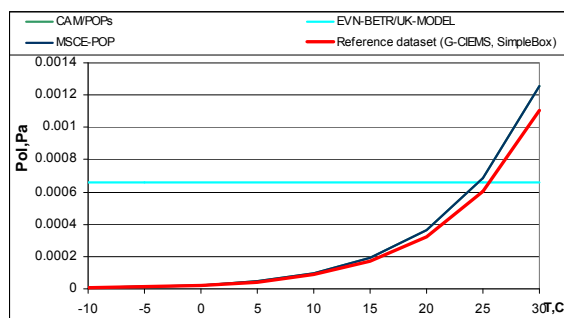


**Fig. 2.** Comparison of temperature dependencies of subcooled liquid vapour pressure of PCB-153 used in data sets of the participating POP models and in "reference data set"

The dispersion of the subcooled liquid vapour pressure of PCB-153 can be characterized by the comparison of its absolute values at  $-10^{\circ}\text{C}$ ,  $10^{\circ}\text{C}$  and  $25^{\circ}\text{C}$  and coefficients of temperature dependence used by the participating models. Above mentioned values and corresponding statistical parameters are given in Table 8.

**Table 8.** Absolute values, coefficients of temperature dependence and statistical parameters of subcooled liquid vapour pressure of PCB-153 for three arbitrary temperatures (-10 °C, 10 °C and 25 °C)

|                    | $p_{OL}$ , Pa |            |          | $a_p$   |
|--------------------|---------------|------------|----------|---------|
|                    | -10°C         | 10°C       | 25°C     |         |
| CAM/POPs           | 5.07E-06      | 9.69E-05   | 6.84E-04 | 10995   |
| G-CIEMS            | 4.80E-06      | 8.82E-05   | 6.06E-04 | 10846.6 |
| SimpleBox          | 4.80E-06      | 8.82E-05   | 6.06E-04 | 10846.6 |
| EVN-BETR/UK-MODEL  | 6.60E-04      | 6.60E-04   | 6.60E-04 | -       |
| MSCE-POP           | 5.07E-06      | 9.69E-05   | 6.84E-04 | 10995   |
| Reference data set | 4.80E-06      | 8.82E-05   | 6.06E-04 | 10846.6 |
| <i>min</i>         | 4.80E-06      | 8.82E-05   | 6.06E-04 | 10846.6 |
| <i>max</i>         | 6.60E-04      | 6.60E-04   | 6.84E-04 | 10995.0 |
| <i>arith. mean</i> | 1.14E-04      | 1.86E-04   | 6.41E-04 | 10906.0 |
| <i>median</i>      | 4.93E-06      | 9.26E-05   | 6.33E-04 | 10846.6 |
| <i>geom. mean</i>  | 1.11E-05      | 1.27E-04   | 6.40E-04 | 10905.7 |
| <i>max/min</i>     | 1.1 / 137.6*  | 1.1 / 7.5* | 1.1      | 1.0     |

\* - the first value is calculated without the temperature independent value of  $p_{OL}$  (EVN-BETR and UK-MODEL), the second value is calculated taking it into account

If not take into account temperature independent value of subcooled liquid vapour pressure of PCB-153 included in EVN-BETR and UK-MODEL, all the rest models use close temperature dependencies of  $p_{ol}$ . Scattering between its values at all considered temperatures (-10, 10 and 25 °C) is about 1.1. However, considering temperature independent value of  $p_{ol}$  of EVN-BETR and UK-MODEL, one can see that for all three temperatures the difference between maximum and minimum values increases up to several order of magnitude. For the first given temperature (-10 °C) it is rather high (max/min ratio equals to 138). At 10 °C, it is considerably smaller (max/min ratio equals to 7.5). For all models max/min ratio for coefficients of temperature dependence equals practically to 1.0.

Comparison of subcooled liquid vapour pressure values of PCB-28 and PCB-180 used in the participating models and “reference data sets” are presented in Fig. B.3 and B.4 in Annex B. Statistical evaluation of absolute values and coefficients of temperature dependencies is given in Table B.6 and B.7.

For all three temperatures the difference in maximum and minimum values of  $p_{ol}$  between all models is less for PCB-28 than that for PCB-153 and PCB-180. If not taking into account temperature independent value of  $p_{ol}$ , max/min ratio for PCB-28 varies within factor 1.3. For PCB-180 max/min ratio of  $p_{ol}$  values lies within factor 7.

### 3.3. The octanol/water partition coefficient

The octanol/water partition coefficient ( $K_{ow}$ , dimensionless) is used in the participating models for the estimation of the POP partitioning in the organic carbon/water system ( $K_{oc}$ ) on the basis of regression dependencies and of the partition coefficient in the octanol/air system ( $K_{oa}$ ) (Subsections 3.4 and 3.5). Thus, this parameter mainly influences on the description of the following processes: gas-particle partitioning in the atmosphere (in accordance with absorption model), gaseous exchange between the atmosphere and soil (partitioning in soil compartment), and gaseous exchange between the atmosphere and vegetation (partitioning among vegetation compartment).  $K_{ow}$  is also included by CliMoChem models in the calculation of the water particle-bound fraction of a pollutant for modelling diffusion process from seawater to atmosphere.

The most part of participating models (CAM/POPs, SimpleBox, G-CIEMS, EVN-BETR and UK-MODEL CliMoChem and DEHM-POP) involve the octanol/water partition coefficient of the considered PCBs in the form of the temperature dependence. As usual the temperature dependencies of this parameter are equated by downward exponents with different values of  $K_{ow}$  at reference temperature (for example at 10°C) as the pre-exponential multiplier and with the values of

the second - temperature coefficient of these dependencies defined with the help of the enthalpy or the internal energy of phase transfer. The exception is CAM/POPs model, in which the temperature dependence of  $K_{ow}$  is recalculated from temperature dependencies of the Henry's law constant and the octanol/air partition coefficient. MSCE-POP model contents temperature independent values of  $K_{ow}$ . These data together with coefficients of  $K_{ow}$  temperature dependencies for PCB-153 are presented in Table 9.

Temperature dependencies of the octanol/water partition coefficient of PCB-153 used in the calculations by the participating models and in "reference data set" are compared in Fig.3.

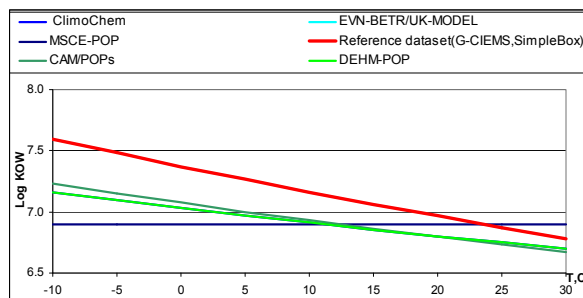


Fig. 3. Comparison of temperature dependencies of  $\log K_{ow}$  of PCB-153 used in the models and in "reference data set"

Table 9. The octanol/water partition coefficient of PCB-153 (data sets of the participating POP models)\*

| Model                 | Description  | Numerical values                |          | Comments  | Reference                 |
|-----------------------|--|---------------------------------|----------|---|---------------------------|
| CAM POPs              | Temperature dependent:<br>$K_{ow} = K_{oa} \cdot H/RT$<br>where $T$ - temperature ( $^{\circ}K$ );<br>$R$ - Universal Gas Constant; $H$ - Henry's law constant; $K_{oa}$ - Octanol/air partition coefficient (dimensionless)             | -                               | -        | These values are calculated with the help of temperature dependencies of $H$ and $K_{oa}$ .   | This study                |
| SimpleBox             | Temperature dependent:<br>$K_{ow} = K_{ow}^0 \exp(a_{Kow}(1/T - 1/T_0))$<br>where $T$ - temperature (K), $K_{ow}^0$ is the value at the reference temperature $T_0$ , and $a_{Kow}$ is a parameter of temperature dependence.            | $K_{ow}^0(T_0)$ , dimensionless | 1.45E+07 | Same to the "reference data set"  | Li et al., 2003           |
|                       |  | $a_{Kow}$                       | 3740.7   |   |                           |
|                       |  | $T_0, K$                        | 283.15   |   |                           |
| G-CIEMS               | Temperature dependent:<br>$K_{ow} = K_{ow}^0 \exp(a_{Kow}(1/T - 1/T_0))$<br>where $T$ - temperature (K), $K_{ow}^0$ is the value at the reference temperature $T_0$ , and $a_{Kow}$ is a parameter of temperature dependence.            | $K_{ow}^0(T_0)$ , dimensionless | 1.45E+07 | Same to the "reference data set"  | Li et al., 2003           |
|                       |  | $a_{Kow}$                       | 3740.7   |   |                           |
|                       |  | $T_0, K$                        | 283.15   |   |                           |
| EVN-BETR and UK-MODEL | Temperature dependent:<br>$K_{ow} = K_{ow}^0 \exp(a_{Kow}(1/T - 1/T_0))$<br>where $T$ - temperature (K), $K_{ow}^0$ is the value at the reference temperature $T_0$ , and $a_{Kow}$ is a parameter of temperature dependence.            | $K_{ow}^0$ , dimensionless      | 1.45E+07 | For $10^{\circ}C$ , calculated as $K_{ow}(T_0) = 10^{\log K_{ow}} \cdot a$ ,<br>$a = \exp[(\Delta H_{sol}/R) \cdot (1/T_0 - 1/T)]$ .<br>$\Delta H_{sol} = -31.1$ KJ/mol: Enthalpy of solution (from octanol to water)<br>here: $a_{Kow} = \Delta H_{sol}/R$   | Li et al., 2003           |
|                       |  | $a_{Kow}$                       | 3740.5   |   |                           |
|                       |  | $T_0, K$                        | 283.15   |   |                           |
| ClimoChem             | Temperature dependent:<br>$K_{ow} = K_{ow}^0 \exp(a_{Kow}(1/T - 1/T_0))$<br>where $T$ - temperature (K), $K_{ow}^0$ is the value at the reference temperature $T_0$ , and $a_{Kow}$ is a parameter of temperature dependence ( $-dH/R$ ) | $K_{ow}^0$ , dimensionless      | 8.17E+06 | $K_{ow}(T) = K_{ow}(T_{ref}) \exp((dHK_{ow}/R)(1/T_{ref} - 1/T))$<br>dimensionless<br>$T$ = temperature (283.15K);<br>$T_{ref}$ = reference temperature (298.15 K)<br>$K_{ow}(T_{ref})$ = Octanol/water partition coefficient at $T_{ref}$ PCB 153: 5.62E+6;<br>$dHK_{ow}$ = phase transfer enthalpy (J/mol) PCB 153: -17500<br>$R$ = universal gas constant (8.3145 J/mol K) | Beyer et al., 2002        |
|                       |  | $a_{Kow}$                       | 2104.8   |   |                           |
|                       |  | $T_0, K$                        | 283.15   |   |                           |
| DEHM-POP              | Temperature dependent:<br>$K_{ow} = K_{ow}^0 \exp(a_{Kow}(1/T - 1/T_0))$<br>where $T$ - temperature (K), $K_{ow}^0$ is the value at the reference temperature $T_0$ , and $a_{Kow}$ is a parameter of temperature dependence ( $-dH/R$ ) | $K_{ow}^0$ , dimensionless      | 8.17E+06 | $K_{ow}(283.15) = K_{ow}^0(298.15) \exp(a_{Kow}(1/T - 1/T_0))$ ,<br>where $K_{ow}^0(298.15) = 5.62E+6$ for PCB 153<br>$a_{Kow} = dHK_{ow}/R$<br>$dHK_{ow}$ = phase transfer enthalpy (J/mol) PCB 153: -17500<br>$R$ = universal gas constant (8.3145 J/mol K)   | Beyer et al., 2002        |
|                       |  | $a_{Kow}$                       | 2102.4   |   |                           |
|                       |  | $T_0, K$                        | 283.15   |   |                           |
| MSCE-POP              | Temperature independent  | $K_{ow}$ , dimensionless        | 7.94E+6  | $\log K_{ow} = 6.9$   | Mackay et al., v.1., 1992 |

\* - for the sake of comparability, the base values and coefficients of temperature dependencies of the considered parameters are given here for the temperature 283.15 K ( $T_0$ ) and the way they were recalculated from original dependencies is specified in the field "Comments".

Comparison of the plots of temperature dependencies of the octanol/water partition coefficient of PCB-153 used in CAM/POPs, CliMoChem, DEHM-POP models and in “reference data set” (also in SimpleBox, G-CIEMS, and EVN-BETR/UK-MODEL) shows not substantial differences between values of  $\log K_{ow}$  used by the models (except temperature independent value presented by MSCE-POP). To evaluate the scattering of  $K_{ow}$ , the variability of this parameter values used by the participating models is determined at three fixed temperature (-10°C, 10°C and 25°C). Absolute values, coefficients of temperature dependence and statistical parameters of octanol/water partition coefficient of PCB-153 for three arbitrary temperatures are given in Table 10.

The difference between all models in terms of absolute values of octanol/water partition coefficient of PCB-153 used for modelling is not large for all considered temperatures (max/min ratios of  $K_{ow}$  vary from 5 to 2). If not take into account the temperature independent value of MSCE-POP, max/min ratio at -10°C comes down to 3. Besides, the difference between statistical parameters characterizing the values averaged between models at three various temperatures (arithmetic and geometric means, and median) is not substantial (factor 3-4) within the temperature interval (-10 - 25°C). It is seen that the values of this parameter at all considered temperatures are the largest for “reference data set” including SimpleBox, G-CIEMS and EVN-BETR/UK-MODEL respectively. At the same time, CAM/POPs, CliMoChem, and DEHM-POP have close values between one another which are lower than the first ones. For all these models and “reference data set” scattering of this parameter at 25°C is minimum. For the models max/min ratio of coefficients of temperature dependences equals to 2.0.

**Table 10.** Absolute values, coefficients of temperature dependence and statistical parameters of octanol/water partition coefficient of PCB-153 for three arbitrary temperatures (-10 °C, 10 °C and 25 °C)

|                    | $K_{ow}$   |            |            | $a_{Kow}$ |
|--------------------|------------|------------|------------|-----------|
|                    | -10°C      | 10°C       | 25°C       |           |
| CAM/POPs           | 1.72E+07   | 8.51E+06   | 5.42E+06   | -         |
| SimpleBox          | 3.96E+07   | 1.45E+07   | 7.46E+06   | 3740.7*   |
| G-CIEMS            | 3.96E+07   | 1.45E+07   | 7.46E+06   | 3740.7*   |
| EVN-BETR/UK-MODEL  | 3.96E+07   | 1.45E+07   | 7.46E+06   | 3740.5*   |
| CliMoChem          | 1.44E+07   | 8.17E+06   | 5.62E+06   | 2104.8**  |
| DEHM-POP           | 1.44E+07   | 8.17E+06   | 5.62E+06   | 2102.4**  |
| MSCE-POP           | 7.94E+06   | 7.94E+06   | 7.94E+06   | -         |
| Reference data set | 3.96E+07   | 1.45E+07   | 7.46E+06   | 3740.7*   |
| <i>min</i>         | 7.94E+06   | 7.94E+06   | 5.42E+06   | 2102.4    |
| <i>max</i>         | 3.96E+07   | 1.45E+07   | 7.94E+06   | 3740.7    |
| <i>arith. mean</i> | 2.59E+07   | 1.13E+07   | 6.93E+06   | 3085.8    |
| <i>median</i>      | 2.70E+07   | 1.13E+07   | 7.46E+06   | 3740.5    |
| <i>geom. mean</i>  | 2.16E+07   | 1.08E+07   | 6.86E+06   | 2971.3    |
| <i>max/min</i>     | 2.8/5.0*** | 1.8/1.8*** | 1.4/1.5*** | 1.8       |

\*, \*\* - difference in absolute values obtained from identical temperature dependencies can be explained by accuracy of coefficient recalculation

\*\*\* - the first value is calculated without the temperature independent value of  $K_{ow}$  (MSCE-POP), the second value is calculated taking it into account

Comparison of octanol/water partition coefficient values of PCB-28 and PCB-180 used in the participating models and “reference data sets” are presented in Fig. B.5 and B.6 in Annex B. Statistical evaluation of absolute values and coefficients of temperature dependencies is given in Table B.9 and B.10.

Differences in absolute values of octanol/water partition coefficient between all models for PCB-28 and PCB-180 are also not large. Max/min ratio of  $K_{OW}$  values for PCB-28 varies from 2 to 4; and for PCB-180 – from 2 to 3. If the temperature independent values of MSCE-POP are not taken into account, max/min ratio for PCB-28 lies within factor 1.2 and for PCB-180 – within factor 1-3. For these congeners,  $K_{OW}$  values are changing with temperature increase within factor 3-4 for considered interval of temperatures (-10-25°C). Scattering of coefficients of temperature dependences among all models for PCB-28 lies within factors 1 and for PCB-180 – within factor 4.

### 3.4. The octanol/air partition coefficient

The octanol/air partition coefficient ( $K_{oa}$ , dimensionless) is used by EVN-BETR and UK-MODEL, G-CIEMS and DEHM-POP in the description of POP gas-particle partitioning in the atmosphere as absorption from air into an octanol-like film of particle phase according to [Finizio et al., 1997; Falconer and Harner, 2000]. Besides, this parameter is included into descriptions of the gaseous exchange between air and vegetation. It should be mentioned that EVN-BETR and UK-MODEL and CliMoChem models do not use  $K_{oa}$  parameter straight as input information for modelling but recalculate it from  $K_{ow}$  and  $K_{aw}$ .

The participating models and “reference data set” contain this parameter in the form of temperature dependence. Coefficients of these dependencies are presented in Table 11.

**Table 11.** The octanol/air partition coefficient of PCB-153 (data sets of the participating POP models)\*

| Model                 | Description   | Numerical values                   |                     | Comments   | Reference                 |
|-----------------------|---|------------------------------------|---------------------|--|---------------------------|
| CAM/POPs              | Temperature dependent:<br>$K_{oa} = 10^{(a/T+b)}$<br>where: $T$ - temperature;<br>$P$ - liquid vapour pressure $p_{oi}$ (Pa)  | $a$                                | -529-19.25<br>logP  | These values are calculated with the help of temperature dependencies of $p_{oi}$  | Harner et al., 1996; 1998 |
|                       |   | $b$                                | 8.2995-0.95<br>logP |  |                           |
| SimpleBox             | Temperature dependent:<br>$K_{oa} = K_{oa}^0 \exp(a_{K_{oa}}(1/T - 1/T_0))$<br>where $T$ - temperature (K),<br>$K_{oa}^0$ is the value at the reference temperature $T_0$ ,<br>and $a_{K_{oa}}$ is a parameter of temperature dependence. | $K_{oa}^0(T_0)$ ,<br>dimensionless | 2.05E+10            | Same to the “reference data set”   | Li et al., 2003           |
|                       |   | $a_{K_{oa}}$                       | 11294.2             |  |                           |
|                       |   | $T_0, K$                           | 283.15              |  |                           |
| G-CIEMS               | Temperature dependent:<br>$K_{oa} = K_{oa}^0 \exp(a_{K_{oa}}(1/T - 1/T_0))$<br>where $T$ - temperature (K),<br>$K_{oa}^0$ is the value at the reference temperature $T_0$ ,<br>and $a_{K_{oa}}$ is a parameter of temperature dependence. | $K_{oa}^0(T_0)$ ,<br>dimensionless | 2.05E+10            | Same to the “reference data set”<br>$K_{oa}$ is used as optional only when the input value is given.   | Li et al., 2003           |
|                       |   | $a_{K_{oa}}$                       | 11294.2             |  |                           |
|                       |   | $T_0, K$                           | 283.15              |  |                           |
| EVN-BETR and UK-MODEL | Temperature dependent:<br>$K_{oa} = K_{ow} / K_{aw}$  | $K_{oa}^0(T_0)$ ,<br>dimensionless | 6.97E+09            | At 10°C, calculated as $K_{oa} = K_{ow} / K_{aw}$  |                           |
|                       |   | $T_0, K$                           | 283.15              |  |                           |
| DEHM-POP              | Temperature dependent:<br>$K_{oa} = K_{oa}^0 \exp(a_{K_{oa}}(1/T - 1/T_0))$<br>where $T$ - temperature (K),<br>$K_{oa}^0$ is the value at the reference temperature $T_0$ ,<br>and $a_{K_{oa}}$ is a parameter of temperature dependence. | $K_{oa}^0(T_0)$ ,<br>dimensionless | 2.74E+10            | $K_{oa}(283.15) = K_{oa}^0(298.15) \exp(a_{K_{oa}}(1/T - 1/T_0))$ ,<br>where $K_{oa}^0(298.15) = 4.14E+9, 1.16E+8, 1.68E+10$<br>for PCB 153, 28 and 180 respectively<br>$a_{K_{oa}} = dHK_{oa}/R$<br>$dH K_{oa}$ = phase transfer enthalpy (J/mol)<br>PCB 153: -88400<br>$R$ = universal gas constant (8.3145 J/mol K) | Beyer et al., 2002        |
|                       |   | $a_{K_{oa}}$                       | 10636.8             |  |                           |
|                       |   | $T_0, K$                           | 283.15              |  |                           |
| MSCE-POP              | Temperature dependent:<br>$K_{oa} = K_{oa}^0 \exp(a_{K_{oa}}(1/T - 1/T_0))$<br>where $T$ - temperature (K), $K_{oa}^0$ is the value at the reference temperature $T_0$ , and $a_{K_{oa}}$ is a parameter of temperature dependence.       | $K_{oa}^0(T_0)$ ,<br>dimensionless | 3.64E+10            | Coefficients of the exponential equation are recalculated from the standard form of temperature dependence:<br>$\log K_{oa} = 4695/T(K) - 6.02$<br>with the help of the following formulas:<br>$a_p = \ln(10) \cdot 4695$ ,<br>$K_{oa}^0(T_0) = 10^{(4695/T_0 - 6.02)}$  | Harner and Bidleman, 1996 |
|                       |   | $a_{K_{oa}}$                       | 10811               |  |                           |
|                       |   | $T_0, K$                           | 283.15              |  |                           |

\* - for the sake of comparability, the base values and coefficients of temperature dependencies of the considered parameters are given here for the temperature 283.15 K ( $T_0$ ) and the way they were recalculated from original dependencies is specified in the field "Comments".

Following the data submitted comparison of temperature dependencies of the octanol/air partition coefficient used by the models and in “reference data set” is presented in Fig. 4.

MSCE-POP has performed the calculations with the help of the highest values of octanol/air partition coefficient of PCB-153 among other participating models. Describing equations of temperature dependence of  $K_{oa}$  in different ways, CAM/POPs and DEHM-POP nevertheless use practically similar values of this parameters for PCB-153. The values of  $K_{oa}$  calculated with “reference data set” (also SimpleBox, G-CIEMS) are somewhat lower than previous ones. EVN-BETR/UK-MODEL uses the lowest values of this parameter than other participating models.

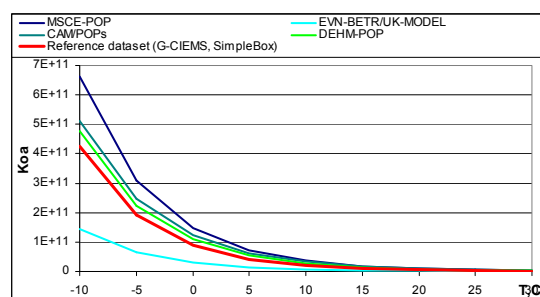


**Fig. 4.** Comparison of temperature dependencies of octanol/air partition coefficient of PCB-153 used in the participating POP models and in “reference data set”

In order to characterize the spread of octanol/air partition coefficient of PCB-153, the comparison of its absolute values at three arbitrary temperatures (-10°C, 10°C and 25°C) between the participating models is made. Absolute values of  $K_{oa}$ , coefficients of temperature dependencies and their statistical parameters are presented in Table 12.

**Table 12.** Absolute values, coefficients of temperature dependencies and statistical parameters of octanol/air partition coefficient of PCB-153 for three arbitrary temperatures (-10 °C, 10 °C and 25 °C)

|                    | $K_{oa}$ |          |          | $a_{K_{oa}}$ |
|--------------------|----------|----------|----------|--------------|
|                    | -10°C    | 10°C     | 25°C     |              |
| CAM/POPs           | 5.10E+11 | 3.29E+10 | 5.45E+09 | -            |
| SimpleBox          | 4.25E+11 | 2.05E+10 | 2.76E+09 | 11294.2      |
| G-CIEMS            | 4.25E+11 | 2.05E+10 | 2.76E+09 | 11294.2      |
| EVN-BETR/UK-MODEL  | 1.45E+11 | 6.97E+09 | 9.37E+08 | -            |
| DEHM-POP           | 4.76E+11 | 2.74E+10 | 4.14E+09 | 10636.8      |
| MSCE-POP           | 6.63E+11 | 3.64E+10 | 5.33E+09 | 10811        |
| Reference data set | 4.25E+11 | 2.05E+10 | 2.76E+09 | 11294.2      |
| <i>min</i>         | 1.45E+11 | 6.97E+09 | 9.37E+08 | 10636.8      |
| <i>max</i>         | 6.63E+11 | 3.64E+10 | 5.45E+09 | 11294.2      |
| <i>arith. mean</i> | 4.38E+11 | 2.36E+10 | 3.45E+09 | 11066.1      |
| <i>mediana</i>     | 4.25E+11 | 2.05E+10 | 2.76E+09 | 11294.2      |
| <i>geom. mean</i>  | 4.05E+11 | 2.13E+10 | 3.03E+09 | 11062.4      |
| <i>max/min</i>     | 5        | 5        | 6        | 1            |

At all considered temperatures there is not a large difference in values of  $K_{oa}$  obtained with the use of existing temperature dependencies. The difference between absolute values of this parameter used by the participants at the first two temperatures is smaller than it is at the last one (max/min ratios come up from 5 to 6). Max/min ratio of coefficients of temperature dependences of  $K_{oa}$  equals to 1.0.

Comparison of octanol/air partition coefficient values of PCB-28 and PCB-180 used in the participating models and in “reference data sets” are presented in Fig. B.7 and B.8 in Annex B. Statistical evaluation of absolute values and coefficients of temperature dependencies is given in Table B.12 and B.13.

Differences in absolute values of octanol/water partition coefficient between all models for PCB-28 are less than that for PCB-153 and PCB-180. Max/min ratios between absolute values of  $K_{oa}$  used by all models at the three considered temperatures range from 2 to 5 for PCB-28 and from 6 to 8 for PCB-180. Max/min ratio of coefficients of temperature dependences of  $K_{oa}$  for these congeners equals practically to 1.0.

### 3.5. The organic carbon/water partition coefficient

The organic carbon/water partition coefficient ( $K_{oc}$ , L/kg) strongly influences on the description of processes of POP sorption by soil and sediments. Partition coefficients in the “organic carbon-water” system selected by the participating models for modelling of PCB-153 are presented in Table 13.

**Table 13.** The organic carbon/water partition coefficient of PCBs,  $dm^3/kg$  (data sets of the participating POP models)

| Model                 | Description  | Numerical values |      | Comments   | Reference   |
|-----------------------|--|------------------|------|--|---|
| CAM/POPs              | Regression relation:<br>$K_{oc} = regc K_{ow}^b$<br>where $regc$ and $b$ are regression coefficients | $regc$           | 0.41 | $K_{oc}$ is calculated from $K_{ow}$ , where $K_{ow}$ is the temperature dependent octanol-water partitioning coefficient                                  | Karickhoff, 1981<br>Mackay, 1991<br>Schnoor, 1996 |
|                       |  | $b$              | 1    |  |   |
| SimpleBox             | Regression relation:<br>$K_{oc} = regc K_{ow}^b$<br>where $regc$ and $b$ are regression coefficients | $regc$           | 0.41 | Same to the “reference data set”<br>$K_{oc}$ is calculated from $K_{ow}$ , where $K_{ow}$ is the temperature dependent octanol-water partition coefficient | Karickhoff, 1981                                  |
|                       |  | $b$              | 1    |  |   |
| G-CIEMS               | Regression relation:<br>$K_{oc} = regc K_{ow}^b$<br>where $regc$ and $b$ are regression coefficients | $regc$           | 1.26 |  |   |
|                       |  | $b$              | 0.81 |  |   |
| EVN-BETR and UK-MODEL | Regression relation:<br>$K_{oc} = regc K_{ow}^b$<br>where $regc$ and $b$ are regression coefficients | $regc$           | 0.41 |  | Karickhoff, 1981                                  |
|                       |  | $b$              | 1    |  |   |
| CliMoChem             | Regression relation:<br>$K_{oc} = regc K_{ow}^b$<br>where $regc$ and $b$ are regression coefficients | $regc$           | 0.35 | $K_{oc}$ is calculated from $K_{ow}$ , where $K_{ow}$ is the temperature dependent octanol-water partition coefficient                                     | Seth et al., 1999                                 |
|                       |  | $b$              | 1    |  |   |
| DEHM-POP              | Regression relation:<br>$K_{oc} = regc K_{ow}^b$<br>where $regc$ and $b$ are regression coefficients | $regc$           | 0.41 |  | Mackay, 1999                                      |
|                       |  | $b$              | 1    |  |   |
| MSCE-POP              | Regression relation:<br>$K_{oc} = regc K_{ow}^b$<br>where $regc$ and $b$ are regression coefficients | $regc$           | 0.41 |  | Karickhoff, 1981                                  |
|                       |  | $b$              | 1    |  |   |

All models use one and the same approach to estimate this parameter – recalculation from octanol/water partition coefficient with the use of simple regression relationships. It is seen that for determination of  $K_{oc}$ , regression coefficient equals to 0.41 is most frequently used. G-CIEMS uses regression equation different from other models. Hence, final value of  $K_{oc}$  is most substantially affected by the difference in  $K_{ow}$  values. Temperature dependencies of organic carbon/water partition coefficient of PCB-153 used in the calculations by the participating models and in “reference data set” are compared in Fig.5.

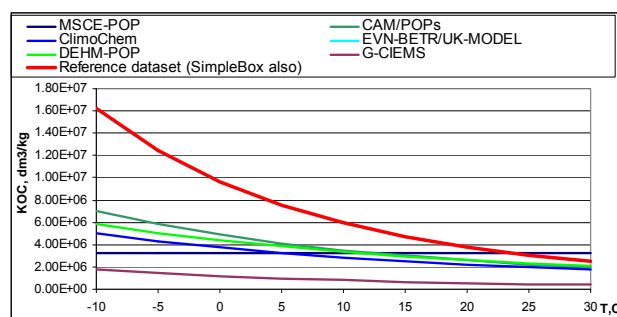


**Fig. 5.** Comparison of temperature dependencies of organic carbon/water partition coefficient of PCB-153 used in the participating POP models and in “reference data set”

Values of  $K_{oc}$  used in “reference data set” and also in EVN-BETR/UK-MODEL and SimpleBox models are the highest among all models practically within the whole considered temperature interval. For CAM/POPs, CliMoChem, and DEHM-POP (including MSCE-POP temperature independent value of  $K_{oc}$ ) its values differ from each other not substantially. Values of this parameter used in G-CIEMS are lower than those used in other models. Table 14 presents the range of absolute values of organic

carbon/water partition coefficient of PCB-153 recalculated from  $K_{ow}$  values taken at three arbitrary temperatures (-10°C, 10°C and 25°C).

The difference between the highest and the lowest values of  $K_{oc}$  used by all participating models is less than an order of magnitude (max/min ratio comes down from 9 to 7 for the considered temperatures). Although, in the case of  $K_{ow}$  at these temperatures the max/min ratio decreases from 5 to 2. For models using one and the same approach to determination of  $K_{oc}$  (all models except for G-CIEMS), its values differ within factors of 2-5.

**Table 14.** Absolute values and statistical parameters of organic carbon/water partition coefficient of PCB-153 for three arbitrary temperatures (-10°C, 10°C and 25°C).

|                    | $K_{oc}$ , dm <sup>3</sup> /kg |          |          |
|--------------------|--------------------------------|----------|----------|
|                    | -10°C                          | 10°C     | 25°C     |
| CAM/POPs           | 7.06E+06                       | 3.50E+06 | 2.23E+06 |
| SimpleBox          | 1.62E+07                       | 5.95E+06 | 3.06E+06 |
| G-CIEMS            | 1.80E+06                       | 7.96E+05 | 4.65E+05 |
| EVN-BETR/UK-MODEL  | 1.62E+07                       | 5.95E+06 | 3.06E+06 |
| CliMoChem          | 5.03E+06                       | 2.86E+06 | 1.97E+06 |
| DEHM-POP           | 5.89E+06                       | 3.35E+06 | 2.31E+06 |
| MSCE-POP           | 3.26E+06                       | 3.26E+06 | 3.26E+06 |
| Reference data set | 1.62E+07                       | 5.95E+06 | 3.06E+06 |
| <i>min</i>         | 1.80E+06                       | 7.96E+05 | 4.65E+05 |
| <i>max</i>         | 1.62E+07                       | 5.95E+06 | 3.26E+06 |
| <i>arith. mean</i> | 8.96E+06                       | 3.95E+06 | 2.42E+06 |
| <i>mediana</i>     | 6.47E+06                       | 3.42E+06 | 2.68E+06 |
| <i>geom. mean</i>  | 6.91E+06                       | 3.41E+06 | 2.14E+06 |
| <i>max/min</i>     | 5.0/9.0 *                      | 2.1/7.5* | 1.7/7.0* |

\* - the first value is calculated without the values of  $K_{oc}$  used in G-CIEMS, the second value is calculated taking it into account.

Comparison of organic carbon/water partition coefficient temperature dependencies of PCB-28 and PCB-180 used in the participating models and “reference data sets” are presented in Fig. B.9 and B.10 in Annex B. Statistical evaluation of absolute values and coefficients of temperature dependencies is given in Table B.15 and B.16.

Difference between the highest and the lowest values of organic carbon/water partition coefficient is less than an order of magnitude. For the considered temperature interval, max/min ratios for PCB-28 and PCB-180 come down from 4 to 2.

### 3.6. Water solubility

Solubility in water ( $S_w$ , mol/m<sup>3</sup>) is an important characteristic of a pollutant defining its behaviour in the atmosphere, precipitation, soils and water. The data on water solubility of PCB-153 used by EVN-BETR/UK-MODEL, G-CIEMS and SimpleBox models which contain this parameter temperature independent are presented in Table 15. With the help of subcooled liquid-vapour pressure, this parameter can be used for estimation of Henry’s law constant if the latter is not available as input data. CAM/POPs, CliMoChem, DEHM-POP, and MSCE-POP do not include this parameter as input data in the calculations. Values of water solubility of PCB-153 used in the participating models and in “reference data set” are of the same order.

**Table 15.** Water solubility of PCB-153 (data sets of the participating POP models)

| Model                 | Description              | Numerical values                 |          | Comments   | Reference       |
|-----------------------|--------------------------|----------------------------------|----------|--|-----------------|
| G-CIEMS               | Temperature independent. | $S_{WL}(T)$ , mol/m <sup>3</sup> | 1.80E-05 | Same to the "reference data set" $T = 10^\circ\text{C}$<br>When Henry's law constants is not given as input, water solubility is used to estimate Henry's law constant | Li et al., 2003 |
| SimpleBox             | Temperature independent  | $S_{WL}(T)$ , mol/m <sup>3</sup> | 1.80E-05 | Same to the "reference data set"<br>$T = 10^\circ\text{C}$   | Li et al., 2003 |
| EVN-BETR/<br>UK-MODEL | Temperature independent  | $S_{WL}(T)$ , mol/m <sup>3</sup> | 3.07E-05 | $T = 25^\circ\text{C}$   | Li et al., 2003 |

The data on water solubility of PCB-28 and PCB-180 used in EVN-BETR/UK-MODEL and SimpleBox models which contain this parameter temperature independent are given in Table B.17 in Annex B. Values of  $S_{WL}$  used in EVN-BETR/UK-MODEL exceed those of SimpleBox about 2 times.

### 3.7. Degradation rate constants of PCBs in the environmental media

The multi-compartment models contain a different number of the environmental media included in their descriptions (See Chapter 2). The degradation process of POP in each medium is characterised by the values of its half-life ( $t_{1/2}$ ) or degradation rate constant ( $k_d$ ) which are connected with each other. Models CAM/POPs, G-CIEMS, EVN-BETR and UK-MODEL, CliMoChem and MSCE-POP use information on separate degradation rate constants (or half-lives) for the three environmental compartments (air, soil, and water). Degradation process in vegetation is considered by EVN-BETR, G-CIEMS and CliMoChem models. In EVN-BETR and UK-MODEL, degradation processes in sediment is also taken into account.

The degradation process in the atmosphere is mainly considered as the gas-phase reaction of a pollutant with hydroxyl radicals and all other reactions are neglected. The temperature-dependent second order rate constants of this reaction are used by CAM/POPs, CliMoChem and MSCE-POP models. Values of the pre-exponential multiplier and coefficients of temperature dependence for PCB-153 rate constant in the atmosphere are displayed in Table 16. No temperature dependence of degradation rate constants in air is used by EVN-BETR and UK-MODEL, SimpleBox and G-CIEMS.

In all models except for CliMoChem degradation processes in other media than air are temperature independent. Degradation of POPs in soil, water, sediment and vegetation are described as a first-order process. These data are also presented in Table 16.

**Table 16.** Degradation rate constants (or half-lives) of PCB-153 in the environmental media (data sets of the participating POP models)\*

| Model     | Description  | Numerical values                               |          | Comments   | Reference          |
|-----------|--|--|----------|--|--------------------|
| CAM/ POPs | Degradation in atmosphere:<br>Temperature dependent:<br>$k_{air} = k_{air}^0 \exp(-a_{kair}(1/T - 1/T_0))$<br>where $T$ - temperature (K), $k_{air}^0$ is the value at the reference temperature $T_0$ , and $a_{kair}$ is a parameter of temperature dependence | $k_{air}^0(T_0)$ , cm <sup>3</sup> / (molec·s) | 2.11E-13 | Coefficients of the exponential equation are recalculated from the following temperature dependence:<br>$K_{OH} = K_{OH}^0 \exp(a(1/T_0 - 1/T))$<br>where $K_{OH}^0 = 2.7\text{E-}13$ is the value at the reference temperature $T_0$ (298 K),<br>$a = 1400$ is parameter of temperature dependence.   | This study         |
|           |  | $a_{kair}$                                     | 1400     |  |                    |
|           |  | $T_0$ , K                                      | 283.15   |  |                    |
| CliMoChem | Degradation in atmosphere:<br>Temperature dependent:<br>$k_{air} = k_{air}^0 \exp(-a_{kair}(1/T - 1/T_0))$<br>where $T$ - temperature (K), $k_{air}^0$ is the value at the reference temperature $T_0$ , and $a_{kair}$ is a parameter of temperature dependence | $k_{air}^0(T_0)$ , cm <sup>3</sup> / (molec·s) | 1.18E-13 | $k_{air}(T) = k_{air}(T_{ref}) \exp((-E_{air}/R)(1/T - 1/T_0))$<br>$T$ = temperature (283.15 K),<br>$T_0$ = reference temperature (298.15 K)<br>$k_{air}(T_0)$ = degradation rate constant at $T_0$ (cm <sup>3</sup> /d),<br>PCB 153: 1.42E-8;<br>$E_{air}$ = activation energy (J/mol), PCB 153: 15400;<br>$R$ = universal gas constant (8.3145 J/mol K )<br>$k_{air}^0$ = degradation rate constant at 283.15 (cm <sup>3</sup> /d),<br>PCB 153: 1.02E-08<br>$a_{kair} = E_a/R$ | Beyer et al., 2002 |
|           |  | $a_{kair}$                                     | 1852.2   |  |                    |
|           |  | $T_0$ , K                                      | 283.15   |  |                    |

| Model  | Description   | Numerical values                                     |   | Comments  | Reference   |
|--|---|--|---|---|---|
|  | Degradation in soil:<br>Temperature dependent:<br>$k_{soil} = k_{soil}^0 \exp(-a_{ksoil}(1/T - 1/T_0))$<br>where $T$ - temperature (K),<br>$k_{soil}^0$ is the value at the<br>reference temperature $T_0$ , and<br>$a_{ksoil}$ is a parameter of<br>temperature dependence       | $k_{soil}^0(T_0)$ ,<br>1/s                           | 6.16E-10  | $k_{soil}(T) = k_{soil}(T_{ref}) \exp((-E_{asoil}/R)(1/T - 1/T_0))$<br>$T$ = temperature (283.15 K),<br>$T_0$ = reference temperature (298.15 K)<br>$k_{soil}(T_0)$ = degradation rate constant at $T_0$ (1/d),<br>PCB 153: 1.01E-4;<br>$E_{asoil}$ = activation energy (J/mol) PCB 153: 30000<br>$R$ = universal gas constant (8.3145 J/mol K )<br>$k_{soil}^0$ = degradation rate constant at 283.15 (1/d),<br>PCB 153: 5.32E-05<br>$a_{ksoil} = E_{asoil}/R$         |   |
|  |   | $a_{ksoil}$  | 3608.2  |   |   |
|  |   | $T_0$ , K  | 283.15  |   |   |
|  | Degradation in water:<br>Temperature dependent:<br>$k_{water} = k_{water}^0 \exp(-a_{kwater}(1/T - 1/T_0))$<br>where $T$ - temperature (K),<br>$k_{water}^0$ is the value at the<br>reference temperature $T_0$ ,<br>and $a_{kwater}$ is a parameter of<br>temperature dependence | $k_{water}^0(T_0)$ ,<br>1/s                          | 8.47E-10  | $k_{water}(T) = k_{water}(T_{ref}) \exp((-E_{awater}/R)(1/T - 1/T_0))$<br>$T$ = temperature (283.15 K),<br>$T_0$ = reference temperature (298.15 K)<br>$k_{water}(T_0)$ = degradation rate constant at $T_0$ (1/d),<br>PCB 153: 1.39E-4;<br>$E_{awater}$ =activation energy (J/mol), PCB 153: 30000<br>$R$ = universal gas constant (8.3145 J/mol K )<br>$k_{water}^0$ =degradation rate constant at 283.15 (1/d),<br>PCB 153: 7.32E-05;<br>$a_{kwater} = E_{awater}/R$ |   |
|  |   | $a_{kwater}$   | 3608.2  |   |   |
|  |   | $T_0$ , K  | 283.15  |   |   |
|  | Degradation in vegetation**:<br>Temperature dependent:<br>$k_{veg} = k_{veg}^0 \exp(-a_{kveg}(1/T - 1/T_0))$<br>where $T$ - temperature (K),<br>$k_{veg}^0$ is the value at the<br>reference temperature $T_0$ ,<br>and $a_{kveg}$ is a parameter of<br>temperature dependence    | $k_{veg}^0(T_0)$ ,<br>1/s                            | 1.14E-07  | $k_{veg}(T) = k_{veg}(T_{ref}) \exp((-E_{aveg}/R)(1/T - 1/T_0))$<br>$T$ = temperature (283.15 K),<br>$T_0$ = reference temperature (298.15 K)<br>$k_{veg}(T_0)$ = degradation rate constant at $T_0$ (1/d),<br>PCB 153: 1.37E-2;<br>$E_{aveg}$ = activation energy (J/mol), PCB 153: 15400<br>$R$ = universal gas constant (8.3145 J/mol K )<br>$k_{veg}(T_0)$ = degradation rate constant at $T_0$ (1/d),<br>PCB 153: 9.86E-03;<br>$a_{kveg} = E_{aveg}/R$             |   |
|  |   | $a_{kveg}$   | 1852.2  |   |   |
|  |   | $T_0$ , K  | 283.15  |   |   |
| MSCE-POP   | Degradation in atmosphere:<br>Temperature dependent:<br>$k_{air} = k_{air}^0 \exp(-a_{kair}(1/T - 1/T_0))$<br>where $T$ - temperature (K),<br>$k_{air}^0$ is the value at the<br>reference temperature $T_0$ ,<br>and $a_{kair}$ is a parameter of<br>temperature dependence      | $k_{air}^0(T_0)$ ,<br>cm <sup>3</sup> /<br>(molec·s) | 1.18E-13  | Coefficients of the exponential equation are<br>recalculated from the following temperature<br>dependence: $k_{air} = A \cdot \exp(-E_a/RT)$<br>with the help of the following formulas: $a_{kair}=E_a/R$ ,<br>$k_{air}^0 = A \cdot \exp(-E_a/RT_0)$ , where $A = 8.12 \text{ E-11}$ is the<br>pre-exponential multiplier value, cm <sup>3</sup> /(molec·s);<br>$E_a = 15380$ is the activation energy of interaction<br>with OH-radical in air, J/mol                  | <i>Beyer and<br/>Matthies,<br/>2001</i>           |
|  |   | $a_{kair}$   | 1849.8  |   |   |
|  |   | $T_0$ , K  | 283.15  |   |   |
|  | Degradation in soil:<br>Temperature independent   | $k_{soil}$ , 1/s                                     | 1.17E-09  | Degradation rate constant in soil is converted<br>from half-life values (PCB-153: 165000 hours):<br>$k_d = 0.693/t_{1/2}$ , where $k_d$ is the first-order rate<br>constant (s <sup>-1</sup> ) and $t_{1/2}$ is the half-life (s).  | <i>Sinkkonen<br/>and<br/>Paasivirta,<br/>2000</i> |
| Degradation in water:<br>Temperature independent | $k_{water}$ ,<br>1/s  | 1.6E-09  | Degradation rate constant in water is converted<br>from half-life values (PCB-153: 120000 hours):<br>$k_d = 0.693/t_{1/2}$ , where $k_d$ is the first-order rate<br>constant (s <sup>-1</sup> ) and $t_{1/2}$ is the half-life (s). |   |   |
| SimpleBox  | Degradation in atmosphere:<br>Temperature independent   | $k_{air}$ , 1/s                                      | 3.50E-08  | Same half-lives as in "reference data set" :<br>PCB-153: 5500 hours   | <i>Mackay<br/>et al.,<br/>1992</i>                |
|  | Degradation in soil:<br>Temperature independent   | $k_{soil}$ , 1/s                                     | 3.50E-09  | Same half-lives as in "reference data set" :<br>PCB-153: 55000 hours  |   |
|  | Degradation in water:<br>Temperature independent  | $k_{water}$ , 1/s                                    | 3.50E-09  | Same half-lives as in "reference data set" :<br>PCB-153: 55000 hours  |   |
| G-CIEMS  | Degradation in atmosphere:<br>Temperature independent   | $k_{air}$ , 1/s                                      | 3.50E-08  | Same half-lives as in "reference data set" :<br>PCB-153: 5500 hours   | <i>Mackay<br/>et al.,<br/>1992</i>                |
|  | Degradation in soil:<br>Temperature independent   | $k_{soil}$ , 1/s                                     | 3.50E-09  | Same half-lives as in "reference data set" :<br>PCB-153: 55000 hours  |   |
|  | Degradation in water:<br>Temperature independent  | $k_{water}$ , 1/s                                    | 3.50E-09  | Same half-lives as in "reference data set" :<br>PCB-153: 55000 hours  |   |
| EVN-BETR and UK-<br>MODEL                        | Degradation in atmosphere:<br>Temperature independent   | $k_{air}$ , 1/s                                      | 3.50E-08  | Same half-lives as in "reference data set" :<br>PCB-153: 5500 hours   | <i>Mackay<br/>et al.,<br/>1992</i>                |
|  | Degradation in soil:<br>Temperature independent   | $k_{soil}$ , 1/s                                     | 3.50E-09  | Same half-lives as in "reference data set" :<br>PCB-153: 55000 hours  |   |
|  | Degradation in water:<br>Temperature independent  | $k_{water}$ , 1/s                                    | 3.50E-09  | Same half-lives as in "reference data set" :<br>PCB-153: 55000 hours  |   |
|  | Degradation in sediment:<br>Temperature independent   | $k_{sed}$ , 1/s                                      | 3.50E-09  | Same half-lives as in "reference data set" :<br>PCB-153: 55000 hours  |   |
|  | Degradation in vegetation:<br>Temperature independent   | $k_{veg}$ , 1/s                                      | 1.13E-08  | PCB-153 half-life in vegetation: 17000 hours  |   |

\* - for the sake of comparability, the base values and coefficients of temperature dependences of the considered parameters are given here for the temperature 283.15 K ( $T_0$ ) and the way they were recalculated from original dependencies is specified in the field "Comments".

\*\* - because of insufficient data on degradation rate constants in vegetation, the values are taken from atmospheric degradation [Möller, 2002] and multiplied with an average OH-radical concentration of 970000 1/cm<sup>3</sup> [Beyer et al., 2002].

The second-order rate constants of PCB-153 degradation process in the air in the form of temperature dependencies are compared in Fig. 6.

Following the data reported, CliMoChem and MSCE-POP models use one and the same values of temperature dependent rate constants of PCB-153 degradation in the atmosphere. CAM/POPs provides the highest values.

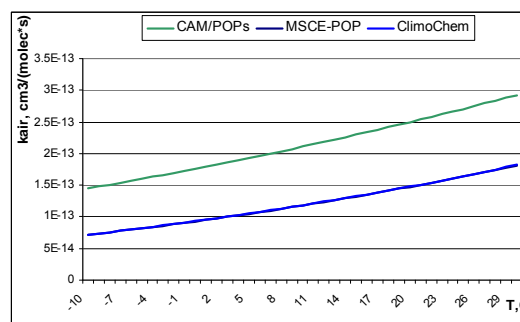


**Fig. 6.** Comparison of temperature dependencies of degradation rate constant of PCB-153 in the atmosphere

The comparison of temperature dependencies of second-order rate constants of PCB-28 and PCB-180 used in the participating models are presented in Fig. B.11 and B.12 in Annex B.

CliMoChem and MSCE-POP models also use one and the same values of degradation rate constants in the atmosphere for PCB-28 and PCB-180.

In the “reference data set” the rate constants of degradation processes in all environmental media are assumed temperature independent. For these purpose data on suggested half-life groups were taken from [Mackay *et al.* 1992] and converted into the first-order degradation rate constants. In order to have possibility to compare values of degradation rate constant of PCB-153 used in all participating models and in the “reference data set”, the rate constants of the second order degradation process in air were yearly averaged for the models which keep this parameter temperature dependent. This calculation was made with the use of monthly averaged temperatures calculated on the basis of meteorological data for 1997, 1998 and 1999 in Europe. Then multiplying the second order rate constants by mean annual OH-radical concentration in the surface layer of 2 km depth at the latitude of 45°N ( $0.8 \cdot 10^6$  molec/cm<sup>3</sup>) [Yu Lu and Khall, 1991], the first order degradation rate constants were calculated for CAM/POPs, CliMoChem, and MSCE-POP models. The results on PCB-153 are presented in Table 17 (for results on PCB-28 and PCB-180 see Tables B.19 and B.21 in Annex B). However, the usage of the mean annual OH-radical concentration for all the models which in reality include this parameter in different ways is rather rough assumption. For an example, in CliMoChem it varies depending on the temperature and in MSCE-POP - depending on the season.

**Table 17.** Monthly averaged temperatures calculated on the basis of meteorological data for 1997, 1998 and 1999 in Europe and the yearly average degradation rate constants of PCB-153 for the models which use temperature dependence of these parameters

| Month   | Temperatures, °C |          |         | CAM/POPs<br>air,<br>cm <sup>3</sup> ·molec <sup>-1</sup> ·s <sup>-1</sup> | MSCE-POP<br>air,<br>cm <sup>3</sup> ·molec <sup>-1</sup> ·s <sup>-1</sup> | CliMoChem   |   |   |   |
|---|------------------|----------|---------|---|---|---|---|---|---|
|   | Over land        | Over sea | Average |   |   | air,<br>cm <sup>3</sup> ·molec <sup>-1</sup> ·s <sup>-1</sup> | soil, s <sup>-1</sup><br>(for Over land temp) | sea, s <sup>-1</sup><br>(for Over sea temp) | veg., s <sup>-1</sup><br>(for aver. temp) |
| Jan   | 4                | 4        | 4       | 1.90E-13  | 1.02E-13  | 1.03E-13  | 4.67E-10                                      | 6.43E-10                                    | 9.89E-08                                  |
| Feb   | 4                | 3        | 4       | 1.90E-13  | 1.02E-13  | 1.03E-13  | 4.67E-10                                      | 6.13E-10                                    | 9.89E-08                                  |
| Mar   | 7                | 5        | 6       | 1.97E-13  | 1.07E-13  | 1.08E-13  | 5.37E-10                                      | 6.74E-10                                    | 1.04E-07                                  |
| Apr   | 11               | 6        | 9       | 2.07E-13  | 1.15E-13  | 1.16E-13  | 6.44E-10                                      | 7.06E-10                                    | 1.11E-07                                  |
| May   | 17               | 10       | 13      | 2.22E-13  | 1.26E-13  | 1.27E-13  | 8.37E-10                                      | 8.47E-10                                    | 1.22E-07                                  |
| Jun   | 21               | 14       | 17      | 2.38E-13  | 1.38E-13  | 1.38E-13  | 9.92E-10                                      | 1.01E-09                                    | 1.33E-07                                  |
| Jul   | 22               | 16       | 19      | 2.46E-13  | 1.44E-13  | 1.45E-13  | 1.03E-09                                      | 1.10E-09                                    | 1.39E-07                                  |
| Aug   | 22               | 16       | 19      | 2.46E-13  | 1.44E-13  | 1.45E-13  | 1.03E-09                                      | 1.10E-09                                    | 1.39E-07                                  |
| Sep   | 18               | 13       | 15      | 2.30E-13  | 1.32E-13  | 1.32E-13  | 8.74E-10                                      | 9.68E-10                                    | 1.28E-07                                  |
| Oct   | 14               | 10       | 12      | 2.18E-13  | 1.24E-13  | 1.24E-13  | 7.35E-10                                      | 8.47E-10                                    | 1.19E-07                                  |
| Nov   | 10               | 7        | 9       | 2.07E-13  | 1.15E-13  | 1.16E-13  | 6.16E-10                                      | 7.39E-10                                    | 1.11E-07                                  |
| Dec   | 6                | 5        | 6       | 1.97E-13  | 1.07E-13  | 1.08E-13  | 5.13E-10                                      | 6.74E-10                                    | 1.04E-07                                  |
| Averaged second-order rate constants, cm <sup>3</sup> ·molec <sup>-1</sup> ·s <sup>-1</sup> |                  |          |         | 2.16E-13  | 1.22E-13  | 1.22E-13  | -   | -   | -   |
| Averaged first-order rate constants, s <sup>-1</sup>  |                  |          |         | 1.72E-07  | 9.73E-08  | 9.78E-08  | 7.29E-10                                      | 8.27E-10                                    | 1.18E-07                                  |

The rate constants of the first order degradation process in soil, sea and vegetation used in CliMoChem model which keeps these parameters temperature dependent were yearly averaged. This calculation was also made with the use of monthly averaged temperatures calculated on the basis of meteorological data for 1997, 1998 and 1999 in Europe.

To illustrate the dispersion of absolute values of the first-order degradation rate constants of PCB-153 in the atmosphere and in other media used in the participating models and in the “reference data set”, statistical treatment of these parameters is made and some statistics are given in Table 18.

**Table 18.** Absolute values and statistical parameters of degradation rate constants of first order (PCB-153)

|                    | $k_{air} \text{ s}^{-1}$ | $k_{soil} \text{ s}^{-1}$ | $k_{water} \text{ s}^{-1}$ | $k_{sediment} \text{ s}^{-1}$ | $k_{veg} \text{ s}^{-1}$ |
|--------------------|--------------------------|---------------------------|----------------------------|-------------------------------|--------------------------|
| CAM/POPs           | 1.72E-07                 | -                         | -                          | -                             | -                        |
| CliMoChem          | 9.78E-08                 | 7.29E-10                  | 8.27E-10                   | -                             | 1.18E-07                 |
| MSCE-POP           | 9.73E-08                 | 1.17E-09                  | 1.60E-09                   | -                             | -                        |
| SimpleBox          | 3.50E-08                 | 3.50E-09                  | 3.50E-09                   | -                             | -                        |
| G-CIEMS            | 3.50E-08                 | 3.50E-09                  | 3.50E-09                   | -                             | -                        |
| EVN-BETR/UK-MODEL  | 3.50E-08                 | 3.50E-09                  | 3.50E-09                   | 3.50E-09                      | 1.13E-08                 |
| Reference data set | 3.50E-08                 | 3.50E-09                  | 3.50E-09                   | 3.50E-09                      | -                        |
| <i>min</i>         | 3.50E-08                 | 7.29E-10                  | 8.27E-10                   | -                             | -                        |
| <i>max</i>         | 1.72E-07                 | 3.50E-09                  | 3.50E-09                   | -                             | -                        |
| <i>arith. mean</i> | 7.25E-08                 | 2.65E-09                  | 2.74E-09                   | -                             | -                        |
| <i>median</i>      | 3.50E-08                 | 3.50E-09                  | 3.50E-09                   | -                             | -                        |
| <i>geom.mean</i>   | 5.89E-08                 | 2.24E-09                  | 2.42E-09                   | -                             | -                        |
| <i>max/min</i>     | 4.9                      | 4.8                       | 4.2                        | 1.0                           | 10.4                     |

There is a large difference in absolute values of degradation rate constant of PCB-153 (s<sup>-1</sup>) between the models which are using and not using its temperature dependencies of degradation rate constants. It is exemplified by the differences in highest and lowest values of these parameters for degradation processes in air, soil, and water, sediments and vegetation. Max/min ratios for degradation processes in air, soil, and water vary within factor of 4-5. The difference between temperature dependent values of degradation rate constant of PCB-153 in air is within a factor of 2. EVN-BETR and UK-MODEL, SimpleBox, G-CIEMS and the “reference data set” contain one and the same values of temperature independent rate constants taken from [Mackay *et al.* 1992]. The difference of degradation rate constant in vegetation between EVN-BETR and UK-MODEL and CliMoChem models (max/min ratio) is around 10. Degradation in sediments is considered in EVN-BETR and UK-MODEL only.

Statistical evaluation of absolute values of the first-order degradation rate constants of PCB-28 and PCB-180 in the atmosphere and in other media used in the participating models and in the “reference data set” are presented in Table B.20 and B.22 in Annex B.

Among all media the largest difference in the values of first-order rate constants between the models for PCB-28 is observed for the degradation in water and for PCB-180 - for the degradation in soil. Max/min ratios of degradation rate constant values in air, soil and water for PCB-28 vary from 2 to 12; and for PCB-180 – from 3 to 10. Max/min ratio of rate constants for degradation in vegetation between CliMoChem and EVN-BETR and UK-MODEL for PCB-28 equals to 7 and for PCB-180 it is around 6. Degradation in sediments is considered in EVN-BETR and UK-MODEL only.

Difference in temperature dependent values of degradation rate constant in air between CAM/POPs, CliMoChem and MSCE-POP models for PCB-180 is within factor 2. In CliMoChem and MSCE-POP models these values for PCB-28 are equal.

## COMPARISON OF PROCESS PARAMETERIZATIONS AND RESULTS OF COMPUTATIONAL EXPERIMENTS FOR PCB-153

This Chapter is devoted to the analysis of model approaches to the description of main processes determining PCBs behaviour in the environment. These are gas/particle partitioning, dry deposition of particulate phase, wet deposition, gaseous exchange between the atmosphere and different types of underlying surface (soil, water, vegetation) and degradation processes. The comparison of the results of calculation experiments obtained by different models is presented here together with brief description of model approaches to the parameterization of the considered processes used in the participating models. More detailed description of these approaches is presented in Annex C. An overview of descriptions of degradation processes used for PCB modelling is given above in Chapter 3. The presentation in this Chapter concerns mainly PCB-153 (substance of the first priority), appropriate data on other considered pollutants (PCB-28 and PCB-180) are presented in Annexes D and E. The exposition in subsequent Sections devoted to each of the above processes (except for degradation) has one and the same structure which goes as follows.

First, we present short summary of the descriptions of the considered process submitted by participants (at present descriptions of considered processes is available for seven models: EVN-BETR and UK-MODEL, CliMoChem, G-CIEMS, DEHM-POP, SimpleBox, CAM/POPs and MSCE-POP).

Second, the description of input data used for calculation experiments with PCB – 153 on each basic process is presented. The input data for modelling include several sets of given air concentrations in different phases (if needed) and environmental conditions (averaged ambient temperatures, organic content in the atmospheric aerosol, TSP, precipitation intensity, mean wind velocity, etc.) relevant for each experiment.

Third, the intercomparison of results of computation experiment carried out by the participating models is presented. This analysis consists of two parts. The first part concerns the comparison of obtained absolute values and some statistical parameters for each experiment included in this process. The second is devoted to the pairwise comparison of the model output. The set of statistical parameters used for the comparison is different for different processes.

### 4.1. Gas/particle partitioning

#### 4.1.1. Model approaches

Basically, there exist two approaches to model evaluation of the fraction of particulate phase of a pollutant in the atmosphere. The first is based on the Junge-Pankow adsorption model [Junge, 1977; Pankow, 1987]. In this case POP fraction  $\varphi$  adsorbed on the atmospheric aerosol particles is calculated using vapor pressure of the subcooled liquid  $p_{oi}$ :

$$\varphi = \frac{c \cdot \theta}{p_{ol} + c \cdot \theta} \quad (3)$$

where  $c$  is the constant depending on thermodynamic parameters of adsorption process and on properties of aerosol particle surface;

$\theta$  is the specific surface of aerosol particles,  $m^2/m^3$ .

This approach is used in SimpleBox, CAM/POPs and MSCE-POP models. In all these models the temperature dependence of  $p_{ol}$  is taken into account. Besides, CAM/POPs model additionally uses 12-bin structure of sulphate aerosol for calculations of gas/aerosol partitioning.

The second is based on absorption model of gas/aerosol partitioning [*Finizio et al.*, 1997; *Falconer and Harner*, 2000]. Under this approach the fraction of POPs absorbed by organic matter of aerosol particles is calculated with the use of particle/gas partitioning coefficient  $K_{PA}$  defined via octanol/air partitioning coefficient  $K_{oa}$ :

$$\varphi = \frac{K_{PA} \cdot TSP}{(K_{PA} \cdot TSP + 1)} \quad (4)$$

Here  $\varphi$  is the fraction of compound sorbed to particles,  $K_{PA}$  is the gas-particle partitioning coefficient, and TSP is the total suspended particle concentration.  $K_{PA}$  is calculated using different regression relations via  $K_{oa}$ , in particular [*Falconer and Harner*, 2000]:

$$\log K_{PA} = m_r \log K_{oa} + \log f_{om} - 11.91, \quad (5)$$

where  $m_r$  - constant expected to have a value close to +1 for equilibrium partitioning;

$K_{oa}$  - octanol-air partition coefficient;

$f_{om}$  - fraction of organic matter in the particles.

This approach is used in DEHM-POP and experimental version of MSCE-POP.

To calculate gas-particle partitioning coefficient CliMoChem used another equation taken from [*Finizio et al.* 1997]:

$$K_{PA} = K_{oa}^{0.55} \cdot 10^{-8.23} \quad (6)$$

EVN-BETR and UK-MODEL and G-CIEMS calculated this coefficient with the help of equations (7) and (8), respectively:

$$K_{PA} = 3.5 \cdot K_{oa} \quad (7)$$

$$K_{PA} = y \cdot K_{oa} / (\tilde{\rho} \cdot 1000), \quad (8)$$

where  $y$  is the organic matter mass fraction, and  $\tilde{\rho}$  is the density of aerosol particles.

Below the results of calculations of  $\varphi$  for different environmental conditions carried out by the above seven models are analyzed.

#### 4.1.2. Input data

Nine sets of input data (different ambient temperatures in the range from  $-12^\circ\text{C}$  to  $32^\circ\text{C}$ ) are proposed for modelling experiments with PCB-153.

**Table 19.** Input data for computation experiments with PCB-153 describing gas/particle partitioning

| N   | Experiment 1 | Experiment 2 | Experiment 3 | Experiment 4 | Experiment 5 | Experiment 6 | Experiment 7 | Experiment 8 | Experiment 9 |
|---|--------------|--------------|--------------|--------------|--------------|--------------|--------------|--------------|--------------|
| Averaged ambient temperature, C                       | -12          | -5           | 0            | 6            | 10           | 15           | 20           | 26           | 32           |
| Total Suspended Matter, TSP, $\mu\text{g}/\text{m}^3$ | 30           | 30           | 30           | 30           | 30           | 30           | 30           | 49           | 66           |
| Organic content in the aerosol, %                     | 20           | 20           | 20           | 20           | 20           | 20           | 20           | 20           | 20           |

**Output** of computation experiments describing gas/particle partitioning process is PCB particulate fraction in the atmosphere.

### 4.1.3. Comparison of the results

This section contains the analysis of the results of experiments on the calculations of particulate fraction  $\varphi$  of the considered pollutants obtained by the participating models. Here we present numerical results for the first priority substance (PCB-153) only. The corresponding results for substances of the second priority (PCB-28 and PCB-180) can be found in Annexes D and E.

The analysis is performed into two stages. At the first stage we present an analysis of the values of calculated fractions of particulate phase and characterize the spread in these values between models in each of the experiments. At the second stage we analyze pairwise differences between participating models using the regression analysis.

**Analysis of the experiments.** Here we use the following statistical parameters for each experiment:

- the value  $m_\varphi$  of fractions of particulate phase averaged between participating models;
- the value of square deviation  $\sigma_\varphi$  between results obtained by different models;

First of the above parameters illustrates the level of particulate phase fraction calculated by all considered models. The second parameter characterizes the dispersion of this fraction between the models.

Calculation results for PCB-153 together with  $m_\varphi$  and  $\sigma_\varphi$  are presented in Table 20. In Table 21 short comments to the calculations made by participants can be found. For two models (G-CIEMS and MSCE-POP) two versions of calculations are presented. Namely, for G-CIEMS calculations of gas-particle partitioning using molecular weight only (G-CEIMS 1) and using absorption scheme (G-CIEMS 2) were carried out. For MSCE-POP model calculations based on the adsorption (based on  $p_{oi}$  values; MSCE-POP 1) and absorption (based on  $K_{oa}$  values; MSCE-POP 2) schemes are presented. The comparison of calculated fractions of the particulate phase is illustrated also by the plot below.

**Table 20.** Calculation results: fractions of particulate phase of PCB-153 calculated by models and statistical parameters used for evaluation

| Exp. No | T (°C) | EVN-BETR and UK-MODEL | DEHM-POP | G-CIEMS |       | CAM/POPs | MSCE-POP |       | CliMoChem | SimpleBox* | $m_\varphi$ | $\sigma_\varphi$ |
|---------|--------|-----------------------|----------|---------|-------|----------|----------|-------|-----------|------------|-------------|------------------|
|         |        |                       |          | 1       | 2     |          | 1        | 2     |           |            |             |                  |
| 1       | -12    | 0.93                  | 0.83     | 0.96    | 0.78  | 0.94     | 0.874    | 0.869 | 0.163     | 0.978      | 0.81        | 0.25             |
| 2       | -5     | 0.75                  | 0.62     | 0.89    | 0.53  | 0.85     | 0.698    | 0.693 | 0.098     | 0.939      | 0.67        | 0.25             |
| 3       | 0      | 0.68                  | 0.44     | 0.79    | 0.35  | 0.73     | 0.522    | 0.519 | 0.068     | 0.882      | 0.55        | 0.25             |
| 4       | 6      | 0.46                  | 0.26     | 0.61    | 0.18  | 0.53     | 0.315    | 0.315 | 0.044     | 0.765      | 0.39        | 0.23             |
| 5       | 10     | 0.33                  | 0.17     | 0.48    | 0.11  | 0.39     | 0.208    | 0.21  | 0.033     | 0.656      | 0.29        | 0.20             |
| 6       | 15     | 0.19                  | 0.095    | 0.32    | 0.058 | 0.24     | 0.118    | 0.121 | 0.023     | 0.500      | 0.19        | 0.15             |
| 7       | 20     | 0.11                  | 0.053    | 0.21    | 0.031 | 0.14     | 0.065    | 0.068 | 0.017     | 0.349      | 0.12        | 0.11             |
| 8       | 26     | 0.086                 | 0.042    | 0.12    | 0.014 | 0.12     | 0.032    | 0.053 | 0.018     | -          | 0.06        | 0.04             |
| 9       | 32     | 0.057                 | 0.029    | 0.063   | 0.007 | 0.078    | 0.016    | 0.036 | 0.017     | -          | 0.04        | 0.03             |

\* - only 7 experiments for Simple Box

**Table 21. Comments**

| Model assumptions   | Models                | Physical-chemical data set | Other Comments   |
|---------------------|-----------------------|----------------------------|--|
| Adsorption approach | CAM/POPs              | Own                        | equation (3);<br>$c$ is 0.172 Pa·m [Pankow, 1987; Falconer et al., 1994; Bidleman et al., 1998]<br>Additional input data of 12 size-bin structure is applied on the TSP in the experiment  |
|                     | SimpleBox             | "Reference"                | equation (3);<br>JungeConst = 0.172 Pa·m by default;<br>$P_L$ = liquid-phase vapor pressure at ambient temperature<br>$T$ (Pa) = $P_L(25C) \cdot \exp((H_{vap}^0/8.314) \cdot (1/298 - 1/T))$<br>$H_{vap}^0$ = Enthalpy of vaporization (J/mol) = $\Delta U_{aw}$ in "reference data set";<br>SimpleBox takes specific aerosol surface as input; calculations done only for 'standard' aerosol characteristics (TSP 30 mg/m <sup>3</sup> ; $f_{oc}$ 20%), with aerosol surface set to $1.5 \cdot 10^{-4}$ m <sup>2</sup> /m <sup>3</sup> |
|                     | MSCE-POP 1            | Own                        | current version – equation (3);<br>Assumed that $c = 0.172$ Pa·m [Junge, 1977] for background aerosol and $\theta = 1.5 \cdot 10^{-4}$ m <sup>2</sup> /m <sup>3</sup> [Whitby, 1978].  |
| Absorption approach | EVN-BETR and UK-MODEL | Own                        | equation (7);<br>own dataset of EVN-BETR and UK-MODEL is extremely close to the "reference dataset"; $K_{oa}$ was calculated from $K_{ow}/K_{aw}$  |
|                     | CliMoChem             | Own                        | equations (4) and (6); $K_{oa}$ was calculated from $K_{ow}/K_{aw}$  |
|                     | DEHM-POP              | Own                        | equations (4) and (5)  |
|                     | G-CIEMS 2             | "Reference"                | equation (8)   |
|                     | MSCE-POP 2            | Own                        | experimental version – equations (4) and (5);  |
| Other               | G-CIEMS 1             | "Reference"                | Gas/particle partitioning is calculated from only molecular weight (for preliminary assessment purpose)  |

The plot of dependence of  $\varphi$  on  $T$  calculated by participating models is presented in Fig. 7.

It is seen that practically all models (except CliMoChem) closely describe temperature dependence of particulate fraction. For the lower temperatures, values of fraction of particulate phase of PCB-153 calculated by CliMoChem are much lower than ones calculated by other participating models. Considering results of the first seven of the experiments, the highest results of this parameter are obtained by SimpleBox model.

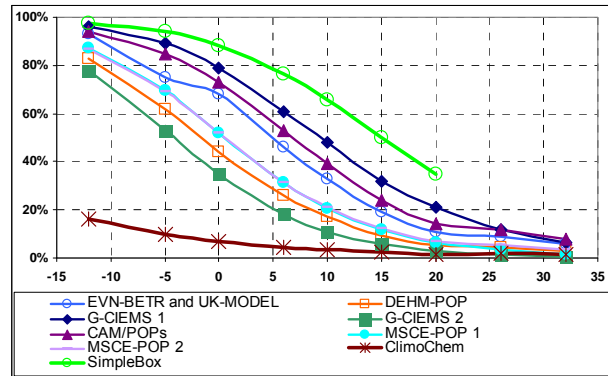


**Fig. 7. Calculation results of the participating models (gas-particle partitioning)**

We recall that the experiments differ mainly by ambient air temperature  $T$  (and some other parameters, see Section 4.1.2). For each temperature within the considered interval of temperatures (-12°C - 32°C), square deviation  $\sigma_\varphi$  between different model calculations (see last column in Table 20) do not exceed the averaged value of particulate phase fractions. It is testify that all models give close enough results in terms of absolute values.

**Pairwise comparison of model results.** Here the analysis of pairwise differences between calculation results obtained by different models by means of the regression analysis is presented. Namely, the relation between calculated fractions  $\varphi_T^1$  and  $\varphi_T^2$  obtained by each two models for different values of temperature  $T$  is supposed to be:

$$\varphi_T^2 = \alpha_{12} \varphi_T^1 + \beta_{12} + \omega_{12}, \quad (9)$$

where  $\alpha_{12}$  and  $\beta_{12}$  are regression coefficients;

$\omega_{12}$  is the random component of the regression relation ("white noise").

For evaluation of closeness of calculated results obtained by models, we shall use regression coefficients  $\alpha_{12}$  and  $\beta_{12}$  (characterizing a non-random component of the regression relation), the residual square deviation, that is, square deviation  $\sigma_{12}^{\text{res}}$  of  $\omega_{12}$  (characterizing the magnitude of random component) and the correlation coefficient  $r_{12}$ .

Table 22 contains the values of regression coefficients  $\alpha$  and  $\beta$  calculated for all pairs of models. The differences between the models are explained mainly by scaling coefficients  $\alpha$  ranging from 0.13 to 3.78. For the most part of the models (not including CliMoChem results),  $\alpha$  varies far less (from 0.71 to 1.15). Coefficients  $\beta$  are not very large for all pairs of models (lying in the range from  $-0.13$  to 0.48). This is a numerical expression of the fact that shapes of curves expressing temperature dependencies of  $\varphi$  (Fig. 7) are similar for these models.

**Table 22.** Coefficients of regression dependence between the models ( $\alpha / \beta$ )

|                       | DEHM-POP     | G-CIEMS 1   | G-CIEMS 2    | CAM/POPs     | MSCE-POP1    | MSCE-POP2    | CliMoChem    | SimpleBox*  |
|-----------------------|--------------|-------------|--------------|--------------|--------------|--------------|--------------|-------------|
| EVN-BETR and UK-MODEL | 0.87 / -0.07 | 1.03 / 0.08 | 0.81 / -0.09 | 1.02 / 0.04  | 0.96 / -0.07 | 0.94 / -0.05 | 0.14 / 0.00  | 0.75 / 0.36 |
| DEHM-POP              | –            | 1.11 / 0.18 | 0.94 / -0.04 | 1.11 / 0.13  | 1.09 / 0.01  | 1.06 / 0.02  | 0.17 / 0.01  | 0.73 / 0.47 |
| G-CIEMS 1             | –            | –           | 0.73 / -0.13 | 0.97 / -0.03 | 0.89 / -0.12 | 0.87 / -0.11 | 0.13 / -0.01 | 0.81 / 0.23 |
| G-CIEMS 2             | –            | –           | –            | 1.15 / 0.18  | 1.14 / 0.06  | 1.11 / 0.07  | 0.18 / 0.01  | 0.73 / 0.51 |
| CAM/POPs              | –            | –           | –            | –            | 0.93 / -0.10 | 0.91 / -0.08 | 0.14 / -0.01 | 0.75 / 0.31 |
| MSCE-POP 1            | –            | –           | –            | –            | –            | 0.98 / 0.01  | 0.15 / 0.01  | 0.71 / 0.44 |
| MSCE-POP 2            | –            | –           | –            | –            | –            | –            | 0.16 / 0.00  | 0.72 / 0.44 |
| CliMoChem             | –            | –           | –            | –            | –            | –            | –            | 3.78 / 0.48 |

\* - by 7 experiments only

This fact is once more confirmed by calculated correlation coefficients (Table 23) which is very high for all pairs of models (from 0.83 to 1.00).

**Table 23.** Correlation coefficients  $\sigma$

|                       | DEHM-POP | G-CIEMS 1 | G-CIEMS 2 | CAM/POPs | MSCE-POP 1 | MSCE-POP 2 | CliMoChem | SimpleBox* |
|-----------------------|----------|-----------|-----------|----------|------------|------------|-----------|------------|
| EVN-BETR and UK-MODEL | 0.98     | 0.99      | 0.96      | 1.00     | 0.99       | 0.99       | 0.93      | 0.97       |
| DEHM-POP              | –        | 0.94      | 1.00      | 0.97     | 1.00       | 1.00       | 0.98      | 0.91       |
| G-CIEMS 1             | –        | –         | 0.91      | 0.99     | 0.96       | 0.96       | 0.87      | 0.99       |
| G-CIEMS 2             | –        | –         | –         | 0.94     | 0.99       | 0.99       | 0.99      | 0.87       |
| CAM/POPs              | –        | –         | –         | –        | 0.98       | 0.98       | 0.91      | 0.98       |
| MSCE-POP 1            | –        | –         | –         | –        | –          | 1.00       | 0.97      | 0.93       |
| MSCE-POP 2            | –        | –         | –         | –        | –          | –          | 0.97      | 0.93       |
| CliMoChem             | –        | –         | –         | –        | –          | –          | –         | 0.83       |

\* - by 7 experiments only

Thus, all models describe temperature dependence of the fraction of particulate phase of PCB-153 in the atmosphere similarly. The difference of model results can be explained by difference in base values of  $K_{oa}$  or  $p_{oi}$  since the change of these values leads to scaling of calculated values of  $\varphi$ .

To assess the reliability of comparative analysis given above calculations of pairwise residual square deviation  $\sigma$  were done (Table 24).

**Table 24.** Residual square deviation,  $\sigma$

|                       | DEHM-POP | G-CIEMS 1 | G-CIEMS 2 | CAM/POPs | MSCE-POP 1 | MSCE-POP 2 | CliMoChem | SimpleBox* |
|-----------------------|----------|-----------|-----------|----------|------------|------------|-----------|------------|
| EVN-BETR and UK-MODEL | 0.167    | 0.157     | 0.214     | 0.075    | 0.124      | 0.130      | 0.050     | 0.146      |
| DEHM-POP              | –        | 0.321     | 0.063     | 0.237    | 0.069      | 0.056      | 0.027     | 0.245      |
| G-CIEMS 1             | –        | –         | 0.312     | 0.105    | 0.236      | 0.244      | 0.068     | 0.084      |
| G-CIEMS 2             | –        | –         | –         | 0.309    | 0.139      | 0.126      | 0.017     | 0.286      |
| CAM/POPs              | –        | –         | –         | –        | 0.161      | 0.167      | 0.058     | 0.112      |
| MSCE-POP 1            | –        | –         | –         | –        | –          | 0.018      | 0.036     | 0.216      |
| MSCE-POP 2            | –        | –         | –         | –        | –          | –          | 0.035     | 0.216      |
| CliMoChem             | –        | –         | –         | –        | –          | –          | –         | 0.320      |

\* - by 7 experiments only

It is seen that the values of  $\sigma$  range from 0.017 to 0.32. This testify the possibility of usage regression analysis for evaluation of the difference between model calculations. Maximum values of the random component are characteristic of the comparisons between G-CIEMS 1 and G-CIEMS 2, between G-CIEMS 1 and DEHM-POP, between EVN-BETR and UK-MODEL and G-CIEMS 2, between CAM/POPs and G-CIEMS 2, between G-CIEMS 1 and MSCE-POP and between SimpleBox and following models: DEHM-POP, G-CIEMS 2, MSCE-POP and CliMoChem.

The results obtained for PCB-180 are similar to the results on PCB-153. Values of fraction of particulate phase of PCB-180 calculated by CliMoChem are much lower than ones calculated by other participating models. We remark also that taking into account the real dispersion of TSP in the atmosphere can essentially affect the calculations (see plots of temperature dependence of  $\varphi$  for PCB-180 in Annex E). Correlation coefficients for all models vary from 0.75 to 1.00.

Results on PCB-28 (Annex D) to some extent differ from the results on above two congeners. The highest values of this parameter are obtained by SimpleBox model. Fractions of particulate phase calculated by EVN-BETR and UK model are also larger than those calculated by DEHM-POP, CliMoChem and MSCE-POP. The results obtained by other models are close to one another. Correlation coefficients for all models vary from 0.98 to 1.00.

## 4.2. Dry deposition of the particulate phase

### 4.2.1. Model approaches

Dry deposition velocity  $v_d$  is used in all models for the description of dry deposition flux of the particulate phase to different types of underlying surface:

$$F_{dep} = v_d \cdot C_{part}, \quad (10)$$

where  $F_{dep}$  is the deposition flux of POP particulate phase to a given type of underlying surface;

$C_{part}$  is the concentration of POP particulate phase in the atmosphere.

The differences between models in the description of this process lie in the method of calculation of deposition velocity. SimpleBox, EVN-BETR and UK-MODEL and G-CIEMS models use one and the same value of dry deposition velocity for all considered types of underlying surfaces. CliMoChem model takes into account the dependence of dry deposition velocity on underlying surface type and its seasonal variations. DEHM-POP, CAM/POPs and MSCE-POP models calculate dry deposition velocity to different types of underlying surface on the basis of current meteorological conditions (such as the friction velocity, the Monin-Obukhov length and the roughness parameter). Due to high scattering of dry deposition velocity values used by the participating models (see Table 25), large range of calculated values of dry deposition flux takes place.

**Table 25.** Dry deposition velocity, m/s

| Type of underlying surface | EVN-BETR and UK-MODEL | DEHM-POP |        |        | G-CIEMS | CAM/POPs | MSCE-POP |        |        | CliMoChem                         | SimpleBox |
|----------------------------|-----------------------|----------|--------|--------|---------|----------|----------|--------|--------|-----------------------------------|-----------|
|                            |                       | Min      | Max    | Aver   |         |          | Min      | Max    | Aver   |                                   |           |
| Grass                      | 0.003                 | 0.0003   | 0.0194 | 0.0100 | 0.0025  | 0.0042   | 0.0007   | 0.0023 | 0.0015 | 0.000647                          | 0.001     |
| Forest                     | 0.003                 | 0.0058   | 0.0172 | 0.0117 | 0.0025  | 0.0750   | 0.0005   | 0.0175 | 0.0090 | 0.0005 (conif)<br>0.00518 (decid) | 0.001     |
| Bare soil                  | 0.003                 | 0.0003   | 0.0250 | 0.0125 | 0.0025  | 0.0039   | 0.0007   | 0.0023 | 0.0015 | 0.003009                          | 0.001     |
| Seawater                   | 0.003                 | 0.0002   | 0.0128 | 0.0064 | 0.0025  | 0.0017   | 0.0001   | 0.0010 | 0.0006 | 0.003009                          | 0.001     |

Below we compare ranges of calculated values of dry deposition flux obtained by all participating models.

#### 4.2.2. Input data

The following four sets of input data are proposed for modelling experiments with PCB-153.

**Table 26.** Input data for computation experiments with PCB-153 describing dry deposition of particulate phase

| N   | Experiment 1 | Experiment 2 | Experiment 3 | Experiment 4 |
|---|--------------|--------------|--------------|--------------|
| Type of underlying surfaces                               | Grass        | Forest       | Bare soil    | Seawater     |
| Mean wind velocity, m/sec                                 | 4            | 4            | 4            | 4            |
| Air concentration of particulate phase, ng/m <sup>3</sup> | 1            | 1            | 1            | 1            |

**Output:** calculated PCB dry deposition fluxes to grass, forest, bare soil, and seawater, ng/m<sup>2</sup>/h.

#### 4.2.3. Comparison of the results

The results of calculation of particulate dry deposition flux for PCB-153 were presented by seven models: EVN-BETR and UK-MODEL, DEHM-POP, G-CIEMS, CliMoChem, SimpleBox, CAM/POPs and MSCE-POP. According to descriptions of dry deposition accepted in these models parameterizations of the flux are one and the same for all PCB congeners so that the results concern also congeners PCB-28 and PCB-180.

Three of the seven participated models (EVN-BETR and UK-MODEL, SimpleBox and G-CIEMS) do not distinguish different types of underlying surface in calculation of particulate dry deposition fluxes. For two models (DEHM-POP and MSCE-POP) range of calculated values depending on environmental parameters not included into the formulation of calculation experiment is presented.

The plot of calculation results for the particulate dry deposition flux to different type of underlying surface are presented in Fig. 8. Of note that mean deposition flux to forest (10.23 ng/m<sup>2</sup>/h) given in the plot for CliMoChem model was calculated for the sake of comparison as arithmetic mean of fluxes to coniferous and deciduous forest obtained by the model (presented in the plot as bars). The corresponding numerical values are given in Table 27.

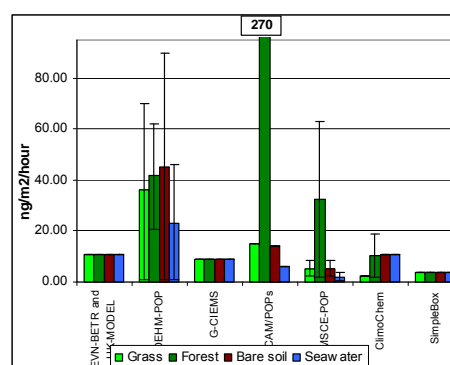


**Fig. 8.** Particulate dry deposition flux from the atmosphere to different types of underlying surface, ng/m<sup>2</sup>/h

Since there is large dispersion in the values of the deposition flux calculated by different models (See Table 27) we do not use statistical parameters for determining average levels of dry deposition flux but restrict ourselves by comparison of the values themselves. The additional reason for such an approach is that in two models from seven the range of calculated values of deposition flux are given and it is reasonable to include these ranges into consideration instead of comparison of mean values only. Short comments to the calculations made by participants can be found in Table 28.

**Table 27.** Particulate dry deposition flux from the atmosphere to different types of underlying surface, ng/m<sup>2</sup>/h

| Type of underlying surface | EVN-BETR and UK-MODEL | DEHM-POP |     |       | G-CIEMS | CAM/POPs | MSCE-POP |       |       | CliMoChem          | SimpleBox |
|----------------------------|-----------------------|----------|-----|-------|---------|----------|----------|-------|-------|--------------------|-----------|
|                            |                       | Min      | Max | Aver* |         |          | Min      | Max   | Aver* |                    |           |
| Grass                      | 11                    | 0.93     | 70  | 36    | 9       | 15       | 2.52     | 8.28  | 5.40  | 2.33               | 3.6       |
| Forest                     | 11                    | 20.9     | 62  | 42    | 9       | 270      | 1.80     | 63.00 | 32.40 | 1.80**<br>18.65*** | 3.6       |
| Bare soil                  | 11                    | 0.93     | 90  | 45    | 9       | 14       | 2.52     | 8.28  | 5.40  | 10.83              | 3.6       |
| Seawater                   | 11                    | 0.76     | 46  | 23    | 9       | 6.1      | 0.36     | 3.60  | 1.98  | 10.83              | 3.6       |

\* - calculated as arithmetic mean between minimum and maximum;

\*\* - for coniferous forest;

\*\*\* - for deciduous forest.

**Table 28.** Comments

| Models                | Comments  |
|-----------------------|---|
| EVN-BETR and UK-MODEL | Independent on underlying surface type;<br>Calculations are made for all considered PCB congeners together  |
| SimpleBox             | Independent on underlying surface type;<br>SimpleBox works with one single deposition velocity (10-3 m/s) of aerosol particles, regardless character of aerosol or surface.<br>Calculations are made for all considered PCB congeners together;<br>No TSP used in model. Assumed that 'standard' specific aerosol surface of 0.00015 m <sup>2</sup> /m <sup>3</sup> corresponds with TSP 30 mg/m <sup>3</sup> , so that<br>Drydep flux = drydep velocity · TSP = 0.001 m/s · 30 mg/m <sup>3</sup> · 1000 µg/mg · 3600 s/hr = 108000 µg/m <sup>2</sup> /hr |
| G-CIEMS               | Independent on underlying surface type;<br>Calculations are made for all considered PCB congeners together  |
| CAM/POPs              | Dependent on underlying surface type ;<br>Calculations are made for all considered PCB congeners together   |
| CliMoChem             | Dependent on underlying surface type ;<br>Calculations are made for all considered PCB congeners together;<br>Flux = dry particle deposition velocity * air concentration of particulate phase  |
| DEHM-POP              | Dependent on underlying surface type ;<br>Calculations are made for all considered PCB congeners together   |
| MSCE-POP              | Dependent on underlying surface type ;<br>Calculations are made for all considered PCB congeners together   |

Taking into account all calculated values, it is seen that the values of dry deposition flux for different models are mostly of the same order. The lowest value of the flux to grass is obtained by CliMoChem model. The flux to forest calculated by CAM/POPs model is essentially larger than that calculated by other models. The max/min value of fluxes to bare soil calculated by all participating models is within a factor of 13. Mean values of the flux to seawater calculated by MSCE-POP model are lower than values obtained by all other models. In general, the largest discrepancy of calculated fluxes to different types of underlying surface takes place for forest: maximum (CAM/POPs) and minimum (CliMoChem for coniferous forest) calculated values differ 150 times.

To evaluate the similarity between models we use correlation coefficients where appropriate (that is, between models where depositions to different types of underlying surface differ from one another). These correlation coefficients are presented in Table 29.

**Table 29.** Correlation coefficients

|          | CAM/POPs | MSCE-POP | CliMoChem |
|----------|----------|----------|-----------|
| DEHM-POP | 0.40     | 0.47     | 0.01      |
| CAM/POPs | -        | 1.00     | 0.25      |
| MSCE-POP | -        | -        | 0.21      |

The correlation coefficients between mean values of particulate dry deposition flux to different types of underlying surface calculated by DEHM-POP and MSCE-POP models and by DEHM-POP and CAM/POPs models are equal to 0.47 and 0.40, respectively. Correlation between CAM/POPs and MSCE-POP model is very high. Correlation between CliMoChem (taking into account the average value of the flux to forest) and the above three models is poor.

Values of average dry deposition flux for different models agree mostly within an order of magnitude. The type of underlying surface essentially affects deposition fluxes. For models distinguishing different types of underlying surface the best correlation is for CAM/POPs and MSCE-POP.

## 4.3. Wet deposition

### 4.3.1. Model approaches

All participating models use similar approach to the description of wet scavenging of POPs based on the calculation of separate washout for particulate and gaseous phases of a pollutant. Total dimensionless washout ratio  $W_T$  is determined by the Eq. (11):

$$W_T = W_G (1 - \phi) + W_P \phi, \quad (11)$$

where  $W_G$  is the washout ratio of the gas phase;  
 $W_P$  is the washout ratio of a substance associated with aerosol particles;  
 $\phi$  is the substance fraction associated with aerosol particles.

Under such approach the concentration of the phase  $i$  (gaseous or particulate) in precipitation is expressed as

$$C_{p,i} = W_i \cdot C_{a,i}, \quad (12)$$

where  $C_{p,i}$  - concentration of the phase  $i$  in precipitation;  
 $W_i$  - value of washout ratio for the phase  $i$ ;  
 $C_{a,i}$  - concentration of the phase  $i$  in air.

For the description of gaseous phase scavenging with precipitation, the instantaneous equilibrium between the gaseous phase in the air and the dissolved phase in precipitation is assumed. For calculations of washout or scavenging ratio for gaseous phase, all the models use the inverse relation of dimensionless Henry's law constant taken in the form of temperature dependence.

For the description of particle bound phase scavenging with precipitation, the constant washout or scavenging ratio ( $W$  or  $Q$ , dimensionless) determined experimentally or estimated theoretically is used in MSCE-POP, EVN-BETR and UK-MODEL, DEHM-POP, G-CIEMS and CliMoChem models. The differences between model descriptions is mostly determined by the difference of washout or scavenging ratio values used for the calculation of particulate phase scavenging. Values of this parameter are given in Table 30.

**Table 30.** Scavenging ratio (washout ratio) for the particle phase of PCB-153

| Model                 | Description and comments   | Numerical values                      | Reference                        |
|-----------------------|--|---------------------------------------|----------------------------------|
| G-CIEMS               | Fixed scavenging ratio for atmospheric particles. Scavenging ratio is one and the same over all land and water surfaces. | 10,000-200,000, depending on the case |                                  |
| EVN-BETR and UK-MODEL | Rain Scavenging ratio  | 200000                                | This study                       |
|                       | Snow Scavenging Ratio  | 1000000                               |                                  |
| CliMoChem             | scavenging ratio: the air volume scavenged by the falling rain is scavratio-times greater than the rainwater volume      | 200000                                | <i>Mackay and Paterson, 1991</i> |
| DEHM-POP              | $\Lambda_{bc}$ is the below cloud scavenging coefficient   | 100000                                | <i>Christensen, 1997</i>         |
|                       | $\Lambda_c$ is the in cloud scavenging coefficient   | 700000                                |                                  |
| MSCE-POP              | Washout ratio for the particle phase   | 150000                                | <i>Sweetman and Jones 2000</i>   |

The scattering of scavenging ratio (or washout ratio) is rather large. For these models, its values vary from 10000 to 700000. The DEHM-POP model uses constant scavenging ratios but makes distinction between in-cloud and below-cloud scavenging. Besides in this model, description of wet deposition process is dependent on height of precipitation formation. The EVN-BETR and UK-MODEL use constant scavenging ratios for rain and snow scavenging separately.

To calculate the particulate wet deposition flux, CAM/POPs includes the value of scavenging rate (in  $s^{-1}$ ) dependent on mean particle/drop collection efficiency and do not use the value of scavenging ratio. Besides, this model uses 12-bin structure of Sulphate aerosol for calculations of particulate phase scavenging. In CAM/POPs rain and snow scavenging are also considered separately. In SimpleBox model aerosol washout of a pollutant is determined with the help of constant value of aerosol collection efficiency, which varies greatly with the size of the particles and depends also on the chemical.

Below the results of model calculations of PCB-153 concentration in precipitation for different environmental conditions made by six models (EVN-BETR and UK-MODEL, G-CIEMS, CAM/POPs, SimpleBox, CliMoChem and MSCE-POP) are presented. As it will be seen, the variability of approaches to calculation of the scavenging ratio lead to essential differences in model calculations of concentrations in precipitation.

### 4.3.2. Input data

Six sets of input data are proposed for modelling experiments with PCB-153.

**Table 31.** Input data for computation experiments with PCB-153 describing wet deposition

| N   | Experiment 1 | Experiment 2 | Experiment 3 | Experiment 4 | Experiment 5 | Experiment 6 |
|---|--------------|--------------|--------------|--------------|--------------|--------------|
| Precipitation intensity, mm/hour                        | 1            | 1            | 1            | 10           | 10           | 10           |
| Precipitation height, m                                 | 1000         | 1000         | 1000         | 1000         | 1000         | 1000         |
| Average ambient temperature, °C                         | -1           | 3            | 15           | -1           | 3            | 15           |
| Air concentration, gaseous phase, pg/m <sup>3</sup>     | 7            | 7.3          | 33.7         | 7            | 7.3          | 33.7         |
| Air concentration, particulate phase, pg/m <sup>3</sup> | 5.3          | 4.8          | 1.5          | 5.3          | 4.8          | 1.5          |

**Output:** calculated wet deposition fluxes, ng/m<sup>2</sup>/hour and total (dissolved+particulate) concentrations of PCB in precipitation, pg/l.

### 4.3.3. Comparison of the results

Numerical results of experiments on calculations of concentration in precipitation and wet deposition fluxes obtained by the participating models and their analysis are presented in this Section for PCB-153. The corresponding results for other substances can be found in Annexes D and E.

*Analysis of the experiments.* Similar to the case of gas/particle partitioning process, we use the following statistical parameters for each experiment:

- $m$  is the average concentration in precipitation calculated by participating models;
- $\sigma$  is the square deviation of results obtained by different models;

Since additional experiments on wet deposition (last three experiments) were made only by three participating models, statistical processing is performed for the calculation results of the first three experiments. It should be mentioned that results of Experiments 4, 5 and 6 calculated by G-CIEMS, MSCE-POP and SimpleBox show the same concentration in precipitation as in Experiments 1, 2, and 3, respectively. Fluxes between Experiments 1, 2, 3 and Experiments 4, 5, 6 differ ten times in accordance with the different values of precipitation intensity given (See Table 31). Calculated values of concentration in precipitation for PCB-153 together with  $m$  and  $\sigma$  are presented in Table 32. Comparison of absolute values of calculated wet deposition fluxes for PCB-153 and the above mentioned statistical parameters for each experiment are given in Table 33. Short comments to the calculations can be found in Table 34.

For the first two of the experiments, square deviation  $\sigma_{\varphi}$  between different model calculations of concentration in precipitation and wet deposition flux (see last column in Tables 32 and 33) do not exceed the averaged value of these parameters. In the third experiment square deviation to some extent overdraws the average value of both parameters. It corresponds to the fact that in the first two experiments calculated values of concentrations in precipitation vary within a factor of six whereas for the last experiment the difference between maximum and minimum values is equal to 14. The lowest values of this parameter is obtained by MSCE-POP model. Considering absolute values of wet deposition flux, it is seen that max/min ratio lies within an order of magnitude for the first two experiments and comes up to 36 times for the highest temperature. The highest values of wet deposition flux are calculated by CAM/POPs model, and the lowest ones – by CliMoChem model. Since for high temperatures the calculated fraction of gaseous phase of PCB-153 in the atmosphere is high enough (about 80% on the average, see the description of gas/particle partitioning), the maximum dispersion of calculated results between models take place for that temperature in which pollutant presents in the atmosphere mostly in the gaseous phase.

**Table 32.** Calculation results: total (dissolved + particulate) concentrations of PCB-153 in precipitation, pg/l

| No | $T$ (°C) | EVN-BETR and UK model | G-CIEMS | CAM/POPs | MSCE-POP | CliMoChem | SimpleBox | $m$  | $\sigma$ |
|----|----------|-----------------------|---------|----------|----------|-----------|-----------|------|----------|
| 1  | -1       | 1870                  | 1070    | 3042     | 808      | 2325      | 1094      | 1702 | 870      |
| 2  | 3        | 1510                  | 967     | 2130     | 729      | 4424      | 984       | 1791 | 1384     |
| 3  | 15       | 1480                  | 310     | 3262     | 237      | 1263      | 338       | 1148 | 1165     |

**Table 33.** Calculation results: wet deposition flux of PCB-153, ng/m<sup>2</sup>/hour

| No | $T$ (°C) | EVN-BETR and UK model | G-CIEMS | CAM/POPs | MSCE-POP | CliMoChem | SimpleBox | $m$   | $\sigma$ |
|----|----------|-----------------------|---------|----------|----------|-----------|-----------|-------|----------|
| 1  | -1       | 1.870                 | 1.070   | 3.042    | 0.808    | 0.313     | 1.094     | 1.366 | 0.964    |
| 2  | 3        | 1.510                 | 0.967   | 2.130    | 0.729    | 0.283     | 0.984     | 1.100 | 0.643    |
| 3  | 15       | 1.480                 | 0.310   | 3.262    | 0.237    | 0.091     | 0.338     | 0.953 | 1.237    |

**Table 34. Comments**

| Models                | Physical-chemical data set | Comments   |
|-----------------------|----------------------------|--|
| EVN-BETR and UK-MODEL | Own                        | Fugacity approach; $D_{air-surface} = Q \cdot \text{Surface Area} \cdot \text{Particles in air fraction} \cdot K_{QA} \cdot U_R \cdot Z_{air}$<br>In the case of deposition in vegetation, the percentage of rain interception due to vegetation is taken into account. $U_R$ - rain rate = $8.84 \times 10^{-5}$ m/h;   |
| SimpleBox             | "Reference"                | Concentration in air adjusted by setting emission to air.<br>Wet deposition flux (mol/m <sup>2</sup> /s) = (GasWashout (m/s) + AerosolWashout (m/s)) · CONC <sub>air</sub> (mol/m <sup>3</sup> )<br>GasWashout = RAIN <sub>rate</sub> (m/s) · FR <sub>gas</sub> (-) / K <sub>n</sub> (-)<br>AerosolWashout = RAIN <sub>rate</sub> (m/s) · (1-FR <sub>gas</sub> (-)) · COLLECT <sub>eff</sub> (-)<br>RAIN <sub>rate</sub> = precipitation intensity from input set<br>FR <sub>gas</sub> = fraction of substance in gas phase = 1 - FR <sub>aerosol</sub><br>K <sub>n</sub> = dimensionless Henry's Law Constant at ambient temperature = $K_n(25C) \cdot \exp((H^0_{vap} - H^0_{sol})/8.314 \cdot (1/298 - 1/T))$<br>$H^0_{vap}, H^0_{sol}$ = Enthalpy of vaporization, dissolution in water = $\Delta U_a, \Delta U_w$ from reference data set<br>COLLECT <sub>eff</sub> = aerosol collection efficiency = $2 \cdot 10^5 \text{ m}^3(\text{air})/\text{m}^3(\text{rain})$ by default<br>CONC <sub>air</sub> = total PCB concentration in air (mol/m <sup>3</sup> ) |
| CAM/POPs              | Own                        | Dependent on aerosol size distribution:<br>a typical 12 size-bin structure of Sulphate Aerosol as additional input data in this experiment   |
| CliMoChem             | Own                        | surface fraction of grass, coniferous forest and deciduous forest of the vegetation area: 0.63; 0.17; 0.2 [Möller, 2002] fraction of rain falling on grass, coniferous forest and deciduous forest: 0.068, 0.35, 0.193 [Wania et al., 2001];<br>Wet gaseous deposition flux = $1/k_{AW}$ temperature dependent · rainfall velocity · air concentration gaseous phase<br>Wet particle deposition flux = wet deposition velocity · air concentration particulate phase (the rain fraction falling on vegetation and vegetation covered soil was considered when calculating the flux to these compartments)  |
| MSCE-POP              | Own                        | Equation (12);<br>Washout ratio for the gaseous phase $W_g = 1/K_H$ is calculated with the help of temperature dependent dimensionless Henry's law constant; washout ratio for particulate phase determined experimentally is used.  |
| G-CIEMS               | "Reference"                | $F = R_{ain} \cdot C_{air}/H + (TSP/\rho) \cdot Q \cdot C_{particle}$ , where $F$ is total mass flux by this process, $R_{ain}$ is rain rate, $C_{air}$ is gaseous concentration of chemical, $H$ is Henry's law constant, $TSP$ is particulate concentration, $\rho$ is density of particles, $Q$ is scavenging ratio of particles, and $C_{particle}$ is volumetric chemical concentration in particles.   |

**Pairwise comparison of the models.** Let us proceed with pairwise comparison of calculation results obtained by different models. Such comparison was made only for the values of concentrations in precipitation since the values of wet deposition fluxes are proportional to the concentrations practically in all models' results (except for CliMoChem). As in the case of gas/aerosol partitioning, the relation between calculated concentrations in precipitation  $c^1$  and  $c^2$  obtained by compared models for different environmental conditions (for first three experiments only) is described by the equation (9).

Below brief analysis of the correlation coefficient  $r_{12}$  of the compared models, regression coefficients  $\alpha_{12}$  and  $\beta_{12}$  and residual square deviation  $\sigma_{12}^{res}$  is given.

Correlation coefficients for concentration in precipitation calculated by the models is presented in Table 35. The comparison of calculated values of concentrations in precipitation is also displayed in Fig. 9.

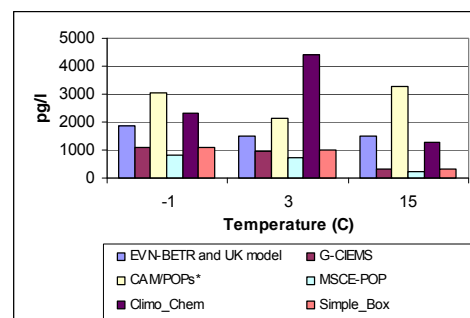


**Fig. 9. Concentration in precipitation calculated by different models for different values of ambient temperatures, pg/l**

**Table 35. Correlation coefficients for concentration in precipitation**

|                       | G-CIEMS | CAM/POPs | MSCE-POP | CliMoChem | SimpleBox |
|-----------------------|---------|----------|----------|-----------|-----------|
| EVN-BETR and UK model | 0.66    | 0.27     | 0.66     | -0.12     | 0.67      |
| G-CIEMS               | -       | -0.55    | 1.00     | 0.67      | 1.00      |
| CAM/POPs              | -       | -        | -0.55    | -0.99     | -0.54     |
| MSCE-POP              | -       | -        | -        | 0.67      | 1.00      |
| CliMoChem             | -       | -        | -        | -         | 0.66      |

Most close results are obtained by G-CIEMS and SimpleBox, by G-CIEMS and MSCE-POP models and by MSCE-POP and SimpleBox models (correlation coefficient in all cases is equal to 1.00). The values of concentrations in precipitation obtained by the rest three models are essentially higher. Temperature dependence of concentrations in precipitation obtained by EVN-BETR and UK-MODEL and G-CIEMS, by EVN-BETR and UK-MODEL and MSCE-POP are close but with some shift. Results of CliMoChem are also well correlated with G-CIEMS, MSCE-POP and SimpleBox models. No correlation is observed between CAM/POPs and all other models and between EVN-BETR and UK-MODEL and CliMoChem model.

Regression coefficients  $\alpha_{12}$  and  $\beta_{12}$  (characterizing a non-random component of the regression relation) are presented in Table 36.

**Table 36.** Coefficients of regression dependence between the models ( $\alpha / \beta$ ) for concentration in precipitation

|                                     | G-CIEMS       | CAM/POPs      | MSCE-POP      | CliMoChem      | SimpleBox     |
|-------------------------------------|---------------|---------------|---------------|----------------|---------------|
| EVN-BETR and UK model               | 1.250 / -1242 | 0.738 / 1616  | 0.941 / -933  | -0.871 / 4082  | 1.253 / -1225 |
| G-CIEMS                             | -             | -0.801 / 3438 | 0.750 / 4     | 2.616 / 624    | 0.992 / 30    |
| CAM/POPs                            | -             | -             | -0.282 / 1385 | -2.649 / 10117 | -0.369 / 1844 |
| MSCE-POP                            | -             | -             | -             | 3.475 / 616    | 1.322 / 24    |
| CliMoChem                           | -             | -             | -             | -              | 0.169 / 355   |
| Mean concentration in precipitation | 782           | 2811          | 591           | 2671           | 805           |

The differences between the models is determined by scaling coefficient  $\alpha$ , which varies within a very wide range from  $-0.87$  to  $3.48$ . However, it is seen that this coefficients are very close to 1 for the most part of considered pairs of models (range from 0.8 to 1.3). Coefficients  $\beta$  are small enough compared with mean values of concentrations in precipitation for the most part of model pairs also (see last line in Table 36). The highest values of this parameter is obtained for the comparison of results of CAM/POPs and CliMoChem models. The lowest values of  $|\beta|$  are observed for the results of the following pair of models: MSCE-POP and G-CIEMS. Taking into account both these regression coefficients' values, G-CIEMS and MSCE-POP, G-CIEMS and SimpleBox, and MSCE-POP and SimpleBox show the most close results in the experiments of wet deposition process.

Pairwise residual square deviation  $\sigma$  presented in Table 37 (characterizing the magnitude of random component  $\omega_{12}$ ) is allowed to reveal the reliability of comparative analysis given above.

**Table 37.** Residual square deviation,  $\sigma$  for concentration in precipitation

|                       | G-CIEMS | CAM/POPs | MSCE-POP | CliMoChem | SimpleBox |
|-----------------------|---------|----------|----------|-----------|-----------|
| EVN-BETR and UK model | 439     | 818      | 329      | 2259      | 432       |
| G-CIEMS               | -       | 709      | 1        | 1687      | 6         |
| CAM/POPs              | -       | -        | 366      | 345       | 486       |
| MSCE-POP              | -       | -        | -        | 1692      | 4         |
| CliMoChem             | -       | -        | -        | -         | 433       |

Values of  $\sigma$  vary within wide range from 1 to 2259. The highest values of the random component are characteristic of the comparisons between CliMoChem and EVN-BETR and UK-MODEL, between CliMoChem and G-CIEMS, between CliMoChem and MSCE-POP. The lowest values are obtained for G-CIEMS and MSCE-POP, G-CIEMS and SimpleBox, and MSCE-POP and SimpleBox.

The results of calculation experiments with PCB-28 and PCB-180 (see Annexes D and E) show also large dispersion between the absolute values of concentrations in precipitation and wet deposition fluxes calculated by different models. For PCB-28 there is a good correlation between results of

MSCE-POP, ClimoChem and SimpleBox (correlation coefficient is equal to 1). Calculated concentrations of PCB-180 in precipitation are also well correlated between these three models (correlation coefficient vary from 0.91 to 1) and between CAM/POPs and EVN-BETR and UK model (correlation coefficient is equal to 0.76).

For better understanding of model approaches to the description of wet deposition process, sensitivity study with respect to model descriptions and their parameterizations is reasonable. Special attention is to be paid for the description of wet scavenging of gaseous phase of POPs.

## **4.4. Gaseous exchange between atmosphere and soil**

### **4.4.1. Model approaches**

Within theory of intermedia diffusion, there exists a large diversity of approaches to the description of atmosphere/soil gaseous exchange. Here we present just very rough classification of similarities and distinctions of approaches used; details can be found in Table 41 and Annex C.

Gaseous exchange between atmosphere and soil is described by all participating models using resistance analogy but with some peculiarities. Processes of redistribution between different phases in soil are taken into account practically in all models (except for CAM/POPs, in which diffusion to low soil layers is considered). EVN-BETR and UK-MODEL implements fugacity approach for description of gaseous exchange between the atmosphere and soil compartments using three different diffusion transport velocity values for soil air-phase, soil water-phase and soil air boundary layer diffusion. In addition to dry gaseous deposition and revolatilization, in CliMoChem model process of bioturbation is also considered. This model takes also into consideration the percentage of vegetation coverage of soil. For the description of pollutant absorption from gas phase by soil and its volatilization from soil, SimpleBox uses two overall air-soil mass transfer coefficients (gas and soil-referenced) calculated considering processes of advection, diffusion and degradation. G-CIEMS also exploits two thin-film theory of intermedia diffusion (with restricted diffusion for soil-side mass transfer) using two mass transfer coefficients calculated with the help of molecular diffusivity and effective diffusion. For the calculation of atmosphere/soil flux, in MSCE-POP model three different resistances (turbulent air sublayer, laminar surface air sublayer and surface soil resistances) and effective diffusion coefficients are used. In addition, processes of vertical diffusion and advection with water flux and degradation of the pollutant in soil are considered in this model. The rest two models (DEHM-POP and CAM/POPs) evaluate air/soil exchange flux also using effective diffusion coefficients.

The difference between model approaches to the description of air/soil exchange is also in the number and thickness of considered soil layers. EVN-BETR and UK-MODEL, DEHM-POP, G-CIEMS, CliMoChem and SimpleBox model use one vertical layer in soil compartment which thickness varies from 5 to 15 cm. CAM/POPs uses three layers (5 cm altogether), and in MSCE-POP multi-layer approach (20 cm altogether) is used. Thus, all models consider different depth of soil compartment which varies from 5 to 20 cm.

Below the results of calculation experiments on air/soil exchange obtained by seven models are compared. Two models (G-CIEMS and MSCE-POP) presented two versions of calculations each (see below).

Since accumulation and clearance processes in soil require large time (decades), investigation of accumulation/clearance dynamics of POPs in soil is of importance. This investigation is exemplified by calculation experiments made by CAM/POPs, EVN-BETR and UK model, SimpleBox and MSCE-POP models in the end of this section.

#### 4.4.2. Input data

Four sets of input data are proposed for modelling experiments with PCB-153.

*Table 38. Input data for computation experiments with PCB-153 describing air/soil exchange*

| N   | Experiment 1 | Experiment 2 | Experiment 3 | Experiment 4 |
|---|--------------|--------------|--------------|--------------|
| Averaged ambient temperature, °C                    | 10           | 10.9         | 12.9         | 13.9         |
| Air concentration, gaseous phase, pg/m <sup>3</sup> | 0.8          | 5.5          | 6.8          | 2.8          |
| Bulk soil density, kg/m <sup>3</sup>                | 1210         | 1080         | 890          | 1360         |
| Volumetric water content in soil, %                 | 20.6         | 41.4         | 26.4         | 16.8         |
| Volumetric air content in soil, %                   | 20           | 20           | 20           | 20           |
| Fraction of organic carbon in soil, %               | 7.1          | 17.7         | 12.3         | 4            |

**Output:** calculation of PCB-153 soil concentrations, ng/g and gaseous fluxes from and to soil and/or net gaseous flux to soil, ng/m<sup>2</sup>/d.

#### 4.4.3. Comparison of the results

Here we present numerical results of calculations of soil concentrations and net gaseous flux to soil obtained by the participating models and their analysis for PCB-153. The corresponding results for other substances can be found in Annexes D and E.

Similar to the cases of gas/particle partitioning and wet deposition, the analysis is performed into two stages. At the first stage we present an analysis of the calculated concentrations and net gaseous fluxes to soil and characterize the dispersion in these values in each experiment. At the second stage we analyze pairwise differences between participating models using the regression analysis. In addition the analysis of accumulation and clearance processes calculated by four models (CAM/POPs, EVN-BETR and UK model, SimpleBox and MSCE-POP) is performed.

**Analysis of the experiments.** Here we use the following statistical parameters for each experiment:

- $m$  is the average soil concentrations for participating models;
- $\sigma$  is the square deviation;

EVN-BETR and UK model, SimpleBox, and DEHM-POP models have made calculations on these experiments using steady-state approach. CliMoChem and CAM/POPs models have obtained results for equilibrium state. For G-CIEMS model two versions of calculations are presented: for steady-state (G-CIEMS 1) and at equilibrium using interim calculation parameters of the model (G-CIEMS 2). For MSCE-POP model two calculation versions are presented as well: steady-state calculations (MSCE-POP 1) and calculations from dynamic model (MSCE-POP 2). In the latter case calculations for 60 year period with air concentration roughly simulating the trend of PCB air concentrations and additional two years with constant air concentrations equal to that specified in the input data. In this case soil concentrations in the end of calculation period were used for comparison. Fig. 10 illustrates air concentration trend used in calculations for Experiment 1.

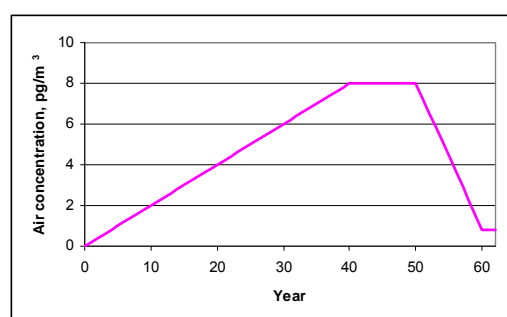


**Fig. 10.** Air concentration trend used for calculations for MSCE-POP model (MSCE-POP 2) for Experiment 1

Calculation results for PCB-153 soil concentrations together with  $m$  and  $\sigma$  are presented in Table 39. Net gaseous fluxes to soil of PCB-153 calculated by the models and statistical parameters used for its evaluation are given in Table 40. Table 41 contains appropriate comments to the calculations made by each model.

The analysis of the results submitted by participants shows that there is rather large differences between calculated both soil concentrations values and net gaseous flux values. It is confirmed by the fact that square deviation values exceed the average values in both cases. For calculated soil concentrations, results obtained by SimpleBox model are essentially lower than other ones. The comparison of calculated net gaseous fluxes shows that calculations of CAM/POPs differ from other model results in several order of magnitude. Below we analyze pairwise differences between participating models.

**Table 39.** Calculation results: soil concentrations of PCB-153 (ng/g) calculated by models and statistical parameters used for evaluation

| No | Air conc, pg/m <sup>3</sup> | EVN-BETR and UK-MODEL | DEHM-POP | G-CIEMS |        | CAM/POPs | MSCE-POP |        | CliMoChem | SimpleBox | $m$  | $\sigma$ |
|----|-----------------------------|-----------------------|----------|---------|--------|----------|----------|--------|-----------|-----------|------|----------|
|    |                             |                       |          | 1       | 2      |          | 1        | 2      |           |           |      |          |
| 1  | 0.8                         | 0.0020                | 0.4635   | 0.0071  | 0.0831 | 0.5719   | 0.0184   | 0.1047 | 0.0822    | 0.0001    | 0.15 | 0.21     |
| 2  | 5.5                         | 0.0138                | 7.6195   | 0.0652  | 1.3089 | 8.6991   | 0.1454   | 0.8284 | 0.9207    | 0.0013    | 2.18 | 3.43     |
| 3  | 6.8                         | 0.0177                | 6.3204   | 0.0652  | 0.9334 | 6.4227   | 0.2045   | 1.1675 | 1.0491    | 0.0015    | 1.80 | 2.63     |
| 4  | 2.8                         | 0.0042                | 1.3987   | 0.0123  | 0.1140 | 0.7934   | 0.0518   | 0.2951 | 0.0962    | 0.0003    | 0.31 | 0.48     |

**Table 40.** Calculation results: net gaseous flux to soil, of PCB-153 (ng/m<sup>2</sup>/d) calculated by models and statistical parameters used for evaluation

| No | Air conc, pg/m <sup>3</sup> | EVN-BETR and UK-MODEL | G-CIEMS  |     | CAM/POPs | MSCE-POP |           | CliMoChem | SimpleBox | $m^*$    | $\sigma^*$ |
|----|-----------------------------|-----------------------|----------|-----|----------|----------|-----------|-----------|-----------|----------|------------|
|    |                             |                       | 1        | 2   |          | 1        | 2         |           |           |          |            |
| 1  | 0.8                         | 8.19E-04              | 3.71E-04 | 0.0 | 3.51E-13 | 2.98E-02 | 8.96E-03  | 0.0       | 7.16E-02  | 1.86E-02 | 2.83E-02   |
| 2  | 5.5                         | 5.81E-03              | 1.66E-03 | 0.0 | 5.01E-12 | 2.29E-01 | 1.57E-01  | 0.0       | 4.95E-01  | 1.48E-01 | 1.95E-01   |
| 3  | 6.8                         | 7.66E-03              | 2.56E-03 | 0.0 | 2.06E-12 | 2.54E-01 | 8.23E-02  | 0.0       | 6.08E-01  | 1.59E-01 | 2.40E-01   |
| 4  | 2.8                         | 3.16E-03              | 1.49E-03 | 0.0 | 3.94E-13 | 7.66E-02 | -7.14E-02 | 0.0       | 2.48E-01  | 4.29E-02 | 1.11E-01   |

\* - statistical parameters are calculated for models using steady-state and dynamic approaches.

**Table 41.** Comments

| Models               | Physical-chemical data set | Numbers of layers in soil compartment | Thickness of considered soil layers, cm | Comments  |
|----------------------|----------------------------|---------------------------------------|---|---|
| EVN-BETR and K-MODEL | Own                        | 1                                     | 10                                      | Steady-state<br>Fugacity approach<br>Redistribution between different phases in soil<br>Individual/own dataset extremely close to the reference dataset;<br>The flux was calculated as Gaseous flux = $D_{\text{air-soil}} \cdot \text{Fugacity (Pa)}$<br>$D_{\text{air-soil}} = (\text{Soil Area} \cdot Z_{\text{air}}) / [(Z_{\text{air}} / (\text{MTCas} \cdot Z_{\text{air}} + \text{MTCsw} \cdot Z_{\text{water}})) + 1 / \text{MTCsabl}]$<br>Soil Area = $8.36 \cdot 10^{12} \text{ m}^2$<br>MTCas : soil air-phase diffusion transport velocity = 0.04 m/h<br>MTCsw : soil water-phase diffusion transport velocity = $1 \cdot 10^5 \text{ m/h}$<br>MTCsabl : soil air boundary layer transport velocity = 1 m/h |

| Models                | Physical-chemical data set | Numbers of layers in soil compartment | Thickness of considered soil layers, cm | Comments   |  |
|-----------------------|----------------------------|---------------------------------------|---|--|--|
| SimpleBox             | Reference                  | 1                                     | 5                                       | <p>Steady-state</p> <p>Redistribution between different phases in soil and other processes;</p> <p>Concentration in air adjusted by setting emission to air.</p> <p>Transport between air and soil entirely by gas exchange. Other exchange mechanisms "switched off"; vegetation "switched off".</p> <p>Transport across air-soil interface calculated by two-resistance model. Air side: film diffusion; soil side: steady-state penetration into half-infinite porous medium with homogeneous degradation.</p> <p>Calculated concentration in soil is bulk, wet concentration in ng PCB per g of wet soil; concentration on dry weight basis added.</p> <p>Absorption from gas phase by soil (mol/m<sup>2</sup>/s) = FR<sub>gas</sub> (-) · k<sub>as</sub>(gas) (m/s) · CONC<sub>air</sub> (mol/m<sup>3</sup>)</p> <p>Volatilization from soil (mol/m<sup>2</sup>/s) = k<sub>as</sub>(soil) (m/s) · CONC<sub>soil</sub> (mol/m<sup>3</sup>)</p> <p>k<sub>as</sub>(gas) = overall gas-referenced air-soil mass transfer coefficient = k<sub>as.air</sub> · k<sub>as.soil</sub> / (k<sub>as.air</sub> · (Kh/K<sub>sw</sub>) + k<sub>as.soil</sub>)</p> <p>k<sub>as</sub>(soil) = overall soil-referenced air-soil mass transfer coefficient = k<sub>as.air</sub> · k<sub>as.soil</sub> / (k<sub>as.air</sub> + k<sub>as.soil</sub>/(Kh/K<sub>sw</sub>))</p> <p>k<sub>as.air</sub> (m/s) = partial mass transfer coefficient for air-side of the air-soil interface = 1.05 · 10<sup>-3</sup> m/s by default</p> <p>k<sub>as.soil</sub> (m/s) = partial mass transfer coefficient for soil-side of the air-soil interface = V<sub>eff</sub> + Deff / PENdepth</p> <p>PENdepth (m) = penetration depth of PCB in soil = V<sub>eff</sub> + SQRT(V<sub>eff</sub><sup>2</sup> + 4 · KDEG · Deff) / 2 · KDEG</p> <p>V<sub>eff</sub> (m/s) = effective (water+solids) downward advection of PCB into soil</p> <p>Deff (m<sup>2</sup>/s) = effective (gas+water+solid) diffusion coefficient of PCB in soil</p> <p>KDEG (s<sup>-1</sup>) = first-order degradation rate constant of PCB in soil</p> <p>Kh (-) = dimensionless air-water equilibrium constant</p> <p>K<sub>sw</sub> (-) = dimensionless soil-water equilibrium constant</p> |  |
| CAM/POPs              | Own                        | 3                                     | 5 (0-1, 1-3, 3-5)                       | <p>Equilibrium;</p> <p>Diffusion to low soil layers;</p> <p>Two transfer processes: the chemical transfer between deep soil layers and surface soil, and the exchange of the chemical vapour between the soil surface and the atmosphere.</p>  |  |
| CiMoChem              | Own                        | 1                                     | 10                                      | <p>Equilibrium;</p> <p>The concentrations are at steady-state;</p> <p>Redistribution between different phases in soil</p> <p>Dry gaseous deposition;</p> <p>Revolatilization;</p> <p>Bioturbation;</p> <p>Dry gaseous deposition flux=diffusion rate air to bare soil · (1-particle bound fraction in air) · concentration in air · air volume/(bare soil volume/ thickness of soil layer)</p> <p>Revolatilization flux = diffusion rate bare soil to air · steady state concentration in bare soil · bare soil volume/(bare soil volume/thickness of soil layer)</p> <p>(Model Geometry: box length: 100000 m; box width: 100000 m; fraction of bare soil area to total area: 0.0345)</p>   |  |
| MSCE-POP <sub>1</sub> | Own                        | 7                                     | 20 (0.1, 0.3, 0.6, 1, 2, 5, 11)         | Steady-state;  | <p>Redistribution between different phases in soil;</p> <p>Vertical diffusion and advection with water flux;</p> <p>Degradation of the pollutant.</p> <p>Gaseous exchange with the atmosphere parameterized using three-resistances approach (turbulent air sublayer, laminar surface air sublayer and surface soil resistances). Atmosphere/soil flux is calculated as follows:</p> $F_{dry}^g = \frac{C_a^g - C_s^g}{r_a + r_b + r_s}$ |
| MSCE-POP <sub>2</sub> |                            |                                       |   | Dynamic  |  |
| G-CIEMS 1             | Reference                  | 1                                     | 5                                       | <p>Steady-state</p> <p>Redistribution between different phases in soil</p> <p>Diffusion to low soil layers and other processes</p>   |  |
| G-CIEMS 2             |                            | 1                                     | 5                                       | <p>Equilibrium;</p> <p>Redistribution between different phases in soil</p> <p>Diffusion to low soil layers and other processes</p>   |  |
| DEHM-POP              | Own                        | 1                                     | 15                                      | <p>Steady-state</p> <p>Redistribution between different phases in soil</p>   |  |

**Pairwise comparison of the models.** As in the case of gas/aerosol partitioning, the relation between calculated soil concentrations  $c^1$  and  $c^2$  obtained by compared models for different environmental conditions (including air concentration values) is expressed by the equation (9).

Below brief analysis of the correlation coefficient  $r_{12}$  of the compared models, regression coefficients  $\alpha_{12}$  and  $\beta_{12}$  and residual square deviation  $\sigma_{12}^{res}$  is given.

In spite of the fact that numerical values of soil concentrations are highly different, the variations of the corresponding numerical values caused by change of environmental conditions between different experiments are similarly described by models. This can be seen from values of pairwise correlation coefficients varying in the range from 0.85 to almost 1 (Table 42).

**Table 42.** Correlation coefficients for soil concentrations

|                       | DEHM-POP | G-CIEMS 1 | G-CIEMS 2 | CAM/ POPs | MSCE-POP 1 | MSCE-POP 2 | CliMoChem | SimpleBox |
|-----------------------|----------|-----------|-----------|-----------|------------|------------|-----------|-----------|
| EVN-BETR and UK-MODEL | 0.93     | 0.98      | 0.89      | 0.90      | 1.00       | 1.00       | 0.99      | 0.99      |
| DEHM-POP              | -        | 0.99      | 0.99      | 0.99      | 0.90       | 0.90       | 0.96      | 0.97      |
| G-CIEMS 1             | -        | -         | 0.97      | 0.97      | 0.95       | 0.95       | 0.99      | 0.99      |
| G-CIEMS 2             | -        | -         | -         | 1.00      | 0.85       | 0.85       | 0.94      | 0.93      |
| CAM/POPs              | -        | -         | -         | -         | 0.86       | 0.86       | 0.95      | 0.94      |
| MSCE-POP 1            | -        | -         | -         | -         | -          | 1.00       | 0.97      | 0.98      |
| MSCE-POP 2            | -        | -         | -         | -         | -          | -          | 0.97      | 0.98      |
| CliMoChem             | -        | -         | -         | -         | -          | -          | -         | 1.00      |

For net gaseous flux (Table 43), the best correlation is observed between SimpleBox and EVN-BETR and UK-MODEL, between MSCE-POP 1 and SimpleBox, between EVN-BETR and UK-MODEL and MSCE-POP 1, and between MSCE-POP 2 and CAM/POPs models. It is also seen that results of G-CIEMS 1 are well correlated with data of EVN-BETR and UK-MODEL, MSCE-POP 1, and SimpleBox. There is no correlation between G-CIEMS 1 and two models: MSCE-POP 2 and CAM/POPs.

**Table 43.** Correlation coefficients for net gaseous flux to soil of PCB-153\*

|                       | G-CIEMS 1 | CAM/POPs | MSCE-POP 1 | MSCE-POP 2 | SimpleBox |
|-----------------------|-----------|----------|------------|------------|-----------|
| EVN-BETR and UK-MODEL | 0.96      | 0.63     | 0.97       | 0.63       | 1.00      |
| G-CIEMS 1             | -         | 0.41     | 0.87       | 0.38       | 0.94      |
| CAM/POPs              | -         | -        | 0.77       | 0.91       | 0.68      |
| MSCE-POP 1            | -         | -        | -          | 0.79       | 0.99      |
| MSCE-POP 2            | -         | -        | -          | -          | 0.67      |

\* - statistical parameters are calculated for models using steady-state and dynamic approaches.

Table 44 contains the values of regression coefficients  $\alpha$  and  $\beta$  calculated for all pairs of models in terms of soil concentrations. It is seen that coefficients  $\beta$  are small enough compared with mean values of soil concentrations for all pairs of models (see last line in Table 44) and the differences between the models are explained mainly by scaling coefficient  $\alpha$ . The latter varies in a very wide range (0.0002 - 486.145). The smallest value (0.0002) is characteristic for regression between DEHM-POP and SimpleBox and for regression between CAM/POPs and SimpleBox. The highest value (486.145) is obtained for regression between EVN-BETR and UK-MODEL and CAM/POPs. Pairs of models: G-CIEMS 2 and CliMoChem, MSCE-POP 2 and CliMoChem, and DEHM-POP and CAM/POPs show close results (regression coefficients  $\alpha$  are close enough to 1).

Table 45 contains the values of regression coefficients  $\alpha$  and  $\beta$  calculated for all pairs of models in terms of net gaseous fluxes to soil.

**Table 44.** Coefficients of regression dependence between the models ( $\alpha / \beta$ ) for soil concentrations

|                         | DEHM-POP         | G-CIEMS 1     | G-CIEMS 2      | CAM/POPs              | MSCE-POP 1     | MSCE-POP 2     | CliMoChem             | SimpleBox        |
|-------------------------|------------------|---------------|----------------|-----------------------|----------------|----------------|-----------------------|------------------|
| EVN-BETR and UK-MODEL   | 439.672 / -0.189 | 4.153/ -0.002 | 71.840/ -0.067 | 486.145/ -0.455       | 11.284/ -0.001 | 64.380/ -0.007 | 68.067/ -0.104        | 0.091 / -0.00005 |
| DEHM-POP                | -                | 0.009/ 0.002  | 0.170/ -0.063  | <b>1.142</b> / -0.391 | 0.022/ 0.019   | 0.124/ 0.108   | 0.141 / -0.021        | 0.0002 / 0.0001  |
| G-CIEMS 1               | -                | -             | 18.380/ -0.079 | 123.634 / -0.512      | 2.539/ 0.010   | 14.479/ 0.056  | 16.085 / -0.066       | 0.021 / 0.00001  |
| G-CIEMS 2               | -                | -             | -              | 6.685/ 0.045          | 0.119/ 0.033   | 0.676 / 0.186  | <b>0.799</b> / 0.050  | 0.001 / 0.0002   |
| CAM/POPs                | -                | -             | -              | -                     | 0.018/ 0.031   | 0.103 / 0.176  | 0.121/ 0.040          | 0.0002 / 0.0002  |
| MSCE-POP 1              | -                | -             | -              | -                     | -              | 5.706/ -0.0004 | 5.912 / -0.084        | 0.008 / -0.00003 |
| MSCE-POP 2              | -                | -             | -              | -                     | -              | -              | <b>1.036</b> / -0.083 | 0.001 / -0.00003 |
| CliMoChem               | -                | -             | -              | -                     | -              | -              | -                     | 0.001 / 0.0001   |
| Mean soil concentration | 3.9505           | 0.0375        | 0.6099         | 4.1218                | 0.1050         | 0.5989         | 0.5371                | 0.0008           |

**Table 45.** Coefficients of regression dependence between the models ( $\alpha / \beta$ ) for net gaseous flux to soil of PCB-153\*

|                       | G-CIEMS 1       | CAM/POPs             | MSCE-POP 1      | MSCE-POP 2       | SimpleBox       |
|-----------------------|-----------------|----------------------|-----------------|------------------|-----------------|
| EVN-BETR and UK-MODEL | 0.29 / 2.68E-04 | 4.57E-10 / -3.97E-14 | 35.99 / -0.01   | 20.46 / -0.05    | 80.46 / 0.005   |
| G-CIEMS 1             | -               | 1.01E-09 / 4.26E-13  | 107.21 / -0.02  | 41.17 / -0.02    | 252.85 / -0.03  |
| CAM/POPs              | -               | -                    | 3.90E+10 / 0.07 | 4.07E+10 / -0.04 | 7.50E+10 / 0.21 |
| MSCE-POP 1            | -               | -                    | -               | 0.69 / -0.06     | 2.15 / 0.04     |
| MSCE-POP 2            | -               | -                    | -               | -                | 1.67 / 0.28     |

\* - statistical parameters are calculated for models using steady-state and dynamic approaches.

The difference between the participating models in values of scaling coefficient  $\alpha$  is even more essential for net gaseous fluxes than for concentrations. The best  $\alpha$  value (that means the most close to 1 among others) is equal to 1.7 and is characteristic for regression between MSCE-POP 2 and SimpleBox models.

To assess the reliability of comparative analysis given above calculations of pairwise residual square deviation  $\sigma$  were done (Table 46 and 47).

**Table 46.** Residual square deviation ( $\sigma$ ) for soil concentrations

|                       | DEHM-POP | G-CIEMS 1 | G-CIEMS 2 | CAM/POPs | MSCE-POP 1 | MSCE-POP 2 | CliMoChem | SimpleBox |
|-----------------------|----------|-----------|-----------|----------|------------|------------|-----------|-----------|
| EVN-BETR and UK-MODEL | 2.182    | 0.012     | 0.486     | 3.098    | 0.012      | 0.072      | 0.142     | 0.0001    |
| DEHM-POP              | -        | 0.009     | 0.142     | 0.820    | 0.063      | 0.361      | 0.240     | 0.0003    |
| G-CIEMS 1             | -        | -         | 0.269     | 1.633    | 0.044      | 0.254      | 0.104     | 0.0001    |
| G-CIEMS 2             | -        | -         | -         | 0.171    | 0.078      | 0.449      | 0.313     | 0.0004    |
| CAM/POPs              | -        | -         | -         | -        | 0.075      | 0.432      | 0.293     | 0.0004    |
| MSCE-POP 1            | -        | -         | -         | -        | -          | 0.001      | 0.214     | 0.0002    |
| MSCE-POP 2            | -        | -         | -         | -        | -          | -          | 0.215     | 0.0002    |
| CliMoChem             | -        | -         | -         | -        | -          | -          | -         | 0.0001    |

**Table 47.** Residual square deviation ( $\sigma$ ) for net gaseous flux to soil of PCB-153

|                       | DEHM-POP | G-CIEMS 1 | G-CIEMS 2 | CAM/POPs | SimpleBox |
|-----------------------|----------|-----------|-----------|----------|-----------|
| EVN-BETR and UK-MODEL | 4.46E-04 | 2.95E-12  | 0.04      | 0.13     | 0.03      |
| G-CIEMS 1             | -        | 3.45E-12  | 0.09      | 0.16     | 0.14      |
| CAM/POPs              | -        | -         | 0.12      | 0.07     | 0.31      |
| MSCE-POP 1            | -        | -         | -         | 0.10     | 0.07      |
| MSCE-POP 2            | -        | -         | -         | -        | 0.31      |

It is seen that the values of residual square deviation for soil concentrations lie within the interval 0.0001 - 2.182. The highest value is obtained for the regression between EVN-BETR and UK-MODEL and DEHM-POP models. For models' results of calculated net gaseous flux,  $-\sigma$  ranges from 3.45E-12 to 0.31.

In the cases of PCB-28 and PCB-180 results ( Annexes D and E), there is also a large difference in absolute values both for calculated soil concentrations and net gaseous fluxes. Correlation coefficients for soil concentration of PCB-28 vary in the range from 0.93 to almost 1 between all pairs of models; for net gaseous flux good correlation is observed between SimpleBox and EVN-BETR and UK-MODEL models. Results on soil concentrations and net gaseous fluxes of PCB-180 are well correlated for all model pairs (correlation coefficients range from 0.87 to 1.00 and from 0.85 to 1.00, respectively).

**Accumulation/clearance dynamics of POPs in soil.** The aim of this subsection is to analyze model descriptions of long-term processes of accumulation of selected PCB congeners in soil and clearance of soil compartment at emission termination. To do this, modelling of air/soil exchange with constant air concentration for a sufficiently long period were carried out by CAM/POPs, MSCE-POP, EVN-BETR and UK model, and SimpleBox models using first set of data presented above. In CliMoChem trend was not calculated as it takes way longer than 120 months to reach steady state in this model.

The period under simulation was split into two periods. During the first period (accumulation) air concentrations are kept at the level defined in the corresponding input data set and initial data are assumed to be zero. Soil concentrations obtained in the end of the first period were used as initial data for the second period (clearance). During this period air concentrations are set to zero.

Figs. 11, 12, 13 and 14 show the results of the experiment obtained by CAM/POPs, MSCE-POP, EVN-BETR and UK model, and SimpleBox models, respectively.

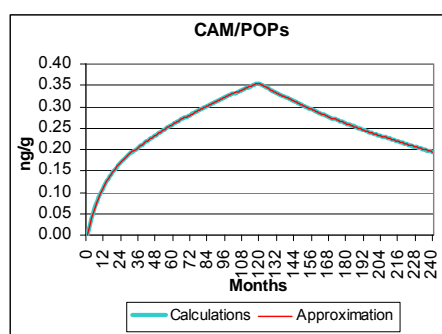


**Fig. 11.** Long-term trends of accumulation and clearance obtained by CAM/POPs model

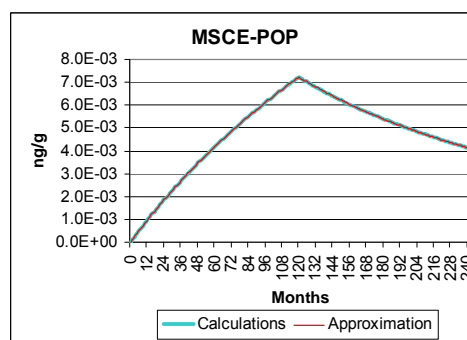


**Fig. 12.** Long-term trends of accumulation and clearance obtained by MSCE-POP model

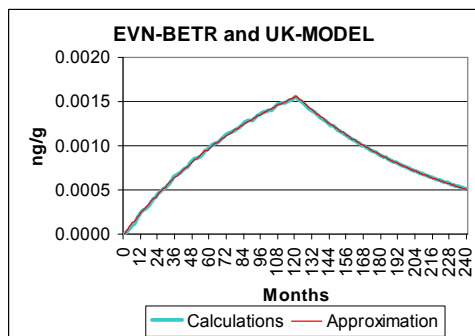


**Fig. 13.** Long-term trends of accumulation and clearance obtained by EVN-BETR and UK-MODEL model

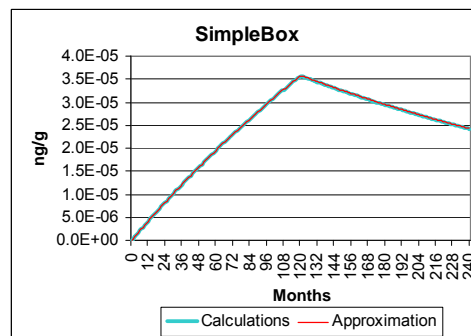


**Fig. 14.** Long-term trends of accumulation and clearance obtained by SimpleBox model

Together with calculated soil concentrations bi-exponential approximation of accumulation and clearance is also shown in the plots. At the accumulation stage this approximation has the form:

$$C_{soil} = C_1(1 - e^{-\lambda_1 t}) + C_2(1 - e^{-\lambda_2 t}), \quad \lambda_1 > \lambda_2$$

where  $t$  is the time, months;

$\lambda_1$  and  $\lambda_2$  are exchange rate constants, month<sup>-1</sup>;

$C_1$  and  $C_2$  are constants determining shares of concentrations involved in fast/slow process.

Such form of the dependence of soil concentrations on time is characteristic of a process with two characteristic times of exchange: fast exchange characteristic time  $T_{1/2}^1 = \ln(2)/\lambda_1$  and slow exchange characteristic time  $T_{1/2}^2 = \ln(2)/\lambda_2$ . At the clearance stage time dependence of soil concentrations has the form:

$$C_{soil} = C_1 e^{-\lambda_1 t} + C_2 e^{-\lambda_2 t}, \quad \lambda_1 > \lambda_2$$

where  $t$  is the time (months);

$\lambda_1$  and  $\lambda_2$  are exchange rate constants, month<sup>-1</sup>;

$C_1$  and  $C_2$  are constants determining shares of concentrations involved in fast/slow process.

with the same interpretation of  $\lambda_1$  and  $\lambda_2$ .

The values of parameters obtained by the approximation with corresponding characteristic times are shown in Table 48. As seen from the plots in Figs. 11–14, bi-exponential approximation well explains the trends of soil concentrations both at accumulation and clearance phases.

**Table 48.** Parameters of multi-exponential approximation

|                    |                   | EVN-BETR and UK model |          | CAM/POPs |          | SimpleBox |          | MSCE-POP |          |
|--------------------|-------------------|-----------------------|----------|----------|----------|-----------|----------|----------|----------|
|                    |                   | Slow                  | Fast     | Slow     | Fast     | Slow      | Fast     | Slow     | Fast     |
| Accumulation phase | $\lambda$         | 8.70E-03              | 8.70E-03 | 5.90E-03 | 9.75E-02 | 3.21E-03  | 3.21E-03 | 2.84E-03 | 1.73E-02 |
|                    | $T_{1/2}$ , years | 6.64                  | 6.64     | 9.79     | 0.59     | 18.00     | 17.99    | 20.37    | 3.35     |
| Clearance phase    | $\lambda$         | 9.30E-03              | 9.61E-03 | 4.03E-03 | 1.00E-02 | 3.25E-03  | 3.25E-03 | 3.27E-03 | 1.00E-02 |
|                    | $T_{1/2}$ , years | 6.21                  | 6.01     | 14.32    | 5.78     | 17.79     | 17.78    | 17.68    | 5.78     |

The analysis of calculated characteristic times for all considered models shows that these models can be divided into two groups. First group (EVN-BETR and UK model and SimpleBox) are characterized by very close characteristic times for fast and slow exponentials. In essence, these models realize mono-exponential trends of POP soil contamination. Also, for these two models characteristic times of accumulation and clearance are very close to each other. The predicted characteristic times differ three times between these two models (6.6 against 18 years).

Another two models (CAM/POPs and MSCE-POP) demonstrate the presence of both fast and slow exponents in soil concentration trends at accumulation and clearance phases. The characteristic times for slow exponential vary between 10 and 20 years depending on model. The characteristic times for fast exponential (fast exchange) vary between 0.6 and 5.8 years.

The results obtained for PCB-28 and PCB-180 are similar and can be found in Annexes D and E.

Thus, there is much similarity in the description of processes of POP accumulation and clearance processes. However, the parameterization of these processes are subject to further clarification.

## 4.5. Gaseous exchange between atmosphere and water

### 4.5.1. Model approaches

Similar to the previous section, in the participating models the description of atmosphere/water gaseous exchange are based on two-film model of intermedia diffusion. Detailed descriptions of this process used in the models can be found in Table 53 and Annex C.

There also exists a large diversity of approaches for the evaluation of transfer velocities at air/water interface. In CliMoChem model diffusion rates - air to water and water to air are calculated using air-over-water and in-water transfer velocities taken from [Mackay and Paterson, 1991] and then dry gaseous deposition and revolatilization fluxes are evaluated using these velocities. For the description of air-water diffusion with the help of fugacity approach, EVN-BETR and UK-MODEL also use constant values of air-water transport velocities. In G-CIEMS air-side and water-side mass transfer coefficient are calculated as the ratio of molecular diffusivity and diffusion path length for air and water. Other participating models use mass transfer velocities, which are dependent on the values of wind speed. Thus, in DEHM-POP model exchange velocities dependent on the wind speed are calculated on the basis of the two-film layer resistance method. In CAM/POPs model the results by [Mackay et al., 1983; Schwarzenbach et al., 1993] are used for calculations of mass transfer velocities. In SimpleBox model absorption from gas phase by water and volatilization from water are calculated with the help of mass transfer coefficients also dependent on the wind speed value. In MSCE-POP model transfer velocities are also dependent on the values of wind speed. In addition, foaming process and expansion of sea area due to wave disturbance are taken into account in this model (see [Strukov, 2001]).

Of note that, EVN-BETR and UK-MODEL, SimpleBox and CAM/POPs models consider gaseous exchange between the atmosphere and freshwater. Other participating models take in consideration seawater compartment. Suspended particulate matter in water compartment is considered in SimpleBox and CliMoChem models. For all models, depth of considered water layers varies in very wide range (3-4600 metres).

Below the results of calculation experiments on air/soil exchange obtained by seven models are compared.

### 4.5.2. Input data

Four sets of input data are proposed for modelling experiments with PCB-153.

**Table 49.** Input data for calculation experiments with PCB-153 describing air/water exchange

| N   | Experiment 1 | Experiment 2 | Experiment 3 | Experiment 4 |
|---|--------------|--------------|--------------|--------------|
| Average ambient temperature, °C                     | 10           | 13.9         | 0            | 25           |
| Air concentration, gaseous phase, pg/m <sup>3</sup> | 14.3         | 3.8          | 2.5          | 23           |
| Mean wind velocity, m/sec                           | 5            | 3.25         | 6            | 2            |

**Output:** calculation of PCB-153 water concentrations, pg/l and gaseous fluxes from and to water and/or net gaseous flux to water, ng/m<sup>2</sup>/d;

### 4.5.3. Comparison of the results

Numerical results of calculations of water concentrations and gaseous flux to water obtained by participating models and their analysis are presented for PCB-153 in this Subsection. The corresponding results for PCB-28 and PCB-180 can be found in Annexes D and E.

The analysis is also performed into two stages. At the first stage we present an analysis of the calculated concentrations and gaseous fluxes to water and characterize the dispersion in these values in each experiment. At the second stage we analyze pairwise differences between participating models using the regression analysis.

*Analysis of the experiments.* For evaluation of results obtained by the participating models, we use the following statistical parameters for each experiment:

- $m$  is the average water concentrations or average gaseous flux to water for participating models;
- $\sigma$  is the square deviation;

Calculated values of water concentrations for PCB-153 together with  $m$  and  $\sigma$  are presented in Table 50. Comparison of absolute values of calculated gaseous flux to water for PCB-153 and the above mentioned statistical parameters for each experiment are given in Table 52. Short comments to the calculations made by participants can be found in Table 53. CAM/POPs model has made calculations on these experiments using dynamic approach. Other participating models used steady-state approach.

If compare the absolute values of calculated water concentrations presented in Table 50, it is seen that there is a large dispersion of water concentration values calculated by the participating models. Results of CliMoChem model differ from other models' results more than order of magnitude. This difference leads to significant bias of averaged values of water concentrations to the maximum values obtained by this model. For each experiment, square deviation  $\sigma_{\phi}$  between different model calculations (see last column in Table 50) substantially exceed the averaged value of water concentrations.

**Table 50.** Calculation results: water concentrations of PCB-153 (pg/l) calculated by all participating models and statistical parameters used for evaluation

| N | EVN-BETR and UK-MODEL | CAM/POPs | DEHM-POP | CliMoChem | G-CIEMS | SimpleBox | MSCE-POP | $m$  | $\sigma$ |
|---|-----------------------|----------|----------|-----------|---------|-----------|----------|------|----------|
| 1 | 5.56                  | 8.40     | 7.10     | 8497.85   | 30.15   | 20.30     | 7.90     | 1225 | 3207     |
| 2 | 0.98                  | 24.00    | 1.25     | 1514.86   | 7.44    | 3.09      | 1.44     | 222  | 570      |
| 3 | 3.11                  | 4.8      | 3.74     | 4103.52   | 5.92    | 5.88      | 3.76     | 590  | 1549     |
| 4 | 2.10                  | 3.0      | 2.51     | 2995.49   | 32.47   | 6.14      | 3.09     | 435  | 1129     |

In Table 51 similar statistical evaluation is presented for a group of participating models, which obtained close results of water concentration values of PCB-153. Differences in their calculated absolute values are within an order of magnitude. At that it can be seen that  $m$  values become more indicative for their comparison. In two cases (experiments 1 and 3), square deviation  $\sigma_{\phi}$  between different results (see last column in Table 51) do not exceed the averaged values of water concentration. For other experiments, the deviations are more remarkable.

**Table 51.** Calculation results: statistical evaluation of PCB-153 water concentrations (pg/l) calculated by models having results of the same order

| N | EVN-BETR and UK-MODEL | CAM/POPs | DEHM-POP | G-CIEMS | SimpleBox | MSCE-POP | $m$  | $\sigma$ |
|---|-----------------------|----------|----------|---------|-----------|----------|------|----------|
| 1 | 5.56                  | 8.40     | 7.10     | 30.15   | 20.30     | 7.90     | 13.2 | 9.8      |
| 2 | 0.98                  | 24.00    | 1.25     | 7.44    | 3.09      | 1.44     | 6.4  | 9.0      |
| 3 | 3.11                  | 4.8      | 3.74     | 5.92    | 5.88      | 3.76     | 4.5  | 1.2      |
| 4 | 2.10                  | 3.0      | 2.51     | 32.47   | 6.14      | 3.09     | 8.2  | 12.0     |

Considering results of calculations of gaseous flux to water (See Table 52), we can observe much better agreement for this parameter than for water concentration results between all models calculations. Square deviation  $\sigma_{\varphi}$  presented in last column of Table 52 do not exceed the averaged value of fluxes. It testifies that all models give rather close results on calculation of gaseous fluxes to water in terms of absolute values.

**Table 52.** Calculation results: Gaseous flux to water of PCB-153 calculated by all participating models and statistical parameters used for evaluation, ng/m<sup>2</sup>/d

| N | EVN-BETR and UK-MODEL | CAM/POPs | CliMoChem | G-CIEMS | SimpleBox | MSCE-POP | <i>m</i> | $\sigma$ |
|---|-----------------------|----------|-----------|---------|-----------|----------|----------|----------|
| 1 | 2.60                  | 2.08     | 0.86      | 1.02    | 4.59      | 2.25     | 2.2      | 1.3      |
| 2 | 0.56                  | 0.62     | 0.21      | 0.25    | 0.74      | 0.54     | 0.5      | 0.2      |
| 3 | 0.66                  | 0.40     | 0.17      | 0.20    | 1.12      | 0.42     | 0.5      | 0.4      |
| 4 | 1.71                  | 1.49     | 0.86      | 1.10    | 1.95      | 2.24     | 1.6      | 0.5      |

**Table 53.** Comments

| Models                | Physical-chemical data set | Depth of considered water layer, metres | Comments  |
|-----------------------|----------------------------|---|---|
| EVN-BETR and UK-MODEL | Own                        | 20                                      | Steady-state approach;<br>Freshwater;<br>Individual/own dataset extremely close to the reference dataset;<br>The flux was calculated as Gaseous flux = $D_{\text{air-water}} \cdot \text{Fugacity (Pa)}$<br>$D_{\text{air-water}} = \text{Water Area} / [(1 / (\text{MTC}_{\text{Casa}} \cdot Z_{\text{air}}) + (1 / (\text{MTC}_{\text{Cass}} \cdot 0.8 \cdot Z_{\text{water}})))]$<br>Fresh water area = $1.7 \cdot 10^{11} \text{ m}^2$<br>MTC <sub>Casa</sub> : Air side air-water transport velocity = 30 m/h<br>MTC <sub>Cass</sub> : water side air-water transport velocity = 0.03 m/h  |
| SimpleBox             | Reference                  | 3                                       | Steady-state approach;<br>Freshwater;<br>Inclusion of suspended particulate matter;<br>Transport between air and water entirely by gas exchange. Other exchange mechanisms "switched off".<br>Concentration in air adjusted by setting emission to air.<br>Transport across air-water interface calculated by classical double film diffusion model.<br>Absorption from gas phase by water (mol/m <sup>2</sup> /s) = FR <sub>gas</sub> (-) · kaw(gas) (m/s) · CONCAir (mol/m <sup>3</sup> )<br>Volatilization from water (mol/m <sup>2</sup> /s) = FR <sub>water</sub> (-) · kaw(water) (m/s) · CONCwater (mol/m <sup>3</sup> )<br>kaw(gas) = overall gas-referenced air-water mass transfer coefficient = $kaw.\text{air} \cdot kaw.\text{water} / (kaw.\text{air} \cdot Kh + kaw.\text{water})$<br>kaw(soil) = overall water-referenced air-water mass transfer coefficient = $kaw.\text{air} \cdot kaw.\text{water} / (kaw.\text{air} + kaw.\text{water}/Kh)$<br>Kh = dimensionless air-water equilibrium constant<br>kaw.air = partial mass transfer coefficient for air-side of the air-water interface (m/s) = $0.01 \cdot (0.3 + 0.2 \cdot \text{WINDspeed}) \cdot (0.018/\text{Molweight})^{(0.67 \cdot 0.5)}$<br>kaw.water = partial mass transfer coefficient for water-side of the air-water interface (m/s) = $0.01 \cdot (0.0004 + 0.00004 \cdot \text{WINDspeed}^2) \cdot (0.032/\text{Molweight})^{(0.5 \cdot 0.5)}$<br>WINDspeed = mean wind velocity from input set<br>Molweight = molecular weight PCB-congener |
| CAM/POPs              | Own                        | Surface water                           | Dynamic approach;<br>Freshwater   |
| CliMoChem             | Own                        | 200                                     | Steady-state approach;<br>Seawater;<br>Inclusion of suspended particulate matter;<br>Only dry gaseous deposition, revolatilization and degradation in water were considered (Model Geometry: box length: 100000 m; box width: 100000 m; fraction of water area to total area: 0.7162)<br>Dry gaseous deposition flux=diffusion rate air to water* concentration in air*volume air/(water volume*depth of water layer)<br>Revolatilization flux = (diffusion rate water to air+degradation rate) * steady state concentration in water * water volume/(water volume/depth of water layer)  |

| Models   | Physical-chemical data set | Depth of considered water layer, metres | Comments   |
|----------|----------------------------|---|--|
| MSCE-POP | Own                        | 4600 (15 layers)                        | Steady-state approach;<br>Seawater;<br>POP flux through the sea surface:<br>$F_z _{z=0} = \alpha_1(c_{ga} / K_{HR}(T) - c_d)((1 - \alpha_2)D_\mu / \delta + \alpha_2 K_{HR} h_f)$<br>$D_\mu = 5.14 \cdot 10^{-10}$ - molecular diffusion coefficient in water, m <sup>2</sup> /s;<br>$\delta_0 = 4 \cdot 10^{-5}$ - surface molecular layer depth at zero wind speed, m;<br>$h_f = 8 \cdot 10^{-3}$ - foam settling rate on the sea surface, m/s;<br>$\alpha_1$ - coefficient of surface sea area expansion due to wave disturbance;<br>$\alpha_2$ - coefficient describes the relative sea surface area covered with foam at strong wind;<br>$\alpha_1$ and $\alpha_2$ are dependent on wind speed absolute value near the surface; |
| G-CIEMS  | Reference                  | 20                                      | Steady-state approach; Seawater  |
| DEHM-POP | Own                        | 75                                      | Steady-state approach; Seawater  |

**Pairwise comparison of model results.** The analysis of pairwise differences between calculation results obtained by all models is performed with the help of regression equation (9). Below brief analysis of the correlation coefficient  $r_{12}$  of the compared models, regression coefficients  $\alpha_{12}$  and  $\beta_{12}$  and residual square deviation  $\sigma_{12}^{res}$  is given.

Pairwise correlation coefficients for water concentrations calculated by all participating models are presented in Table 54. It is seen that their values varies in the very wide range from -0.50 to almost 1. At that, there is no correlation between CAM/POPs and all other models. Results of G-CIEMS model are poor correlated with other models also. However, in spite of the fact that absolute values of water concentrations of EVN-BETR and UK-MODEL, DEHM-POP, CliMoChem, SimpleBox and MSCE-POP differ from each other substantially, the variations of the corresponding numerical values caused by change of environmental conditions between different experiments are similarly described by them. Correlation coefficient for these models is very close to 1.

**Table 54.** Correlation coefficients for water concentrations

|                       | CAM/POPs | DEHM-POP | CliMoChem | G-CIEMS | SimpleBox | MSCE-POP |
|-----------------------|----------|----------|-----------|---------|-----------|----------|
| EVN-BETR and UK-MODEL | -0.48    | 1.00     | 0.99      | 0.46    | 0.95      | 0.99     |
| CAM/POPs              | -        | -0.44    | -0.41     | -0.50   | -0.29     | -0.44    |
| DEHM-POP              | -        | -        | 1.00      | 0.46    | 0.96      | 0.99     |
| CliMoChem             | -        | -        | -         | 0.50    | 0.98      | 1.00     |
| G-CIEMS               | -        | -        | -         | -       | 0.59      | 0.54     |
| SimpleBox             | -        | -        | -         | -       | -         | 0.98     |

Correlation coefficients for values of gaseous flux to water calculated by all models range from 0.73 to 1 (See Table 55). It is evident that results of all participating models well correlated with each other in describing air–water gaseous exchange fluxes. Most close results are obtained between EVN-BETR and UK-MODEL and CAM/POPs, between G-CIEMS and CliMoChem, between G-CIEMS and MSCE-POP models and between MSCE-POP and CliMoChem models (correlation coefficient is all cases is equal to 1.00).

**Table 55.** Correlation coefficients for gaseous flux to water

|                       | CAM/POPs | CliMoChem | G-CIEMS | SimpleBox | MSCE-POP |
|-----------------------|----------|-----------|---------|-----------|----------|
| EVN-BETR and UK-MODEL | 0.99     | 0.92      | 0.90    | 0.96      | 0.92     |
| CAM/POPs              | -        | 0.95      | 0.93    | 0.92      | 0.95     |
| CliMoChem             | -        | -         | 1.00    | 0.77      | 1.00     |
| G-CIEMS               | -        | -         | -       | 0.73      | 1.00     |
| SimpleBox             | -        | -         | -       | -         | 0.78     |

For further evaluation of closeness of calculated results obtained by models, regression coefficients  $\alpha_{12}$  and  $\beta_{12}$  and the residual square deviation,  $\sigma_{12}^{\text{res}}$  are used below.

Values of regression coefficients  $\alpha$  and  $\beta$  for water concentrations calculated for all pairs of models are given in Table 56. It is seen that maximum values of coefficients  $\alpha$  and  $\beta$  are characteristic for the comparison of CliMoChem with other models ( $\alpha$ : -129.469 - 1531.35;  $\beta$ : -220.42 - 5579.09). It is obvious since absolute values of this model's results differ substantially from others. For the rest of pairs of the models,  $\alpha$  varies far less (from -2.33 to 3.76).  $|\beta|$  varies not very much in comparison with mean values of water concentrations (lying in the range from -2.20 to 26.53).

**Table 56.** Coefficients of regression dependence between the models ( $\alpha / \beta$ ) for water concentrations

|                             | CAM/POPs      | DEHM-POP     | CliMoChem          | G-CIEMS       | SimpleBox     | MSCE-POP     |
|-----------------------------|---------------|--------------|--------------------|---------------|---------------|--------------|
| EVN-BETR and UK-MODEL       | -2.33 / 16.89 | 1.29 / -0.13 | 1531.35 / -220.42  | 3.35 / 9.15   | 3.76 / -2.20  | 1.40 / -0.05 |
| CAM/POPs                    | –             | -0.12 / 4.81 | -129.469 / 5579.09 | -0.75 / 26.53 | -0.24 / 11.21 | -0.13 / 5.31 |
| DEHM-POP                    | –             | –            | 1193.26 / -77.47   | 2.62 / 9.44   | 2.96 / -1.95  | 1.09 / 0.08  |
| CliMoChem                   | –             | –            | –                  | 0.002 / 8.90  | 0.003 / -1.91 | 0.001 / 0.14 |
| G-CIEMS                     | –             | –            | –                  | –             | 0.32 / 2.74   | 0.10 / 2.06  |
| SimpleBox                   | –             | –            | –                  | –             | –             | 0.35 / 0.98  |
| Mean concentration in water | 10.05         | 3.65         | 4277.93            | 19.00         | 8.85          | 4.05         |

Coefficients of regression dependence between the models ( $\alpha$  and  $\beta$ ) for gaseous flux to water are presented in Table 57. One can see that in this case the difference between the participating models in  $\alpha$  and  $\beta$  values is much less than for water concentrations. For all models  $\alpha$  varies not substantially (from 0.37 to 3.47), and  $\beta$  ranges from -0.28 to 0.42. The closest results ( $\alpha$  values are close to 1 and  $|\beta|$  values are comparable with mean values of fluxes) are obtained by the following pairs of models: CAM/POPs and EVN-BETR and UK-MODEL; G-CIEMS and CliMoChem; MSCE-POP and EVN-BETR and UK-MODEL; MSCE-POP and CAM/POPs.

**Table 57.** Coefficients of regression dependence between the models ( $\alpha / \beta$ ) for gaseous flux to water

|                            | CAM/POPs    | CliMoChem    | G-CIEMS      | SimpleBox    | MSCE-POP     |
|----------------------------|-------------|--------------|--------------|--------------|--------------|
| EVN-BETR and UK-MODEL      | 0.80 / 0.05 | 0.37 / 0.01  | 0.45 / 0.02  | 1.72 / -0.28 | 0.98 / 0.01  |
| CAM/POPs                   | –           | 0.47 / -0.02 | 0.57 / -0.02 | 2.04 / -0.24 | 1.24 / -0.06 |
| CliMoChem                  | –           | –            | 1.25 / -0.01 | 3.47 / 0.28  | 2.63 / -0.02 |
| G-CIEMS                    | –           | –            | –            | 2.62 / 0.42  | 2.10 / 0.01  |
| SimpleBox                  | –           | –            | –            | –            | 0.46 / 0.40  |
| Mean gaseous flux to water | 1.15        | 0.53         | 0.64         | 2.10         | 1.36         |

Calculations of pairwise residual square deviation  $\sigma$  given in Table 58 and 59 allow to assess the reliability of comparative analysis given above.

**Table 58.** Residual square deviation,  $\sigma$  for water concentrations

|                       | CAM/POPs | DEHM-POP | CliMoChem | G-CIEMS | SimpleBox | MSCE-POP |
|-----------------------|----------|----------|-----------|---------|-----------|----------|
| EVN-BETR and UK-MODEL | 14.58    | 0.20     | 537.54    | 21.96   | 4.29      | 0.61     |
| CAM/POPs              | -        | 3.92     | 4744.96   | 21.35   | 12.86     | 4.28     |
| DEHM-POP              | -        | -        | 326.00    | 21.92   | 3.78      | 0.49     |
| CliMoChem             | -        | -        | -         | 21.43   | 2.96      | 0.26     |
| G-CIEMS               | -        | -        | -         | -       | 10.82     | 3.99     |
| SimpleBox             | -        | -        | -         | -       | -         | 0.97     |

**Table 59.** Residual square deviation,  $\sigma$  for gaseous flux to water

|                       | CAM/POPs | CliMoChem | G-CIEMS | SimpleBox | MSCE-POP |
|-----------------------|----------|-----------|---------|-----------|----------|
| EVN-BETR and UK-MODEL | 0.23     | 0.26      | 0.37    | 0.86      | 0.68     |
| CAM/POPs              | -        | 0.21      | 0.32    | 1.20      | 0.55     |
| CliMoChem             | -        | -         | 0.06    | 1.90      | 0.01     |
| G-CIEMS               | -        | -         | -       | 2.05      | 0.13     |
| SimpleBox             | -        | -         | -       | -         | 1.11     |

It is seen that the values of residual square deviation are maximum for the comparison of water concentrations calculated by CliMoChem with those obtained by other models. For the rest of the model pairs  $\sigma$  lies within the interval 0.2 - 21.96. For results of calculations of gaseous flux to water,  $\sigma$  ranges from 0.01 to 2.05.

For PCB-28 (See Annex D), a difference in absolute values of calculated water concentrations is also large. However, max/min ratio of values of PCB-28 gaseous fluxes to water lies within factor 3-5 only. The results obtained for PCB-180 are similar to the results on PCB-153 and can be found in Annex E. All models (except for DEHM-POP) similarly describe the variations of water concentration values for both congeners caused by change of environmental conditions between different experiments (correlation coefficient is very close 1). Correlation coefficients for values of gaseous flux to water of PCB-28 and PCB-180 calculated by all models range from 0.84 to 1 and from 0.93 to 1.00, respectively.

## 4.6. Gaseous exchange between atmosphere and vegetation

### 4.6.1. Model approaches

Similar to the descriptions of other gaseous exchange processes considered above, in the participating models atmosphere/vegetation gaseous exchange is also described with the help of theory of intermedia diffusion. Detailed descriptions of this process used in the models can be found in Table 63 and Annex C.

Not all models include vegetation as environmental media for calculations. In description of gaseous exchange between vegetation and atmosphere on the basis of fugacity approach, EVN-BETR and UK-MODEL use constant values of air-vegetation transport velocities. In SimpleBox model absorption from gas phase by plant and volatilization from plant are calculated with the help of constant value of mass transfer coefficient. In CliMoChem models fluxes between atmosphere and vegetation are calculated via atmosphere/vegetation diffusion rates. These rates are supposed to be dependent on climatic zones. In CliMoChem three types of vegetation are considered: grass, coniferous forest and deciduous forest. MSCE-POP describes air/vegetation exchange on the basis of resistance analogy. At that mass transfer coefficient is assumed to be directly proportional to  $K_{oa}$  value. Similar to CliMoChem in MSCE-POP grass, coniferous forest and deciduous forest are treated separately. Models G-CIEMS and CAM/POPs use description of air/vegetation exchange similar to that for air/soil but with another parameter values. The model DEHM-POP does not include vegetation compartment.

At present calculation experiments with vegetation are made by EVN-BETR and UK-MODEL, SimpleBox and MSCE-POP. The comparison of the results of calculation experiments are presented below.

## 4.6.2. Input data

Four sets of input data are proposed for modelling experiments with PCB-153.

**Table 60.** Input data for calculation experiments with PCB-153 describing air/vegetation exchange

| N   | Experiment 1 | Experiment 2 | Experiment 3 | Experiment 4 |
|---|--------------|--------------|--------------|--------------|
| Type of vegetation compartment:                     | Grass        | Grass        | Grass        | Grass        |
| Average ambient temperature, °C                     | 5            | 25           | 11           | 18           |
| Air concentration, gaseous phase, pg/m <sup>3</sup> | 6            | 19           | 3            | 14           |
| Mean wind velocity, m/sec                           | 4            | 4            | 4            | 4            |

**Output:** calculation of PCB-153 concentration in vegetation, ng/g dry weight and gaseous fluxes from and to vegetation and/or net gaseous flux to vegetation, ng/m<sup>2</sup>/d;

## 4.6.3. Comparison of the results

Numerical results of experiments on calculations of concentration in vegetation and net gaseous flux to vegetation obtained by participating models and their analysis are presented in this Section for PCB-153. The corresponding results for other substances can be found in Annexes D and E.

Since optional experiments on gaseous exchange between atmosphere and vegetation were made by three participating models only, such statistical parameters as the average concentration in vegetation and net gaseous flux to vegetation and square deviation of these results can not be useful in the analysis of results. It is more reasonable to make comparison of the absolute values themselves. Calculated values of concentration in vegetation for PCB-153 are presented in Table 61. Comparison of absolute values of calculated net gaseous flux to vegetation for PCB-153 are given in Table 62. Short comments to the calculations can be found in Table 63.

It is seen that dispersion of absolute values of concentrations in vegetation calculated by the models is rather large. The difference between maximum and minimum values of this parameter varies within wide range from 3 to 10. Comparing the results on net deposition flux calculations, we can see that in EVN-BETR and UK-MODEL volatilization flux from vegetation exceed flux from air to vegetation for all four experiments (that is re-emissions from plant takes place) in contrary to MSCE-POP and SimpleBox models. At that the difference in absolute values is very large. However, for the last two models, absolute values are very close to each other.

**Table 61.** Calculation results: concentrations of PCB-153 in vegetation calculated by models, ng/g d.w

| N            | Air concentration, pg/m <sup>3</sup> | EVN-BETR and UK-MODEL | SimpleBox * | MSCE-POP |
|--------------|--------------------------------------|-----------------------|-------------|----------|
| Experiment 1 | 6                                    | 0.220                 | 0.401       | 0.104    |
| Experiment 2 | 19                                   | 0.050                 | 0.483       | 0.252    |
| Experiment 3 | 3                                    | 0.053                 | 0.159       | 0.050    |
| Experiment 4 | 14                                   | 0.089                 | 0.529       | 0.217    |

\* - ng/g wet weight.

**Table 62.** Calculation results: net gaseous flux of PCB-153 to vegetation calculated by models, ng/m<sup>2</sup>/d

| N            | Air concentration, pg/m <sup>3</sup> | EVN-BETR and UK-MODEL | SimpleBox | MSCE-POP |
|--------------|--------------------------------------|-----------------------|-----------|----------|
| Experiment 1 | 6                                    | -0.07                 | 0.40      | 0.33     |
| Experiment 2 | 19                                   | -0.03                 | 0.82      | 0.81     |
| Experiment 3 | 3                                    | -0.02                 | 0.18      | 0.16     |
| Experiment 4 | 14                                   | -0.0004               | 0.71      | 0.70     |

**Table 63. Comments**

| Models                | Physical-chemical data set | LAI, m <sup>2</sup> /m <sup>2</sup> | Comments  |
|-----------------------|----------------------------|-------------------------------------|---|
| EVN-BETR and UK-MODEL | Own                        | 4                                   | Steady-state approach;<br>Individual/own dataset extremely close to the reference dataset;<br>The flux was calculated as Gaseous flux = Dair-veg · Fugacity (Pa)<br>Dair-veg = 1/((1/(Veg Area · Veg_airMTC · Z <sub>veg</sub> )) + (1/(Veg Area·Air_VegMTC · Z <sub>air</sub> )))<br>Veg_area: Vegetation area = 8·10 <sup>12</sup> m <sup>2</sup><br>Veg_airMTC: Vegetation side air-vegetation transport velocity = 10.8 m/h<br>Air_VegMTC : Air side air-vegetation transport velocity = 9 m/h  |
| SimpleBox             | "Reference"                | 3.9                                 | Steady-state approach;<br>SimpleBox works with (wet) bulk vegetation densities (900 kg/m <sup>3</sup> by default); concentrations in vegetation expressed on wet weight basis.<br>Specific amount of plant material given in SimpleBox as mass per unit area (1.2 kg/m <sup>2</sup> by default).<br>Fluxes to and from vegetation expressed per unit leaf area.<br>Absorption from gas phase by plant (mol/m <sup>2</sup> /s) = FRgas (-) · kav(gas) (m/s) · CONCair (mol/m <sup>3</sup> )<br>Volatilization from plant (mol/m <sup>2</sup> /s) = kav(gas) (m/s) / Kva (-) · CONCair (mol/m <sup>3</sup> )<br>kav(gas) = overall gas-referenced air-plant mass transfer coefficient = 10 <sup>-3</sup> m/s by default<br>Kva = dimensionless vegetation-air euilibrium constant |
| MSCE-POP              | Own                        | 1                                   | Steady-state approach<br>$\frac{dC_V}{dt} = \frac{1}{R_{tot}} \cdot (C_a^g - C_V / K_{Va}),$<br>where $C_a^g$ - air concentration of a pollutant;<br>$C_V$ - concentration in the vegetation of a given type;<br>$K_{Va}$ - bioconcentration factor (BCF);<br>$R_{tot}$ - total resistance to the gaseous exchange given by the formula.<br>$R_{tot} = R_a + a_v / k,$<br>where $R_a$ - aerodynamic resistance of turbulent atmospheric layer;<br>$k$ - mass transfer coefficient, m/s;<br>$a_v$ - specific surface area of vegetation, m <sup>2</sup> /m <sup>3</sup> (assumed value is 8000, see [Duyzer and van Oss, 1997])  |

The comparison of calculated values of concentrations in vegetation is also displayed in Fig. 15. Calculation results of Simple Box and MSCE-POP models show very close character of variability of concentration values in dependence with variability of input data for each experiments. For these models' result on calculation of net gaseous fluxes, we can see the same tendency.

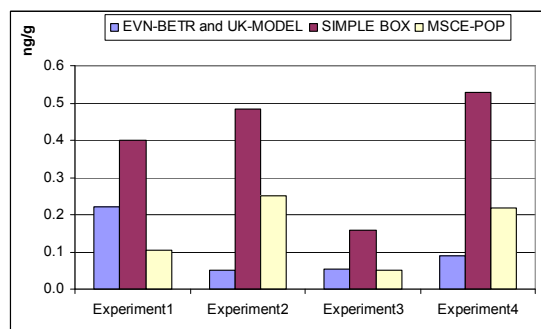


**Fig.15. The comparison of calculated values of concentrations in vegetation**

Correlation coefficients for concentration in vegetation and net gaseous flux calculated by the models are presented in Tables 64 and 65.

**Table 64. Correlation coefficients for concentrations in vegetation**

|                       | SimpleBox | MSCE-POP |
|-----------------------|-----------|----------|
| EVN-BETR and UK-MODEL | 0.15      | -0.30    |
| SimpleBox             | –         | 0.88     |

**Table 65.** Correlation coefficients for net gaseous flux

|                       | SimpleBox | MSCE-POP |
|-----------------------|-----------|----------|
| EVN-BETR and UK-MODEL | 0.27      | 0.34     |
| SimpleBox             | –         | 1.00     |

According to the values of pairwise correlation coefficients for both parameters, only two models SimpleBox and MSCE-POP describe tendency of gaseous exchange variability similarly. Correlation coefficients for concentrations and fluxes are equal to 0.88 and 1.0, respectively. It is evident that results of EVN-BETR and UK-MODEL are not correlated with other models.

The values of coefficients  $\alpha$  and  $\beta$  calculated for the regression between SimpleBox and MSCE-POP models in values of calculated concentration in vegetation and net gaseous flux are presented in Table 66 and 67.

**Table 66.** Coefficients of regression dependence between the models ( $\alpha / \beta$ ) for concentrations in vegetation

|          | SimpleBox     |
|----------|---------------|
| MSCE-POP | 0.51 / -0.044 |

**Table 67.** Coefficients of regression dependence between the models ( $\alpha / \beta$ ) for net gaseous flux

|          | SimpleBox     |
|----------|---------------|
| MSCE-POP | 1.04 / -0.045 |

Considering concentration in vegetation, the differences between these models is determined by scaling coefficient  $\alpha$ , which totals to 0.51 in this case. However, it is seen that  $\alpha$  is very close to 1 for net gaseous flux results. Coefficients  $\beta$  are small enough in both cases compared with mean values of concentrations and fluxes.

For results on PCB-28 and PCB-180 (see Annexes D and E), a dispersion in absolute values of concentrations in vegetation and net deposition fluxes calculated for all experiments by three participating models is also large. However, values of PCB-180 concentrations are closer to each other than results for PCB-28. Thus, the differences between maximum and minimum values of this parameter calculated by the participating models vary within ranges from 3 to 7 and from 13 to 41, respectively. The difference in absolute values of fluxes of both congeners are more substantial than the dispersion of their concentrations. Correlation coefficients for PCB-180 concentration in vegetation vary in the range from 0.63 to 1.00 between all pairs of models; for PCB-28 a good correlation is observed between SimpleBox and EVN-BETR and UK-MODEL and between SimpleBox and MSCE-POP models. Results on net gaseous fluxes of PCB-28 and PCB-180 are well correlated for SimpleBox and MSCE-POP models.

## Conclusions

At the preliminary stage of POP models intercomparison study short descriptions of 13 models were submitted by participants. On the basis of these descriptions a short summary of model types participating in the intercomparison study with indication of model type, spatial and temporal resolution, environmental media used, and processes taken into account was compiled. This analysis was used for the determination of the intercomparison procedure at Stage I.

Stage I of the intercomparison study of POP models was aimed at the comparison of:

- modelling approaches to the description of main processes determining POP fate in the environment, namely:
  - gas/particle partitioning in the atmosphere;
  - dry deposition;
  - wet deposition;
  - gaseous exchange between the atmosphere and different types of underlying surface (soil, seawater, vegetation);
  - degradation;
- values of physical-chemical parameters used for modelling;
- results of calculation experiments on the above processes carried out by participating models.

Values of physical-chemical parameters used by participants for the Stage I calculations strongly affect the results of calculation experiments. Comparison of physical-chemical parameters used in participating models and statistical processing of these data is made. Physical-chemical data sets of individual models are compared also with “reference data sets”, which will be used at follow-up Stage II within sensitivity study with respect to basic processes. Thus, analysis of physical-chemical parameters of PCB-153, PCB-28 and PCB-180 shows the following:

- Henry’s law constant and air-water partition coefficient :
  - All models use temperature dependent Henry’s law constant and air-water partition coefficient (except  $H$  value of EVN-BETR and UK-MODEL). Differences in absolute values of Henry’s law constant between all models are very large for PCB-153 and PCB-180. These values differ from each other more than an order of magnitude. Difference in  $H$  values for PCB-28 is much less than for other congeners. Scattering is going down with temperature.
  - If temperature independent  $H$  values of EVN-BETR and UK-MODEL are not taken into account, max/min ratio of  $H$  and  $K_{aw}$  values for PCB-153 varies within factor 8-9; for PCB-28 - within factor 1-2; and for PCB-180 - within factor 12-22.
- Subcooled liquid vapour pressure:
  - All models use temperature dependent subcooled liquid vapour pressure (except EVN-BETR and UK-MODEL). Differences in absolute values of  $p_{ol}$  between all models are more substantial for PCB-153 and PCB-180 than that for PCB-28.
  - For PCB-153 and PCB-28 there is a high similarity between the values of subcooled liquid vapour pressure presented by models using temperature dependence of this parameter (max/min ratio is about 1.1 and 1.3, respectively). For PCB-180 max/min ratio of  $p_{ol}$  values lies within factor 7.
- Octanol/water partition coefficient:

- Difference in absolute values of octanol/water partition coefficient between all models is not large. Max/min ratio of  $K_{ow}$  values for PCB-153 varies from 2 to 5; for PCB-28 - from 2 to 4; and for PCB-180 – from 2 to 3. If not take into account the temperature independent value of MSCE-POP, max/min ratio for all considered congeners to a variable degree comes down.
- This parameter is changing with temperature within factor 3-4 for considered interval of temperatures (-10-25°C).
- Scattering of coefficients of temperature dependences among all models lies within factors 1 – 4.
- Octanol/air partition coefficient:
  - There is a large similarity in values of octanol/air partition coefficient obtained with the use of existing temperature dependencies.
  - Max/min ratios between absolute values of  $K_{oa}$  used by all participants at different temperatures range from 5 to 6 for PCB-153; from 2 to 5 for PCB-28 and from 6 to 8 for PCB-180.
  - Max/min ratio of coefficients of temperature dependences of  $K_{oa}$  for the considered congeners equals practically to 1.0.
- Organic carbon/water partition coefficient:
  - Difference between the highest and the lowest values of organic carbon/water partition coefficient is less than an order of magnitude. For the considered temperature interval, max/min ratio for PCB-153 comes down from 9 to 7.
  - For models using close values of regression coefficients for recalculation of  $K_{oc}$  from  $K_{ow}$  (all models except for G-CIEMS), its values differ within factors of 2-5 for PCB-153; and within factors 2-4 for PCB-28 and PCB-180.
- Water solubility:
  - Values of water solubility used in EVN-BETR and UK-MODEL, SimpleBox and G-CIEMS models are of the same order. Other models do not use this parameter directly.
- Degradation:
  - There is a large difference in absolute values of first order rate constant for the considered media between the models. For all media max/min ratios for PCB-153 vary within the range of 4-10; for PCB-28 – within the range of 2-12; and for PCB-180 – within the range of 3-10.
  - Degradation in air, soil and water is considered in all models. Max/min ratios for PCB-153 vary from 4 to 5; for PCB-28 – from 2 to 12; and for PCB-180 – from 3 to 10.
  - Degradation in vegetation is included in CliMoChem and EVN-BETR and UK-MODEL. Difference of rate constants between the models (max/min ratio) for PCB-153 is around 10; for PCB-28 it equals to 7 and for PCB-180 it is around 6. Degradation in sediments is considered in EVN-BETR and UK-MODEL only.
  - Temperature dependence of rate constant for degradation in air are considered in CAM/POPs, CliMoChem and MSCE-POP models. The difference between temperature dependent values for the considered congeners is within factors 1-2.
  - Degradation in other media than air is temperature dependent in CliMoChem model only.

In order to analyze similarities and distinctions in model descriptions and parameterisations of the above listed processes and to find out “hot spots” in modelling, a number of calculation experiments

with PCB-153 (first priority) and PCB-28 and PCB-180 (second priority) were carried out by the participating models. The analysis of the results of these experiments revealed that:

- Gas/particle partitioning:
  - For the description of gas/particle partitioning, the models mostly use adsorption and absorption approaches. There is not a large difference in values of particulate fraction calculated by both methods.
  - Tendency in variability of calculated particulate fraction of PCB-153 with temperature is described by all models rather closely and the difference in its absolute values is not substantial. The difference of model results can be explained by the difference in  $K_{oa}$  or  $p_{oi}$  values used. Correlation coefficients for PCB-153 are very high for all pairs of models (from 0.83 to 1.00). The main difference between models is determined by scaling factors (from 0.13 to 3.78).
  - The results obtained for PCB-180 and PCB-28 are similar to the results on PCB-153. Dispersion of their absolute values are not large. Correlation coefficients between all pairs of models for PCB-180 vary from 0.75 to 1.00; and for PCB-28 - from 0.98 to 1.00.
- Dry deposition of the particulate phase:
  - The difference between models in the description of this process lies in different methods of calculation of deposition velocity used by the participating models. A large dispersion in calculated values of dry deposition flux is mainly explained by the high scattering of dry deposition velocity values used. The type of underlying surface essentially affects deposition fluxes. According to descriptions of dry deposition accepted in the participating models, parameterizations of the flux are one and the same for all PCB congeners.
  - The values of dry deposition flux for different models are mostly of the same order. A discrepancy in calculated deposition fluxes comes up to an order of magnitude for models distinguishing different types of underlying surface. The largest discrepancy of calculated fluxes to different types of underlying surface takes place for forest: maximum and minimum calculated values differ 150 times. For models distinguishing different types of underlying surface the best correlation is observed for CAM/POPs and MSCE-POP.
- Wet deposition:
  - All models use the inverse dimensionless Henry's law constant for the calculations of washout or scavenging ratio of gaseous phase. A difference in this parameter values used by the models affects the calculation results. The scattering of constant values of scavenging ratio (or washout ratio) used by the most part of participating models for the description of wet deposition of particle bound phase is rather large. CAM/POPs and SimpleBox do not include scavenging ratio in their parameterizations and use the values of aerosol collection efficiency to evaluate scavenging or washout rate of a pollutant.
  - There is a large difference between model calculations made for experiments on wet deposition process. Values of PCB-153 concentrations in precipitation vary within a factor 6-14. Max/min ratio of absolute values of wet deposition flux lies within an order of magnitude for the first two experiments and comes up to 36 times for the highest temperature. For PCB-153, the best correlations are obtained between G-CIEMS and SimpleBox, between G-CIEMS and MSCE-POP models and between MSCE-POP and SimpleBox models (correlation coefficient in all cases is equal to 1.00). Taking into account regression coefficients' values also, these models show the closest results in the experiments of wet deposition process.

- The results of calculation experiments with PCB-28 and PCB-180 show also a large dispersion between the absolute values of concentrations in precipitation and wet deposition fluxes calculated by different models. For PCB-28 there is a good correlation between results of MSCE-POP, ClimoChem and SimpleBox (correlation coefficient is equal to 1). Calculated concentrations of PCB-180 in precipitation are also well correlated between these three models (correlation coefficient vary from 0.91 to 1) and between CAM/POPs and EVN-BETR and UK model (correlation coefficient is equal to 0.76).
- Gaseous exchange between atmosphere and soil
  - All models use one and the same philosophy for the description of atmosphere/soil gaseous exchange – resistance analogy. The difference between model approaches to the description of air/soil exchange is mostly determined by the variability of mass transfer coefficient or diffusion transport velocity values used by the models. The difference between models is also in the number and thickness of considered soil layers.
  - There is rather large difference in absolute values both for calculated soil concentrations and net gaseous flux of PCB-153. However, all models similarly describe the variations of soil concentration values caused by change of environmental conditions between different experiments. Correlation coefficients vary within the range from 0.85 to almost 1. Results on net gaseous flux of PCB-153 are also well correlated for the most part of model pairs except for pairs between G-CIEMS 1 and two models: MSCE-POP 2 and CAM/POPs.
  - For PCB-28 and PCB-180, a large difference in absolute values also takes place both for calculated soil concentrations and net gaseous flux. Correlation coefficients for soil concentration of PCB-28 vary within the range from 0.93 to almost 1 between all pairs of models; for net gaseous flux, a good correlation is observed between SimpleBox and EVN-BETR and UK-MODEL models. Results on soil concentrations and net gaseous fluxes of PCB-180 are well correlated for all model pairs (correlation coefficients range from 0.87 to 1.00 and from 0.85 to 1.00, respectively).
  - Within the optional experiment on POP accumulation and clearance dynamics in soil, the analysis of calculated characteristic times for four considered models shows that these models can be divided into two groups. First group (EVN-BETR and UK model and SimpleBox) are characterized by very close characteristic times for fast and slow exponentials. In essence, these models realize mono-exponential trends of POP soil contamination. Another two models (CAM/POPs and MSCE-POP) demonstrate the presence of both fast and slow exponents in soil concentration trends at accumulation and clearance phases.
- Gaseous exchange between atmosphere and water:
  - The description of atmosphere/water gaseous exchange in all models is based on two-film model of intermedia diffusion. There exist a large diversity of approaches to the evaluation of transfer velocities at air/water interface.
  - For results on PCB-153, a dispersion in absolute values of water concentrations obtained by all models is large. However, EVN-BETR and UK-MODEL, DEHM-POP, ClimoChem, SimpleBox and MSCE-POP similarly describe the variations of water concentration values caused by change of environmental conditions between different experiments. Correlation coefficient for these models is very close to 1. For calculated PCB-153 gaseous fluxes to water, a better agreement between all models calculations is observed than for water concentration results. Correlation coefficients for values of gaseous flux to water calculated by all models range from 0.73 to 1. It is evident that results of all models are well correlated with each other describing air –water gaseous exchange fluxes.

- For PCB-28, a difference in absolute values of calculated water concentrations is also large. However, max/min ratio of values of PCB-28 gaseous fluxes to water lies within factor 3-5 only. The results obtained for PCB-180 are similar to the results on PCB-153. The most part of models similarly describe the variations of water concentration values for both congeners caused by change of environmental conditions between different experiments (correlation coefficient is very close 1). Correlation coefficients for values of gaseous flux to water of PCB-28 and PCB-180 calculated by all models range from 0.84 to 1 and from 0.93 to 1.00, respectively.
- Gaseous exchange between atmosphere and vegetation (optional):
  - Atmosphere/vegetation gaseous exchange is described in all models with the help of theory of intermedia diffusion. Not all models include vegetation as environmental media for calculations. The difference between models is determined by the difference of mass transfer coefficient or diffusion transport velocity values used.
  - A dispersion of absolute values of PCB-153 concentrations in vegetation and net deposition flux calculated for all experiments by three participating models is large. The difference between maximum and minimum values of concentrations varies within wide range from 3 to 10. Absolute values of PCB-153 fluxes are very close to each other in MSCE-POP and SimpleBox models. In addition, Simple Box and MSCE-POP models show very close character of variability of both calculated parameters in dependence with variability of input data for each experiment.
  - A difference in absolute values of concentrations in vegetation and net deposition fluxes calculated for all experiments is also large both for PCB-28 and PCB-180. However, values of PCB-180 concentrations obtained by the models are closer to each other than results for PCB-28. The difference in absolute values of fluxes of both congeners are more substantial than the dispersion of their concentrations. Correlation coefficients for PCB-180 concentration in vegetation vary within the range from 0.63 to 1.00 between all pairs of models; for PCB-28 a good correlation is observed between SimpleBox and EVN-BETR and UK-MODEL and between SimpleBox and MSCE-POP models. Results on net gaseous fluxes of PCB-28 and PCB-180 are well correlated for SimpleBox and MSCE-POP models.

On the basis of the analysis of physical-chemical properties and of the results of calculation experiments, it was found that maximum differences in model output absolute values takes place for deposition processes (dry deposition of particles and wet deposition), and gaseous exchange processes with underlying surfaces. It is seems reasonable to carry out sensitivity study for their model descriptions at the next stages of model intercomparison.

The results obtained at Stage I of the POP model intercomparison study show that all the participating models are able to simulate main processes determining POP fate in the environment. However, our current understanding of POP behaviour is still incomplete and needs further improvement.

## References

- Achman, Hornbuckle, Eisenreich [1993]  
Atmosphere Handbook, Leningrad [1991] p. 22
- Bamford, H. A., D. L. Poster, and J. E. Baker [2000] Henry's law constants of polychlorinated biphenyl congeners and their variation with temperature. *Journal of Chemical & Engineering Data*, v.45, pp. 1069–1074.
- Bennett D.H., Scheringer, M., McKone, T.E. and K. Hungerbühler [2001] Predicting Long Range Transport: A Systematic Evaluation of Two Multimedia Transport Models, *Environmental Science and Technology*, v. 35, No. 6, pp.1181-1189.
- Beyer A. and M.Matthies [2001] Criteria for Atmospheric Long-range Transport Potential and Persistence of Pesticides and Industrial Chemicals. Umweltforschungsplan des Bundesministerium für welt,Naturschutz und Reaktorsicherheit. Stoffbewertung, Gentechnik, Forderkennzeichen (UFOPLAN) 299 65 402.
- Beyer A., F. Wania, T. Gouin, D. Mackay and M. Matthies [2002] Selecting internally consistent physicochemical properties of organic compounds. *Environmental Toxicology and Chemistry*, v.21, No.5, pp. 941–953.
- Bidleman, T. F., Falconer, R. L. and T. Harner [1998] "Particle/Gas Distribution of Semivolatile Organic Compounds: Field and Laboratory Experiments with Filtration Samplers", in Gas and Particle Partition Measurements of Atmospheric Organic Compounds, edited by D. A. Lane. Gordon and Breach Publishers, Newark, New Jersey.
- Brandes L.J. H. den Hollander and D. van de Meent [1996] SimpleBox 2.0: a nested multimedia fate model for evaluating the environmental fate of chemicals. Report no. 719101029. National Institute of Public Health and the Environment (RIVM), P.O. Box 1, 3720 BA Bilthoven, the Netherlands.
- Breivik K., F. Wania [2002a] Evaluating a model of the historical behavior of two hexachlorocyclohexanes in the Baltic Sea environment. *Environ. Sci. Technol.* v.36, pp.1014-1023.
- Breivik K., F. Wania [2002b] Mass budgets, pathways and equilibrium states of two hexa-chlorocyclohexanes in the Baltic Sea environment. *Environ. Sci. Technol.* v.36, pp.1024-1032.
- Breivik K., Sweetman A., Pacyna J.M., Jones K. [2002] Towards a global historical emission inventory for selected PCB congeners – a mass balance approach. 2. Emissions. *The Science of the Total Environment*, v. 290, pp. 199-224.
- Burkhard L.P., Armstrong D.E. and A.W. Andren [1985] Henry's Law Constants for the Polychlorinated Biphenyls. *Environ. Sci. Technol.*, v.19, pp.590-596.
- Christensen J. [1999] An overview of modelling the Arctic mass budget of metals and sulphur: Emphasis on source apportionment of atmospheric burden and deposition. In: Modelling and sources: A workshop on Techniques and associated uncertainties in quantifying the origin and long-range transport of contaminants to the Arctic. Report and extended abstracts of the workshop, Bergen, 14-16 June 1999. AMAP report 99:4. see also <http://www.amap.no/>
- Christensen J. H. [1997] The Danish Eulerian Hemispheric Model – a three-dimensional air pollution model used for the Arctic. *Atmospheric Environment*, v.31, No. 24, pp.4169–4191.
- Dunnivant F.M., Elzerman A.W., Jurs P.C., M.N. Hasan [1992] Quantitative Structure-Property Relationships for Aqueous Solubilities and Henry's Law Constants of Polychlorinated Biphenyls, *Environ. Sci. Technol.*, v. 23, No. 10, pp. 1250 – 1253.
- Duyzer J.H., van Oss R.F., Verhagen H.L.M., Vervaart M. and B.Boeke [1997] Determination of deposition parameters of a number of persistence organic pollutants by laboratory experiments. TNO-report TNO-MEP-R97/150.
- ENV/JM/MONO(2002)15 [2002] Report of the OECD/UNEP Workshop on the Use of Multimedia Models for Estimating Overall Environmental Persistence and Long range Transport in the Context of PBTS/POPS Assessment. OECD Environment, Health and Safety Publications Series on Testing and Assessment, No.36. Environment Directorate OECD, Paris.
- Falconer R.L. and T.F. Bidleman [1994] Vapor pressures and predicted particle/gas distributions of polychlorinated biphenyl congeners as functions of temperature and ortho-chlorine substitution. *Atmos. Environ.*, v.28, pp.547-554
- Falconer R.L. and T. Harner [2000] Comparison of octanol-air partition coefficient and liquid-phase vapor pressure as descriptors for particle/gas partitioning using laboratory and field data for PCBs and PCNs. *Atmospheric Environment*, v. 34, pp. 4043–4046.
- Falconer R.L. and T.F. Bidleman [1994] Vapor Pressures and Predicted Particle/Gas Distributions of Polychlorinated Biphenyl Congeners as Functions of Temperature and Ortho-Chlorine Substitution, *Atmospheric Environment*, v. 28, No. 3, pp. 547-554.
- Falconer R.L. and T.F. Bidleman, Cotham and E.William [1995] Preferential Sorption of Non-and-Mono-ortho-polychlorinated Biphenyls to Urban Aerosols, *Environ. Sci. Technol.*, v. 29, No. 6, pp. 1666-1673.

- Falkowski P.G., Barber R.T., and V.Smetacek [1998] Biogeochemical Controls and Feedbacks on Ocean Primary Production, *Science*, v.281, pp.200-205.
- Finizio A., D. Mackay T. Bidleman and T. Harner [1997] Octanol-Air Partition Coefficient as a Predictor of Partitioning of Semi-Volatile Organic Chemicals to Aerosols. *Atmospheric Environment*, v.31, No.15, pp.2289-2296.
- Frohn L.M., J.H. Christensen and J. Brandt [2002] Development of a high-resolution nested air pollution model – the numerical approach. *Journal of Computational Physics*, v.179, pp. 68–94.
- Geels C., J.H. Christensen, A.W. Hansen, S. Kiilsholm, N.W. Larsen, S.E. Larsen, T. Pedersen and L.L. Sørensen [2001] Modeling concentrations and fluxes of atmospheric CO<sub>2</sub> in the North East Atlantic Region. *Physics and Chemistry of the Earth (B)*, v.26, No.10, pp. 763–768.
- Gong S.L., Barrie L.A. and J.-P. Blanchet [2003] Canadian Aerosol Module: A size-segregated simulation of atmospheric aerosol processes for climate and air quality models 1.Model Development", *Journal of Geophysical Research*, v. 108, No. D1, pp. 4007, doi:10.1029/2001JD002002,2003.
- Gong S.L., Barrie L.A. and J.-P. Blanchet [1997b] Modeling Sea-salt Aerosols in the Atmosphere, 1.Model Development", *Journal of Geophysical Research*, v. 102, No. D3, pp. 3805-3818.
- Granier L.K. and Chevreuril M. [1997] Behaviour and spatial and temporal variations of polychlorinated biphenyls and lindane in the urban atmosphere of the Paris area, France. *Atmospheric Environment*, v.31, No.22, pp.3787-3802.
- Grell, G. A., J. Dudhia, and D. R. Stauffer [1995] A description of the fifth-generation Penn State/NCAR Mesoscale Model (MM5). NCAR/TN-398+STR. NCAR Technical Note. Mesoscale and Microscale Meteorology Division. National Center for Atmospheric Research. Boulder, Colorado. Pp. 122.
- Gusev A., I. Ilyin, G. Petersen, A. van Pul, D.Syrakov and M. Pekar [2000] Long-range transport model Intercomparison studies: Model intercomparison study for cadmium; About EMEP/MSC-E participation in ATMES-II, EMEP/MSC-E Technical Note 2/2000.
- Harner et al, 1998
- Harner T. and T.F. Bidleman [1996] Measurements of octanol-air partition coefficients for polychlorinated biphenyls. *Chem. Eng. Data*, v.41, pp.895-899.
- Hawker D.W. and D.W.Connell [1988] Octanol-water partition coefficients of polychlorinated biphenyl congeners. *Environ. Sci. Technol.*, v.22, pp.382-387.
- Horstmann M. and M.S. McLachlan [1998] Atmospheric Deposition of Semivolatile Organic Compounds to Tow Forest Canopies, *Atmospheric Environment*, v.32, No. 10, pp.1799-1809.
- Jacobs C.M.J. and W.A.J. van Pul [1996] Long-range atmospheric transport of persistent organic pollutants, I: Description of surface - atmosphere exchange modules and Implementation in EUROS. National institute of public health and the environment, Bilthoven, the Netherlands. Report No722401013.
- Junge C.E. [1977] Basic considerations about trace constituent in the atmosphere is related to the fate of global pollutant. In: Fate of pollutants in the air and water environment. Part I, I.H. Suffet (ed.) (Advanced in *Environ. Sci. Technol.*, v.8), Wiley-Interscience, New York.
- Kalnay E., Kanamitsu M., Kistler R., Collins W., Deaven D., Gandin L., Irdell M., White S., Sh. G., Wollen J., Zhu Y., Chelliah M., Ebisuzaki W., Higgins H., Janowiak J., Ropelewski K.C., Mo. C., Wang J., Leetmaa A., Reynolds R., Jenne R. and D. Joseph [1996] The NCEP/NCAR 40-year reanalysis project. *Bull. Amer. Meteor. Soc.* v.77, pp. 437-471.
- Karickhoff S.W. [1981] Semiempirical estimation of sorbtion of hydrophobic pollutants on natural sediments and soil, *Chemosphere*, v.10, pp.833-846.
- Koziol A. and J. Pudykiewicz [2001] Global scale transport of persistent organic pollutants, *Chemosphere*, v. 45/8, pp. 1181-1200.
- Li Y.F., M.T. Scholtz, and B.J. van Heyst [2000] Global gridded emission inventories of  $\alpha$ -hexachlorocyclohexane. *Journal of Geophysical Research*, v.102, No.D5, pp. 6621–6632.
- Li Y.-F., McMillan A., Scholtz M. T. [1996] Global HCH usage with 1 x 1 degree longitude/latitude resolution. *Environ. Sci. Tech.* v.30, pp.3525-3533.
- Li N., Wania F., Lei D.Y., Daly G.L. [2003] A comprehensive and critical compilation, evaluation and selection of physical chemical property data for selected polychlorinated biphenyls, *J. Phys. Chem. Ref. Data*, v. 32, No. 4, pp. 1545-1590.
- Lindfors V., S.M.Joffe and J.Damski [1991] Determination of the wet and dry deposition of sulphur and nitrogen compounds over the Baltic sea using actual meteorological data. Finnish Meteorological Institute Contributions N 4, Helsinki.
- Mackay D. [1999] Multimedia Environmental Models – The Fugacity Approach, second edition, Lewis Publishers.
- Mackay D., Shiu, W.Y., Ma, K.C. [1992] Illustrated Handbook of Physical-Chemical properties and environmental fate for organic chemicals, v.1: Monoaromatic Hydrocarbons, Chlorobenzenes, and PCBs. Lewis Publishers, INC.

- Mackay D. and Yeun A.T.K. [1983] Mass Transfer Coefficient Correlations for Volatilization of Organic Solutes from Water, *Environmental Science and Technology*, v. 17, pp. 211-217.
- Mackay D. and S. Paterson [1991] Evaluating the Multimedia Fate of Organic Chemicals: A Level III Fugacity Model, *Environmental Science and Toxicology*, v. 25, pp.427-436.
- Malanichev A.,V. Shatalov N. Vulykh, B.Strukov [2002] Modelling of POP Hemispheric Transport, MSC-E Technical Report 8/2002.
- McLachlan M. and M.Horstmann [1998] Forests as filters of airborne organic pollutants: a model. *Environ. Sci. Technol.*, v.32, pp. 413-420.
- McLachlan, M., G. Jeczub and F. Wania [2002] The Influence of Vertical Sorbed Phase Transport on the Fate of Organic Chemicals in Surface Soils, *Environ. Sci. Technol.*, v.36, pp.4860-4867.
- Möller M. [2002] Einfluss der Vegetation auf das Verteilungsverhalten von organischen Schadstoffen in einem Umweltmodell, Diplomarbeit ETHZ Zürich, Swiss Federal Institut of Technology Zurich (ETHZ) (ISBN 3-906734-27-7).
- Murray J.W. [1992] The Oceans, in: Butcher, S.S., Charlson, R.J., Orians, G.H., Wolfe, G.V. (Eds.): *Global Biogeochemical Cycles*. Academic Press, pp.175-211.
- Pacyna, J.M. et al. [1999] Final Report for Project POPCYCLING-Baltic. NILU, P.O. Box 100, N-2007 Kjeller, Norway. CD-ROM.
- Pankow J.F. [1987] Review and comparative analysis of the theories on partitioning between the gas and aerosol particulate phases in the atmosphere. *Atmos. Environ.*, v.21, pp.2275-2283.
- Pekar M., N.Pavlova, A.Gusev, V.Shatalov, N.Vulikh, D.Ioannisian, S.Dutchak, T.Berg and A.-G. Hjellbrekke [1999] Long-range transport of selected persistent organic pollutants. Development of transport models for polychlorinated biphenyls, benzo[a]pyrene, dioxins/furans and lindane Joint report of EMEP Centres: MSC-E and CCC, EMEP Report 4/99.
- Report of the OECD/UNEP Workshop on the Use of Multimedia Models for Estimating Overall Environmental Persistence and Long-Range Transport in the context of PBTs/POPs assessment. [2002] ENV/JM/MONO(2002)15.
- Ruijgrok, W. Tieben H. and P.Eisinga [1997] The dry deposition of particles to a forest canopy: a comparison of model and experimental results. *Atmospheric Environment*, v.31, pp. 399-415.
- Ryaboshapko A., I.Ilyin, R.Artz, R.Bullock, J.Christensen, M.Cohen, A.Dastoor, D.Davignon, R.Draxler, R.Ebinghaus, J.Munthe, G.Petersen, D.Syrakob [2002] Progress report on Intercomparison study of numerical model for long range atmospheric transport of mercury. MSC-E Technical Note 10/2002.
- Ryaboshapko A., R. Artz, R. Bullock, J. Christensen, M. Cohen, A. Dastoor, D. Davignon, R. Draxler, R. Ebinghaus, I. Ilyin, J. Munthe, G. Petersen, D. Syrakov [2003] Intercomparison Study of numerical models for long-range atmospheric transport of mercury. Stage II. Comparison of modeling results with observations obtained during short-term measuring campaigns. MSC-E Technical report 1/2003.
- Scheringer M., Wegmann F. and M.Salzmann [2003] POP model intercomparison study. Stage 1: Process Description and Parameterization for the Models ChemRange and CliMoChem. ETH-Logo. Postadresse und Buwalreferenz.
- Scheringer M. [1996] Räumliche und Zeitliche Reichweite als Indikatoren zur Bewertung von Umweltchemikalien, Diss. ETH Nr.11746, Swiss Federal Institut of Technology Zurich (ETHZ).
- Schwarzenbach, R. P., Gschwend, P. M. and D.M. Imboden [1993] *Environmental Organic Chemistry*. John Wiley & Sons, Inc., New York.
- Sehmel G.A. [1980] Particle and gas dry deposition: a review. *Atmos. Environ.* v.14, pp. 983-1011.
- Seinfeld J.H. [1986] *Atmospheric Chemistry and Physics of Air Pollution*, J. Wiley & Sons, N.Y., pp. 738
- Sellers P. J., Meeson B. W., Closs J., Collatz J., Corprew F., Dazlich D., Hall F. G., Kerr Y., Koster R., Los S., Mitchell K., McManus J., Myers D., Sun K.-J. and P. Try [1995] An Overview of the ISLSCP Initiative Global data sets. On: ISLSCP Initiative Global data sets for land-atmosphere models, 1987-1988, Vol. 1-5. Published on CD by NASA, Vol. 1, USA-NASA-GDAAC-ISLSCP-001, OVERVIEW.DOC.
- Seth R., Mackay D., Muncke J. [1999] Estimating the Organic Carbon Partition Coefficient and its Variability for Hydrophobic Chemicals, *Environmental Science and Technology*, v. 33, pp. 2390-2394.
- Shatalov V., A. Malanichev, N. Vulykh (MSC-E), T. Berg, S. Manø (CCC) [2002] Assessment of POP Transport and Accumulation in the Environment, MSC-E/CCC Technical Report 7/2002
- Shatalov V., A.Malanichev, N.Vulykh, T.Berg and S.Mano [2001] Assessment of POP transport and accumulation in the environment. EMEP Report 4/2001
- Shatalov V., A.Malanichev, T.Berg and R.Larsen [2000] Investigation and assessment of POP transboundary transport and accumulation in different media, EMEP-MS-C-E, Report 4/2000, Part 1,2.
- Siegenthaler U. and F. Joos, [1992] Use of a simple model for studying oceanic tracer distribution and the global carbon cycle. *Tellus* 44B, pp.186-207.

- Sinkkonen S. and J.Paasivirta [2000] Degradation half-life times of PCDDs, PCDFs and PCBs for environmental fate modeling. *Chemosphere*, v. 40, pp.943-949.
- Sofiev M., Maslyayev A. and A. Gusev [1996] Heavy metal model intercomparison. Methodology and results for Pb in 1990, MSC-E Report 2/96.
- Strand A., and Ø. Hov [1996] A model strategy for the simulation of chlorinated hydrocarbon distributions in the global environment. *Water, Air and Soil Pollution*, v.86, pp. 283–316.
- Struijs J. and Van den Berg R. [1995]. Standardized biodegradability tests: extrapolation to aerobic environments. *Water Research*, v 29, Issue 1, Pages 255-262.
- Strukov B., Resnyansky Yu., Zelenko A., Gusev A. and V.Shatalov [2000] Modelling long-range transport and deposition of POPs in the European region with emphasis to sea currents. EMEP/MSC-E Report 5/2000.
- Strukov B.S. [2001] Dynamics of POPs distribution in Sea Water between Different Phases. EMEP/MSC-E Technical Note 1/2001, Meteorological Synthesizing Centre - East, Moscow, Russia.
- Sweetman A.J. and Jones K.C. [2000] Declining PCB concentrations in the U.K. atmosphere: evidence and possible causes. *Environmental Science and Technology*, v.34, No. 5, pp.863-869.
- Vassilyeva G. and V. Shatalov [2002] Behaviour of persistent organic pollutants in soil. MSC-E Technical Note 1/2002.
- Wania F and D. Mackay [2000] The global distribution model. A non-steady state multi-compartmental mass balance model of the fate of persistent organic pollutants in the global environment. Technical Report ([www.uts.utoronto.ca/~wania](http://www.uts.utoronto.ca/~wania))
- Wania F. and C.Dugani [2003] Assessing the long-range transport potential of polybrominated diphenyl ethers: A comparison of four multimedia models. *Environ. Toxicol. Chem.*, v. 22, No. 6, p.1252-1261.
- Wania F. and D. Mackay [2000] A Comparison of Overall Persistence Values and Atmospheric Travel Distances Calculated by various Multi-Media Fate Models. WECC Wania Environmental Chemists Corp., WECC Report 2/2000.
- Wania F. and D. Mackay [1993] An approach to modelling the global distribution of toxaphene: A discussion of feasibility and desirability. *Chemosphere*, v. 27, pp.2079-2094.
- Wania F. and D. Mackay [1995] A global distribution model for persistent organic chemicals. *Sci.Total Environ.* v.160/161, pp.211-232.
- Wania F. and D. Mackay [1999] Global chemical fate of  $\alpha$ -hexachlorocyclohexane. 2. Use of a global distribution model for mass balancing, source apportionment, and trend predictions. *Environ. Toxicol. Chem.*, v.18, pp. 1400-1407.
- Wania F., D. Mackay Y.-F. Li T.F. Bidleman and A.Strand [1999] Global chemical fate of  $\alpha$ -hexachlorocyclohexane. 1. Evaluation of a global distribution model. *Environ. Toxicol. Chem.* v.18, pp.1390-1399.
- Wania F. and G. Daly [2002] Estimating the contribution of degradation in air and deposition to the deep sea to the global loss of PCBs. *Atmos. Environ.*, v.36., iss.36-37, pp. 5581-5593.
- Wania F. and M.S. McLachlan [2001] Estimating the influence of forests on the overall fate of semivolatile organic compounds using a multimedia fate model, *Environmental Science and Technology*, v.35, No. 3, pp. 582-590.
- Wania F., J.Persson A. Di Guardo and M.S. McLachlan [2000] CoZMO-Pop: A Fugacity-Based Multi-Compartmental Mass Balance Model of the Fate of Persistent Organic Pollutants in the Coastal Zone, WECC-Report 1/2000
- Whitby K.T. [1978] The Physical Characteristics of Sulphur Aerosols. *Atmos. Environ.*, v.12, pp.135 – 159.
- WOCE Data Products Committee, 1998: WOCE Global Data, Surface Velocity Programme, Version 1.0, WOCE IPO Report No. 158/98, Southampton, U.K.).
- Yu Lu and M.A.K. Khall [1991] Tropospheric OH: model calculation of spacial, temporal and secular variations. *Chemosphere*, v. 23, pp.397-444.



### DESCRIPTIONS OF THE MODELS

This Annex contains the descriptions of POP models taking part in the intercomparison study.

#### A.1. HYSPLIT 4

*Paul Bartlett*

Persistent organic pollutants (POPs) emit into the atmosphere from near and distant sources, transport and deposit to land and marine surfaces, and enter the food chain through water, flora and fauna. Remedial policy must be directed to the reduction of emissions from the sources, but knowledge of source emissions, pollutant measurements, and distance alone is insufficient information to distinguish the sources most responsible for contamination. Numerical modeling of pollutant transport and environmental fate from individual sources to ecological receptors can close this information gap by taking into account weather patterns and the chemical characteristics of the pollutant affecting atmospheric destruction and deposition, but only when source-to-receptor information is preserved in the results. The approach we use with the HYSPLIT (Hybrid Single Particle Lagrangian Integrated Trajectory) atmospheric transport model can accomplish these objectives. HYSPLIT is a three dimensional Lagrangian model developed by Roland Draxler's team at the National Oceanic and Atmospheric Administration (NOAA). When simulated puffs enter new grids, they are split and follow their own trajectory. Meteorological data is interpolated between date time periods. HYSPLIT was adapted at CBNS (originally by Mark Cohen, presently at NOAA) for the persistent organic pollutants.

The (HYSPLIT) enables us to preserve source-to-receptor identity while simulating atmospheric transport, destruction and deposition of hypothetical emission puffs, from each source point to target receptor areas. The source-to-receptor relationship can be represented, as an output of HYSPLIT, by the ratio deposited to the receptor from one unit emission from the source, the atmospheric transport coefficient (ATC). When ATCs are mapped, the effect of weather patterns and pollutant chemical properties on transport can be evaluated. The product of the ATC and the quantity emitted is the amount deposited to the receptor from that source ( $ATC * \text{Source Quantity Emitted} = \text{Receptor Deposition}$ ). Relative contributions of each source to receptor deposition can be determined and ranked. We are able to use this approach because we are modeling single-hop transport (no re-suspension; one-way deposition) and since the pollutants are transported in trace amounts, interactive effects between the pollutant is insignificant. HYSPLIT algorithms use pollutant chemical properties to estimate vapor-particle partitioning, destruction (hydroxyl radical and photochemical reactions), dispersion and deposition.

This method is made computationally feasible for a large number of sources and congeners by the use of a spatial and congener interpolation program, TRANSCO, which applies an emission inventory to a set of geographically represented standard point source-to-receptor HYSPLIT computer runs.

HYSPLIT has been used by CBNS for source-to-receptor transport modeling of HCB, dioxin, PCBs and atrazine.

#### A.2. EVN-BETR and UK-MODEL

*Andrew Sweetman*

**Introduction:** A fugacity-based, contaminant distribution model was developed at Lancaster University in order to simulate the fate of Persistent Organic Pollutants (POPs) in the entire European Continent. The model calculates steady and non-steady state (dynamic) mass balances of chemical contaminants from inputs describing the environmental characteristics of Europe, the physicochemical properties of the chemical of interest, and contaminant emission rates. The focus is on describing pollutant fate and transport, including transfer, transport and cycling in and between air, vegetation, soil, surface water, sediments and coastal water. GIS software was used to better describe geo-referenced data regarding landcover, water flows, soil organic carbon content, precipitation and temperature information.

**Model segmentation:** Europe was divided into 54 regions using a 5x5 degree grid. A total of 50 cells describe the main bulk of the European continent with four further perimetric boxes, namely: the Atlantic, Mediterranean, Eurasian and Arctic Boxes.

**Flow balance:** Inter-regional flows of air in the upper and lower atmosphere, fresh and coastal water connect the individual regional environments. The movement of air and water in both directions across all regional boundaries, thus, is described with the help of five matrices of volumetric flow rates. The five flow matrices have been compiled with the aid of Geographical Information System (GIS) analysis of available hydrological and meteorological data. Air-flow balances have been extrapolated from data gathered about wind speeds and directions, notably from the BADC trajectory service. The flow matrix for air specifies the 5-year average flow rates ( $\text{m}^3/\text{h}$ ) of air between all connected regions in the upper and lower air compartments.

**Mass balance equations:** There are seven mass balance equations describing the fate of POPs in each region, and therefore 378 equations make up the 54 European regions. This system of seven equations and the seven unknown fugacities have been solved analytically using linear and matrix algebra algorithms.

**Case studies:** We are planning to model the environmental fate of a wide range of POPs, such as Polychlorinated Biphenyls (PCBs), Dibenzo-p-dioxins and Furans (PCDD/Fs), Polycyclic Aromatic Hydrocarbons (PAHs), Polybrominated Diphenyl Ethers (PBDEs) and organochlorine pesticides (OCs). Most of these chemicals are still emitted in considerable amounts into the European environment and constitute a growing hazard. Several emission scenarios will be tested for different chemicals and regions. Pollutants lying in the extreme ends of the physicochemical properties' range will be assessed in terms of persistence and transport potential. Emission estimates have already been compiled for a number of chemicals and the model's output will be tested against measurement data. The ultimate aim is to validate our model with the results of the PASAE (Passive Air Sampling Across Europe) campaign, Lancaster University and our collaborators have just concluded.

### A.3. ELPOS

*Michael Matthies*

The model EUSES-SimpleBox 1.0 (a level III multimedia model) was expanded to calculate the overall persistence and the characteristic travel distance in air and water (long-range transport potential). The new model is called "Environmental Long-range transport and Persistence of Organic Substances" model (ELPOS). Both criteria describe inherent substance properties that can be used for screening, ranking, and chemical assessment. Both criteria account for the intermedia transfer and intramedia degradation and are independent of the chemical amount emitted. The criteria were calculated for 65 current-use pesticides, 23 industrial chemicals, and 21 persistent organic pollutants (POPs). The sensitivity analysis shows that the parameter sensitivity heavily depends on the characteristics of the chemicals as well as assumptions with respect to environmental conditions. The ranking of the chemicals can be affected if uncertainty of the parameters is taken into account, e.g. by using 90<sup>th</sup>-percentiles instead of mean values. The criteria were assessed in relation to a reference scenario with respect to gas-particle partitioning, photo-oxidative degradation, degradability in water and soil (field and laboratory measurements), rain rate and possible degradation on foliage. The model was modified to account for temperature variations within a range of 5° to 30°C. The overall persistence as well as the characteristic travel distance are highly dependent on temperature. While the overall persistence always increases when temperature drops, the characteristic travel distance can increase or decrease, which is caused by opposing processes. The so-called cold condensation effect could be explained by these temperature dependent calculations. The characteristic travel distance was compared to monitoring data of pesticides in rain water, yielding a rough agreement between measurements and model results. A comparison of model results to observed spatial concentration gradients was possible for some PCB congeners, leading to the same chemical ranking in both cases. The 65 current-use pesticides (with the two exceptions Dicofol and Chlorothalonil) exhibit a lower persistence and long-range transport potential than typical POPs (such as hexachlorobenzene or DDT). The pesticides dicofol and chlorothalonil are therefore evaluated more in depth.

## A.4. ChemRange and CliMoChem

*Martin Scheringer and Fabio Wegmann*

**Compartments, coverage and resolution.** Both models are multi-compartment box models and cover the global system, see Fig. A.1. Compartments included are soil, oceanic surface water and tropospheric air in the case of ChemRange and, in addition to these three, vegetation and vegetation soil in CliMoChem. ChemRange is a spatially homogeneous one-dimensional circular system (a “loop”) while CliMoChem is a two-dimensional model containing a flexible number (typically: 20 to 30) latitudinal zones with different temperatures and compartment volumes (the vertical extension is not counted as a dimension here). CliMoChem does not have a spatial resolution in east-west direction; in north-south direction, the spatial resolution is given by the number of zones,  $n$  (the width of a zone is equal to  $180/n$  degrees latitude).

ChemRange is a steady state model without temporal resolution. The temporal resolution of CliMoChem is between 1 month and 1 year.

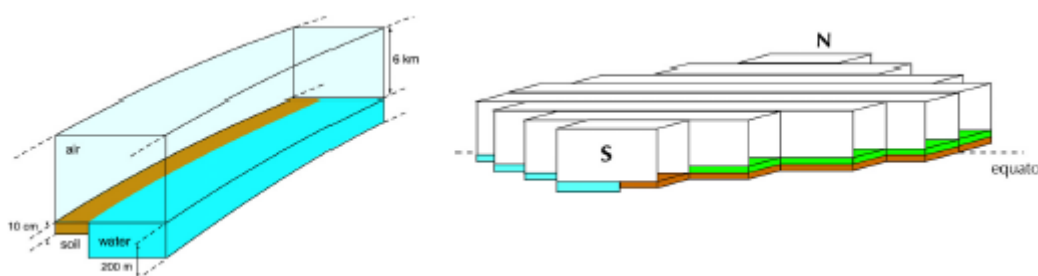


**Fig. A.1.** Geometry of the global multi-compartment box models ChemRange (left) and CliMoChem (right)

### Processes and parameterization

Both models include:

- 1) degradation processes in all compartments, described as first-order processes;
- 2) transport in oceanic surface water and tropospheric air, described as macroscopic eddy diffusion with diffusion coefficients from measurements of large-scale oceanic diffusion and tracer experiments in the troposphere;
- 3) exchange processes between the compartments:
  - diffusive exchange of chemicals in the gas phase (gaseous deposition, volatilization)
  - dry deposition with aerosol particles of particle-bound chemicals
  - wet deposition with aerosol particles
  - rain washout of chemicals in the gas phase
  - deposition to the deep sea of chemicals associated with suspended particles in the ocean water.
  - runoff from soil to ocean water
  - leaf fall from the vegetation to the soil (only CliMoChem)

The diffusive processes are based on two-resistance models for the phase transfer of the chemicals. The advective processes are based on global and long-term averages of rain rates, particle fluxes etc. Association with particles is calculated from the chemicals' KOA (air) and KOC (water) partition coefficients.

In CliMoChem, degradation processes and processes influenced by partition coefficients are temperature dependent.

**Chemicals.** Both models can only be applied to non-polar organic chemicals, not to ionizing compounds or heavy metals. Interaction or conversion of different chemical species is not included in general. With ChemRange, the formation of transformation products such as DDE from DDT can be modeled. A similar extension is planned for CliMoChem.

**Model input.** ChemRange requires five chemical specific input parameters (degradation rate constants for soil, ocean and air as well as Henry's law constant and octanol-water partition coefficient). If possible, the partition coefficients should be internally consistent. If available, the chemical-specific input parameters should be chosen for a temperature around 280K because 298K is too high as a global average.

In addition to the chemical-specific parameters, several environmental parameters are required: concentration of aerosol particles, average aerosol deposition rate, rain rate, concentration of suspended particles in the oceanic surface water, organic carbon export from the surface ocean, fractions of air and water in the soil, several transfer velocities for two-film models, soil runoff rate.

CliMoChem requires degradation rate constants in soil, ocean water, air and vegetation and two partition coefficients (HLC and KOW). All of these parameters must be available as functions of temperature (mostly based on activation energies and enthalpies of phase transfer). Degradation rate constants in air should be second-order constants for reaction with OH radicals.

Environmental parameters required for each latitudinal zone are: fractions of ocean and land, fractions of three types of vegetation (grassland, deciduous and coniferous forests), monthly averages of air temperature at 2m height, OH radical concentrations as functions of temperature. In addition, the same environmental parameters as in ChemRange are required (transfer velocities, aerosol concentrations etc.). Further parameters are leaf fall rates and vegetation growth rates as functions of time and additional vegetation parameters (leaf surface index, fraction of organic matter in leaves, fraction of retained rainwater).

**Emission scenarios.** ChemRange can be used with any combination of continuous sources into one or more compartments and at different locations. Typically, a single point source is used because such a simple scenario is consistent with the evaluative and generic character of the model.

CliMoChem requires a single pulse emission or any combination of pulse emissions (spatially and temporally resolved) as emission scenario. Single pulse emissions are useful for evaluative calculations; temporally and spatially resolved emissions are required for calculations of absolute concentration levels.

**Model results.** ChemRange yields steady-state concentrations, mass fractions and mass flows of the chemical in each medium, the media-specific and overall persistence (calculated as residence times), and the spatial range in each medium (calculated as the 95<sup>th</sup> interquartile distance of the spatial concentration distribution).

The CliMoChem output contains concentrations, mass fractions and mass flows in and between all compartments and latitudinal zones as functions of time. In addition, persistences, spatial ranges, cold condensation potentials are derived from the basic output.

## **A.5. CAM/POPs – Canadian Model for POPs**

### *Sunling Gong*

This model consists of four major components: (1) an active aerosol module (CAM), (2) a surface exchange module for PCBs between water and atmosphere and between soil and atmosphere (Emission), (3) a module to partition PCBs between gas and aerosol phases (Atmospheric Processes) and removal processes and (4) a transport module for tracers (Atmospheric Transport) as shown in Fig. A.2.

The Canadian Aerosol Module (CAM) developed for treating size segregated aerosols in both air quality and climate models [Gong *et al.*, 2003] simulates the mass and number distributions of five major aerosols: sea-salt, sulphate, soil dust, black carbon and organic carbon. CAM provides aerosol surface areas and removal rates for aerosol-bound PCBs

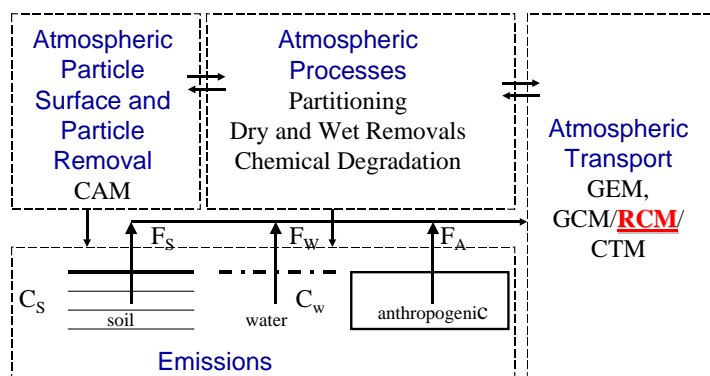


Fig. A.2. Framework of POP model for simulating PCBs

Air-water exchange of PCBs was treated with a method by *Liss and Slater* [1974] who asserts that a chemical must diffuse through layers of water and air in series at rates characterized by mass transfer coefficients  $k_w$  (water side) and  $k_a$  (air side). The dimensionless Henry's Law constant,  $K_{aw}$ , gives the ratio of the concentrations across the air-water interface. The soil-exchange model from [*Jury, 1989; Jury et al., 1983*] was used for the calculating the soil PCB fluxes to the atmosphere. PCB/aerosol partition was simulated with the Junge-Pankow Partition [*Junge, 1977; Pankow, 1987*]. The PCB amount partitioned between gas and aerosol phase depends the aerosol surface area available for adsorption ( $m^2$  aerosol/ $m^3$  air), the liquid-phase saturation vapour pressure of pure compound ( $Pa$ ). Atmospheric degradation of PCBs by OH has also been implemented.

## A.6. G-Ciems

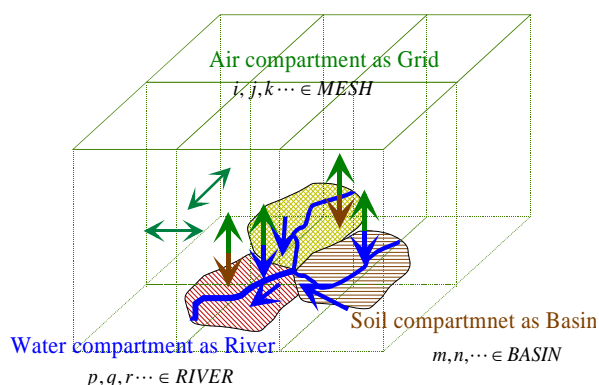
*Noriyuki Suzuki*

**General description.** Grid-Catchment Integrated Environmental Modeling System (G-CIEMS, tentative name) is a geo-referenced multimedia and river environmental fate model system for region-scale environment. The multimedia model is as an expansion of Mackay-type multimedia fate model to multi-box compartments with geo-referenced geographical resolution on GIS software. The model calculates multimedia environmental concentration on specified geographical environmental area.

**Basic modeling items.** Model consists of the following geographical/data items. Each item has relevant information like geographical/hydrological/meteorological and chemical datasets on database format.

Air: grid structure with layers, now 5x5 km size. River: GIS line items representing real geographical river. Soil: GIS polygon items including 7 land use categories and 1 forest vegetation compartment. Average size of soil polygon is around 10km<sup>2</sup> at present. Lake: GIS polygon item, Coastal area and Coastal sea.

**Transport formulation.** Inter-media transport between media are formulated based on basic transport phenomena (diffusive and advective processes). Transport between geographical items with different shape are formulated using projective area between the items.



**User interface.** The model is developed on GIS-based integrated information system as the data management system and the user interface, based on Microsoft Access database.

**POPs modeling ability.** The model can calculate the gross input and output between target area and outer boundary for each transport pathway. This is not directly show a specific transport index but could be a real estimation and reference of the transport potential of the chemicals within/outside the region.

## A.7. INERIS

### *Regis FARRET*

INERIS -French Institute for Industrial Risks and Environment- is a public institute which brings its scientific experience mainly to the Ministry of Environment. The Chronic Risks Division of INERIS covers experience in toxicology, ecotoxicology, modelisation of transfers in the environment, analytical chemistry. Through collaboration between these skills we developed our expertise in Risk Assessment, both at the local level – atmospheric emission of a factory, study of polluted sites– and at the national or international level, for supporting governmental actions.

Risk Assessment of chemical substances are carried out in the frame of the application of the European Directive 93/67 EEC (for new substances) and the Regulation 1488/94 (for existing substances). Therefore, following the Technical Guidance Document, INERIS has experience in the multi-media model EUSES, which includes a local and a regional model.

INERIS is also using other "generic" multimedia models like ELPOS (close to EUSES) and ChemCan. The results are not used directly for supporting national regulation for POPs, but they may be included in specific studies at a national level : For example I am presently performing a multi-criteria study aiming at prioritising pesticides considering their possible impact through atmospheric transport.

Besides, INERIS takes part in international programmes, such as:

- the UN-ECE Convention on Long-Range Transboundary Air Pollution. INERIS is the French National Focus Centre for Integrated Assessment Modelling ; we also take part in the Task-Force on Measurement and Modelling and in several Task-Forces in the Working Group on Effects. We are developing together with the Laboratory of Dynamic Meteorology (Paris 6 University) the regional model CHIMERE with similar principles to EMEP (West) models. It is not a multi-media model, but particles are being included presently and future developments for including POPs and metals may be undertaken.
- the OECD Task-Force on Environmental Exposure Assessment. Here data, scenarios and models are discussed and exchanged, and INERIS is especially involved in the expert group on exposure reporting.
- the OECD expert group on multi-media modelling.
- the UNEP programme of regional evaluation of PTS for the Mediterranean region.

We also have to mention here that the multi-media model ChemFrance was developed in France by *Bintein and Devillers* [1996]. This model allows to choose between several options, each of them accounting for environmental conditions of a specific region of France. However this model is not used for national risk assessments, which are led in the frame of the European Union, as mentioned here above.

## A.8. Globo-POP

### *Knut Breivik*

The Globo-POP model is a zonally averaged global multimedia fate and transport model formulated in fugacity notation. Ten climate zones are distinguished based on a climatic classification of the world. The atmosphere is divided into four vertical layers. The top of the four vertical layers corresponds to pressure levels of 83.5, 50, 11 and 1 kPa or 1.3, 5, 16 and 33 kilometers of altitude. Vertical and horizontal atmospheric advective transport velocities and macro-diffusivities are defined with a monthly resolution, as are temperatures and the

concentrations of OH radicals. Within each latitudinal zone, the Earth's surface is represented by two soil (agricultural and non-cultivated soil), a fresh water, a fresh water sediment and a surface ocean compartment (depth of 200 m). Chemical fate processes considered include: equilibrium phase partitioning between sub-compartments, advective and diffusive transport between compartments (including meridional transport in the atmosphere and ocean), first order degradation in each compartment (second order in atmosphere between vapor phase chemical and OH radical), transfer to the deep sea and fresh water sediment burial. Description of these processes follows standard practice in fugacity-based multimedia fate and transport models, but the impact of temperature on partitioning and degradation is accounted for through the use of activation energies and internal energies of phase transfer. Non-steady state mass balances are formulated over all 90 compartments of the model and solved step-wise by finite difference approximation. The model is programmed in Visual Basic, can be run from any Windows platform and downloaded free-of-charge from [www.utsc.utoronto.ca/~wania](http://www.utsc.utoronto.ca/~wania). Various stages of the evolution of that model are documented in various publications [*Wania and Mackay*, 1993, 1995, 1999, 2000]. Using historical emission estimates the Globo-POP model has been applied to simulate the global fate of  $\alpha$ -HCH [*Wania and Mackay*, 1999; *Wania et al.* 1999] and several PCB congeners [*Wania and Daly*, 2002] over the time frame of several decades. Using hypothetical scenarios it has also been used to assess the long range transport behaviour of persistent organic chemicals using the concept of Arctic Contamination Potential [*Wania and Dugani*, 2003].

## A.9. POPCYCLING-Baltic

*Knut Breivik*

The POPCYCLING-Baltic model is a regional multimedia fate and transport model formulated in fugacity notation. Its aim is to describe the long-term, large-scale fate of persistent organic pollutants in the drainage basin and water body of the Baltic Sea. A product of the EU-project POPCYCLING-Baltic project [*Pacyna et al.* 1999], a full description of the model is given in *F.Wania et al.* [2000]. Its 85 well-mixed compartments represent the atmosphere (4 boxes), the aquatic (26 water and 25 sediment boxes) and terrestrial environment (10 forest canopy, 10 forest soil and 10 agricultural soil boxes). Chemical fate processes considered include: equilibrium phase partitioning between sub-compartments, advective and diffusive transport between compartments, first order degradation in each compartment (second order in atmosphere between vapor phase chemical and OH radical), and fresh water sediment burial. Description of these processes follows standard practice in fugacity-based multimedia fate and transport models, but the impact of temperature on partitioning and degradation is accounted for through the use of activation energies and internal energies of phase transfer. Long term averaged monthly atmospheric advection rates between the four atmospheric compartments (Fig. A.3.A) were derived from a atmospheric transport model. Based upon a complete steady-state mass balance of water (Fig. A.3.B and C) and particulate organic carbon (Fig. A.3.D), a non-steady state contaminant mass balance equation is formulated over each of the 85 compartments and solved step-wise by finite difference approximation. The model is programmed in Visual Basic, can be run from any Windows platform and downloaded from [www.utsc.utoronto.ca/~wania](http://www.utsc.utoronto.ca/~wania).

The model has been evaluated [*Breivik and Wania*, 2002a] and applied [*Breivik and Wania*, 2002b] to derive a quantitative understanding of the historical behavior of  $\alpha$ - and  $\gamma$ -hexachlorocyclohexane from 1970 to 2000.

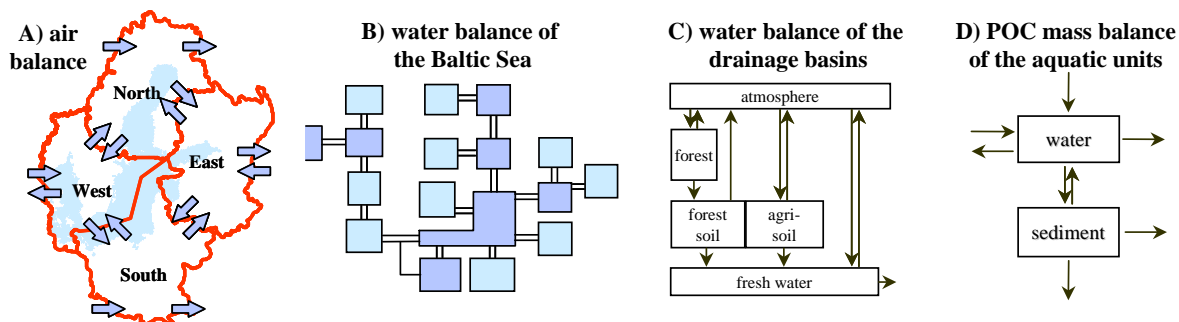


**Fig. A.3.** Major components of the POPCYCLING-Baltic model

## A.10. MEDIA (MEDIA - Multicompartment Environmental Diagnosis and Assessment)

Janusz Pudykiewicz

|   |  |  |  |
|---|--|--|--|
| Type of the model   | Three dimensional, global scale multicompartment environmental transport model including atmosphere, soil, cryosphere and ocean compartments |  |  |
| Description of compartments taken into account in the model | <b>Atmosphere</b>  | <ul style="list-style-type: none"> <li>▪ Three-dimensional atmospheric transport model written in the spherical Gal-Chen terrain following coordinates, horizontal resolution can vary between 0.5 x 0.5 and 2 x 2 degrees, vertical resolution is variable with 15-25 levels</li> <li>▪ Advection is solved using the semi-Lagrangian algorithm</li> <li>▪ Diffusion is solved using a semi-implicit Crank-Nicholson scheme</li> </ul>  |  |
|   | <b>Soil</b>  | <ul style="list-style-type: none"> <li>▪ Column soil model based on advection diffusion equation which is used to simulate water flow and the transport of chemicals in porous medium, typical resolution is of the order of 10 to 15 levels; the first level is located at the surface, the last corresponds to the soil depth</li> <li>▪ Transport of water and chemical species in soil is simulated using Multidimensional Positive Definite Advection Transport Algorithm MPDATA</li> </ul>                                   |  |
|   | <b>Cryosphere</b>  | The equilibrium partition model  |  |
|   | <b>Ocean</b>   | Static version   | The values of the concentration of chemical species in ocean are kept constant |
| Dynamic version of the ocean                                |  | The modified version of High-Latitude Exchange Interior Diffusion-Advection (HILDA) model described originally by <i>Siegenthaler and Joos [1992]</i>  |  |
| Description of processes included in the model              | <b>Atmosphere</b>  | <ul style="list-style-type: none"> <li>▪ Mixing in vertical direction based on the similarity theory</li> <li>▪ Horizontal and vertical advection</li> <li>▪ Scavenging by clouds and precipitation</li> <li>▪ Decay of chemical species with the rate evaluated as a function of temperature and a solar zenith angle</li> <li>▪ Exchange of mass between atmosphere and soil. The exchange is represented by the lower boundary condition at the interface between atmosphere and soil.</li> </ul>                               |  |
|   | <b>Soil</b>  | <ul style="list-style-type: none"> <li>▪ Convective and diffusive transport of chemicals (in three phases) in soil</li> <li>▪ Exchange of mass between the soil system and the atmosphere. The exchange is represented by the lower boundary condition at the interface between soil and atmosphere.</li> <li>▪ Water flow in soil taking into account the forcing at the surface associated with evaporation and precipitation</li> <li>▪ Decay of chemical species with a rate evaluated as a function of temperature</li> </ul> |  |
|   | <b>Cryosphere</b>  | The equilibrium partition of organic compounds in a layer of ice (or snow) takes place between two phases: adsorbed on the surface of ice particles and mixed with interstitial air.   |  |
|   | <b>Ocean</b>   | Static version   | Exchange of pollutant with the atmosphere based on Henry law                   |
| Dynamic version   |  | Advection in the surface layer and exchange of mass with deep water reservoir, exchange of pollutant with the atmosphere   |  |
| Chemicals included in the simulation                        | alpha-HCH and gamma-HCH (lindane)  |  |  |
| Model data base   | <b>Meteorological data</b>   | The NCEP/NCAR 40-year reanalysis project [ <i>Kalnay et al., 1996</i> ]  |  |
|   | <b>Soil and Cryosphere data</b>  | Global data sets for land-atmosphere models [ <i>Sellers et al., 1995</i> ]  |  |
|   | <b>Oceanographic data</b>  | Ocean Circulation Experiment [ <i>WOCE, 1998</i> ]   |  |
| Usage data  | Seasonal usage inventory   | The information about usage of HCH was obtained from: <i>Li et al [1996]</i>   |  |
| Model evaluation  | Evaluation was performed for 1993 and 1994   | Model evaluation was performed for the selected stations in the Arctic   |  |
| Future work   | Improve model parameterizations  | Improvement of the wet scavenging scheme. Additionally we plan also to perform the simulation of environmental cycling of other chemical species. The time frame of the future work with the model is to be determined   |  |
| Model status  | Research model   | <b>MEDIA</b> was developed between 1997 and 2000. The model was used for the assessment of the global scale transport of HCH on the grid with resolution of 2 x 2 degrees. Subsequently it was applied for the evaluation of the transport of lindane from Canadian sources (on a finer grid with the resolution of 1 x 1 degree). Description of the model: <i>Koziol and Pudykiewicz, 2001</i>   |  |

Explanation of acronyms: **MEDIA** – **M**ulticompartment **E**nvironmental **D**iagnosis and **A**ssessment  
**MSC** – **M**eteorological **S**ervice of **C**anada  
**NCEP** – **N**ational **C**enter for **E**nvironmental **P**rediction  
**NCAR** – **N**ational **C**enter for **A**tmospheric **R**esearch  
**WOCE** – **W**orld **O**cean **C**irculation **E**xperiment

## A.11. ADOM-POP

*Gerharg Petersen*

A comprehensive mercury modelling system using the Eulerian reference frame of the Acid Deposition and Oxidant Model (ADOM) has been developed under the Canada-Germany Science & Technology Co-operation Agreement and applied within various projects funded by the European Commission to study the regional transport and deposition fluxes of atmospheric mercury species [Petersen *et al.*, 2001]. As a first step in extending this model system for POPs the cloud mixing, scavenging, chemistry and wet deposition modules of ADOM, originally designed for regional-scale acid precipitation and photochemical oxidants studies have been restructured to accommodate recent developments in atmospheric processes of benzo[a]pyrene (B[a]P). A stand-alone version of these modules referred to as the Tropospheric Chemistry Module (TCM) was designed to simulate the meteorology and chemistry of the entire depth of the troposphere to study cloud mixing, scavenging and physico-chemical processes associated with precipitation systems that generate wet deposition fluxes of B[a]P).

After comprehensive testing under different environmental conditions the TCM has been implemented into the full ADOM-POP model. Within the constraints of the available computer resources and input data, this model incorporates an up-to-date understanding of the detailed physical and chemical processes in the atmosphere. The vertical grid consists of 12 unequally spaced levels between the surface and the top of the model domain at 10 km. The model is run for a grid cell size 55 by 55 km (High Resolution Limited Area Model (HIRLAM) grid) over a 76 by 76 domain.

The transport and diffusion module uses a sophisticated cell-centered flux formulation solver for the 3-dimensional advection-diffusion equation. Dry deposition is modelled in terms of a deposition velocity for gaseous and particle associated mercury species, which is calculated as the inverse of the sum of the aerodynamic, deposition layer and surface canopy resistance. The mass transfer, chemistry and adsorption component of the model has a potential for incorporating numerous species and reactions including mass transfer, aqueous phase and gas phase chemical reactions and adsorption processes on particles. However, this component is restricted at present to the mass transfer of B[a]P from ambient air to cloud droplets and back evaporation after cloud dissipation.

The cloud physics module simulates the vertical distribution of mercury species in clouds. Two different modules are incorporated: one describes stratus (layer) clouds and the other simulates cumulus (convective) type clouds. One or the other or a combination (cumulus deck embedded in a stratus cloud) is used in the calculation depending on the characteristics of the precipitation observed.

The meteorological input data needed by ADOM are three-dimensional fields of wind speed, wind direction, pressure, temperature, relative humidity, vertical velocity and vertical diffusivity, and two-dimensional fields of surface winds, surface pressure, surface air temperature, friction velocity, Monin-Obukhov length, mixing height, cloud base and top height, amount of cloud cover and the amount of precipitation at every one hour model time step. These data sets are derived diagnostically using the weather prediction model HIRLAM.

The geophysical data include files for 8 land use categories (i. e. deciduous forest, coniferous forest, grassland, cropland, urban, desert, water and swamp) and 12 soil categories. The database also includes information on terrain height and the growing season. This geophysical data affects meteorology, dry deposition processes and air-surface exchange of gaseous mercury species.

Initial and boundary conditions are needed for all advected species in the model. Due its relative short atmospheric residence time and due to anthropogenic emissions occurring near the ground concentrations B[a]P is allowed to decrease with height to a value of about 10 % of the boundary value at the model top. In the absence of reliable measurement data, a very low initial value of  $1.5 \cdot 10^{-3}$  ng/m<sup>3</sup> at ground level is used for both B[a]P initial and boundary concentrations.

## A.12. Danish Eulerian Hemispheric Model (DEHM-POP)

*Kaj Mantzius Hansen and Jesper H. Christensen*

The Danish Eulerian Hemispheric Model (DEHM) is a 3-D dynamical atmospheric transport model initially developed to describe the long-range transport of sulphur into the Arctic [Christensen, 1997]. The model has since been further developed to describe the atmospheric transport of lead and CO<sub>2</sub>, and the model results have been thoroughly validated for these compounds [Christensen, 1997; Christensen, 1999; Geels et al., 2001]. The recent development has been to include a scheme with 54 chemical species (e.g. O<sub>3</sub>, NH<sub>3</sub>, and NO<sub>x</sub>) and 110 reactions, mercury, and persistent organic pollutants (POPs) in the model.

The model has a horizontal resolution of 150 km x 150 km and 20 unevenly distributed vertical layers in terrain-following sigma-coordinates extending to about 18 km height. It covers the majority of the northern hemisphere, and is driven by meteorological data from the numerical weather prediction model MM5V2 [Grell et al., 1995]. It is possible to run the model with a two-way nest covering the EMEP region with a resolution of 50 km x 50 km. A full model description can be found in Christensen [1997] and Frohn et al. [2002].

A description of the exchange processes between the land/ocean surfaces and the atmosphere is included in the model to account for the multi-hop transport of POPs. The environmental parameters for the surface compartments and the parameterisation of the air/surface exchange processes have been adapted from a multimedia box model [Strand and Hov, 1996]. The processes described by DEHM are atmospheric advection, diffusion and wet deposition, air/surface gas exchange and degradation in the three media.

The model has been used to study the atmospheric transport of  $\alpha$ -HCH for the years 1991 to 1998. Input to this model run were emissions of  $\alpha$ -HCH from 1990 [Li et al., 2000] and a background concentration in water interpolated from measurements from the late 1980s and early 1990s. The model results are currently being evaluated against measured data.

## A.13. SimpleBox

*Dirk van de Meent*

"SimpleBox is a nested multi-media fate model of the "Mackay type". The environment is modeled as consisting of a set of well-mixed, homogeneous compartments (air, two water compartments, sediments, three soil compartments and two vegetation compartments) in regional, continental and global scales. The model takes emission rates and rate constants for transport and transformation of micropollutants as input and computes steady-state concentrations as output. SimpleBox is a generic model in the sense that it can be customised to represent specific environmental situations. The default settings of the regional and continental scales of the model are set to match the EU procedures for evaluation of substances...

SimpleBox follows the Mackay concept of sequentially carrying out the modelling procedure at different stages of conceptual sophistication or "levels" (Mackay, 1991). In SimpleBox, the non-equilibrium, steady-state computation (level 3) and the quasi-dynamic non-equilibrium, non-steady-state computation (level 4) can be performed. Unlike the fugacity approach as adopted by Mackay, computation of mass flows and concentration levels in SimpleBox is done with concentration-based "piston velocity" type mass transfer coefficients [m.s<sup>-1</sup>]... As is done in the Mackay models, transfer and transformation phenomena are treated as simple pseudo first-order processes." - cited from [Brandes et al., 1996].

## A.14. MSCE-POP

*Victor Shatalov and Mikhail Fedyunin*

Here we present a short description of EMEP/MSCE-POP model. This model is a multicompartment one describing processes in and exchange between basic environmental compartments (atmosphere, soil, seawater,

vegetation). Spatial resolution of the model is 150 km x150 km. At present hemispheric version of the model with resolution 2.5°x2.5° is under development.

**Model structure.** Fig. A.4 presents the structure of the model showing environmental media and processes included.

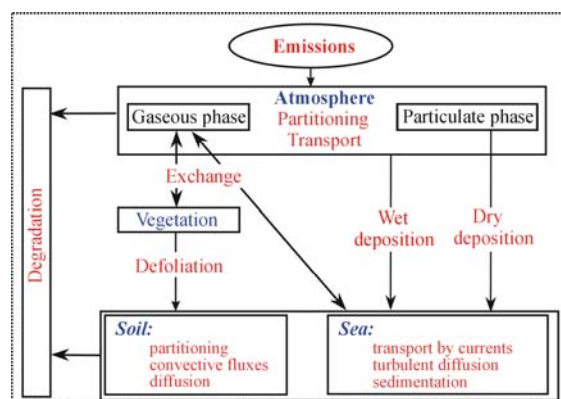


**Fig. A.4.** The scheme of the multicompartiment transport model MSCE-POP

In particular, apart from atmospheric transport the model takes into account the transport of pollutants by sea currents. This can be essential for the pollutants, which tend to be accumulated in the marine environment (e.g. HCB and  $\gamma$ -HCH). Vegetation is considered to describe their transport from vegetation to soil, forest litter as an intermediate media between vegetation and soil was introduced.

Model parameterizations are elaborated for PAHs (B[a]P, B[b]F and B[k]F), HCHs ( $\gamma$ -HCH), PCBs, HCB, and PCDD/Fs. At present there exists a modification of the model for evaluation of B[a]P and PCDD/Fs transboundary transport by country-to-country scheme with resolution 50 km x 50 km.

In the model, such media as the atmosphere, soil, and sea are separated vertically into a number of layers to describe the vertical transport of a pollutant in question. To describe variability of soil and vegetation properties in the horizontal direction the corresponding land-use and leaf area index information is taken into account.

**Time scale.** Due to large accumulation capacities of soil and sea compartments and long periods required for establishing equilibrium, for correct evaluation of POP environmental pollution levels long-term calculations are to be performed. This can be illustrated by plots of long-term dynamics of PCB accumulation in media (Fig. A.5) calculated for the period from 1970 to 2010 under the assumption that emissions from 1995 are constant.

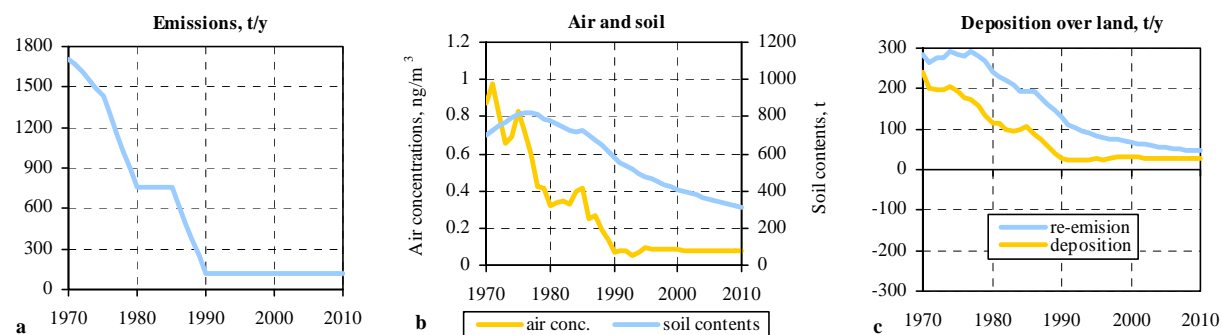


**Fig. A.5.** Long-term dynamics of emissions (a), air concentrations and soil content (b), and re-emission and particle deposition over land (c) for the period from 1970 to 2010 under the assumption that emissions are constant beginning from 1995

From these plots it is seen that contamination levels in soil are determined by a long-term process and can support pollution of other media for a long time period.

**Model reliability.** At present the discrepancies between measured and calculated data for all the pollutants considered are within the order of magnitude. More detailed information on comparison of calculated data against measurements can be found in [*Shatalov et al.*, 2000, 2001, 2002, 2003].

Detailed description of regional version of MSCE-POP model is published in MSC-E Report 4/2000 (vol.2) and of hemispheric version – in MSC-E Report 8/2002 [*Malanichev et al.*, 2002]. Recent model modification can be found in MSC-E Report 4/2003 [*Shatalov et al.*, 2003]; see also MSC-E web site: [www.msce@msceast.org](http://www.msce@msceast.org).

## COMPARISON OF PHYSICAL-CHEMICAL PROPERTIES AND DEGRADATION RATES OF PCB-28 AND PCB-180 BETWEEN INDIVIDUAL MODELS

**Table B.1.** “Reference data sets” of physical-chemical properties and degradation rates of PCB-28 and PCB-180\*

| Description  | Numerical values                       |          | Comments | Reference   |
|--|--|----------|----------|---|
|  | PCB-28                                 | PCB-180  |          |   |
| <i>Air/water Henry's law constant, <math>K_H</math> (Pa·m<sup>3</sup>/mol)</i>   |  |          |          |   |
| Temperature dependent:<br>$H = H_0 \exp(-a_H(1/T - 1/T_0))$<br>where $T$ - temperature (K), $H_0$ is the value at the reference temperature $T_0$ , and $a_H$ is a parameter of temperature dependence.                        | $H_0(T_0)$ ,<br>Pa·m <sup>3</sup> /mol | 9.46E+00 | 1.98E+00 | Coefficients are recalculated from the following temperature dependence:<br>$\log H = \log H(25^\circ\text{C}) - (\Delta U_{aw} + R \cdot 298.15)/(\ln(10) \cdot R) \cdot (1/T - 1/298.15)$<br>where: $T$ - temperature; $R$ - Universal Gas Constant;<br>$\Delta U_{aw}$ - internal energy of phase transfer, kJ/mol (PCB-28: 52.3; PCB-180: 63.6).<br>$H(25^\circ\text{C})$ - Henry 's law constant at 25°C, Pa·m <sup>3</sup> /mol (PCB-28: 30.5; PCB-180: 8.13).  |
|  | $a_H$                                  | 6588.7   | 7947.9   |   |
| <i>Air/water partition coefficient, <math>K_{aw}</math> (dimensionless)</i>  |  |          |          |   |
| Temperature dependent:<br>$K_{aw} = K_{aw}^0 \exp(-a_{Kaw}(1/T - 1/T_0))$<br>where $T$ - temperature (K), $K_{aw}^0$ is the value at the reference temperature $T_0$ , and $a_{Kaw}$ is a parameter of temperature dependence. | $K_{aw}^0(T_0)$ ,<br>dimensionless     | 4.02E-03 | 8.42E-04 | Coefficients are recalculated from the following temperature dependence:<br>$\log K_{aw} = \log K_{aw}(25^\circ\text{C}) - \Delta U_{aw}/(\ln(10) \cdot R) \cdot (1/T - 1/298.15)$<br>where: $T$ - temperature; $R$ - Universal Gas Constant;<br>$\Delta U_{aw}$ - internal energy of phase transfer, kJ/mol (PCB-28: 52.3; PCB-180: 63.6).<br>$K_{aw}(25^\circ\text{C})$ - dimensionless air/water partition coefficient at 25°C, estimated from:<br>$K_{aw}(25^\circ\text{C}) = H(25^\circ\text{C})/(R \cdot 298.15)$ |
|  | $a_{Kaw}$                              | 6290.6   | 7649.7   |   |
| <i>Subcooled liquid vapour pressure, <math>p_{ol}</math> (Pa)</i>  |  |          |          |   |
| Temperature dependent:<br>$p_{ol} = p_{ol}^0 \exp(-a_p(1/T - 1/T_0))$<br>where $T$ - temperature (K), $p_{ol}^0$ is the value at the reference temperature $T_0$ , and $a_p$ is a parameter of temperature dependence.         | $p_{ol}^0(T_0)$ ,                      | 5.24E-03 | 1.51E-05 | Coefficients are recalculated from the following temperature dependence:<br>$\log p_{ol} = \log p_{ol}(25^\circ\text{C}) - (\Delta U_a + R \cdot 298.15)/(\ln(10) \cdot R) \cdot (1/T - 1/298.15)$<br>where: $T$ - temperature; $R$ - Universal Gas Constant;<br>$\Delta U_a$ - internal energy of phase transfer, kJ/mol (PCB-28: 74.2; PCB-180:89.6).<br>$p_{ol}(25^\circ\text{C})$ - vapour pressure at 25°C, Pa (PCB-28: 2.70E-2; PCB-180:1.08E-4).   |
|  | $a_p$                                  | 9222.9   | 11075.2  |   |
| <i>Octanol/water partition coefficient, <math>K_{ow}</math> (dimensionless)</i>  |  |          |          |   |
| Temperature dependent:<br>$K_{ow} = K_{ow}^0 \exp(a_{Kow}(1/T - 1/T_0))$<br>where $T$ - temperature (K), $K_{ow}^0$ is the value at the reference temperature $T_0$ , and $a_{Kow}$ is a parameter of temperature dependence.  | $K_{ow}^0(T_0)$ ,<br>dimensionless     | 8.09E+05 | 2.70E+07 | Coefficients are recalculated from the following temperature dependence:<br>$\log K_{ow} = \log K_{ow}(25^\circ\text{C}) - \Delta U_{ow}/(\ln(10) \cdot R) \cdot (1/T - 1/298.15)$<br>where: $T$ - temperature; $R$ - Universal Gas Constant;<br>$\Delta U_{ow}$ - internal energy of phase transfer, kJ/mol (PCB-28: -26.3 ; PCB-180: -29.1).<br>$K_{ow}(25^\circ\text{C})$ - octanol/water partition coefficient at 25 °C, dimensionless<br>(PCB-28: 4.61E+5; PCB-180:1.45E+7)  |
|  | $a_{Kow}$                              | 3163.3   | 3500.1   |   |

| Description   |                                     | Numerical values |          | Comments  | Reference          |
|---|-------------------------------------|------------------|----------|---|--------------------|
|   |                                     | PCB-28           | PCB-180  |   |                    |
| <i>Octanol/air partition coefficient, <math>K_{oa}</math> (dimensionless)</i>   |                                     |                  |          |   |                    |
| Temperature dependent:<br>$K_{oa} = K_{oa}^0 \exp(a_{K_{oa}}(1/T - 1/T_0))$<br>where $T$ - temperature (K), $K_{oa}^0$ is the value at the reference temperature $T_0$ , and $a_{K_{oa}}$ is a parameter of temperature dependence. | $K_{oa}^0(T_0)$ ,<br>dimensionless  | 3.77E+08         | 1.06E+11 | Coefficients are recalculated from the following temperature dependence:<br>$\log K_{oa} = \log K_{oa}(25^\circ\text{C}) - \Delta U_{oa}/(\ln(10) \cdot R) \cdot (1/T - 1/298.15)$<br>where: $T$ - temperature; $R$ - Universal Gas Constant;<br>$\Delta U_{oa}$ - internal energy of phase transfer, kJ/mol (PCB-28: -78.5; PCB-180: -92.8).<br>$K_{oa}(25^\circ\text{C})$ - octanol/air partition coefficient at $25^\circ\text{C}$ , dimensionless<br>(PCB-28: 7.05E+7; PCB-180:1.46E+10); | Li et al., 2003    |
|   | $a_{K_{oa}}$                        | 9441.9           | 11161.9  |   |                    |
| <i>Organic carbon/water partition coefficient, <math>K_{oc}</math> (dimensionless)</i>  |                                     |                  |          |   |                    |
| Regression relation:<br>$K_{oc} = regc K_{ow}^b$<br>where $regc$ and $b$ are regression coefficients  | <i>regc</i>                         | 0.41             | 0.41     | $K_{oc}$ is calculated from $K_{ow}$ , where $K_{ow}$ is the temperature dependent octanol-water partition coefficient  | Karickhoff, 1981   |
|   | $b$                                 | 1                | 1        |   |                    |
| <i>Water solubility, <math>S_{WL}</math> (mol/m<sup>3</sup>)</i>  |                                     |                  |          |   |                    |
| Temperature independent   | $S_{WL}(T)$ ,<br>mol/m <sup>3</sup> | 5.53E-04         | 7.57E-06 | Values are calculated for $T = 283.15$ with the help of the following temperature dependence:<br>$\log S_{WL} = \log S_{WL}(25^\circ\text{C}) - \Delta U_{W}/(\ln(10) \cdot R) \cdot (1/T - 1/298.15)$<br>where: $R$ - Universal Gas Constant;<br>$\Delta U_{W}$ - internal energy of phase transfer, kJ/mol (PCB-28: 22.0; PCB-180: 26.0).<br>$S_{WL}(25^\circ\text{C})$ - water solubility, mol/m <sup>3</sup> at $25^\circ\text{C}$ (PCB-28: 8.85E-4; PCB-180:1.32E-5).                    | Li et al., 2003    |
| <i>Degradation rate constants, <math>k_d</math> (1/s)</i>   |                                     |                  |          |   |                    |
| Degradation in atmosphere:<br>Temperature independent   | $k_{air}(T)$ ,<br>1/s               | 3.50E-07         | 3.50E-08 | Degradation rate constant in the air is converted from half-life values, $t_{1/2}$ (PCB-28: 550; PCB-180: 5500):<br>$k_d = 0.693/t_{1/2}$<br>where $k_d$ is the first-order rate constant ( $s^{-1}$ ) and $t_{1/2}$ is the half-life (s).  | Mackay et al, 1992 |
| Degradation in soil:<br>Temperature independent   | $k_{soil}(T)$ ,<br>1/s              | 3.50E-09         | 3.50E-09 | Degradation rate constant in soil is converted from half-life values (PCB-28:55000; PCB-180: 55000):<br>$k_d = 0.693/t_{1/2}$<br>where $k_d$ is the first-order rate constant ( $s^{-1}$ ) and $t_{1/2}$ is the half-life (s).  | Mackay et al, 1992 |
| Degradation in water:<br>Temperature independent  | $k_{water}(T)$ ,<br>1/s             | 1.13E-08         | 3.50E-09 | Degradation rate constant in water is converted from half-life values (PCB-28: 17000; PCB-180: 55000):<br>$k_d = 0.693/t_{1/2}$<br>where $k_d$ is the first-order rate constant ( $s^{-1}$ ) and $t_{1/2}$ is the half-life (s).  | Mackay et al, 1992 |
| Degradation in sediment:<br>Temperature independent   | $k_{sed}(T)$ ,<br>1/s               | 3.50E-09         | 3.50E-09 | Degradation rate constant in sediment is converted from half-life values (PCB-28: 55000; PCB-180: 55000):<br>$k_d = 0.693/t_{1/2}$<br>where $k_d$ is the first-order rate constant ( $s^{-1}$ ) and $t_{1/2}$ is the half-life (s).   | Mackay et al, 1992 |

\* - for the sake of comparability, the base values and coefficients of temperature dependences of the considered parameters are given here for the temperature 283.15 K ( $T_0$ ) and the way they were recalculated from original dependencies is specified in the field "Comments".

**Table B.2.** The Henry's law constant and the air/water partition coefficient of PCBs (data sets of the participating POP models)\*

| Model                 | Description   | Numerical values               |          | Comments | Reference   |   |
|-----------------------|---|--------------------------------|----------|----------|---|---|
|                       |   | PCB-28                         | PCB-180  |          |   |   |
| CAM/POPs              | Temperature dependent:<br>$H = H_0 \exp(-a_H(1/T - 1/T_0))$<br>where $T$ - temperature (K), $H_0$ is the value at the reference temperature $T_0$ , and $a$ is a parameter of temperature dependence.<br>Temperature dependent: $K_{aw} = H / (R \cdot T)$        | $H_0$ , Pa·m <sup>3</sup> /mol | -        | 2.53E-01 | Coefficient $a_H$ of the exponential equation are recalculated from the coefficient of the following temperature dependence:<br>$H = H_0 \cdot 10^{(-3416(1/T - 1/T_0))}$<br>with the help of the following formula: $a_H = \ln(10) \cdot 3416$ ,<br>It was obtained from the following temperature dependence:<br>$\log(H/H(25^\circ\text{C})) = \text{slop}(1/T - 1/298)$<br>$H(25^\circ\text{C})$ - Henry's law constant at 25°C, Pa·m <sup>3</sup> /mol (PCB-180: 1.01)   | Achman, Hornbuckle, Eisenreich [1993]           |
|                       |   | $a_H$                          | -        | 7865.6   |   |   |
|                       |   | $T_0$ , K                      | -        | 283.15   |   |   |
| SimpleBox             | Temperature dependent:<br>$H = H_0 \exp(-a_H(1/T - 1/T_0))$<br>where $T$ - temperature (K), $H_0$ is the value at the reference temperature $T_0$ , and $a_H$ is a parameter of temperature dependence.   | $H_0$ , Pa·m <sup>3</sup> /mol | 9.46E+00 | 1.98E+00 | Same to the "reference data set"  | Li et al., 2003                                 |
|                       |   | $a_H$                          | 6588.7   | 7947.9   |   |   |
|                       |   | $T_0$ , K                      | 283.15   | 283.15   |   |   |
| EVN-BETR and UK-MODEL | $H$ is temperature independent.<br>Temperature dependent:<br>$K_{aw} = K_{aw}^0 \exp(-a_{Kaw}(1/T - 1/T_0))$<br>where $T$ - temperature (K), $K_{aw}^0$ is the value at the reference temperature $T_0$ , and $a_{Kaw}$ is a parameter of temperature dependence. | $H$ , Pa·m <sup>3</sup> /mol   | 30.5     | 8.18     | Calculated as $H = \text{Vapour Pressure (Pa)} / \text{Water Solubility (mol/m}^3\text{)}$ at 25°C<br>At 10°C, calculated as:<br>$K_{aw}(T_0) = 10^{\log K_{aw}} \cdot a$<br>$a = \exp[(\Delta H_{vap} / R) \cdot (1/T_0 - 1/T)]$ .<br>$\Delta H_{vap} = 62.8$ kJ/mol: Enthalpy of vaporisation (from water to air)<br>Here $a_{Kaw} = \Delta H_{vap} / R$  | Li et al., 2003                                 |
|                       |   | $K_{aw}$ , dimensionless       | 4.02E-03 | 8.48E-04 |   |   |
|                       |   | $a_{Kaw}$                      | 7553.5   | 7553.5   |   |   |
|                       |   | $T_0$ , °K                     | 283.15   |          |   |   |
| CliMoChem             | Temperature dependent:<br>$K_{aw} = K_{aw}^0 \exp(-a_{Kaw}(1/T - 1/T_0))$<br>where $T$ - temperature (K), $K_{aw}^0$ is the value at the reference temperature $T_0$ , and $a_{Kaw}$ is a parameter of temperature dependence.                                    | $K_{aw}^0$ , dimensionless     | 4.63E-03 | 1.83E-03 | $K_{aw}(T) = K_{aw}(T_{ref}) \exp(dH_{Kaw}/R(1/T_{ref} - 1/T))$ (dimensionless)<br>$T$ = temperature (283.15 K); $T_{ref}$ = reference temperature (298.15 K)<br>$K_{aw}(T_{ref})$ = Henry's law constant at $T_{ref}$ (dimensionless):<br>PCB 28: 1.27E-2; PCB 180: 8.92E-3<br>$dH_{kaw}$ = phase transfer enthalpy (J/mol): PCB 28: 47200; PCB 180: 74100<br>$R$ = universal gas constant (8.3145 J/mol·K)  | Beyer et al., 2002                              |
|                       |   | $a_{Kaw}$                      | 5680     | 8910     |   |   |
|                       |   | $T_0$ , K                      | 283.15   |          |   |   |
| DEHM-POP              | Temperature dependent:<br>$K_{aw} = K_{aw}^0 \exp(-a_{Kaw}(1/T - 1/T_0))$<br>where $T$ - temperature (K), $K_{aw}^0$ is the value at the reference temperature $T_0$ , and $a_{Kaw}$ is a parameter of temperature dependence.                                    | $K_{aw}^0$ , dimensionless     | 4.63E-03 | 1.83E-03 | $K_{aw}(283.15) = K_{aw}^0(298.15) \exp(-a_{Kaw}(1/T - 1/T_0))$ ,<br>where $K_{aw}^0(298.15) = 1.27E-2, 8.92E-3$ for PCB 28 and 180 respectively  | Beyer et al., 2002                              |
|                       |   | $a_{Kaw}$                      | 5680     | 8917     |   |   |
|                       |   | $T_0$ , K                      | 283.15   |          |   |   |
| MSCE-POP              | Temperature dependent:<br>$H = H_0 \exp(-a_H(1/T - 1/T_0))$<br>where $T$ - temperature (K), $H_0$ is the value at the reference temperature $T_0$ , and $a_H$ is a parameter of temperature dependence.<br>Temperature dependent:<br>$K_{aw} = H / (R \cdot T)$   | $H_0$ , Pa·m <sup>3</sup> /mol | 7.642    | 2.388    | Coefficients of the exponential equation are recalculated from the standard form of temperature dependence: $\log H = -A/T(K) + B$<br>with the help of the following formulas:<br>$a_H = \ln(10) \cdot A$ ; $H_0 = 10^{(-A/T_0 + B)}$ ,<br>where $A = \Delta H_w / 2.303R$ ,<br>$B = \log H_{298} + \Delta H_w / 2.303R(298)$ .<br>where $H_{298}$ is Henry's law constant (Pa·m <sup>3</sup> /mol) at 25°C (PCB-28: 28.58; PCB-180: 10.74);<br>$\Delta H_w$ is the enthalpy of volatilization from water, kJ/mol (PCB-28: 61.8; PCB-180: 71.3) | Burkhard et al., 1985<br>Dunnivant et al., 1992 |
|                       |   | $a_H$                          | 7430     | 8575     |   |   |
|                       |   | $T_0$ , K                      | 283.15   | 283.15   |   |   |

\* - for the sake of comparability, the base values and coefficients of temperature dependences of the considered parameters are given here at the temperature 283.15 K ( $T_0$ ) and the way they were recalculated from original dependencies is specified in the field "Comments".

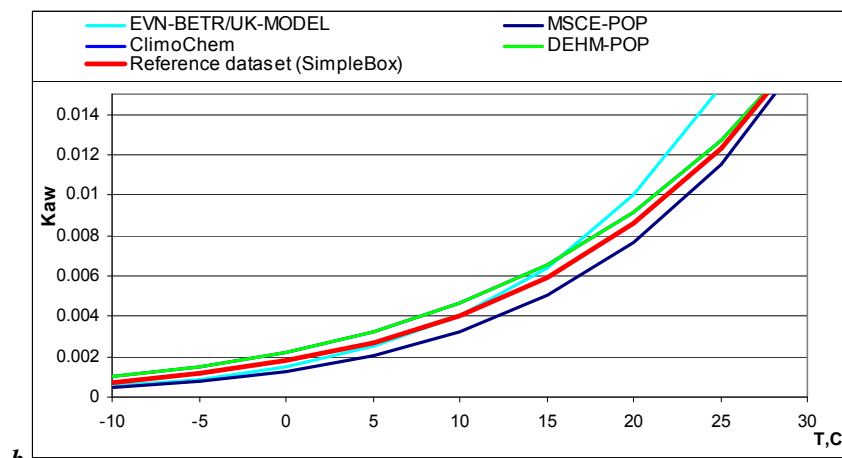
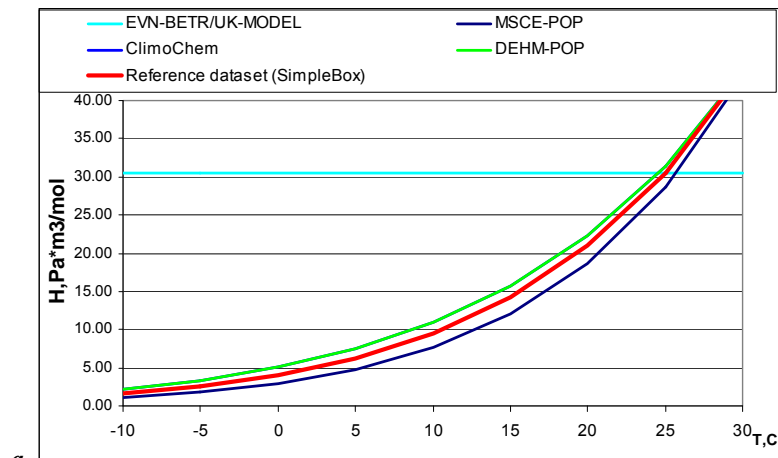


**Fig. B.1.** Comparison of temperature dependencies of Henry's law constant ( $H$ ,  $\text{Pa}\cdot\text{m}^3/\text{mol}$ ) and air/water partition coefficient ( $K_{aw}$ , dimensionless) of PCB-28.

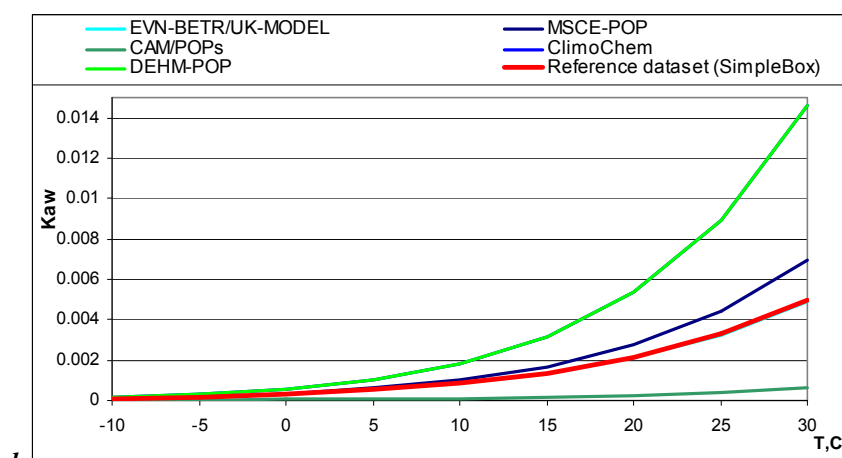
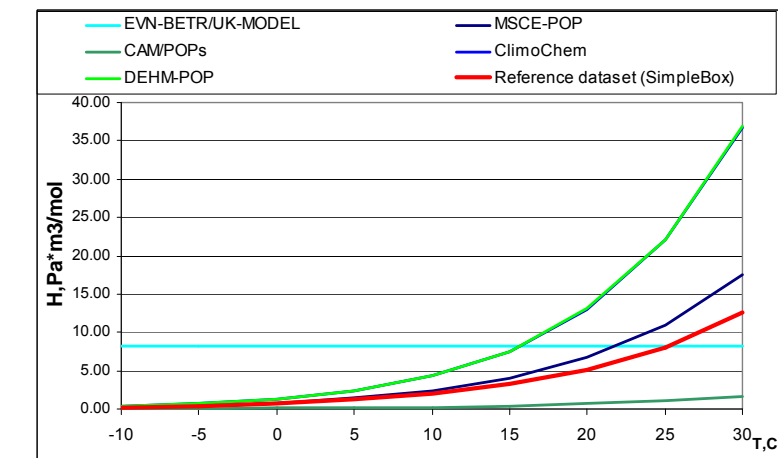


**Fig. B.2.** Comparison of temperature dependencies of Henry's law constant ( $H$ ,  $\text{Pa}\cdot\text{m}^3/\text{mol}$ ) and air/water partition coefficient ( $K_{aw}$ , dimensionless) of PCB-180.

**Table B.3.** Absolute values and statistical parameters of Henry's law constant (H, Pa·m<sup>3</sup>/mol) and air/water partition coefficient (K<sub>aw</sub>, dimensionless) of PCB-28 for three arbitrary temperatures (-10°C, 10°C and 25°C) and coefficients of temperature dependencies

|                       | H, Pa·m <sup>3</sup> /mol |          |          |                | K <sub>aw</sub> , dimensionless |          |          |                  |
|-----------------------|---------------------------|----------|----------|----------------|---------------------------------|----------|----------|------------------|
|                       | -10°C                     | 10°C     | 25°C     | a <sub>H</sub> | -10°C                           | 10°C     | 25°C     | a <sub>Kaw</sub> |
| SimpleBox             | 1.61E+00                  | 9.46E+00 | 3.05E+01 | 6588.7         | 7.43E-04                        | 4.02E-03 | 1.23E-02 | 6290.6           |
| EVN-BETR and UK-MODEL | 3.05E+01                  | 3.05E+01 | 3.05E+01 | -              | 5.29E-04                        | 4.02E-03 | 1.54E-02 | 7553.5           |
| CliMoChem             | 2.21E+00                  | 1.09E+01 | 3.15E+01 | -              | 1.01E-03                        | 4.63E-03 | 1.27E-02 | 5680             |
| DEHM-POP              | 2.21E+00                  | 1.09E+01 | 3.15E+01 | -              | 1.01E-03                        | 4.63E-03 | 1.27E-02 | 5680             |
| MSCE-POP              | 1.04E+00                  | 7.64E+00 | 2.86E+01 | 7430           | 4.75E-04                        | 3.25E-03 | 1.15E-02 | -                |
| "Reference data set"  | 1.61E+00                  | 9.46E+00 | 3.05E+01 | 6588.7         | 7.43E-04                        | 4.02E-03 | 1.23E-02 | 6290.6           |
| min                   | 1.04E+00                  | 7.64E+00 | 2.86E+01 | 6588.7         | 4.75E-04                        | 3.25E-03 | 1.15E-02 | 5680.0           |
| max                   | 3.05E+01                  | 3.05E+01 | 3.15E+01 | 7430.0         | 1.01E-03                        | 4.63E-03 | 1.54E-02 | 7553.5           |
| arith. mean           | 6.53E+00                  | 1.31E+01 | 3.05E+01 | 6869.1         | 7.51E-04                        | 4.09E-03 | 1.28E-02 | 6298.9           |
| median                | 1.91E+00                  | 1.02E+01 | 3.05E+01 | 6588.7         | 7.43E-04                        | 4.02E-03 | 1.25E-02 | 6290.6           |
| geom. mean            | 2.72E+00                  | 1.16E+01 | 3.05E+01 | 6858.0         | 7.22E-04                        | 4.07E-03 | 1.28E-02 | 6263.9           |
| max/min               | 2/29*                     | 1/4*     | 1        | 1.1            | 2                               | 1        | 1        | 1.3              |

\* - the first value is calculated without the temperature independent value of H (EVN-BETR and UK-MODEL), the second value is calculated taking it into account.

**Table B.4.** Absolute values and statistical parameters of Henry's law constant (H, Pa·m<sup>3</sup>/mol) and air/water partition coefficient (K<sub>aw</sub>, dimensionless) of PCB-180 for three arbitrary temperatures (-10°C, 10°C and 25°C) and coefficients of temperature dependencies

|                       | H, Pa·m <sup>3</sup> /mol |          |          |                | K <sub>aw</sub> , dimensionless |          |           |                  |
|-----------------------|---------------------------|----------|----------|----------------|---------------------------------|----------|-----------|------------------|
|                       | -10°C                     | 10°C     | 25°C     | a <sub>H</sub> | -10°C                           | 10°C     | 25°C      | a <sub>Kaw</sub> |
| CAM/POPs              | 3.06E-02                  | 2.53E-01 | 1.02E+00 | 7865.6         | 1.40E-05                        | 1.07E-04 | 4.13E-04  | -                |
| SimpleBox             | 2.35E-01                  | 1.98E+00 | 8.13E+00 | 7947.9         | 1.08E-04                        | 8.42E-04 | 3.28E-03  | 7649.7           |
| EVN-BETR and UK-MODEL | 8.18E+00                  | 8.18E+00 | 8.18E+00 | -              | 1.12E-04                        | 8.48E-04 | 3.25E-03  | 7553.5           |
| CliMoChem             | 3.66E-01                  | 4.31E+00 | 2.21E+01 | -              | 1.67E-04                        | 1.83E-03 | 8.91E-03* | 8910*            |
| DEHM-POP              | 3.66E-01                  | 4.31E+00 | 2.21E+01 | -              | 1.67E-04                        | 1.83E-03 | 8.92E-03* | 8917*            |
| MSCE-POP              | 2.39E-01                  | 2.39E+00 | 1.10E+01 | 8575           | 1.09E-04                        | 1.01E-03 | 4.42E-03  | -                |
| "Reference data set"  | 2.35E-01                  | 1.98E+00 | 8.13E+00 | 7947.9         | 1.08E-04                        | 8.42E-04 | 3.28E-03  | 7649.7           |
| min                   | 3.06E-02                  | 2.53E-01 | 1.02E+00 | 7865.6         | 1.40E-05                        | 1.07E-04 | 4.13E-04  | 7553.5           |
| max                   | 8.18E+00                  | 8.18E+00 | 2.21E+01 | 8575.0         | 1.67E-04                        | 1.83E-03 | 8.92E-03  | 8917.0           |
| arith. mean           | 1.38E+00                  | 3.34E+00 | 1.15E+01 | 8084.1         | 1.12E-04                        | 1.04E-03 | 4.64E-03  | 8136.0           |
| median                | 2.39E-01                  | 2.39E+00 | 8.18E+00 | 7947.9         | 1.09E-04                        | 8.48E-04 | 3.28E-03  | 7649.7           |
| geom. mean            | 3.32E-01                  | 2.32E+00 | 8.40E+00 | 8079.2         | 9.20E-05                        | 8.05E-04 | 3.38E-03  | 8111.6           |
| max/min               | 12/267***                 | 17/32*** | 22/22*** | 1.1            | 12                              | 17       | 22        | 1.2              |

\*- difference in absolute values obtained from identical temperature dependencies can be explained by accuracy of coefficient recalculation.

\*\*\* - the first value is calculated without the temperature independent value of H (EVN-BETR and UK-MODEL), the second value is calculated taking it into account.

**Table B.5.** The subcooled liquid vapour pressure of PCBs (data sets of the participating POP models)\*

| Model                 | Description   | Numerical values |          | Comments | Reference  |   |
|-----------------------|---|------------------|----------|----------|--|---|
|                       |   |                  | PCB-28   |          |  | PCB-180   |
| CAM/POPs              | Temperature dependent:<br>$p_{ol} = p_{ol}^0 \exp(-a_p(1/T - 1/T_0))$<br>where $T$ - temperature (K), $p_{ol}^0$ is the value at the reference temperature $T_0$ ,<br>and $a_p$ is a parameter of temperature dependence. | $p_{ol}^0$ , Pa  | -        | 1.67E-05 | Coefficients of the exponential equation are recalculated from the standard form of temperature dependence:<br>$p_{ol} = 10^{(m/T + b)}$<br>where $T$ - temperature ( $^{\circ}$ K);<br>$m = -5042$ - parameter of temperature dependence, and<br>$b = 13.03$ - parameter depended on molecular weight.<br>It was obtained from the following original equation:<br>$\log(p_{ol}) = -Q / (2.303 RT) + b$<br>where: $T$ - temperature; $R$ - Universal Gas Constant;<br>$Q$ - the heat of vaporisation (kJ/mol) | <i>Harner et al., 1996;</i><br><i>Falconer et al., 1995</i> |
|                       |   | $a_p$            | -        | 11610    |  |   |
|                       |   | $T_0$ , K        | -        | 283.15   |  |   |
| SimpleBox             | Temperature dependent:<br>$p_{OL} = p_{OL}^0 \exp(-a_p(1/T - 1/T_0))$<br>where $T$ - temperature (K), $p_{OL}^0$ is the value at the reference temperature $T_0$ ,<br>and $a_p$ is a parameter of temperature dependence. | $p_{OL}^0$ , Pa  | 5.24E-03 | 1.51E-05 | Same to the "reference data set"   | <i>Li et al., 2003</i>                                      |
|                       |   | $a_p$            | 9222.9   | 11075.2  |  |   |
|                       |   | $T_0$ , K        | 283.15   | 283.15   |  |   |
| EVN-BETR and UK-MODEL | Temperature independent:  | $p_{OL}$ , Pa    | 2.70E-02 | 1.08E-04 | T = 25°C   | <i>Li et al., 2003</i>                                      |
| MSCE-POP              | Temperature dependent:<br>$p_{ol} = p_{ol}^0 \exp(-a_p(1/T - 1/T_0))$<br>where $T$ - temperature (K), $p_{ol}^0$ is the value at the reference temperature $T_0$ ,<br>and $a_p$ is a parameter of temperature dependence. | $p_{OL}^0$ , Pa  | 6.43E-03 | 1.67E-05 | Coefficients of the exponential equation are recalculated from the standard form of temperature dependence:<br>$\log p_{ol} (\text{Pa}) = -A/T(K) + B$<br>with the help of the following formulas:<br>$a_p = \ln(10) \cdot A$<br>$p_{ol}^0 = 10^{(-A/T_0 + B)}$<br>where; $A = 4075$ and $5072$ for PCB-28 and PCB-180 respectively;<br>$B = 12.20$ and $13.03$ for PCB-28 and PCB-180 respectively  | <i>Falconer and Bidleman, 1994</i>                          |
|                       |   | $a_p$            | 9383     | 11610    |  |   |
|                       |   | $T_0$ , K        | 283.15   | 283.15   |  |   |

\* - for the sake of comparability, the base values and coefficients of temperature dependences of the considered parameters are given here at the temperature 283.15 K ( $T_0$ ) and the way they were recalculated from original dependencies is specified in the field "Comments".

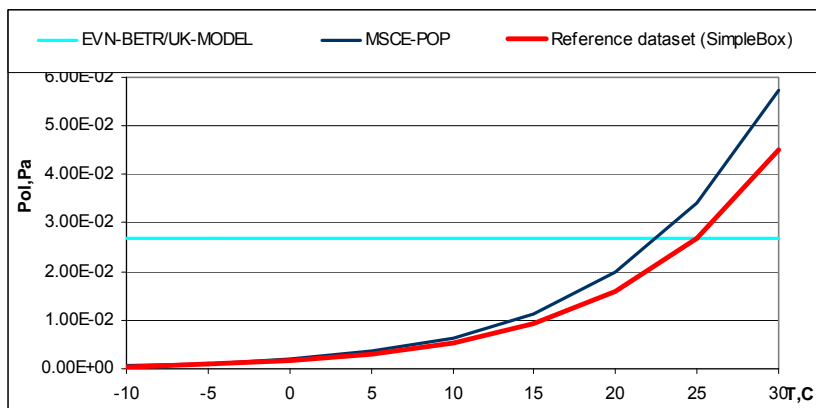


**Fig. B.3.** Comparison of temperature dependencies of subcooled liquid vapour pressure of PCB-28 used in data sets of the participating POP models and in “reference data set”

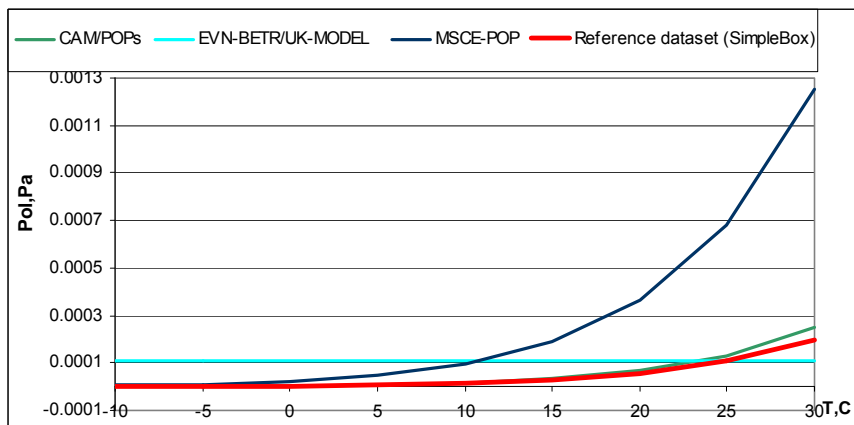


**Fig. B.4.** Comparison of temperature dependencies of subcooled liquid vapour pressure of PCB-180 used in data sets of the participating POP models and in “reference data set”

**Table B.6.** Absolute values, coefficients of temperature dependence and statistical parameters of subcooled liquid vapour pressure of PCB-28 for three arbitrary temperatures (-10 °C, 10 °C and 25 °C)

|                    | $p_{0L}$ , Pa |          |          | $a_p$  |
|--------------------|---------------|----------|----------|--------|
|                    | -10°C         | 10°C     | 25°C     |        |
| SimpleBox          | 4.41E-04      | 5.24E-03 | 2.70E-02 | 9222.9 |
| EVN-BETR/UK-MODEL  | 2.70E-02      | 2.70E-02 | 2.70E-02 | -      |
| MSCE-POP           | 5.18E-04      | 6.43E-03 | 3.41E-02 | 9383   |
| Reference data set | 4.41E-04      | 5.24E-03 | 2.70E-02 | 9222.9 |
| <i>min</i>         | 4.41E-04      | 5.24E-03 | 2.70E-02 | 9222.9 |
| <i>max</i>         | 2.70E-02      | 2.70E-02 | 3.41E-02 | 9383.0 |
| <i>arith. mean</i> | 7.10E-03      | 1.10E-02 | 2.88E-02 | 9276.3 |
| <i>median</i>      | 4.79E-04      | 5.84E-03 | 2.70E-02 | 9222.9 |
| <i>geom. mean</i>  | 1.28E-03      | 8.31E-03 | 2.86E-02 | 9276.0 |
| <i>max/min</i>     | 1.2/61.3*     | 1.2/5.2* | 1.3      | 1.02   |

\* - the first value is calculated without the temperature independent value of  $p_{0L}$  (EVN-BETR and UK-MODEL), the second value is calculated taking it into account

**Table B.7.** Absolute values, coefficients of temperature dependence and statistical parameters of subcooled liquid vapour pressure of PCB-180 for three arbitrary temperatures (-10 °C, 10 °C and 25 °C)

|                    | $p_{0L}$ , Pa |          |          | $a_p$   |
|--------------------|---------------|----------|----------|---------|
|                    | -10°C         | 10°C     | 25°C     |         |
| CAM/POPs           | 7.40E-07      | 1.67E-05 | 1.31E-04 | 11610   |
| SimpleBox          | 7.73E-07      | 1.51E-05 | 1.08E-04 | 11075.2 |
| EVN-BETR/UK-MODEL  | 1.08E-04      | 1.08E-04 | 1.08E-04 | -       |
| MSCE-POP           | 5.07E-06      | 9.69E-05 | 6.84E-04 | 11610   |
| Reference data set | 7.73E-07      | 1.51E-05 | 1.08E-04 | 11075.2 |
| <i>min</i>         | 7.40E-07      | 1.51E-05 | 1.08E-04 | 11075.2 |
| <i>max</i>         | 1.08E-04      | 1.08E-04 | 6.84E-04 | 11610.0 |
| <i>arith. mean</i> | 2.31E-05      | 5.04E-05 | 2.28E-04 | 11342.6 |
| <i>median</i>      | 7.73E-07      | 1.67E-05 | 1.08E-04 | 11342.6 |
| <i>geom. mean</i>  | 3.00E-06      | 3.31E-05 | 1.62E-04 | 11339.4 |
| <i>max/min</i>     | 6.8/145.9*    | 6.4/7.2* | 6.3      | 1.05    |

\* - the first value is calculated without the temperature independent value of  $p_{0L}$  (EVN-BETR and UK-MODEL), the second value is calculated taking it into account

**Table B.8.** The octanol/water partition coefficient of PCBs (data sets of the participating POP models)\*

| Model                 | Description  | Numerical values           |          | Comments  | Reference   |   |
|-----------------------|--|----------------------------|----------|---|---|---|
|                       |  | PCB-28                     | PCB-180  |   |   |   |
| CAM/POPs              | Temperature dependent:<br>$K_{ow} = K_{oa} \cdot H/RT$<br>where $T$ - temperature (K); $R$ - Universal Gas Constant;<br>$H$ - Henry's law constant; $K_{oa}$ - Octanol/air partition coefficient (dimensionless)                             | -                          | -        | These values are calculated with the help of temperature dependencies of $H$ and $K_{oa}$ . | This study  |   |
| SimpleBox             | Temperature dependent:<br>$K_{ow} = K_{ow}^0 \exp(a_{Kow}(1/T - 1/T_0))$<br>where $T$ - temperature (K), $K_{ow}^0$ is the value at the reference temperature $T_0$ ,<br>and $a_{Kow}$ is a parameter of temperature dependence.             | $K_{ow}^0$ , dimensionless | 8.09E+05 | 2.70E+07  | Same to the "reference data set"  | <i>Li et al., 2003</i>  |
|                       |  | $a_{Kow}$                  | 3163.3   | 3500.1  |   |   |
|                       |  | $T_0$ , K                  | 283.15   | 283.15  |   |   |
| EVN-BETR and UK-MODEL | Temperature dependent:<br>$K_{ow} = K_{ow}^0 \exp(a_{Kow}(1/T - 1/T_0))$<br>where $T$ - temperature (K), $K_{ow}^0$ is the value at the reference temperature $T_0$ ,<br>and $a_{Kow}$ is a parameter of temperature dependence.             | $K_{ow}^0$ , dimensionless | 8.02E+05 | 2.69E+07  | For 10°C, calculated as<br>$K_{ow}(T_0) = 10^{\log K_{ow}} \cdot a$ ,<br>$a = \exp[(\Delta H_{sol}/R) \cdot (1/T_0 - 1/T)]$ .<br>$\Delta H_{sol} = -31.1$ KJ/mol:<br>Enthalpy of solution (from octanol to water)<br>Here: $a_{Kow} = \Delta H_{sol}/R$   | <i>Li et al., 2003</i>  |
|                       |  | $a_{Kow}$                  | 3740.5   | 3740.5  |   |   |
|                       |  | $T_0$ , K                  | 283.15   | 283.15  |   |   |
| CliMoChem             | Temperature dependent:<br>$K_{ow} = K_{ow}^0 \exp(a_{Kow}(1/T - 1/T_0))$<br>where $T$ - temperature (K), $K_{ow}^0$ is the value at the reference temperature $T_0$ ,<br>and $a_{Kow}$ is a parameter of temperature dependence ( $-dH/R$ ). | $K_{ow}^0$ , dimensionless | 9.41E+05 | 1.84E+07  | $K_{ow}(T) = K_{ow}(T_{ref}) \exp((dHK_{ow}/R)(1/T_{ref} - 1/T))$<br>dimensionless<br>$T$ = temperature (283.15 K);<br>$T_{ref}$ = reference temperature (298.15 K)<br>$K_{ow}(T_{ref})$ = Octanol/water partition coefficient at $T_{ref}$<br>PCB 28: 5.13E+5; PCB 180: 1.54E+7<br>$dHK_{ow}$ = phase transfer enthalpy (J/mol)<br>PCB 28: -28400; PCB 180: -8270<br>$R$ = universal gas constant (8.3145 J/mol·K) | <i>Beyer et al., 2002</i>                                       |
|                       |  | $a_{Kow}$                  | 3415.7   | 994.6   |   |   |
|                       |  | $T_0$ , K                  | 283.15   | 283.15  |   |   |
| DEHM-POP              | Temperature dependent:<br>$K_{ow} = K_{ow}^0 \exp(a_{Kow}(1/T - 1/T_0))$<br>where $T$ - temperature (K), $K_{ow}^0$ is the value at the reference temperature $T_0$ ,<br>and $a_{Kow}$ is a parameter of temperature dependence ( $-dH/R$ ). | $K_{ow}^0$ , dimensionless | 9.41E+05 | 1.84E+07  | $K_{ow}(283.15) = K_{ow}^0(298.15) \exp(a_{Kow}(1/T - 1/T_0))$ ,<br>where $K_{ow}^0(298.15) = 5.13E+5$ ;<br>1.54E+7 for PCB-28 and 180 respectively;<br>$a_{Kow} = dHK_{ow}/R$<br>$dHK_{ow}$ = phase transfer enthalpy (J/mol)<br>PCB 28: -28400; PCB 180: -8270<br>$R$ = universal gas constant (8.3145 J/mol·K)   | <i>Beyer et al., 2002</i>                                       |
|                       |  | $a_{Kow}$                  | 3414.5   | 994.6   |   |   |
|                       |  | $T_0$ , K                  | 283.15   | 283.15  |   |   |
| MSCE-POP              | Temperature independent  | $K_{ow}$ , dimensionless   | 6.31E+5  | 2.29E+7   | PCB-28: $\log K_{ow} = 5.8$<br>PCB-180: $\log K_{ow} = 7.36$  | <i>Mackay et al., 1992</i> ;<br><i>Hawker and Connell, 1988</i> |

\* - for the sake of comparability, the base values and coefficients of temperature dependences of the considered parameters are given here for the temperature 283.15 K ( $T_0$ ) and the way they were recalculated from original dependencies is specified in the field "Comments".

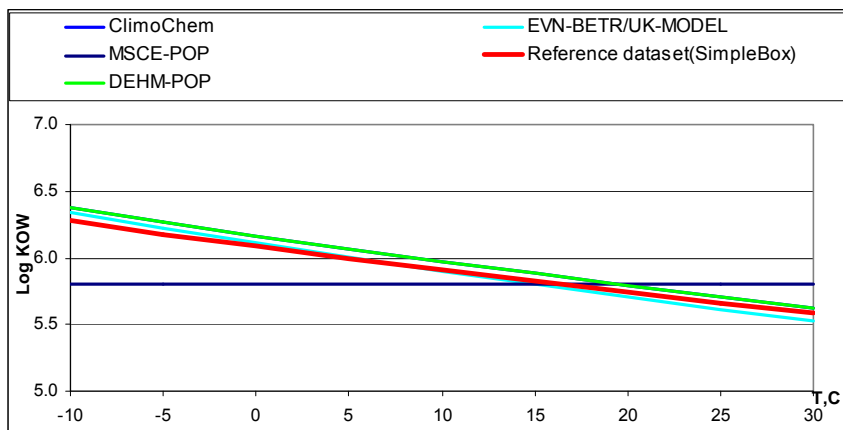


Fig. B.5. Comparison of temperature dependencies of  $\log K_{ow}$  of PCB-28 used in the models and in “reference data set”

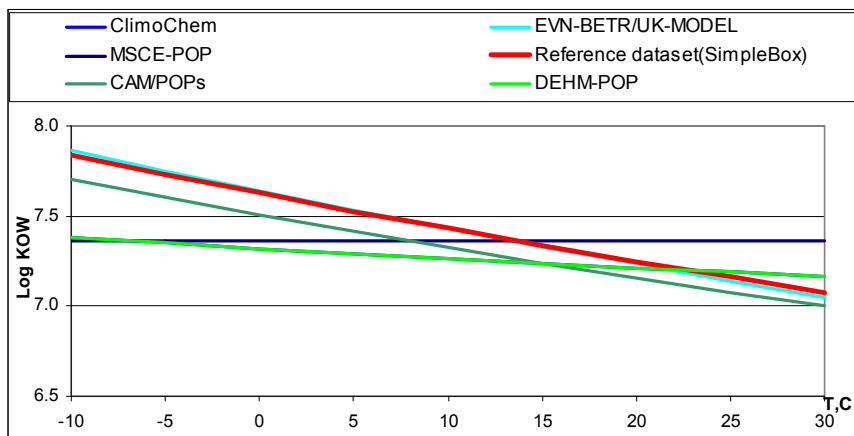


Fig. B.6. Comparison of temperature dependencies of  $\log K_{ow}$  of PCB-180 used in the models and in “reference data set”

**Table B.9.** Absolute values, coefficients of temperature dependence and statistical parameters of octanol/water partition coefficient of PCB-28 for three arbitrary temperatures (-10 °C, 10 °C and 25 °C)

|                    | $K_{ow}$  |           |           | $a_{Kow}$ |
|--------------------|-----------|-----------|-----------|-----------|
|                    | -10°C     | 10°C      | 25°C      |           |
| SimpleBox          | 1.89E+06  | 8.09E+05  | 4.61E+05  | 3163.3    |
| EVN-BETR/UK-MODEL  | 2.19E+06  | 8.02E+05  | 4.13E+05  | 3740.5    |
| CliMoChem          | 2.35E+06  | 9.41E+05  | 5.13E+05  | 3415.7*   |
| DEHM-POP           | 2.35E+06  | 9.41E+05  | 5.13E+05  | 3414.5*   |
| MSCE-POP           | 6.31E+05  | 6.31E+05  | 6.31E+05  | -         |
| Reference data set | 1.89E+06  | 8.09E+05  | 4.61E+05  | 3163.3    |
| <i>min</i>         | 6.31E+05  | 6.31E+05  | 4.13E+05  | 3163.3    |
| <i>max</i>         | 2.35E+06  | 9.41E+05  | 6.31E+05  | 3740.5    |
| <i>arith. mean</i> | 1.88E+06  | 8.25E+05  | 5.06E+05  | 3433.5    |
| <i>median</i>      | 2.19E+06  | 8.09E+05  | 5.13E+05  | 3415.1    |
| <i>geom. mean</i>  | 1.71E+06  | 8.16E+05  | 5.01E+05  | 3427.4    |
| <i>max/min</i>     | 1.2/3.7** | 1.2/1.5** | 1.2/1.5** | 1.2       |

\* - difference in absolute values obtained for identical temperature dependencies can be explained by accuracy of coefficient recalculation;

\*\* - the first value is calculated without the temperature independent value of  $K_{ow}$  (MSCE-POP), the second value is calculated taking it into account

**Table B.10.** Absolute values, coefficients of temperature dependence and statistical parameters of octanol/water partition coefficient of PCB-180 for three arbitrary temperatures (-10 °C, 10 °C and 25 °C)

|                    | $K_{ow}$  |           |           | $a_{Kow}$ |
|--------------------|-----------|-----------|-----------|-----------|
|                    | -10°C     | 10°C      | 25°C      |           |
| CAM/POPs           | 5.11E+07  | 2.12E+07  | 1.20E+07  | -         |
| SimpleBox          | 6.91E+07  | 2.70E+07  | 1.45E+07  | 3500.1*   |
| EVN-BETR/UK-MODEL  | 7.34E+07  | 2.69E+07  | 1.38E+07  | 3740.5*   |
| CliMoChem          | 2.40E+07  | 1.84E+07  | 1.54E+07  | 994.6     |
| DEHM-POP           | 2.40E+07  | 1.84E+07  | 1.54E+07  | 994.6     |
| MSCE-POP           | 2.29E+07  | 2.29E+07  | 2.29E+07  | -         |
| Reference data set | 6.91E+07  | 2.70E+07  | 1.45E+07  | 3500.1*   |
| <i>min</i>         | 2.29E+07  | 1.84E+07  | 1.20E+07  | 994.6     |
| <i>max</i>         | 7.34E+07  | 2.70E+07  | 2.29E+07  | 3740.5    |
| <i>arith. mean</i> | 4.27E+07  | 2.27E+07  | 1.64E+07  | 2307.5    |
| <i>median</i>      | 2.40E+07  | 2.29E+07  | 1.54E+07  | 2247.4    |
| <i>geom. mean</i>  | 3.68E+07  | 2.24E+07  | 1.61E+07  | 1897.0    |
| <i>max/min</i>     | 3.1/3.2** | 1.5/1.5** | 1.3/1.9** | 3.8       |

\* - difference in absolute values obtained from identical temperature dependencies can be explained by accuracy of coefficient recalculation

\*\* - the first value is calculated without the temperature independent value of  $K_{ow}$  (MSCE-POP), the second value is calculated taking it into account

**Table B.11.** The octanol/air partition coefficient of PCBs (data sets of the participating POP models)\*

| Model                 | Description   | Numerical values                   |          | Comments         | Reference  |  |
|-----------------------|---|------------------------------------|----------|------------------|--|--|
|                       |   | PCB-28                             | PCB-180  |                  |  |  |
| CAM/POPs              | Temperature dependent:<br>$K_{oa} = 10^{(a/T + b)}$<br>where $T$ - temperature;<br>$P$ - liquid vapour pressure $p_{oi}$ (Pa)   | $a$                                | -        | -529-19.25 logP  | These values are calculated with the help of temperature dependencies of $p_{oi}$  | Harner et al, 1996; 1998   |
|                       |   | $b$                                | -        | 8.2995-0.95 logP |  |  |
| SimpleBox             | Temperature dependent:<br>$K_{oa} = K_{oa}^0 \exp(a_{Koa}(1/T - 1/T_0))$<br>where $T$ - temperature (K),<br>$K_{oa}^0$ is the value at the reference temperature $T_0$ ,<br>and $a_{Koa}$ is a parameter of temperature dependence. | $K_{oa}^0(T_0)$ ,<br>dimensionless | 3.77E+08 | 1.06E+11         | Same to the "reference data set"   | Li et al., 2003  |
|                       |   | $a_{Koa}$                          | 9441.9   | 11161.9          |  |  |
|                       |   | $T_0, K$                           | 283.15   | 283.15           |  |  |
| EVN-BETR and UK-MODEL | Temperature dependent:  | $K_{oa}^0(T_0)$ ,<br>dimensionless | 1.99E+08 | 3.18E+10         | At 10°C, calculated as $K_{oa} = K_{ow} / K_{aw}$  |  |
|                       |   | $T_0, K$                           | 283.15   | 283.15           |  |  |
| DEHM-POP              | Temperature dependent:<br>$K_{oa} = K_{oa}^0 \exp(a_{Koa}(1/T - 1/T_0))$<br>where $T$ - temperature (K), $K_{oa}^0$ is the value at the reference temperature $T_0$ ,<br>and $a_{Koa}$ is a parameter of temperature dependence.    | $K_{oa}^0(T_0)$ ,<br>dimensionless | 5.84E+08 | 9.78E+10         | $K_{oa}(283.15) = K_{oa}^0(298.15) \exp(a_{Koa}(1/T - 1/T_0))$ ,<br>where $K_{oa}^0(298.15) = 1.16E+8, 1.68E+10$ for PCB-28 and 180 respectively<br>$a_{Koa} = dHK_{oa}/R$<br>$dHK_{oa}$ = phase transfer enthalpy (J/mol)<br>PCB 28: -75620; PCB-180: -82410<br>$R$ = universal gas constant (8.3145 J/mol·K)   | Beyer et al., 2002   |
|                       |   | $a_{Koa}$                          | 9095.0   | 9911.6           |  |  |
|                       |   | $T_0, K$                           | 283.15   | 283.15           |  |  |
| MSCE-POP              | Temperature dependent:<br>$K_{oa} = K_{oa}^0 \exp(a_{Koa}(1/T - 1/T_0))$<br>where $T$ - temperature (K), $K_{oa}^0$ is the value at the reference temperature $T_0$ ,<br>and $a_{Koa}$ is a parameter of temperature dependence.    | $K_{oa}^0(T_0)$ ,<br>dimensionless | 5.78E+8  | 2.07E+11         | Coefficients of the exponential equation are recalculated from the standard form of temperature dependence:<br>$\log K_{oa} = A/T(K) - B$<br>with the help of the following formulas:<br>$a_p = \ln(10) \cdot A$ ,<br>$K_{oa}^0(T_0) = 10^{(A/T_0 - B)}$<br>where: $A = 3792^a$ and $4535^b$ for PCB-28 and PCB-180 respectively;<br>$B = 4.63^a$ and $4.70^b$ for PCB-28 and PCB-180 respectively | <sup>a</sup> -estimated with the use of data [Harner and Bidleman 1996] for PCB-29<br><sup>b</sup> -Harner and Bidleman [1996] |
|                       |   | $a_{Koa}$                          | 8731     | 10442            |  |  |
|                       |   | $T_0, K$                           | 283.15   | 283.15           |  |  |

\* - for the sake of comparability, the base values and coefficients of temperature dependences of the considered parameters are given here for the temperature 283.15 K ( $T_0$ ) and the way they were recalculated from original dependencies is specified in the field "Comments".

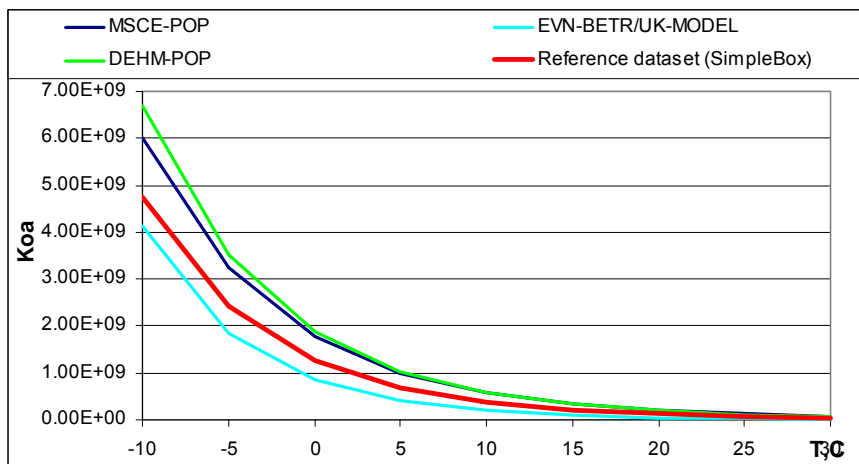


Fig. B.7. Comparison of temperature dependencies of octanol/air partition coefficient of PCB-28 used in the participating POP models and in “reference data set”

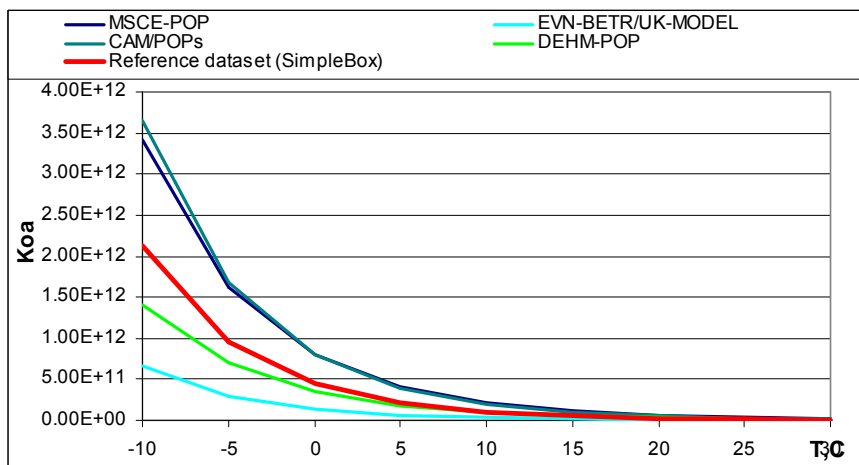


Fig. B.8. Comparison of temperature dependencies of octanol/air partition coefficient of PCB-180 used in the participating POP models and in “reference data set”

**Table B.12.** Absolute values, coefficients of temperature dependencies and statistical parameters of octanol/air partition coefficient of PCB-28 for three arbitrary temperatures (-10 °C, 10 °C and 25 °C)

|                    | $K_{oa}$ |          |          | $a_{K_{oa}}$ |
|--------------------|----------|----------|----------|--------------|
|                    | -10°C    | 10°C     | 25°C     |              |
| SimpleBox          | 4.75E+09 | 3.77E+08 | 7.04E+07 | 9441.9       |
| EVN-BETR/UK-MODEL  | 4.14E+09 | 2.00E+08 | 2.68E+07 | -            |
| DEHM-POP           | 6.71E+09 | 5.84E+08 | 1.16E+08 | 9095.0       |
| MSCE-POP           | 6.02E+09 | 5.78E+08 | 1.23E+08 | 8731         |
| Reference data set | 4.75E+09 | 3.77E+08 | 7.04E+07 | 9441.9       |
| <i>min</i>         | 4.14E+09 | 2.00E+08 | 2.68E+07 | 8731.0       |
| <i>max</i>         | 6.71E+09 | 5.84E+08 | 1.23E+08 | 9441.9       |
| <i>arith. mean</i> | 5.27E+09 | 4.23E+08 | 8.12E+07 | 9177.5       |
| <i>mediana</i>     | 4.75E+09 | 3.77E+08 | 7.04E+07 | 9268.5       |
| <i>geom. mean</i>  | 5.19E+09 | 3.95E+08 | 7.17E+07 | 9172.7       |
| <i>max/min</i>     | 2        | 3        | 5        | 1.1          |

**Table B.13.** Absolute values, coefficients of temperature dependencies and statistical parameters of octanol/air partition coefficient of PCB-180 for three arbitrary temperatures (-10 °C, 10 °C and 25 °C)

|                    | $K_{oa}$ |          |          | $a_{K_{oa}}$ |
|--------------------|----------|----------|----------|--------------|
|                    | -10°C    | 10°C     | 25°C     |              |
| CAM/POPs           | 3.65E+12 | 1.97E+11 | 2.91E+10 | -            |
| SimpleBox          | 2.12E+12 | 1.06E+11 | 1.46E+10 | 11161.9      |
| EVN-BETR/UK-MODEL  | 6.58E+11 | 3.17E+10 | 4.26E+09 | -            |
| DEHM-POP           | 1.40E+12 | 9.78E+10 | 1.68E+10 | 9911.6       |
| MSCE-POP           | 3.41E+12 | 2.07E+11 | 3.24E+10 | 10442        |
| Reference data set | 2.12E+12 | 1.06E+11 | 1.46E+10 | 11161.9      |
| <i>min</i>         | 6.58E+11 | 3.17E+10 | 4.26E+09 | 9911.6       |
| <i>max</i>         | 3.65E+12 | 2.07E+11 | 3.24E+10 | 11161.9      |
| <i>arith. mean</i> | 2.23E+12 | 1.10E+11 | 1.65E+10 | 10669.4      |
| <i>mediana</i>     | 2.12E+12 | 1.06E+11 | 1.46E+10 | 10802.0      |
| <i>geom. mean</i>  | 1.93E+12 | 9.37E+10 | 1.38E+10 | 10656.2      |
| <i>max/min</i>     | 6        | 7        | 8        | 1.1          |

**Table B.14.** The organic carbon/water partition coefficient of PCBs (data sets of the participating POP models)

| Model                 | Description  | Numerical values |        | Comments | Reference  |   |
|-----------------------|--|------------------|--------|----------|--|---|
|                       |  |                  | PCB-28 |          |  | PCB-180   |
| CAM/POPs              | Regression relation:<br>$K_{oc} = regc K_{ow}^b$<br>where <i>regc</i> and <i>b</i> are regression coefficients | <i>regc</i>      | -      | 0.41     | $K_{oc}$ is calculated from $K_{ow}$ , where $K_{ow}$ is the temperature dependent octanol-water partition coefficient                                     | Karickhoff, 1981;<br>Mackay, 1991;<br>Schnoor, 1996 |
|                       |  | <i>b</i>         | -      | 1        |  |   |
| SimpleBox             | Regression relation:<br>$K_{oc} = regc K_{ow}^b$<br>where <i>regc</i> and <i>b</i> are regression coefficients | <i>regc</i>      | 0.41   | 0.41     | Same to the "reference data set"<br>$K_{oc}$ is calculated from $K_{ow}$ , where $K_{ow}$ is the temperature dependent octanol-water partition coefficient | Karickhoff, 1981                                    |
|                       |  | <i>b</i>         | 1      | 1        |  |   |
| EVN-BETR and UK-MODEL | Regression relation:<br>$K_{oc} = regc K_{ow}^b$<br>where <i>regc</i> and <i>b</i> are regression coefficients | <i>regc</i>      | 0.41   | 0.41     |  | Karickhoff, 1981                                    |
|                       |  | <i>b</i>         | 1      | 1        |  |   |
| CliMoChem             | Regression relation:<br>$K_{oc} = regc K_{ow}^b$<br>where <i>regc</i> and <i>b</i> are regression coefficients | <i>regc</i>      | 0.35   | 0.35     | $K_{oc}$ is calculated from $K_{ow}$ , where $K_{ow}$ is the temperature dependent octanol-water partition coefficient                                     | Seth et al., 1999                                   |
|                       |  | <i>b</i>         | 1      | 1        |  |   |
| DEHM-POP              | Regression relation:<br>$K_{oc} = regc K_{ow}^b$<br>where <i>regc</i> and <i>b</i> are regression coefficients | <i>regc</i>      | 0.41   | 0.41     |  | Mackay, 1999  |
|                       |  | <i>b</i>         | 1      | 1        |  |   |
| MSCE-POP              | Regression relation:<br>$K_{oc} = regc K_{ow}^b$<br>where <i>regc</i> and <i>b</i> are regression coefficients | <i>regc</i>      | 0.41   | 0.41     |  | Karickhoff, 1981                                    |
|                       |  | <i>b</i>         | 1      | 1        |  |   |

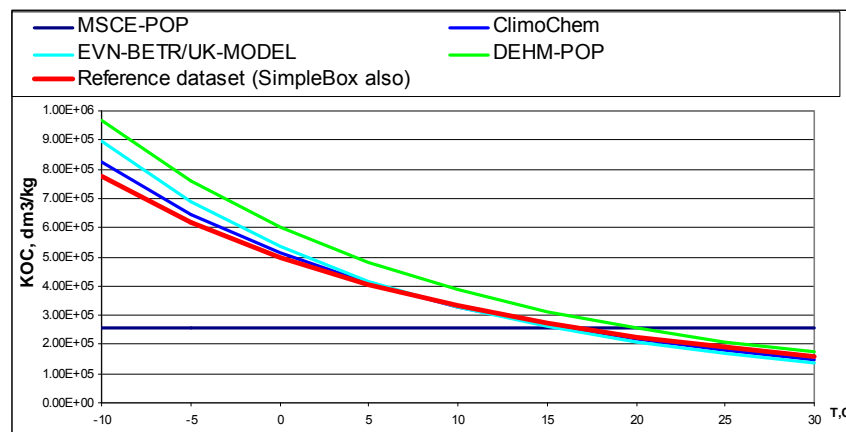


**Fig. B.9.** Comparison of temperature dependencies of organic carbon/water partition coefficient of PCB-28 used in the participating POP models and in "reference data set"

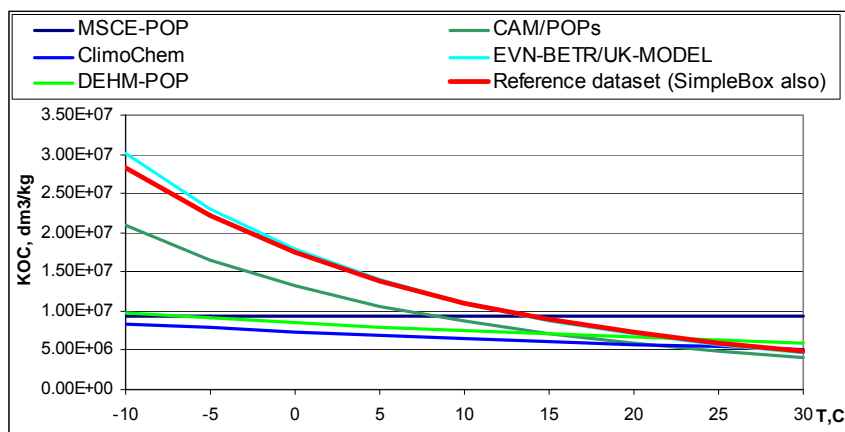


**Fig. B.10.** Comparison of temperature dependencies of organic carbon/water partition coefficient of PCB-180 used in the participating POP models and in “reference data set”

**Table B.15.** Absolute values and statistical parameters of organic carbon/water partition coefficient of PCB-28 for three arbitrary temperatures (-10 °C, 10 °C and 25 °C).

|                    | $K_{oc}$ , $\text{dm}^3/\text{kg}$ |          |          |
|--------------------|------------------------------------|----------|----------|
|                    | -10°C                              | 10°C     | 25°C     |
| SimpleBox          | 7.75E+05                           | 3.32E+05 | 1.89E+05 |
| EVN-BETR/UK-MODEL  | 8.97E+05                           | 3.29E+05 | 1.69E+05 |
| CliMoChem          | 8.24E+05                           | 3.29E+05 | 1.80E+05 |
| DEHM-POP           | 9.65E+05                           | 3.86E+05 | 2.10E+05 |
| MSCE-POP           | 2.59E+05                           | 2.59E+05 | 2.59E+05 |
| Reference data set | 7.75E+05                           | 3.32E+05 | 1.89E+05 |
| <i>min</i>         | 2.59E+05                           | 2.59E+05 | 1.69E+05 |
| <i>max</i>         | 9.65E+05                           | 3.86E+05 | 2.59E+05 |
| <i>arith. mean</i> | 7.49E+05                           | 3.28E+05 | 1.99E+05 |
| <i>mediana</i>     | 8.00E+05                           | 3.31E+05 | 1.89E+05 |
| <i>geom. mean</i>  | 6.93E+05                           | 3.25E+05 | 1.97E+05 |
| <i>max/min</i>     | 3.7                                | 1.5      | 1.5      |

**Table B.16.** Absolute values and statistical parameters of organic carbon/water partition coefficient of PCB-180 for three arbitrary temperatures (-10 °C, 10 °C and 25 °C).

|                    | $K_{oc}$ , dm <sup>3</sup> /kg |          |          |
|--------------------|--------------------------------|----------|----------|
|                    | -10°C                          | 10°C     | 25°C     |
| CAM/POPs           | 2.09E+07                       | 8.68E+06 | 4.92E+06 |
| SimpleBox          | 2.83E+07                       | 1.11E+07 | 5.94E+06 |
| EVN-BETR/UK-MODEL  | 3.01E+07                       | 1.10E+07 | 5.67E+06 |
| CliMoChem          | 8.41E+06                       | 6.44E+06 | 5.40E+06 |
| DEHM-POP           | 9.85E+06                       | 7.54E+06 | 6.32E+06 |
| MSCE-POP           | 9.39E+06                       | 9.39E+06 | 9.39E+06 |
| Reference data set | 2.83E+07                       | 1.11E+07 | 5.94E+06 |
| <i>min</i>         | 8.41E+06                       | 6.44E+06 | 4.92E+06 |
| <i>max</i>         | 3.01E+07                       | 1.11E+07 | 9.39E+06 |
| <i>arith. mean</i> | 1.93E+07                       | 9.32E+06 | 6.23E+06 |
| <i>mediana</i>     | 2.09E+07                       | 9.39E+06 | 5.94E+06 |
| <i>geom. mean</i>  | 1.69E+07                       | 9.15E+06 | 6.10E+06 |
| <i>max/min</i>     | 3.6                            | 1.7      | 1.9      |

**Table B.17.** Water solubility of PCBs (data sets of the participating POP models)

| Model                       | Description              | Numerical values                    |          |          | Comments   | Reference              |
|-----------------------------|--------------------------|-------------------------------------|----------|----------|--|------------------------|
|                             |                          |                                     | PCB-28   | PCB-180  |  |                        |
| SimpleBox                   | Temperature independent  | $S_{WL}(T)$ ,<br>mol/m <sup>3</sup> | 5.53E-04 | 7.57E-06 | Same to the "reference data set"<br>$T = 10\text{ °C}$ | <i>Li et al., 2003</i> |
| EVN-BETR<br>and<br>UK-MODEL | Temperature independent. | $S_{WL}(T)$ ,<br>mol/m <sup>3</sup> | 8.85E-04 | 1.32E-05 | $T = 25\text{ °C}$                                     | <i>Li et al., 2003</i> |

**Table B.18.** Degradation rate constants of PCBs in the environmental media (data sets of the participating POP models)\*

| Model     | Description   | Numerical values                               |          | Comments | Reference   |                       |
|-----------|---|--|----------|----------|---|-----------------------|
|           |   | PCB-28   | PCB-180  |          |   |                       |
| CAM/POPs  | Degradation in atmosphere:<br>Temperature dependent:<br>$k_{air} = k_{air}^0 \exp(-a_{kair}(1/T - 1/T_0))$<br>where $T$ - temperature (K), $k_{air}^0$ is the value at the reference temperature $T_0$ , and $a_{kair}$ is a parameter of temperature dependence        | $k_{air}^0(T_0)$ ,<br>cm <sup>3</sup> /molec·s | -        | 1.25E-13 | Coefficients of the exponential equation are recalculated from the following temperature dependence:<br>$K_{OH} = K_{OH}^0 \exp(a/(1/T_0 - 1/T))$<br>where $K_{OH}^0 = 1.6E-13$ is the value at the reference temperature $T_0$ (298 K),<br>$a = 1400$ is parameter of temperature dependence.  | This study            |
|           |   | $a_{kair}$                                     | -        | 1400     |   |                       |
|           |   | $T_0, K$                                       | -        | 283.15   |   |                       |
| ClimoChem | Degradation in atmosphere:<br>Temperature dependent:<br>$k_{air} = k_{air}^0 \exp(-a_{kair}(1/T - 1/T_0))$<br>where $T$ - temperature (K), $k_{air}^0$ is the value at the reference temperature $T_0$ , and $a_{kair}$ is a parameter of temperature dependence        | $k_{air}^0(T_0)$ ,<br>cm <sup>3</sup> /molec·s | 7.95E-13 | 7.15E-14 | $k_{air}(T) = k_{air}(T_{ref}) \exp((Ea_{air}/R)(1/T - 1/T_0))$<br>$T$ = temperature (283.15 K), $T_0$ = reference temperature (298.15 K)<br>$k_{air}(T_0)$ = degradation rate constant at $T_0$ (cm <sup>3</sup> /d),<br>PCB 28: 9.21E-8 ; PCB 180: 9.04E-9<br>$Ea_{air}$ = activation energy (J/mol) PCB 28: 13700; PCB 180: 17800<br>$R$ = universal gas constant (8.3145 J/mol·K)<br>$k_{air}^0$ = degradation rate constant at 283.15 (cm <sup>3</sup> /d),<br>PCB 28: 6.87E-08; PCB-180: 6.18E-09<br>$a_{kair} = Ea/R$                | Beyer et al.,<br>2002 |
|           |   | $a_{kair}$                                     | 1647.7   | 2140.8   |   |                       |
|           |   | $T_0, K$                                       | 283.15   | 283.15   |   |                       |
|           | Degradation in soil:<br>Temperature dependent:<br>$k_{soil} = k_{soil}^0 \exp(-a_{ksoil}(1/T - 1/T_0))$<br>where $T$ - temperature (K), $k_{soil}^0$ is the value at the reference temperature $T_0$ , and $a_{ksoil}$ is a parameter of temperature dependence         | $k_{soil}^0(T_0)$ ,<br>1/d                     | 3.90E-09 | 3.07E-10 | $k_{soil}(T) = k_{soil}(T_{ref}) \exp((Ea_{soil}/R)(1/T - 1/T_0))$<br>$T$ = temperature (283.15 K), $T_0$ = reference temperature (298.15 K)<br>$k_{soil}(T_0)$ = degradation rate constant at $T_0$ (1/d),<br>PCB 28: 6.40E-4 ; PCB 180: 5.04E-5<br>$Ea_{soil}$ = activation energy (J/mol) PCB 28: 30000; PCB 180: 30000<br>$R$ = universal gas constant (8.3145 J/mol·K )<br>$k_{soil}^0$ = degradation rate constant at 283.15 (1/d)<br>PCB 28: 3.37E-04; PCB-180: 2.65E-05<br>$a_{ksoil} = Ea_{soil} / R$                              | Beyer et al.,<br>2002 |
|           |   | $a_{ksoil}$                                    | 3608.2   | 3608.2   |   |                       |
|           |   | $T_0, K$                                       | 283.15   | 283.15   |   |                       |
|           | Degradation in water:<br>Temperature dependent:<br>$k_{water} = k_{water}^0 \exp(-a_{kwater}(1/T - 1/T_0))$<br>where $T$ - temperature (K), $k_{water}^0$ is the value at the reference temperature $T_0$ , and $a_{kwater}$ is a parameter of temperature dependence   | $k_{water}^0(T_0)$ ,<br>1/d                    | 7.01E-08 | 4.22E-10 | $k_{water}(T) = k_{water}(T_{ref}) \exp((Ea_{water}/R)(1/T - 1/T_0))$<br>$T$ = temperature (283.15 K), $T_0$ = reference temperature (298.15 K)<br>$k_{water}(T_0)$ = degradation rate constant at $T_0$ (1/d),<br>PCB 28: 1.15E-2 ; PCB 180: 6.93E-5<br>$Ea_{water}$ = activation energy (J/mol)<br>PCB 153: 30000; PCB 28: 30000 ; PCB 180: 30000<br>$R$ = universal gas constant (8.3145 J/mol·K )<br>$k_{water}^0$ = degradation rate constant at 283.15 (1/d),<br>PCB 28: 6.06E-03; PCB-180: 3.65E-05<br>$a_{kwater} = Ea_{water} / R$ | Beyer et al.,<br>2002 |
|           |   | $a_{kwater}$                                   | 3608.2   | 3608.2   |   |                       |
|           |   | $T_0, K$                                       | 283.15   | 283.15   |   |                       |
|           | Degradation in vegetation*:<br>Temperature dependent:<br>$k_{veg} = k_{veg}^0 \exp(-a_{kveg}(1/T - 1/T_0))$<br>where $T$ - temperature (K),<br>$k_{veg}^0$ is the value at the reference temperature $T_0$ ,<br>and $a_{kveg}$ is a parameter of temperature dependence | $k_{veg}^0(T_0)$ ,<br>1/d                      | 7.71E-07 | 6.94E-08 | $k_{veg}(T) = k_{veg}(T_{ref}) \exp((Ea_{veg}/R)(1/T - 1/T_0))$<br>$T$ = temperature (283.15 K), $T_0$ = reference temperature (298.15 K)<br>$k_{veg}(T_0)$ = degradation rate constant at $T_0$ (1/d)*,<br>PCB 28: 8.93E-2 ; PCB 180: 8.77E-3<br>$Ea_{veg}$ = activation energy (J/mol) PCB 28: 13700 ; PCB 180: 17800<br>$R$ = universal gas constant (8.3145 J/mol·K )<br>$k_{veg}(T_0)$ = degradation rate constant at $T_0$ (1/d),<br>PCB 28: 6.66E-02; PCB-180: 6.00E-03<br>$a_{kveg} = Ea_{veg} / R$                                 | Beyer et al.,<br>2002 |
|           |   | $a_{kveg}$                                     | 1647.7   | 2140.8   |   |                       |
|           |   | $T_0, K$                                       | 283.15   | 283.15   |   |                       |

| Model                 | Description  | Numerical values  |          |          | Comments  | Reference   |
|-----------------------|--|---|----------|----------|---|---|
|                       |  |   | PCB-28   | PCB-180  |   |   |
| MSCE-POP              | Degradation in atmosphere:<br>Temperature dependent:<br>$k_{air} = k_{air}^0 \exp(-a_{kair}(1/T - 1/T_0))$<br>where $T$ - temperature (K), $k_{air}^0$ is the value at the reference temperature $T_0$ , and $a_{kair}$ is a parameter of temperature dependence | $k_{air}^0(T_0)$ ,<br>$\text{cm}^3/(\text{molec}\cdot\text{s})$ | 7.95E-13 | 7.16E-14 | Coefficients of the exponential equation are recalculated from the following temperature dependence:<br>$k_{air} = A \cdot \exp(-Ea/RT)$<br>with the help of the following formulas:<br>$a_{kair} = Ea/R$ ,<br>$k_{air}^0 = A \cdot \exp(-Ea/RT_0)$<br>where $A = 2.70 \text{ E-}10$ and $1.40 \text{ E-}10$ are the pre-exponential multiplier values for PCB-28 and PCB-180 respectively, $\text{m}^3/(\text{molec}\cdot\text{s})$ ;<br>$E_A = 13720$ and $17840$ are the activation energies of interaction with OH-radical in air for PCB-28 and PCB-180 respectively, $\text{J/mol}$ | <i>Anderson and Hites, 1996; Beyer and Matthies, 2001</i> |
|                       |  | $a_{kair}$  | 1650.1   | 2145.6   |   |   |
|                       |  | $T_0, \text{K}$   | 283.15   | 283.15   |   |   |
| MSCE-POP              | Degradation in soil:<br>Temperature independent  | $k_{soil}, 1/\text{s}$  | 7.4E-09  | 5.83E-10 | Degradation rate constant in soil is converted from half-life values (PCB-28: 26000 hours; PCB-180: 330000 hours):<br>$k_d = 0.693/t_{1/2}$<br>where $k_d$ is the first-order rate constant ( $\text{s}^{-1}$ ) and $t_{1/2}$ is the half-life (s).   | <i>Sinkkonen and Paasivirta, 2000</i>                     |
|                       | Degradation in water:<br>Temperature independent   | $k_{water}, 1/\text{s}$   | 1.33E-07 | 8.02E-10 | Degradation rate constant in water is converted from half-life values (PCB-28: 1450 hours; PCB-180: 240000 hours):<br>$k_d = 0.693/t_{1/2}$<br>where $k_d$ is the first-order rate constant ( $\text{s}^{-1}$ ) and $t_{1/2}$ is the half-life (s).   |   |
| SimpleBox             | Degradation in atmosphere:<br>Temperature independent  | $k_{air}, 1/\text{s}$   | 3.50E-07 | 3.50E-08 | Same half-lives as in "reference data set": PCB-28: 550; PCB-180: 5500 hours  | <i>Mackay et al. 1992</i>                                 |
|                       | Degradation in soil:<br>Temperature independent  | $k_{soil}, 1/\text{s}$  | 3.50E-09 | 3.50E-09 | Same half-lives as in "reference data set": PCB-28: 55000; PCB-180: 55000 hours   |   |
|                       | Degradation in water:<br>Temperature independent   | $k_{water}, 1/\text{s}$   | 1.13E-08 | 3.50E-09 | Same half-lives as in "reference data set": PCB-28: 17000; PCB-180: 55000 hours   |   |
| EVN-BETR and UK-MODEL | Degradation in atmosphere:<br>Temperature independent  | $k_{air}, 1/\text{s}$   | 3.50E-07 | 3.50E-08 | Same half-lives as in "reference data set": PCB-28: 550; PCB-180: 5500 hours  | <i>Mackay et al. 1992</i>                                 |
|                       | Degradation in soil:<br>Temperature independent  | $k_{soil}, 1/\text{s}$  | 3.50E-09 | 3.50E-09 | Same half-lives as in "reference data set": PCB-28: 55000; PCB-180: 55000 hours   |   |
|                       | Degradation in water:<br>Temperature independent   | $k_{water}, 1/\text{s}$   | 1.13E-08 | 3.50E-09 | Same half-lives as in "reference data set": PCB-28: 17000; PCB-180: 55000 hours   |   |
|                       | Degradation in sediment:<br>Temperature independent  | $k_{sed}, 1/\text{s}$   | 3.50E-09 | 3.50E-09 | Same half-lives as in "reference data set": PCB-28: 55000; PCB-180: 55000 hours   |   |
|                       | Degradation in vegetation:<br>Temperature independent  | $k_{veg}, 1/\text{s}$   | 1.13E-07 | 1.13E-08 | Half-lives: PCB-28: 1700; PCB-180: 17000 hours  |   |

\* - for the sake of comparability, the base values and coefficients of temperature dependences of the considered parameters are given here at the temperature 283.15 K ( $T_0$ ) and the way they were recalculated from original dependencies is specified in the field "Comments".

\*\* - because of insufficient data about vegetation degradation rate constants, the values are taken from atmospheric degradation [Möller, 2002] and multiplied with an average OH-radical concentration of  $970000 \text{ l}/\text{cm}^3$  [Beyer et al., 2002].

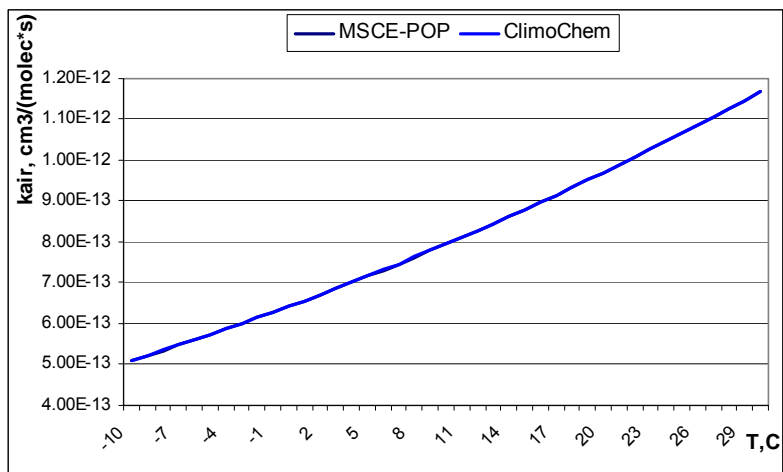


Fig. B.11. Comparison of temperature dependencies of degradation rate constant of PCB-28 in the atmosphere

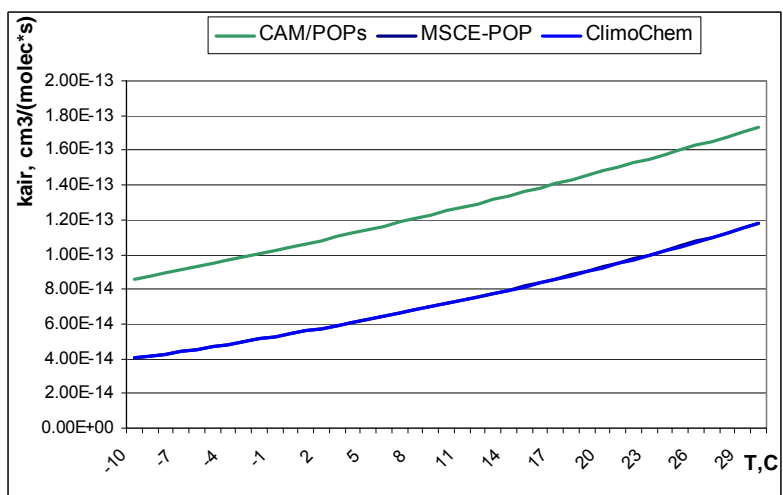


Fig. B.12. Comparison of temperature dependencies of degradation rate constant of PCB-180 in the atmosphere

**Table B.19.** Monthly averaged temperatures calculated on the basis of meteorological data for 1997, 1998 and 1999 in Europe and the yearly average degradation rate constants of PCB-28 for the models which use temperature dependence of this parameter

| Month   | Temperatures, °C |          |         | MSCE-POP   |  |  |  |  | CliMoChem  |  |  |  |  |
|---|------------------|----------|---------|--|--|--|--|--|--|--|--|--|--|
|   | Over land        | Over sea | Average | air, cm <sup>3</sup> ·molec <sup>-1</sup> ·s <sup>-1</sup> | air, cm <sup>3</sup> ·molec <sup>-1</sup> ·s <sup>-1</sup> | soil, s <sup>-1</sup> (for Over land temp) | sea, s <sup>-1</sup> (for Over sea temp) | veg., s <sup>-1</sup> (for aver. temp) | air, cm <sup>3</sup> ·molec <sup>-1</sup> ·s <sup>-1</sup> | air, cm <sup>3</sup> ·molec <sup>-1</sup> ·s <sup>-1</sup> | soil, s <sup>-1</sup> (for Over land temp) | sea, s <sup>-1</sup> (for Over sea temp) | veg., s <sup>-1</sup> (for aver. temp) |
| Jan   | 4                | 4        | 4       | 7.01E-13   | 7.01E-13   | 2.96E-09                                   | 5.32E-08                                 | 6.80E-07                               | 7.01E-13   | 7.01E-13   | 2.96E-09                                   | 5.08E-08                                 | 6.80E-07                               |
| Feb   | 4                | 3        | 4       | 7.01E-13   | 7.01E-13   | 2.96E-09                                   | 5.08E-08                                 | 6.80E-07                               | 7.01E-13   | 7.01E-13   | 2.96E-09                                   | 5.08E-08                                 | 6.80E-07                               |
| Mar   | 7                | 5        | 6       | 7.31E-13   | 7.31E-13   | 3.4E-09                                    | 5.57E-08                                 | 7.09E-07                               | 7.31E-13   | 7.31E-13   | 3.4E-09                                    | 5.57E-08                                 | 7.09E-07                               |
| Apr   | 11               | 6        | 9       | 7.79E-13   | 7.79E-13   | 4.08E-09                                   | 5.84E-08                                 | 7.55E-07                               | 7.79E-13   | 7.79E-13   | 4.08E-09                                   | 5.84E-08                                 | 7.55E-07                               |
| May   | 17               | 10       | 13      | 8.45E-13   | 8.45E-13   | 5.3E-09                                    | 7.01E-08                                 | 8.20E-07                               | 8.45E-13   | 8.45E-13   | 5.3E-09                                    | 7.01E-08                                 | 8.20E-07                               |
| Jun   | 21               | 14       | 17      | 9.15E-13   | 9.15E-13   | 6.28E-09                                   | 8.37E-08                                 | 8.87E-07                               | 9.15E-13   | 9.15E-13   | 6.28E-09                                   | 8.37E-08                                 | 8.87E-07                               |
| Jul   | 22               | 16       | 19      | 9.51E-13   | 9.51E-13   | 6.55E-09                                   | 9.13E-08                                 | 9.22E-07                               | 9.51E-13   | 9.51E-13   | 6.55E-09                                   | 9.13E-08                                 | 9.22E-07                               |
| Aug   | 22               | 16       | 19      | 9.51E-13   | 9.51E-13   | 6.55E-09                                   | 9.13E-08                                 | 9.22E-07                               | 9.51E-13   | 9.51E-13   | 6.55E-09                                   | 9.13E-08                                 | 9.22E-07                               |
| Sep   | 18               | 13       | 15      | 8.8E-13  | 8.79E-13   | 5.54E-09                                   | 8.01E-08                                 | 8.53E-07                               | 8.8E-13  | 8.79E-13   | 5.54E-09                                   | 8.01E-08                                 | 8.53E-07                               |
| Oct   | 14               | 10       | 12      | 8.28E-13   | 8.28E-13   | 4.66E-09                                   | 7.01E-08                                 | 8.03E-07                               | 8.28E-13   | 8.28E-13   | 4.66E-09                                   | 7.01E-08                                 | 8.03E-07                               |
| Nov   | 10               | 7        | 9       | 7.79E-13   | 7.79E-13   | 3.9E-09                                    | 6.12E-08                                 | 7.55E-07                               | 7.79E-13   | 7.79E-13   | 3.9E-09                                    | 6.12E-08                                 | 7.55E-07                               |
| Dec   | 6                | 5        | 6       | 7.31E-13   | 7.31E-13   | 3.25E-09                                   | 5.57E-08                                 | 7.09E-07                               | 7.31E-13   | 7.31E-13   | 3.25E-09                                   | 5.57E-08                                 | 7.09E-07                               |
| Averaged second-order rate constants, cm <sup>3</sup> ·molec <sup>-1</sup> ·s <sup>-1</sup> |                  |          |         | 8.16E-13   | 8.16E-13   | -  | -  | -                                      | 8.16E-13   | 8.16E-13   | -  | -  | -                                      |
| Averaged first-order rate constants, s <sup>-1</sup>  |                  |          |         | 6.53E-07   | 6.53E-07   | 4.62E-09                                   | 6.85E-08                                 | 7.92E-07                               | 6.53E-07   | 6.53E-07   | 4.62E-09                                   | 6.85E-08                                 | 7.92E-07                               |

**Table B.20.** Absolute values and statistical parameters of degradation rate constants of first order (PCB-28)

|                    | $k_{air}$ , s <sup>-1</sup> | $k_{soil}$ , s <sup>-1</sup> | $k_{water}$ , s <sup>-1</sup> | $k_{sediment}$ , s <sup>-1</sup> | $k_{veg}$ , s <sup>-1</sup> |
|--------------------|-----------------------------|------------------------------|-------------------------------|----------------------------------|-----------------------------|
| CliMoChem          | 6.53E-07                    | 4.62E-09                     | 6.85E-08                      | -                                | 7.92E-07                    |
| MSCE-POP           | 6.53E-07                    | 7.4E-09                      | 1.33E-07                      | -                                | -                           |
| SimpleBox          | 3.50E-07                    | 3.50E-09                     | 1.13E-08                      | -                                | -                           |
| EVN-BETR/UK-MODEL  | 3.50E-07                    | 3.50E-09                     | 1.13E-08                      | 3.50E-09                         | 1.13E-07                    |
| Reference data set | 3.50E-07                    | 3.50E-09                     | 1.13E-08                      | 3.50E-09                         | -                           |
| <i>min</i>         | 3.50E-07                    | 3.50E-09                     | 1.13E-08                      | -                                | -                           |
| <i>max</i>         | 6.53E-07                    | 7.40E-09                     | 1.33E-07                      | -                                | -                           |
| <i>arith. mean</i> | 4.71E-07                    | 4.50E-09                     | 4.71E-08                      | -                                | -                           |
| <i>median</i>      | 3.50E-07                    | 3.50E-09                     | 1.13E-08                      | -                                | -                           |
| <i>geom.mean</i>   | 4.49E-07                    | 4.30E-09                     | 2.65E-08                      | -                                | -                           |
| <i>max/min</i>     | 1.9                         | 2.1                          | 11.8                          | 1.0                              | 7.0                         |

**Table B.21.** Monthly averaged temperatures calculated on the basis of meteorological data for 1997, 1998 and 1999 in Europe and the yearly average degradation rate constants of PCB-180 for the models which use temperature dependence of this parameter

| Month   | Temperatures, °C |          |         | CAM/POPs   | MSCE-POP   | CliMoChem  |   |   |   |
|---|------------------|----------|---------|--|--|--|---|---|---|
|   | Over land        | Over sea | Average | air, $\text{cm}^3 \cdot \text{molec}^{-1} \cdot \text{s}^{-1}$ | air, $\text{cm}^3 \cdot \text{molec}^{-1} \cdot \text{s}^{-1}$ | air, $\text{cm}^3 \cdot \text{molec}^{-1} \cdot \text{s}^{-1}$ | soil, $\text{s}^{-1}$<br>(for Over land temp) | sea, $\text{s}^{-1}$<br>(for Over sea temp) | veg., $\text{s}^{-1}$<br>(for aver. temp) |
| Jan   | 4                | 4        | 4       | 1.12E-13   | 6.08E-14   | 6.07E-14   | 2.33E-10                                      | 3.2E-10                                     | 5.89E-08                                  |
| Feb   | 4                | 3        | 4       | 1.12E-13   | 6.08E-14   | 6.07E-14   | 2.33E-10                                      | 3.06E-10                                    | 5.89E-08                                  |
| Mar   | 7                | 5        | 6       | 1.16E-13   | 6.42E-14   | 6.42E-14   | 2.68E-10                                      | 3.36E-10                                    | 6.23E-08                                  |
| Apr   | 11               | 6        | 9       | 1.23E-13   | 6.97E-14   | 6.96E-14   | 3.21E-10                                      | 3.52E-10                                    | 6.76E-08                                  |
| May   | 17               | 10       | 13      | 1.32E-13   | 7.75E-14   | 7.74E-14   | 4.17E-10                                      | 4.22E-10                                    | 7.51E-08                                  |
| Jun   | 21               | 14       | 17      | 1.41E-13   | 8.6E-14  | 8.58E-14   | 4.94E-10                                      | 5.04E-10                                    | 8.33E-08                                  |
| Jul   | 22               | 16       | 19      | 1.46E-13   | 9.04E-14   | 9.03E-14   | 5.15E-10                                      | 5.5E-10                                     | 8.76E-08                                  |
| Aug   | 22               | 16       | 19      | 1.46E-13   | 9.04E-14   | 9.03E-14   | 5.15E-10                                      | 5.5E-10                                     | 8.76E-08                                  |
| Sep   | 18               | 13       | 15      | 1.36E-13   | 8.17E-14   | 8.15E-14   | 4.36E-10                                      | 4.82E-10                                    | 7.91E-08                                  |
| Oct   | 14               | 10       | 12      | 1.29E-13   | 7.55E-14   | 7.54E-14   | 3.67E-10                                      | 4.22E-10                                    | 7.32E-08                                  |
| Nov   | 10               | 7        | 9       | 1.23E-13   | 6.97E-14   | 6.96E-14   | 3.07E-10                                      | 3.68E-10                                    | 6.76E-08                                  |
| Dec   | 6                | 5        | 6       | 1.16E-13   | 6.42E-14   | 6.42E-14   | 2.56E-10                                      | 3.36E-10                                    | 6.23E-08                                  |
| Averaged second-order rate constants, $\text{cm}^3 \cdot \text{molec}^{-1} \cdot \text{s}^{-1}$ |                  |          |         | 1.28E-13   | 7.42E-14   | 7.41E-14   | -   | -   | -   |
| Averaged first-order rate constants, $\text{s}^{-1}$  |                  |          |         | 1.02E-07   | 5.94E-08   | 5.93E-08   | 3.64E-10                                      | 4.13E-10                                    | 7.19E-08                                  |

**Table B.22.** Absolute values and statistical parameters of degradation rate constants of first order (PCB-180)

|                    | $k_{\text{air}}, \text{s}^{-1}$ | $k_{\text{soil}}, \text{s}^{-1}$ | $k_{\text{water}}, \text{s}^{-1}$ | $k_{\text{sediment}}, \text{s}^{-1}$ | $k_{\text{veg.}}, \text{s}^{-1}$ |
|--------------------|---------------------------------|----------------------------------|-----------------------------------|--------------------------------------|----------------------------------|
| CAM/POPs           | 1.02E-07                        | -                                | -                                 | -                                    | -                                |
| CliMoChem          | 5.93E-08                        | 3.64E-10                         | 4.13E-10                          | -                                    | 7.19E-08                         |
| MSCE-POP           | 5.94E-08                        | 5.83E-10                         | 8.02E-10                          | -                                    | -                                |
| SimpleBox          | 3.50E-08                        | 3.50E-09                         | 3.50E-09                          | -                                    | -                                |
| EVN-BETR/UK-MODEL  | 3.50E-08                        | 3.50E-09                         | 3.50E-09                          | 3.50E-09                             | 1.13E-08                         |
| Reference data set | 3.50E-08                        | 3.50E-09                         | 3.50E-09                          | 3.50E-09                             | -                                |
| <i>min</i>         | 3.50E-08                        | 3.64E-10                         | 4.13E-10                          | -                                    | -                                |
| <i>max</i>         | 1.02E-07                        | 3.50E-09                         | 3.50E-09                          | -                                    | -                                |
| <i>arith. mean</i> | 5.43E-08                        | 2.29E-09                         | 2.34E-09                          | -                                    | -                                |
| <i>median</i>      | 4.72E-08                        | 3.50E-09                         | 3.50E-09                          | -                                    | -                                |
| <i>geom. mean</i>  | 4.99E-08                        | 1.56E-09                         | 1.70E-09                          | -                                    | -                                |
| <i>max/min</i>     | 2.9                             | 9.6                              | 8.5                               | 1.0                                  | 6.4                              |

## DESCRIPTIONS OF MAIN PROCESSES

This Annex contains the descriptions of the main processes determining POP environmental behavior used in the participating models.

### C.1. Gas/particle partitioning

#### EVN-BETR and UK-MODEL

The gas-particle partitioning is described with the help of the Finizio Aerosol Partition coefficient  $K_{QA}$ . Its dependence on the octanol-air partition coefficient  $K_{oa}$  is depicted by the following formula:

$$K_{QA} = 3.5 \cdot K_{oa}$$

The fugacity capacity of the bulk air compartment can then be written as the sum of the gaseous and particle-bound chemical fraction:

$$(1 - \text{particles in air volume fraction}) \cdot Z_{air} + (\text{particles in air volume fraction}) \cdot K_{QA} \cdot Z_{air}$$

where  $Z_{air} = 1/(R \cdot T)$  is the fugacity capacity in air;

$T$  - corrected environmental temperature for annual mean of 9°C;

$R$  - gas constant = 8.314 Pa·m<sup>3</sup>/mol K;

Particles in air volume fraction -  $2 \cdot 10^{-11}$ ;

$K_{oa} = K_{ow} / K_{aw} - 51616649$  for PCB 153 at the averaged ambient temperature  $T$ ;

Averaged ambient temperature = 9°C (base temperature).

#### CliMoChem

cited from [Scheringer et al., 2003]

The gas/particle partitioning is calculated as follows [Finizio et al., 1997]:

$$K_{partair} = 0.55 \cdot \lg\left(\frac{K_{ow}}{K_h}\right) - 8.23$$

This equation is used to calculate the fraction Phi, which indicates the particle-bound fraction of the substance. Phi-values range from 0-1.

$$\lg k_{partair} = K_{partair} + 6 = 0.55 \cdot \lg\left(\frac{K_{ow}}{K_h}\right) - 2.23 \quad \text{in (m}^3/\text{g)}$$

$$Phi = \frac{k_{partair} \cdot tsp}{(1 + k_{partair} \cdot tsp)}$$

| Parameter | Description                            | Numeric value                                     | Reference                                   |
|-----------|--|---|---|
| $tsp$     | Total suspended particles              | $86 \cdot 10^{-6} \text{ g/m}^3$                  | <i>Bennett et al.</i> [2001] only mentioned |
| $Phi$     | particle-bound fraction of substance   | between 0-1                                       |   |
| $K_h$     | Henry's law constant                   | depending on substance, See Chapter 3 and Annex B |   |
| $K_{ow}$  | Octanol/water partitioning coefficient | depending on substance, See Chapter 3 and Annex B |   |

## G-CIEMS

When  $K_{oa}$  is not available as input:

$$K_{qa} = 6 \cdot 10^6 / P_{ls},$$

where  $K_{qa}$  is dimensionless particle/gas partition coefficient and  $P_{ls}$  is liquid vapour pressure. Final partitioning is calculated with TSP and density of aerosol particles in fugacity format. Vapour pressure is temperature corrected when the temperature is different from 25 °C.

When  $K_{oa}$  is available as input:

$$K_{qa} = y \cdot K_{oa} / (\rho / 1000),$$

where,  $K_{qa}$  is dimensionless particle/gas partition coefficient,  $y$  is organic matter mass fraction, and  $\rho$  is the density of aerosol particles.

(Note: G-CIEMS model can calculate V/P partitioning from only molecular weight (for preliminary assessment purpose) or from  $K_{oa}$ . Two output 1 and 2 is presented in Chapter 4 as G-CIEMS-1 and G-SIEMS-2).

## DEHM-POP

The gas-particle partitioning is calculated using the absorption model:

$$\phi = \frac{K_p TSP}{(K_p TSP + 1)},$$

where  $\phi$  is the fraction of compound sorbed to particles,  $K_p$  is gas-particle partitioning coefficient, and TSP is the total suspended particulate matter [e.g. *Falconer and Harner, 2000*].  $K_p$  is calculated using the  $K_{oa}$  approach:

$$\log K_p = m_r \log K_{oa} + \log f_{om} - 11.91,$$

where  $m_r$  is a constant expected to have a value close to +1 for equilibrium partitioning,  $K_{oa}$  is the octanol-air partitioning coefficient,  $f_{om}$  is the fraction of organic matter in the particles, and 11.91 is a constant determined by the intercept  $br = \log f_{om} - 11.91$  [*Finizio et al., 1997, Falconer and Harner, 2000*].

The temperature dependent  $K_{oa}$  is calculated using the expression:

$$K_{oa}(T) = K_{oa}(T_{ref}) \exp\left(\frac{\Delta U_{oa}}{R} \left(\frac{1}{T_{ref}} - \frac{1}{T}\right)\right),$$

where  $\Delta U_{oa}$  is the internal energy of phase transfer,  $R$  is the universal gas constant,  $T$  is the temperature and  $K_{oa}(T_{ref})$  is the value of  $K_{oa}$  at the reference temperature  $T_{ref}$  [*Beyer et al., 2002*].

## SimpleBox

cited from [*Brandes et al., 1996*]

Air-aerosol partition coefficients are usually not known. However, some information is frequently available on the fraction of the chemical that occurs in association with the aerosol phase. SimpleBox uses this information for the computations. A value for the fraction of the chemical that is associated with the aerosol phase,  $FRas_{aerosol}$ , can be entered directly, or estimated on the basis of the chemical's vapor pressure, according to *Junge* [1977]. In this equation, the sub-cooled liquid vapour pressure should be used. For solids, a correction is applied according to *Mackay* [1991]:

If  $MELTINGPOINT < TEMPERATURE_{[S]}$  (substance is liquid):

$$FRass_{aerosol[S]} = \frac{CONST \cdot \theta}{VAPORPRESSURE(T) + CONST \cdot \theta}$$

If  $MELTINGPOINT > TEMPERATURE_{[S]}$  (substance is solid):

$$FRass_{aerosol[S]} = \frac{CONST \cdot \theta}{VAPORPRESSURE(T) \cdot e^{6.79 \cdot (1 - \frac{MELTINGPOINT}{TEMPERATURE_{[S]}})} + CONST \cdot \theta}$$

with  $FRass_{aerosol[S]}$  - fraction of the chemical in air that is associated with aerosol particles at scale S [-] (A);

$VAPORPRESSURE(T)$  - vapor pressure of the chemical at temperature  $T$  at scale S [Pa] (A);

$MELTINGPOINT$  - melting point of the chemical [K] (A);

$CONST$  - constant [Pa·m] (C);

$\theta$  - surface area of aerosol phase [ $m_{aerosol}^2/m_{air}^3$ ] (C);

$TEMPERATURE_{[S]}$  - temperature at the air-water interface at scale S [K] (A).

with the product  $CONST \cdot \theta$  set equal to  $10^{-4}$  Pa.

## CAM/POPs

In the CAM/POPs model, the process of POP partitioning between the gas and particulate phases in atmosphere is based on Junge-Pankow adsorption model [Junge, 1977; Pankow, 1987] POP fraction  $\Phi$  adsorbed on the atmospheric aerosol particles is given by:

$$\Phi = \frac{c \cdot \Theta}{P_L^0 + c \cdot \Theta}$$

where,  $\Phi$  - fraction of POPs adsorbed on aerosol particles;

$\Theta$  - aerosol surface area available for adsorption,  $m^2$  aerosol/ $m^3$  air;

$P_L^0$  - liquid-phase saturation vapour pressure of pure compound, Pa;

$c$  - parameter that depends on the thermodynamics of the adsorption process and surface properties of the aerosol (Pa · cm).

Junge's proposed value of the parameter  $c$  is 17.2 Pa · cm [Pankow, 1987; Falconer et al., 1994; Bidleman et al., 1998].

The liquid vapour pressure,  $P_L^0$ , are derived from:

$$\log_{10} P_L^0 = \frac{m}{T} + b,$$

where the slope ( $m$ ) and the intercept ( $b$ ) are estimated to calculate liquid vapour pressure of POPs with changing air temperature [Falconer et al., 1995; Harner et al., 1996]. Temperature dependence of  $P_L^0$  for each congener can be seen in Table C.1.

**Table C.1.** Liquid vapour pressure of PCBs as a function of air temperature

|              | PCB-153 | PCB-180 |
|--------------|---------|---------|
| slope, m     | 4775    | 5042    |
| intercept, b | 12.85   | 13.03   |

Aerosol surface area,  $\Theta$ , is calculated by multiplying aerosol number density by its wet surface area.

## MSCE-POP

In the **current model version (MSCE-POP 1)** the characterization of POP partitioning between the gas and particulate phase of a pollutant is performed using subcooled liquid vapour pressure  $p_{ol}$  (Pa). According to the Junge-Pankow adsorption model [Junge, 1977; Pankow, 1987] POP fraction  $\varphi$  adsorbed on the atmospheric aerosol particles equals to:

$$\varphi = \frac{c \cdot \theta}{p_{ol} + c \cdot \theta}$$

where  $c$  is the constant depending on thermodynamic parameters of adsorption process and on properties of aerosol particle surface. It assumed  $c = 0.17 \text{ Pa}\cdot\text{m}$  [Junge, 1977] for background aerosol;

$\theta$  is the specific surface of aerosol particles,  $\text{m}^2/\text{m}^3$ . Assumed  $\theta = 1.5 \cdot 10^{-4}$  [Whitby, 1978].

The temperature dependence of  $p_{ol}$  (Pa) is parameterized in the model by:

$$p_{ol} = p_{ol}^0 \cdot e^{-a_P \left( \frac{1}{T} - \frac{1}{T_0} \right)},$$

where  $T_0 = 283.15 \text{ K}$  is the reference temperature,  $T$  (K) is the ambient temperature,  $p_{ol}^0$  is  $p_{ol}$  value at reference temperature, and  $a_P$  is the coefficient of temperature dependence. The values of  $p_{ol}^0$  and  $a_P$  for considered PCB congeners used in the model are presented in Table C.2.

**Table C.2.** Coefficients of  $p_{ol}$  temperature dependence for three PCB congeners used in MSCE-POP model

| Congener | $p_{ol}^0$           | $a_P$ |
|----------|----------------------|-------|
| PCB-28   | $6.43 \cdot 10^{-3}$ | 9383  |
| PCB-153  | $9.69 \cdot 10^{-5}$ | 10995 |
| PCB-180  | $1.67 \cdot 10^{-5}$ | 11610 |

At present the work on modification of the description of gas aerosol partitioning within MSCE-POP model is ongoing. The approach using the octanol-air partitioning coefficient absorption model presented in [Falconer and Harner, 2000] is tested. Under this approach POP fraction  $\varphi$  adsorbed on the atmospheric aerosol particles is calculated as:

$$\varphi = \frac{K_p \cdot TSP}{1 + K_p \cdot TSP}$$

where  $K_p$  is the particle-gas partitioning coefficient and  $TSP$  is the total suspended particle concentration ( $\mu\text{g}\cdot\text{m}^{-3}$ ). The constant  $K_p$  is calculated for PCBs via  $K_{oa}$  by the following regression equations [Falconer and Harner, 2000]:

$$\log K_p = \log K_{oa} + \log f_{om} - 11.91, \quad (\text{experimental version - MSCE-POP 2})$$

where  $K_{oa}$  is the octanol/air partitioning coefficient and  $f_{om}$  is the fraction of organic matter in the atmospheric aerosol involved in partitioning.

The temperature dependence of  $K_{oa}$  is parameterized in the model by:

$$K_{oa} = K_{oa}^0 \cdot e^{-a_K \left( \frac{1}{T} - \frac{1}{T_0} \right)},$$

where  $K_{oa}^0$  is  $K_{oa}$  value at reference temperature, and  $a_K$  is the coefficient of temperature dependence.

The values of  $K_{oa}^0$  and  $a$  for considered PCB congeners used in the model are presented in Table C.3.

**Table C.3.** Coefficients of  $K_{oa}$  temperature dependence for three PCB congeners used in MSCE-POP model

| Congener | $K_{oa}^0$           | $a_K$ |
|----------|----------------------|-------|
| PCB-28   | $5.78 \cdot 10^8$    | 8731  |
| PCB-153  | $3.64 \cdot 10^{10}$ | 10811 |
| PCB-180  | $2.07 \cdot 10^{11}$ | 10442 |

## C.2. Dry deposition of the particulate phase

### EVN-BETR and UK-MODEL

The intermedia transport of chemicals is described using D-values (mol/Pa-h), which represent how fast advective and reactive/degradation processes are occurring. In the case of the air to surface exchange, the D-value defining dry particle deposition is:

$$D_{air-surface} = \text{Surface Area} \cdot \text{Particles in air volume fraction} \cdot V_q \cdot Z_{air} \cdot K_{QA}$$

Knowing these values can help calculate the flux of a chemical entering a region and, thus, its amount in the compartment under study.

Surface area - compartment specific;

Particles in air volume fraction -  $2 \cdot 10^{-11}$ ;

$V_q$  - dry deposition velocity = 10.8 m/h.

### CliMoChem

cited from [Scheringer et al., 2003]

**Dry deposition to baresoil<sup>a</sup>, water, vegetation-covered soil<sup>b</sup>**

$$\frac{dC_{gas}}{dt} = -Phi \left( v_{dry} \cdot \left( \frac{A_i}{V_{gas}} \right) \right) \cdot C_{gas}$$

| Parameter | Description   | Numeric Value | Reference                   |
|-----------|---|---------------|-----------------------------|
| $C_{gas}$ | concentration of substance in gaseous phase         |               |                             |
| $Phi$     | particle-bound fraction of the substance (see C.1.) | between 0-1   |                             |
| $v_{dry}$ | deposition rate                                     | 260 m/d       | [Mackay and Paterson, 1991] |
| $A_i$     | Area, i = baresoil, water, vegetation-covered soil  | variable      |                             |
| $V_{gas}$ | Volume of gaseous phase                             | variable      |                             |

<sup>a</sup>If the year consists of exactly four seasons with varying temperatures,  $v_{dry}$  for deposition to baresoil is changing taking into account that in the cold season the atmosphere is more stable and the deposition rate therefore is smaller. The spring and fall values are interpolations between the summer and winter values.  $v_{dry}$  changes as follows [Wania and McLachlan, 2001]:

| season | $v_{dry} =$     |
|--------|-----------------|
| winter | $v_{dry} / 2$   |
| spring | $v_{dry} / 1.5$ |
| summer | $v_{dry}$       |
| fall   | $v_{dry} / 1.5$ |

<sup>b</sup>If the year consists of exactly four seasons with varying temperatures,  $v_{dry}$  for deposition to vegetation-covered soil is changing taking into account that in the cold season the atmosphere is more stable and the deposition rate therefore is smaller. The spring and fall values are interpolations between the summer and winter values.  $v_{dry}$  changes as follows [Wania and McLachlan, 2001]:

| season | $v_{dry} =$   |
|--------|---|
| winter | $v_{dry} / (2 \cdot \text{VegGrass} + 5 \cdot \text{VegCon} + 3 \cdot \text{VegDec})$     |
| spring | $v_{dry} / (1.5 \cdot \text{VegGrass} + 2.5 \cdot \text{VegCon} + 2 \cdot \text{VegDec})$ |
| summer | $v_{dry}$   |
| fall   | $v_{dry} / (1.5 \cdot \text{VegGrass} + 2.5 \cdot \text{VegCon} + 2 \cdot \text{VegDec})$ |

The vegetation cover consists of three types: Grass, Coniferous Forest and Deciduous Forest. The variables VegGrass, VegCon and VegDec describe the fraction of the vegetation-covered soil occupied by the different cover types. Their numeric value is between 0-1 and depends on the climatic zone.

## Dry deposition to vegetation

$$\frac{dC_{gas}}{dt} = -Phi \left( v_{dry} \cdot \left( \frac{A_{veg}}{V_{gas}} \right) \right) \cdot C_{gas}$$

| Parameter | Description   | Numeric Value                         |
|-----------|---|---------------------------------------|
| $C_{gas}$ | concentration of substance in gaseous phase                         |                                       |
| $Phi$     | particle-bound fraction of the substance (see C.1.)                 | between 0-1                           |
| $v_{dry}$ | deposition rate   | variable, depending on climatic zone* |
| $A_{veg}$ | Area of vegetation (identical with Area of vegetation-covered soil) | variable                              |
| $V_{gas}$ | Volume of gaseous phase   | variable                              |

\* - the model contains three types of vegetation. For each type, the deposition rate ( $v_{dry}$ ) is different (see table below). Depending on the composition of a climatic zone,  $v_{dry}$  is calculated as follows:

$$v_{dry_i} = fraction_{grass_i} \cdot v_{dry_{grass}} + fraction_{dec_i} \cdot v_{dry_{dec}} + fraction_{con_i} \cdot v_{dry_{con}}$$

| Parameter            | Description  | Numeric Value | Reference                             |
|----------------------|--|---------------|---------------------------------------|
| $v_{dry_i}$          | deposition rate in climatic zone i                                   |               |                                       |
| $v_{dry_{grass}}$    | deposition rate to grass   | 55.92 m/d     | <i>Horstmann and McLachlan [1998]</i> |
| $v_{dry_{dec}}$      | deposition rate to deciduous forest                                  | 447.6 m/d     | <i>McLachlan [1998]</i>               |
| $v_{dry_{con}}$      | deposition rate to coniferous forest                                 | 43.2 m/d      | <i>Möller [2002]</i>                  |
| $fraction_{grass_i}$ | fraction of grass of total vegetation in climatic zone i             | variable      |                                       |
| $fraction_{dec_i}$   | fraction of deciduous forest of total vegetation in climatic zone i  | variable      |                                       |
| $fraction_{con_i}$   | fraction of coniferous forest of total vegetation in climatic zone i | variable      |                                       |

Because of increased stability of the atmosphere in the spring, fall and winterseason, the deposition rates  $v_{dry_{grass}}$ ,  $v_{dry_{dec}}$  and  $v_{dry_{con}}$  are divided by 3 for the winterseason and by 2 for the spring and fall seasons (given that the year consists of exactly four seasons with varying temperature [*Wania and McLachlan, 2001*]).

## G-CIEMS

$$F = v_{Dep} \cdot (TSP/\rho) \cdot C_{particle}$$

Where  $F$  is mass flux of compound for this chemical,  $v_{Dep}$  is dry deposition velocity of particles,  $TSP$  is particulate concentration of weight/volume dimension,  $\rho$  is density of aerosol particles,  $C_{particle}$  is compound volumetric concentration in particles. Same value is used on all land and water surfaces.

## DEHM-POP

The dry deposition of particulate phase is calculated as a flux given by the atmospheric concentration times a deposition velocity [*Christensen, 1997*]. The deposition velocity is highly dependent on the meteorological conditions and the surface properties. The size of the particles is assumed to be  $1\mu\text{m}$  [*Christensen, 1997*].

For unstable conditions in the atmosphere (when  $L < 0$ , i.e. at day time with clear sky), the deposition velocity is calculated using:

$$v_d = \frac{u^*}{a} \left( 1 + \left( \frac{-300}{L} \right)^{2/3} \right),$$

where  $u^*$  is the surface friction velocity,  $a$  is a constant depending on the surface properties, and  $L$  is the Monin-Obukhov length.

For stable conditions in the atmosphere (when  $L > 0$ , i.e. at night time with clear sky), the deposition velocity is calculated using:

$$v_d = \frac{u^*}{a}$$

The surface friction velocity is calculated using:

$$u^* = \frac{0.35 \cdot U}{\ln(10) \cdot z},$$

where  $U$  is the wind speed and  $z$  is the roughness length which depends on the properties of the surface, and varies seasonally.

The Monin-Obukhov length is calculated using:

$$L = \frac{(u^*)^3 \cdot T}{0.35 \cdot g \cdot \left(\frac{-H_d}{c_p \rho}\right)},$$

where  $T$  is the temperature,  $g$  is the gravitational constant ( $g = 9.82$ ),  $H_d$  is the heat flux,  $c_p$  is the specific heat at constant pressure, and  $\rho$  is the air density.  $L$  is positive (stable atmosphere) when the heat flux is negative (night time clear sky) and negative (unstable atmosphere) when the heat flux is positive (day time clear sky).

## SimpleBox

cited from [Brandes et al., 1996]

Value for the deposition mass transfer coefficients  $DRYDEP_{aerosol}$  may be obtained by means of:

$$DRYDEP_{aerosol[S]} = AEROSOLDEPRATE_{[S]} \cdot FRass_{aerosol[S]}$$

with  $DRYDEP_{aerosol[S]}$ : mass transfer coefficient for dry deposition of aerosol-associated chemical at scale S [m<sub>air</sub>/s] (D);

$AEROSOLDEPRATE_{[S]}$  - deposition velocity of the aerosol particles at scale S with which the chemical is associated [m/s] (A);

$FRass_{aerosol[S]}$ : fraction of the chemical in air that is associated with aerosol particles at scale S [-] (A).

Deposition mass flows of the chemical depend on the rate of dry aerosol deposition. Deposition velocities of aerosols vary greatly with the size of the particles. As chemicals may be associated with particles of a specific size, the deposition velocities depend also on the chemical. The values given are typical values, to be used as a starting point:

$$AEROSOLDEPRATE_{[S]} = 0.1 \text{ cm/s}$$

with  $AEROSOLDEPRATE_{[S]}$ : deposition velocity of the aerosol particles with which the chemical is associated at scale S [m/s] (A)

## CAM/POPs

Removal of POPs particles is coupled with the dry deposition of aerosols in the CAM model. The dry deposition flux can be written as:

$$F_d = -v_d \cdot C_p,$$

where  $v_d$  is the deposition velocity and  $C_p$  is the particle concentration [Gong et al. 2003].

Dry deposition flux of POPs gas is written as:

$$F_d = -v_d \cdot C_g,$$

where the dry deposition velocity of gas,  $v_d$ , is calculated in CAM model [Gong et al. 2003].

## MSCE-POP

### *Dry deposition to grass and bare soil*

According to model of [Sehmel, 1980], deposition flux over grass is calculated as

$$F = C_p \cdot (A_{soil} u_*^2 + B_{soil}) z_0^{C_{soil}},$$

where as above  $u_*$ , is the friction velocity;

$z_0$  is the surface roughness, mm;

$A_{soil} = 0.02$ ,  $B_{soil} = 0.01$ ,  $C_{soil} = 0.33$ .

### *Dry deposition to forest*

According to model of [Ruijgrok et al., 1997], deposition flux over forest is calculated as

$$F = C_p \cdot E \frac{u_*^2}{u_h},$$

where  $u_h$  is the wind speed at forest height  $h = z_b$ ;

$u_*$  is the friction velocity, m/s;

$E = \alpha u_*^\beta (1 + \gamma \exp((RH - 80)/20))$ ,  $\alpha = 0.048$ ,  $\beta = 0.3$  and  $\gamma = 0.25$ ,  $RH=80$ .

### *Dry deposition to seawater*

According to model of [Lindfors et al., 1991], deposition flux over seawater is calculated as:

$$F = C_p \cdot (A_{sea} u_*^2 + B_{sea}),$$

where  $u_*$  is the friction velocity, m/s;

$A_{sea} = 0.15$ ,  $B_{sea} = 0.013$

Similar to DEHM-POP model values of deposition flux depend on meteorological conditions (friction velocity  $u_*$ ). Therefore, in the results of calculation experiments we present the range of obtained values of the flux together with its value at average environmental parameters.

## C.3. Wet deposition

### EVN-BETR and UK-MODEL

In a similar way as for the dry particle deposition, wet scavenging is defined as the result of:

$$D_{air-surface} = Q \cdot \text{Surface Area} \cdot \text{Particles in air fraction} \cdot K_{QA} \cdot U_R \cdot Z_{air}$$

In the case of deposition in vegetation, the percentage of rain interception due to vegetation is taken into account.

$U_R$  - rain rate =  $8.84 \times 10^{-5}$  m/h;

Q - Rain Scavenging ratio = 200000;

Or Snow Scavenging Ratio = 1000000

## CliMoChem

cited from [Scheringer et al., 2003]

### Wet deposition from gaseous phase to baresoil and water

$$\frac{dC_{gas}}{dt} = -(1 - Phi) \left( v_{rain} \cdot \left( \frac{A_i}{V_{gas}} \right) \cdot \frac{1}{K_h} \right) \cdot C_{gas}$$

| Parameter  | Description   | Numeric value   | Reference                        |
|------------|---|---|----------------------------------|
| $C_{gas}$  | concentration of substance in gaseous phase         |   |                                  |
| $Phi$      | particle-bound fraction of the substance (see C.1.) | between 0-1   |                                  |
| $v_{rain}$ | global annual average precipitation                 | $2.33 \cdot 10^{-3}$ m/d  | <i>Mackay and Paterson, 1991</i> |
| $A_i$      | area, i = baresoil, water                           | variable  |                                  |
| $V_{gas}$  | volume of gaseous phase                             | variable  |                                  |
| $K_h$      | Henry's law constant                                | depending on substance, compare substance property sheets, See Chapter 3 and Annex B. |                                  |

### Wet deposition from gaseous phase to vegetation-covered soil

$$\frac{dC_{gas}}{dt} = -(1 - Phi) \left( v_{rain} \cdot \left( \frac{A_{vsoil}}{V_{gas}} \right) \cdot \frac{1}{K_h} \right) \cdot (1 - f_{rt}) \cdot C_{gas}$$

| Parameter   | Description   | Numeric value  | Reference  |
|-------------|---|--|--|
| $C_{gas}$   | concentration of substance in gaseous phase         |  |  |
| $Phi$       | particle-bound fraction of the substance (see C.1.) | between 0-1  |  |
| $v_{rain}$  | global annual average precipitation                 | $2.33 \cdot 10^{-3}$ m/d   | <i>Mackay and Paterson, 1991</i>                         |
| $A_{vsoil}$ | area of vegetation-covered soil                     | variable   |  |
| $V_{gas}$   | volume of gaseous phase                             | variable   |  |
| $K_h$       | Henry's law constant                                | depending on substance, compare substance property sheets See Chapter 3 and Annex B. |  |
| $f_{rt}$    | fraction of rain falling on vegetation (leaves etc) | depending on vegetation type and season*   | <i>Horstmann and McLachlan, 1998; Wania et al., 2000</i> |

\* - for deciduous and coniferous forest, the  $f_{rt}$ -value is 0.35 for the summer season, for grass, the  $f_{rt}$ -value is 0.12 for the summer season. In the winter season, the value is at 10% of the summer season, in spring and fall season, the value is at the linear interpolation value between summer and winter season. Because the composition of the vegetation varies with the climatic zones, the contributions of grass, coniferous and deciduous forest to the overall  $f_{rt}$ -value of a specific climate zone differ and are proportional to the fraction of the respective vegetation type in a climatic zone.

### Wet deposition from gaseous phase to vegetation

$$\frac{dC_{gas}}{dt} = -(1 - Phi) \left( v_{rain} \cdot \left( \frac{A_{vsoil}}{V_{gas}} \right) \cdot \frac{1}{K_h} \right) \cdot f_{rt} \cdot C_{gas}$$

| Parameter   | Description  | Numeric value   | Reference                        |
|-------------|--|---|----------------------------------|
| $C_{gas}$   | concentration of substance in gaseous phase            |   |                                  |
| $Phi$       | particle-bound fraction of the substance (see C.1.)    | between 0-1   |                                  |
| $v_{rain}$  | global annual average precipitation                    | $2.33 \cdot 10^{-3}$ m/d  | <i>Mackay and Paterson, 1991</i> |
| $A_{vsoil}$ | area of vegetation (= area of vegetation-covered soil) | variable  |                                  |
| $V_{gas}$   | volume of gaseous phase                                | variable  |                                  |
| $K_h$       | Henry's law constant                                   | depending on substance, compare substance property sheets, See Chapter 3 and Annex B. |                                  |
| $f_{rt}$    | fraction of rain falling on vegetation (leaves etc)    | depending on vegetation type and season*  | <i>Wania et al., 2000</i>        |

\* - for deciduous and coniferous forest, the  $f_{rt}$ -value is 0.35 for the summer season, for grass, the  $f_{rt}$ -value is 0.12 for the summer season. In the winter season, the value is at 10% of the summer season, in spring and fall season, the value is at the linear interpolation value between summer and winter season. Because the composition of the vegetation varies with the climatic zones, the contributions of grass, coniferous and deciduous forest to the overall  $f_{rt}$ -value of a specific climate zone differ and are proportional to the fraction of the respective vegetation type in a climatic zone.

### Wet deposition from particulate phase to bare soil and water

$$\frac{dC_{gas}}{dt} = -Phi \left( v_{rain} \cdot scav_{ratio} \cdot \left( \frac{A_i}{V_{gas}} \right) \right) \cdot C_{gas}$$

| Parameter      | Description   | Numeric value            | Reference                        |
|----------------|---|--------------------------|----------------------------------|
| $C_{gas}$      | concentration of substance in gaseous phase   |                          |                                  |
| $Phi$          | particle-bound fraction of the substance (see C.1)  | between 0-1              |                                  |
| $v_{rain}$     | global annual average precipitation   | $2.33 \cdot 10^{-3}$ m/d | <i>Mackay and Paterson, 1991</i> |
| $scav_{ratio}$ | scavenging ratio: the air volume scavenged by the falling rain is scavratio-times greater than the rainwater volume | $2 \cdot 10^5$           | <i>Mackay and Paterson, 1991</i> |
| $A_i$          | area, i = baresoil,water  | variable                 |                                  |
| $V_{gas}$      | volume of gaseous phase   | variable                 |                                  |

### Wet deposition from particulate phase to vegetation-covered soil

$$\frac{dC_{gas}}{dt} = -Phi \left( v_{rain} \cdot scav_{ratio} \cdot \left( \frac{A_{vsoil}}{V_{gas}} \right) \right) \cdot (1 - f_{rt}) \cdot C_{gas}$$

| Parameter      | Description   | Numeric value  | Reference                        |
|----------------|---|--|----------------------------------|
| $C_{gas}$      | concentration of substance in gaseous phase   |  |                                  |
| $Phi$          | particle-bound fraction of the substance (see C.1)  | between 0-1  |                                  |
| $v_{rain}$     | global annual average precipitation   | $2.33 \cdot 10^{-3}$ m/d   |                                  |
| $scav_{ratio}$ | scavenging ratio: the air volume scavenged by the falling rain is scavratio-times greater than the rainwater volume | $2 \cdot 10^5$   | <i>Mackay and Paterson, 1991</i> |
| $A_{vsoil}$    | area of vegetation-covered soil (= area of vegetation)  | variable   |                                  |
| $V_{gas}$      | volume of gaseous phase   | variable   |                                  |
| $K_h$          | Henry's law constant  | depending on substance, compare substance property sheets, See Chapter 3 and Annex B |                                  |
| $f_{rt}$       | fraction of rain falling on vegetation (leaves etc)   | depending on vegetation type and season*   | <i>Wania et al., 2000</i>        |

\* - for deciduous and coniferous forest, the  $f_{rt}$ -value is 0.35 for the summer season, for grass, the  $f_{rt}$ -value is 0.12 for the summer season. In the winter season, the value is at 10% of the summer season, in spring and fall season, the value is at the linear interpolation value between summer and winter season. Because the composition of the vegetation varies with the climatic zones, the contributions of grass, coniferous and deciduous forest to the overall  $f_{rt}$ -value of a specific climate zone differ and are proportional to the fraction of the respective vegetation type in a climatic zone.

### Wet deposition from particulate phase to vegetation

$$\frac{dC_{gas}}{dt} = -Phi \left( v_{rain} \cdot scav_{ratio} \cdot \left( \frac{A_{vsoil}}{V_{gas}} \right) \right) \cdot f_{rt} \cdot C_{gas}$$

| Parameter      | Description   | Numeric value  | Reference                        |
|----------------|---|--|----------------------------------|
| $C_{gas}$      | concentration of substance in gaseous phase   |  |                                  |
| $Phi$          | particle-bound fraction of the substance (see C.1.)   | between 0-1  |                                  |
| $v_{rain}$     | global annual average precipitation   | $2.33 \cdot 10^{-3}$ m/d   |                                  |
| $scav_{ratio}$ | scavenging ratio: the air volume scavenged by the falling rain is scavratio-times greater than the rainwater volume | $2 \cdot 10^5$   | <i>Mackay and Paterson, 1991</i> |
| $A_{vsoil}$    | area of vegetation (= area of vegetation-covered soil)  | variable   |                                  |
| $V_{gas}$      | volume of gaseous phase   | variable   |                                  |
| $K_h$          | Henry's law constant  | depending on substance, compare substance property sheets, See Chapter 3 and Annex B |                                  |
| $f_{rt}$       | fraction of rain falling on vegetation (leaves etc)   | depending on vegetation type and season*   | <i>Wania et al., 2000</i>        |

\* - for deciduous and coniferous forest, the  $f_{rt}$ -value is 0.35 for the summer season, for grass, the  $f_{rt}$ -value is 0.12 for the summer season. In the winter season, the value is at 10% of the summer season, in spring and fall season, the value is at the linear interpolation value between summer and winter season. Because the composition of the vegetation varies with the climatic zones, the contributions of grass, coniferous and deciduous forest to the overall  $f_{rt}$ -value of a specific climate zone differ and are proportional to the fraction of the respective vegetation type in a climatic zone.

## G-CIEMS

$$F = R_{rain} \cdot C_{air} / H + (TSP/\rho) \cdot Q \cdot C_{particle},$$

where  $F$  is total mass flux by this process,  $R_{rain}$  is rain rate,  $C_{air}$  is gaseous concentration of chemical,  $H$  is Henry's law constant,  $TSP$  is particulate concentration,  $\rho$  is density of particles,  $Q$  is scavenging ratio of particles, and  $C_{particle}$  is volumetric chemical concentration in particles.

Same  $Q$  value is assumed over all land and water surfaces.

## DEHM-POP

The wet deposition is given as a flux calculated as the product between the air concentration and a scavenging ratio [Christensen, 1997]. Different scavenging ratios are used for in-cloud scavenging and below-cloud scavenging. It is assumed that air pollution is scavenged more efficient in the clouds than below the clouds. The below cloud scavenging rate at a given height  $\sigma$  is given by:

$$W(\sigma) = \frac{\Lambda_{bc} P_a(\sigma)}{H \rho_w},$$

where  $\Lambda_{bc}$  is the below cloud scavenging coefficient,  $P_a$  is the total precipitation at the level,  $H$  is an effective thickness for scavenging ( $H = 1000$  m), and  $\rho_w$  is the density of water. The in cloud scavenging rate at a given height  $\sigma$  is given by:

$$W(\sigma) = \frac{\Lambda_c P(\sigma)}{H \rho_w},$$

where  $\Lambda_c$  is the below cloud scavenging coefficient,  $P_a$  is the total precipitation created inside the cloud layer. The used scavenging ratios are:  $\Lambda_{bc} = 100000$  and  $\Lambda_c = 700000$ .

The total amount of pollutant scavenged by the wet deposition is then dependent on the actual height of the formation of the precipitation, and on the vertical concentration profile.

## SimpleBox

cited from [Brandes et al., 1996]

Value for the deposition mass transfer coefficient *WASHOUT* may be obtained by means of:

$$WASHOUT_{[S]} = RAINRATE_{[S]} \cdot SCAVratio_{[S]}$$

with  $WASHOUT_{[S]}$  - mass transfer coefficient for wet atmospheric deposition at scale  $S$  [ $m_{air} \cdot s^{-1}$ ] (D);  
 $RAINRATE_{[S]}$  - rate of wet precipitation at scale  $S$  [ $m_{rain} \cdot s^{-1}$ ] (A);  
 $SCAVratio_{[S]}$  - scavenging ratio (quotient of the total concentration in rainwater and the total concentration in air) of the chemical at scale  $S$  [-] (A).

The scavenging ratio may be known from measurements or estimated:

$$SCAVratio_{[S]} = \frac{1 - FRass_{aerosol[S]} + FRass_{aerosol[S]} COLLECTeff_{[S]}}{K_{air-water[S]}}$$

with  $SCAVratio_{[S]}$  - scavenging ratio (quotient of the total concentration in rainwater and the total concentration in air) of the chemical at scale  $S$  [-] (A);  
 $FRass_{aerosol[S]}$  - fraction of the chemical in air that is associated with aerosol particles at scale  $S$  [-] (A);  
 $K_{air-water[S]}$  - air-water equilibrium distribution constant at scale  $S$  [ $mol \cdot m_{air}^{-3} / mol \cdot m_{water}^{-3}$ ] (A);  
 $COLLECTeff_{[S]}$  - aerosol collection efficiency at scale  $S$  [-] (A),

The first term represents an estimate of the (equilibrium) distribution between rain water in air and the gas phase of air. The second term represents the scavenging of aerosol particles by rain droplets. The proportionality constant of  $2 \cdot 10^5$  is taken from Mackay [1991].

Deposition mass flows of the chemical depend on the rate of wet precipitation. Collection efficiencies of aerosols vary greatly with the size of the particles. As chemicals may be associated with particles of a specific size, the collection efficiencies depends also on the chemical. The values given are typical values, to be used as a starting point:

$$COLLECTeff_{[S]} = 2 \cdot 10^5$$

with  $COLLECTeff_{[S]}$  - aerosol collection efficiency at scale S [-] (A).

**Table C4.** RAINRATE of the scales

| Scale       | RAINRATE, mm/y |
|-------------|----------------|
| Regional    | 700            |
| Continental | 700            |
| Moderate    | 700            |
| Arctic      | 250*           |
| Tropic      | 1300*          |

\* - from Wania and Mackay [1995]

## CAM/POPs

The precipitation scavenging of POPs particles by falling rain or snow is coupled with the wet removal of aerosols in the CAM model.

The particulate wet deposition flux,  $F_p$ , can be written as:

$$F_p = (-\Psi_{rain\ or\ snow} h) C_p,$$

where  $h$  is the falling distance,  $C_p$  is the particulate phase POPs concentration,  $\psi$  is the scavenging rate for rain or snow [Gong *et al.* 1997].

The gas phase POPs are assumed to be in quasi-steady equilibrium with the rain drop. The air-water equilibrium coefficient,  $K_{aw}$ , is a dimensionless partition coefficient that can be derived from Henry's Law constant,  $H$  ( $\text{Pa} \cdot \text{m}^3/\text{mol}$ ) [Seinfeld, 1986].

$$K_{aw} = H / (R \cdot T)$$

and,  $H = H_0 \exp(a(1/T_0 - 1/T))$ ,

where  $T$  is the temperature (K) and  $R$  is the gas constant ( $8.314 \text{ Pa} \cdot \text{m}^3/\text{mol} \cdot \text{K}$  or  $\text{J}/\text{mol}/\text{K}$ ),  $H_0$  is the value at the reference temperature  $T_0$ , and  $a$  is a parameter of temperature dependence.

|       | PCB-153 | PCB-180 |
|-------|---------|---------|
| $H_0$ | 2.43    | 1.01    |
| $T_0$ | 298 °K  | 298 °K  |
| $a$   | 3.4E+3  | 3.4E+3  |

The net wet deposition flux,  $F_w$ , is then written as:

$$F_w = (-p / K_{AW}) \cdot C_G$$

where  $p$  is the precipitation rate, usually reported in mm/h and  $C_G$  is the gas phase POPs concentration.

## MSCE-POP

### *Wet deposition of particulate phase*

The values of concentration in precipitation are given by the formula:

$$C_w^s = W_p C_a^p,$$

where  $C_a^p$  - the particle bound phase concentration in the air surface layer, ng/m<sup>3</sup>;  
 $C_w^s$  - the suspended phase concentration in precipitation water, ng/m<sup>3</sup>;  
 $W_p = 1.5 \cdot 10^5$  - the dimensionless washout ratio for the particulate phase.

### *Wet deposition of gaseous phase*

$$C_w^d = W_g C_a^g,$$

where  $C_w^d$  - the dissolved phase concentration in precipitation water, ng/m<sup>3</sup>;  
 $C_a^g$  - the gaseous phase concentration in air, ng/m<sup>3</sup>;  
 $W_g = 1/K_H$  - the dimensionless washout ratio for the gaseous phase;  
 $K_H$  - the dimensionless Henry's law constant.

## C.4. Gaseous exchange between atmosphere and soil

### EVN-BETR and UK-MODEL

#### *Air-soil diffusion*

$$D_{air-soil} = (Soil\ Area \cdot Z_{air}) / [(Z_{air} / (MTC_{as} \cdot Z_{air} + MTC_{sw} \cdot Z_{water})) + 1 / MTC_{sabl}]$$

where *Average soil depth* = 10 cm;  
*Soil Area* = 8.36 10<sup>12</sup> m<sup>2</sup>;  
 $Z_{water} = Z_{air} / K_{AW} = 543$  mol/m<sup>3</sup> Pa;  
 $MTC_{as}$  - soil air-phase diffusion transport velocity = 0.04 m/h;  
 $MTC_{sw}$  - soil water-phase diffusion transport velocity = 1 x 10<sup>-5</sup> m/h;  
 $MTC_{sabl}$  - soil air boundary layer transport velocity = 1 m/h.

#### *Air-soil rain dissolution*

$$D_{air-soil} = Soil\ Area \cdot U_R \cdot Z_{water}$$

## CliMoChem

cited from [Scheringer et al., 2003]

### *Diffusion from atmosphere to baresoil and vegetation-covered soil*

$$\frac{dC_{gas}}{dt} = -(1 - Phi) \left\{ \frac{1}{v_{gasS}} + \frac{1}{vG + \frac{vL}{K_h} + \frac{vS}{\frac{K_h}{regc \cdot rhoom \cdot foc \cdot K_{ow}}}} \right\}^{-1} \cdot \frac{A_f}{V_{gas}} \cdot C_{gas}$$

| Parameter    | Description  | Numeric Value  | Reference   |
|--------------|--|--|---|
| $C_{gas}$    | concentration of substance in gaseous phase  |  |   |
| $\Phi$       | particle-bound fraction of the substance (see C.1)   | between 0-1  |   |
| $v_{gasS}$   | transfer velocity on the interface soil-atmosphere: air over soil  | 24 m/d   | <i>Mackay and Paterson, 1991; Jury et al., 1983</i> |
| $vG$         | transfer velocity on the interface soil-atmosphere: air filled pores   | calculation see below  |   |
| $vL$         | transfer velocity on the interface soil-atmosphere: water filled pores   | calculation see below  |   |
| $vS$         | transfer velocity on the interface soil-atmosphere: sorbed phase   | calculation see below  |   |
| $f_{oc}$     | fraction of organic matter in soil: different for different types of soil.   | baresoil: 0.02<br>vegetation-covered soil: variable,<br>calculation see below        | assumed   |
| $regc$       | regression coefficient from equation $K_{oc}=regc \cdot K_{ow}$ , where $K_{oc}$ is the partitioning coefficient of organic carbon and water | 0.35 L/kg  | <i>Seth et al., 1999</i>                            |
| $\rho_{oom}$ | density of organic matter  | 2.5 kg/L   | <i>Seth et al., 1999</i>                            |
| $A_i$        | Area, i=bare soil, vegetation-covered soil   | variable   |   |
| $V_{gas}$    | Volume of gaseous phase  | variable   |   |
| $K_h$        | Henry's law constant   | depending on substance compare substance property sheets, See Chapter 3 and Annex B. |   |
| $K_{ow}$     | Octanol/water partitioning coefficient   | depending on substance compare substance property sheets, See Chapter 3 and Annex B. |   |

Analogous to the procedure in subsection C.3, the parameter  $v_{gasS}$  is changed if the year consists of exactly four seasons with varying temperatures (compare tables below).

*bare soil:*

| season | $v_{gasS} =$   |
|--------|----------------|
| winter | $v_{gasS}/2$   |
| spring | $v_{gasS}/1.5$ |
| summer | $v_{gasS}$     |
| fall   | $v_{gasS}/1.5$ |

*vegetation-covered soil:*

| season | $v_{gasS} =$  |
|--------|---|
| winter | $v_{gasS}/(2 \cdot VegGrass + 5 \cdot VegCon + 3 \cdot VegDec)$     |
| spring | $v_{gasS}/(1.5 \cdot VegGrass + 2.5 \cdot VegCon + 2 \cdot VegDec)$ |
| summer | $v_{gasS}$  |
| fall   | $v_{gasS}/(1.5 \cdot VegGrass + 2.5 \cdot VegCon + 2 \cdot VegDec)$ |

The vegetation cover consists of three types: Grass, Coniferous Forest and Deciduous Forest. The variables VegGrass, VegCon and VegDec describe the fraction of the vegetation-covered soil occupied by the different cover types. Their numeric value is between 0-1 and depend on the climatic zone.

Calculation of  $vG$ ,  $vL$ ,  $vS$  [*Jury et al., 1983*].

When calculating the  $v_i$ -value, the corresponding  $D_i$ -value must be used (eg. for calculating  $vG$ , the  $DG$ -value is used):

$$v_i = \frac{D_i}{\frac{h_{soil}}{2}} \cdot \left[ \frac{K_h}{regc \cdot \rho_{oom} \cdot f_{oc} \cdot K_{ow} (1 - frac_{wsoil} - frac_{airsoil}) + frac_{wsoil} + frac_{airsoil} \cdot K_h} \right]$$

| Parameter        | Description  | Numeric value   | Reference                         |
|------------------|--|---|-----------------------------------|
| $v_i$            | $vG, vS, vL$   |   |                                   |
| $DG$             | diffusion coefficient in soil air pores  | $8.0469 \cdot 10^{-3} \text{ m}^2/\text{d}$ (calculation see below)                   |                                   |
| $DL$             | diffusion coefficient in soil water pores  | $3.10885 \cdot 10^{-6} \text{ m}^2/\text{d}$ (calculation see below)                  |                                   |
| $DS$             | diffusion coefficient in soil sorbed phase   | $5.5 \cdot 10^{-7} \text{ m}^2/\text{d}$  | <i>Elzein and Balesdent, 1995</i> |
| $h_{soil}$       | height of soil   | 0.1 m   |                                   |
| $regc$           | regression coefficient from equation $K_{oc} = regc K_{ow}$ where $K_{oc}$ is the partitioning coefficient of organic carbon and water | 0.35 L/kg   | <i>Seth et al., 1999</i>          |
| $\rho_{oom}$     | density of organic matter  | 2.5 kg/L  | <i>Seth et al., 1999</i>          |
| $frac_{wsoil}$   | part of water in soil  | 0.3   | <i>Scheringer, 1996</i>           |
| $frac_{airsoil}$ | part of air in soil  | 0.2   | <i>Scheringer, 1996</i>           |
| $f_{oc}$         | fraction of organic matter in soil: different for different types of soil.   | baresoil: 0.02<br>vegetation-covered soil: variable, calculation see below            | assumed                           |
| $K_h$            | Henry's law constant   | depending on substance, compare substance property sheets, See Chapter 3 and Annex B. |                                   |
| $K_{ow}$         | Octanol/water partitioning coefficient   | depending on substance, compare substance property sheets, See Chapter 3 and Annex B. |                                   |

$$DG = 0.43 \cdot \left( \frac{frac_{airsoil}^{\frac{10}{3}}}{(frac_{airsoil} + frac_{wsoil})^2} \right)$$

$$DL = 0.000043 \cdot \left( \frac{frac_{wsoil}^{\frac{10}{3}}}{(frac_{airsoil} + frac_{wsoil})^2} \right)$$

Calculation of the fraction of organic matter ( $f_{oc}$ ) in the vegetation covered soil

The model contains three types of vegetation. For each type, the  $f_{oc}$  is different (see table below). Depending on the composition of a climatic zone,  $f_{oc}$  is calculated as follows:

$$f_{oc_i} = fraction_{grass_i} \cdot f_{oc_{grass}} + fraction_{dec_i} \cdot f_{oc_{dec}} + fraction_{con_i} \cdot f_{oc_{con}}$$

| Parameter            | Description  | Numeric value | Reference                  |
|----------------------|--|---------------|----------------------------|
| $f_{oc_i}$           | fraction of organic matter in vegetation-covered soil in climatic zone i |               |                            |
| $f_{oc_{grass}}$     | fraction of organic matter in grass covered soil                         | 0.19          | <i>Meijer et al., 2002</i> |
| $f_{oc_{dec}}$       | fraction of organic matter in deciduous forest covered soil              | 0.71          |                            |
| $f_{oc_{con}}$       | fraction of organic matter in coniferous forest covered soil             | 0.55          |                            |
| $fraction_{grass_i}$ | fraction of grass of total vegetation in climatic zone i                 | variable      |                            |
| $fraction_{dec_i}$   | fraction of deciduous forest of total vegetation in climatic zone i      | variable      |                            |
| $fraction_{con_i}$   | fraction of coniferous forest of total vegetation in climatic zone i     | variable      |                            |

### *Diffusion from baresoil and vegetation-covered soil to the atmosphere*

$$\frac{dC_{gas}}{dt} = \frac{K_h}{regc \cdot \rho_{oom} \cdot f_{oc} \cdot K_{ow}} \cdot \left( \frac{1 - \frac{tsp}{\rho_{part}} + k_{partair} \cdot \rho_{part} \cdot \frac{tsp}{\rho_{part}}}{1 - frac_{airsoil} - frac_{wsoil} + frac_{airsoil} \cdot \frac{K_h}{regc \cdot \rho_{oom} \cdot f_{oc} \cdot K_{ow}} \cdot \frac{frac_{wsoil}}{regc \cdot \rho_{oom} \cdot f_{oc} \cdot K_{ow}}} \right)^{-1} \cdot \left[ \frac{1}{v_{gasS}} + \frac{1}{vG + \frac{vL}{K_h} + \frac{vS}{\frac{K_h}{regc \cdot \rho_{oom} \cdot f_{oc} \cdot K_{ow}}}} \right] \cdot \frac{A_i}{V_{gas}} \cdot C_{soil}$$

For explanation of the grey part in the formula see subsection 1.

| Parameter        | Description  | Numeric value  | Reference   |
|------------------|--|--|---|
| $C_{gas}$        | concentration of substance in gaseous phase  |  |   |
| $C_{soil}$       | concentration of substance in soil   |  |   |
| $regc$           | regression coefficient from equation $K_{oc} = regc K_{ow}$ , where $K_{oc}$ is the partitioning coefficient of organic carbon and water | 0.35 L/kg  | <i>Seth et al.</i> , 1999   |
| $\rho_{oom}$     | density of organic matter  | 2.5 kg/L   | <i>Seth et al.</i> , 1999   |
| $tsp$            | total suspended particles  | $86 \cdot 10^{-6} \text{ g/m}^3$   | Bennett et al., 2001, only mentioned  |
| $\rho_{opart}$   | density of aerosols  | $2 \cdot 10^6 \text{ g/m}^3$   | <a href="http://www.mpi-hd.mpg.de/dustgroup/~graps/earth/properties.html">http://www.mpi-hd.mpg.de/dustgroup/~graps/earth/properties.html</a> |
| $k_{partair}$    | $k_{partair} = 0.55 \lg(K_{ow}/K_h) - 2.23$ (compare with 1)   | in $\text{m}^3/\text{g}$   | <i>Finizio et al.</i> , 1997  |
| $frac_{airsoil}$ | part of air in soil  | 0.2  | <i>Scheringer</i> , 1996  |
| $frac_{wsoil}$   | part of water in soil  | 0.3  | <i>Scheringer</i> , 1996  |
| $f_{oc}$         | fraction of organic matter in soil: different for different types of soil.   | baresoil: 0.02<br>vegetation-covered soil: variable, calculation see subsection 1    | assumed   |
| $A_i$            | Area, i = baresoil, vegetation-covered soil  | variable   |   |
| $V_{gas}$        | volume of gaseous phase  | variable   |   |
| $K_h$            | Henry's law constant   | depending on substance compare substance property sheets, See Chapter 3 and Annex B. |   |
| $K_{ow}$         | octanol/water partitioning coefficient   |  |   |

## G-CIEMS

Typical formulation as that uses two thin-film theory of intermedia diffusion, with restricted diffusion for soil-side mass transfer. Air-side mass transfer coefficient is calculated as the ratio of molecular diffusivity and diffusion path length for air and the thickness of assumed air-side stagnant layer. Soil-side mass transfer coefficient is calculated by molecular diffusivity and effective diffusion path length for cavity air in soil, which is calculated by Millington-Quirk equation.

$$B_{ae} = B_a \cdot v_a^{10/3} / (v_a + v_w)^2$$

Where  $B_{ae}$  is effective diffusivity,  $B_a$  is molecular diffusivity in air,  $v_a$  is volumetric air content in soil,  $v_w$  is volumetric water content in soil. Effective mass transfer for soil side is calculated by combining this effective diffusivity with diffusion path length in soil. Total diffusive exchange process is calculated by combining effective mass transfer process in soil and normal mass transfer process in air-side.

Bulk soil compartment is assumed to be in equilibrium for chemical among soil organic matter, cavity air and cavity water. Soil concentration in our model is calculated as theoretical dry-base concentration assuming all content in bulk soil matrix is concentrated onto dry soil particles.

## DEHM-POP

The air/soil gas exchange,  $F_{exc,s}$  is given by:

$$F_{exc,s} = v_e (C_a / \rho_a - C_s / H_{s/a}),$$

where  $v_e$  is the exchange velocity,  $C_a$  is the concentration in the lowermost atmospheric layer,  $C_s$  is the concentration in the soil,  $\rho_a$  is the density of air at the measured height, and  $H_{s/a}$  is the partitioning coefficient between soil and soil air.  $v_e$  is given by:

$$v_e = \frac{D_G^{air} a^{10/3} (1-l-a)^{-2} + D_L^{water} l^{10/3} (1-l-a)^{-2} H_{w/a}}{0.5 z_s},$$

where  $D_G^{air}$  is the air diffusion coefficient,  $D_L^{water}$  is the liquid diffusion coefficient,  $l$  and  $a$  is the water and air fractions in soil respectively,  $z_s$  is the soil depth, and  $H_{w/a}$  is the dimensionless Henry law constant [*Strand and Hov*, 1996].

The partitioning between the soil air and the soil itself is given by:

$$H_{s/a} = \rho_b f_{OC} K_{OC} H_{w/a} + H_{w/a} + a,$$

where  $\rho_b$  is the density,  $f_{OC}$  is the organic carbon fraction, and  $K_{OC}$  is the organic carbon partitioning coefficient [Strand and Hov, 1996].  $K_{OC}$  is calculated as:  $K_{OC} = 0.41 \cdot K_{OW}$  [Mackay, 1999], where  $K_{OW}$  is the temperature dependent octanol-water partitioning coefficient given by:

$$K_{OW}(T) = K_{OW}(T_{ref}) \exp\left(\frac{\Delta U_{OW}}{R}\right) \left(\frac{1}{T_{ref}} - \frac{1}{T}\right),$$

where  $T$  is the temperature,  $T_{ref}$  is the reference temperature  $T_{ref} = 298.15$  K,  $R$  is the molar gas constant ( $R = 8.314$  J/mol K), and  $\Delta U_{OW}$  is the energy of the phase transfer from octanol to water [Beyer et al., 2002].

Values used for the three modelled PCB congeners are [Beyer et al., 2002]:

$$\text{PCB 153: } K_{OW}(T_{ref}) = 5.62 \cdot 10^6 \quad \Delta U_{OW} = -17.5 \times 10^3 \text{ J/mol}$$

$$\text{PCB 28: } K_{OW}(T_{ref}) = 5.13 \cdot 10^5 \quad \Delta U_{OW} = -18.4 \times 10^3 \text{ J/mol}$$

$$\text{PCB 180: } K_{OW}(T_{ref}) = 1.54 \cdot 10^7 \quad \Delta U_{OW} = -8.27 \times 10^3 \text{ J/mol}$$

The water air partitioning coefficient (the dimensionless Henry's law coefficient) is assumed temperature dependent and is given by:

$$H_{w/a} = \exp\left(-\frac{\Delta H_H}{RT} + \frac{\Delta S_H}{R}\right),$$

where  $T$  is the temperature,  $R$  is the molar gas constant,  $\Delta H_H$  is the enthalpy (the slope when  $H_{w/a}$  is plotted against  $1/T$ ) and  $\Delta S_H$  is the entropy of the phase change from the dissolved phase to the gas phase (the intercept when  $H_{w/a}$  is plotted against  $1/T$ ) [Bamford et al., 2000].  $\Delta H_H$  and  $\Delta S_H$  are determined from laboratory experiments.

Values used for the three modelled PCB congeners are [Bamford et al., 2000]:

$$\text{PCB 153: } \Delta H_H = 66.1 \times 10^3 \text{ J/mol and } \Delta S_H = 190 \text{ J/(mol K)}$$

$$\text{PCB 28: } \Delta H_H = 32.5 \times 10^3 \text{ J/mol and } \Delta S_H = 74 \text{ J/(mol K)}$$

$$\text{PCB 180: } \Delta H_H = 143.6 \times 10^3 \text{ J/mol and } \Delta S_H = 447 \text{ J/(mol K)}$$

The soil concentrations assuming equilibrium in the modelling experiments are found by setting the flux equal to zero and isolating:

$$F_{exc,s} = v_e(C_a / \rho_a - C_s / H_{s/a}) = 0 \Rightarrow (C_a / \rho_a - C_s / H_{s/a}) = 0 \Rightarrow C_s = C_a H_{s/a} / \rho_a.$$

## SimpleBox

cited from [Brandes et al., 1996]

Values for the overall mass transfer coefficients for gas absorption and volatilization may be estimated using the classical two-film resistance model. In the case of transport across the air-soil interface, the soil-side of the interface is treated as a pair of parallel resistances (air phase and water phase of the soil). The following equations may be used:

$$GASABS_{soil[S]} = \frac{kasl_{air[S]} \cdot kasl_{soilair[S]} + kasl_{air[S]} \cdot kasl_{soilwater[S]} / K_{air-water[S]}}{kasl_{air[S]} + kasl_{soilair[S]} + kasl_{soilwater[S]} / K_{air-water[S]}} - (1 - FRass_{aerosol[S]})$$

with  $GASABS_{soil[S]}$  - overall mass transfer coefficient for gas absorption across the air-soil interface, referenced to air at scale S [ $m_{air} \cdot s^{-1}$ ] (D);

$kasl_{air[S]}$  - partial mass transfer coefficient at the air-side of the air-soil interface at scale S [ $m_{air} \cdot s^{-1}$ ] (A);

- $kasl_{soilair[S]}$  - partial mass transfer coefficient at the soilair-side of the air-soil interface at scale S [ $m_{air} \cdot s^{-1}$ ] (A);
- $kasl_{soilwater[S]}$  - partial mass transfer coefficient at the soilwater-side of the air-soil interface at scale S [ $m_{water} \cdot s^{-1}$ ] (A);
- $K_{air-water[S]}$  - air-water equilibrium distribution constant at scale S [ $m_{water}^3 \cdot m_{air}^{-3}$ ] (A);
- $FRass_{aerosol[S]}$  - fraction of the chemical in air that is associated with aerosol particles at scale S [-] (A).

And, since the quotient of the mass transfer coefficients for gas absorption and volatilization is equal to the volume-based intermedia partition coefficient:

$$VOLAT_{soil\ i[S]} = \frac{GASABS_{soil\ i[S]} \cdot K_{air-water[S]}}{1 - FRass_{aerosol[S]} \cdot K_{soil\ i-water[S]}}$$

- with  $VOLAT_{soil\ i[S]}$  - overall mass transfer coefficient for volatilization across the air-soil interface, referenced to soil at scale S [ $m_{soil} \cdot s^{-1}$ ] (D);
- $GASABS_{soil\ i[S]}$  - overall mass transfer coefficient for gas absorption across the air-soil interface, referenced to air at scale S [ $m_{air} \cdot s^{-1}$ ] (D);
- $FRass_{aerosol[S]}$  - fraction of the chemical in air that is associated with aerosol particles at scale S [-] (A);
- $K_{air-water[S]}$  - air-water equilibrium distribution constant at scale S [ $m_{water}^3 \cdot m_{air}^{-3}$ ] (A);
- $K_{soil\ i-water[S]}$  - soil i-water equilibrium distribution constant at scale S [ $m_{water}^3 \cdot m_{soil}^{-3}$ ] (A);

The partial mass transfer coefficients at the air-soil interface may be derived using the reasoning suggested by Mackay *et al.* [1992].

According to this reasoning, the value for the air side may be taken equal to the value at the air-water interface:

$$kasl_{air} = kaw_{air}$$

- with  $kasl_{air}$  - partial mass transfer coefficient at the air-side of the air-soil interface [ $m_{air} \cdot s^{-1}$ ] (A);
- $kaw_{air}$  - partial mass transfer coefficient at the air-side of the air-water interface [ $m_{air} \cdot s^{-1}$ ] (A).

Mass transfer in the soil air phase is treated as molecular diffusion in the gas phase of a porous solid medium, characterized by an effective diffusivity of  $10^{-3} m^2 \cdot hr^{-1}$  and a diffusion path length of 5 cm. This leads to:

$$kasl_{soilair} = 5.56 \cdot 10^{-6} m / s^{-1}$$

- with  $kasl_{soilair}$  - partial mass transfer coefficient at the soilair-side of the air-soil interface [ $m_{air} \cdot s^{-1}$ ] (A).

Mass transfer in the soil water phase is similarly treated as molecular diffusion in the water phase of a porous solid medium, characterized by an effective diffusivity of  $10^{-7} m^2 \cdot hr^{-1}$  and a diffusion path length of 2 cm, leading to:

$$kasl_{soilwater} = 5.56 \cdot 10^{-10} m \cdot s^{-1}$$

- with  $kasl_{soilwater}$  - partial mass transfer coefficient at the soilwater-side of the air-soil interface [ $m_{water} \cdot s^{-1}$ ] (A).

## CAM/POPs

The exchange process depends on the balance between two transfer processes: the chemical transfer between deep soil layers and surface soil, and the exchange of the chemical vapour between the soil surface and the atmosphere.

PCBs move through the soil by advective diffusion. Quantitatively, it is given by Fick's Law. The rate of change of concentration of PCBs in the soil is simplified as:

$$\frac{\partial C_G}{\partial t} = D_{ES} \frac{\partial^2 C_G}{\partial z^2}$$

where  $C_G$  is the gaseous phase concentration in soil and  $D_{ES}$  ( $m^2/s$ ) is the effective diffusivity of the chemical in the soil matrix. The effective diffusivity will be written as a function of  $K_{SA}$  and  $K_{AW}$  assuming that the porosity is not equal to zero and the water body still contains soil particles. The expression may be simplified as:

$$D_{ES} = \frac{\left[ \left( \frac{a^{10/3}}{\phi^2} \right) \cdot D_{PCBair} + \left( \frac{\theta^{10/3}}{\phi^2} \right) \cdot \frac{D_{PCBwater}}{K_{AW}} \right]}{K_{SA} + a + \frac{\theta}{K_{AW}}}$$

where  $a$  is the volumetric air content ( $m^3$ air/ $m^3$ soil),  $\theta$  is the volumetric water content ( $m^3$ water/ $m^3$ soil), and  $\phi$  is the porosity (volume pore space/volume soil),  $D_{PCB,air}$  is the air-side POPs diffusion coefficients in the soil matrix,  $D_{PCB,water}$  is the water-side POPs diffusion coefficients in the soil matrix.

$D_{PCB,air}$  ( $cm^2/s \cdot 10^{-2}$ )

| Congener | T = 0 °C | T = 5 °C | T = 10 °C | T = 15 °C | T = 20 °C | T = 25 °C |
|----------|----------|----------|-----------|-----------|-----------|-----------|
| PCB153   | 4.12     | 4.26     | 4.39      | 4.53      | 4.67      | 4.81      |
| PCB180   | 3.99     | 4.12     | 4.25      | 4.38      | 4.52      | 4.65      |

$D_{PCB,water}$  ( $cm^2/s \cdot 10^{-6}$ )

| POPs   | T = 0 °C | T = 5 °C | T = 10 °C | T = 15 °C | T = 20 °C | T = 25 °C |
|--------|----------|----------|-----------|-----------|-----------|-----------|
| PCB153 | 2.55     | 3.00     | 3.50      | 4.05      | 4.65      | 5.30      |
| PCB180 | 2.45     | 2.89     | 3.36      | 3.89      | 4.47      | 5.10      |

$K_{sa}$  is the soil-air partition coefficient (volume air/volume soil).

$$K_{sa} = \frac{K_{sw}}{K_{aw}} = 0.411 \cdot f_{OC} \cdot \rho_b \cdot K_{oa} \quad \text{and, } \rho_b = \rho_{soil} \cdot (1 - \phi)$$

where  $\rho_b$  is the bulk soil density (in kg/L),  $\rho_{soil}$  is soil density (kg/L),  $f_{OC}$  is the mass fraction of organic carbon present in the particulate matter in soil (kg organic carbon /kg soil).

$K_{oa}$  is the octanol-air partition coefficient.

$$\log_{10} K_{oa} = a/T + b$$

$$a = -529 - 19.25 \log P \quad \text{and} \quad b = 8.2995 - 0.95 \log P$$

where  $T$  is temperature (K),  $P$  is vapour pressure, and  $a$  and  $b$  are parameters depended on vapour pressure of POPs.

## MSCE-POP

**Partitioning.** The scheme of exchange processes used in the model is displayed in Fig.C1.

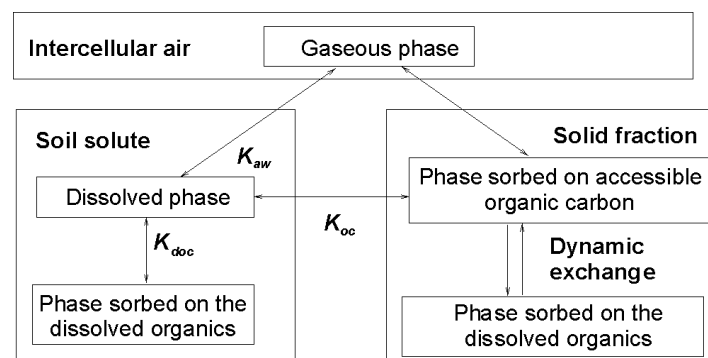


Fig.C1. Scheme of POP processes in soil used in MSCE-POP model

The total volume concentration in soil  $C$  is expressed as the sum of the concentration  $C^0$  of a pollutant in gaseous, dissolved, sorbed on dissolved organics, and sorbed on accessible part of solid soil fraction phases and concentration  $C^1$  of a pollutant sorbed on deep (potentially accessible) soil solid matter. It is supposed that all phases except for that sorbed on potentially accessible soil solids are in the instantaneous equilibrium with one another. Following [Jacobs and van Pul, 1996], the concentration  $C^0$ ,  $\text{ng/m}^3$  is then expressed via mass concentration  $C_s$  of a pollutant absorbed by the soil matter,  $\text{ng/kg}$ , volume concentration  $C_d$  of a pollutant dissolved in the soil water,  $\text{ng/m}^3$ , volume concentration  $C_{doc}$  of a pollutant sorbed on the dissolved organics,  $\text{ng/m}^3$ , and gas-phase volume concentration  $C_g$  of a pollutant in the soil air,  $\text{ng/m}^3$ :

$$C_T = \rho_s C_s + \alpha_w (C_d + C_{doc}) + \alpha_a C_g,$$

where  $\rho_s = 1350$  - bulk density of solid soil material,  $\text{kg/m}^3$ ;

$\alpha_w = 0.3$  - volumetric water content of the soil;

$\alpha_a = 0.2$  - volumetric air content of the soil.

The concentration in each phase may be represented by  $C^0$  using soil partitioning coefficients  $R_s$ ,  $R_d$  and  $R_g$ :

$$C = R_s C^s = R_d C^d = R_g C^g,$$

where  $R_d = \alpha_w + (\rho_s f_{oc} K_{oc} + \alpha_a K_H) / (1 + c_{doc} K_{doc})$ ;

$$R_s = R_d (1 + c_{doc} K_{doc}) / (f_{oc} K_{oc});$$

$$R_g = R_d (1 + c_{doc} K_{doc}) / K_H;$$

$f_{oc}$  is the fraction of organic carbon in soil;

$K_H$  is the dimensionless Henry's law constant (see above),

$K_{oc}$  is the organic carbon distribution coefficient;

$K_{doc}$  is dissolved organic carbon/water partitioning coefficient.

The other two partitioning coefficients are calculated via the octanol/water partitioning coefficient  $K_{ow}$  of a pollutant in question by the following regression equations:

$$K_{oc} = 0.41 \cdot K_{ow}$$

[Karikhoff, 1981], and

$$\log K_{doc} = 0.98 \log K_{ow} - 0.39 \quad \text{for PAHs}$$

$$\log K_{doc} = 0.93 \log K_{ow} - 0.54 \quad \text{for PCBs}$$

[J.Poershman and F.D.Kopinke, 2001]. The latter relation obtained for a number of POPs with wide range of  $K_{ow}$  can be also used for other POPs (PCDD/Fs, HCB,  $\gamma$ -HCH) [Vasilieva and Shatalov, 2002].

The exchange of a POP between easily accessible and potentially accessible OC fractions is assumed to be a process of first order:

$$\frac{dC^0}{dt} = k(C^1 - C^0)$$

$$\frac{dC^1}{dt} = k(C^0 - C^1)$$

with mass transfer coefficient  $k$  chosen in such a way that the characteristic time for the exchange process equals 1 year. The fraction  $f_{acc}$  of easily accessible fraction was assumed to be 30%.

**Vertical transport.** The migration of a pollutant over the vertical profile in soil is assumed to be due to diffusion and transport with convective water flux  $J_w$ . The corresponding equation is:

$$\frac{\partial C}{\partial t} + \frac{J_w}{R_d} \frac{\partial C}{\partial z} = D_E \frac{\partial^2 C}{\partial z^2} - k_{soil} C$$

where  $D_E$  is the effective gas-liquid diffusion coefficient,  $m^2/s$ ,  
 $k_{soil}$  is the degradation rate constant for soil,  $s^{-1}$ .

The coefficient  $D_E$  is determined by the following equation:

$$D_E = \frac{\xi_g D_g}{R_g} + \frac{\xi_l D_l}{R_d} + D_b,$$

where  $D_g, D_l$  are the molecular diffusion coefficient for gas and liquid;

$\xi_g = a^{10/3} / \phi^2$ ,  $\xi_l = \theta^{10/3} / \phi^2$  are gas and liquid tortuosity factors;

$\phi$  is the porosity of soil (assumed  $\phi = 0.5$ );

$D_b$  is effective diffusion coefficient due to bioturbation (assumed  $D_b = 6 \cdot 10^{-12}$ , [McLachlan et al., 2002]).

Liquid flux  $J_w$  is supposed to be equal to precipitation intensity  $h_p$ ,  $m/c$  during rain events and has opposite direction (upward) for certain period after rain events. This period is chosen to be 5 days as model assumption. Preliminary estimations show low model sensitivity to this parameter. The value of the upward flux is chosen in such a way that 60% of precipitation amount is evaporated to the atmosphere (evaluated on the basis of data from [Atmosphere Handbook, 1991]).

**Gaseous exchange with the atmosphere.** The gaseous exchange between soil and the atmosphere is parameterized using resistance analogy.

The gaseous flux of POP from the atmosphere into the soil is driven by the difference between atmospheric gas concentration  $C_a^g$  at the air reference level ( $z_a$  - equal to half of the height of the lower atmospheric layer) and the soil gas-phase concentration  $C_s^g$  at the soil reference level at depth  $z_s = \Delta z_1/2$  ( $\Delta z_1$  - is the upper soil layer thickness). In the course of pollutant transport from the air reference level to the soil reference level it overcomes three resistances (see Fig. C.2).

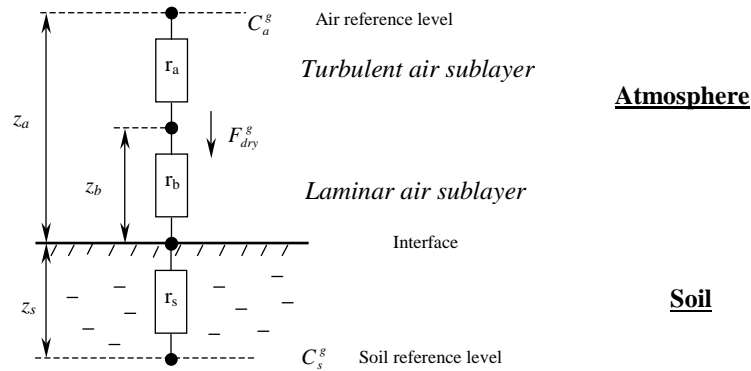


**Fig. A2.** Resistance scheme used for the description of gaseous exchange between soil and the atmosphere

- Turbulent air sublayer resistance  $r_a$ ,  $s/m$  that is the resistance to transporting through turbulent air sublayer (from  $z_a$  to  $z_b$ . The latter is laminar sublayer height);
- Laminar surface air sublayer resistance  $r_b$ ,  $s/m$  that is the resistance to transporting through laminar surface air sublayer ( $z_b$ ) to the interface;
- Surface soil resistance  $r_s$ ,  $s/m$  that is the resistance to transporting from surface soil interface to the soil reference level ( $z_s$ ).

Hence, the formula for atmosphere/soil flux is:

$$F_{dry}^g = \frac{C_a^g - C_s^g}{r_a + r_b + r_s},$$

where  $r_a$  is atmospheric resistance, and:

$$C_s^g = \frac{C(z_1) (2D_E / \Delta z_1 - qJ_w / R_d)}{R_g (2D_E / \Delta z_1 + pJ_w / R_d)}$$

$$r_s = \frac{1}{R_g (2D_E / \Delta z_1 + pJ_w / R_d)}$$

$$r_b = \frac{2}{\kappa U_*} \left( \frac{Sc}{Pr} \right)^{2/3}$$

where Pr = 0.71 - Prandtl number;

Sc =  $n/D_a$  - Schmidt number;

$n = 1.5 \cdot 10^{-5}$  - kinematic viscosity of air, m<sup>2</sup>/s;

$D_a$  - the molecular diffusion coefficient of the pollutant in air, m<sup>2</sup>/s;

$D_E$  - the molecular diffusion coefficient of the pollutant in air, m<sup>2</sup>/s;

$J_w$  - the convective water flux equal to mean annual precipitation intensity, m/c;

$R_d$  - the soil partitioning coefficient, see 2.16 above, dimensionless;

$u_*$  - the friction velocity, m/s;

$p = 1$  and  $q = 0$  for downward water flux and  $p = 0$  and  $q = 1$  for upward water flux.

## C.5. Gaseous exchange between atmosphere and seawater

### EVN-BETR and UK-MODEL

#### Air-Water Diffusion

$$D = \text{Sea Area} / \left[ \left( 1 / (MTC_{\text{air}} \cdot Z_{\text{air}}) \right) + \left( 1 / (MTC_{\text{sea}} \cdot 0.8 \cdot Z_{\text{water}}) \right) \right]$$

where Average Seawater depth = 87.5 m;

Sea Area =  $5.63 \cdot 10^{12}$  m<sup>2</sup>;

$MTC_{\text{air}}$  - air side air-sea transport velocity = 30 m/h;

$MTC_{\text{sea}}$  - sea side air-sea transport velocity = 0.03 m/h.

#### Rain Dissolution to Water

$$D = \text{Sea Area} \cdot \text{Rain Rate} \cdot Z_{\text{water}}$$

### CliMoChem

cited from [Scheringer et al., 2003]

#### Diffusion from atmosphere to seawater

$$\frac{dC_{\text{gas}}}{dt} = -(1 - \text{Phi}) \cdot \left( \frac{V_{\text{gasW}} \cdot V_{\text{water}}}{K_h \cdot V_{\text{gasW}} + V_{\text{water}}} \right) \frac{A_{\text{water}}}{V_{\text{gas}}} \cdot C_{\text{gas}}$$

| Parameter          | Description   | Numeric value   | Reference                 |
|--------------------|---|---|---------------------------|
| $C_{\text{gas}}$   | concentration of substance in gaseous phase                         |   |                           |
| $\text{Phi}$       | particle-bound fraction of substance (see C.1)                      | between 0-1   |                           |
| $V_{\text{gasW}}$  | transfer velocity on the interface atmosphere-water: air over water | 72 m/d  | Mackay and Paterson, 1991 |
| $V_{\text{water}}$ | transfer velocity on the interface atmosphere-water: in water       | 0.72 m/d  |                           |
| $A_{\text{water}}$ | Area of water   | variable  |                           |
| $V_{\text{gas}}$   | Volume of gaseous phase   | variable  |                           |
| $K_h$              | Henry's law constant  | depending on substance<br>compare substance<br>property sheets, See<br>Chapter 3 and Annex B. |                           |

## Diffusion from seawater to atmosphere

$$\frac{dC_{\text{gas}}}{dt} = (1 - \text{Phisusp}w) \cdot \left( \frac{\left(1 - \frac{tsp}{\rho_{\text{part}}}\right) \cdot \frac{1}{R \cdot T} + \frac{tsp}{\rho_{\text{part}}} \cdot k_{\text{partair}} \cdot \rho_{\text{part}} \cdot \frac{1}{R \cdot T}}{\left(1 - \text{sea}_{\text{part}}\right) \cdot \frac{1}{K_{\text{hmin}} \cdot R \cdot T_w} + \text{sea}_{\text{part}} \cdot \frac{1}{K_{\text{hmin}} \cdot R \cdot T_w} \cdot \text{fossusp} \cdot \text{regc} \cdot \rho_{\text{oom}} \cdot K_{\text{owmin}}}} \right) \cdot \left( \frac{v_{\text{gasW}} \cdot v_{\text{water}}}{K_h \cdot v_{\text{gasW}} \cdot v_{\text{water}}} \right) \cdot \frac{A_{\text{water}}}{V_{\text{gas}}} \cdot C_{\text{water}}$$

| Parameter                  | Description  | Numeric value  | Reference   |
|----------------------------|--|--|---|
| $C_{\text{gas}}$           | concentration of substance in gaseous phase  |  |   |
| $\text{Phisusp}w$          | waterparticle-bound fraction of substance  | calculation see below  |   |
| $tsp$                      | total suspended particles (in gaseous phase)   | $86 \cdot 10^{-6} \text{ g/m}^3$   | <i>Bennett et al.</i> , 2001, only mentioned  |
| $\rho_{\text{part}}$       | density of aerosols  | $2 \cdot 10^6 \text{ g/m}^3$   | <a href="http://www.mpi-hd.mpg.de/dustgroup/~graps/earth/properties.html">http://www.mpi-hd.mpg.de/dustgroup/~graps/earth/properties.html</a> |
| $R$                        | universal gas constant   | 8.3145 J/mol·K   |   |
| $T$                        | Temperature  | variable   |   |
| $k_{\text{partair}}$       | $k_{\text{partair}} = 0.55 \lg(K_{\text{ow}}/K_h) - 2.23$ (compare with 1)   | in $\text{m}^3/\text{g}$   | <i>Finizio et al.</i> , 1997  |
| $T_w$                      | Temperature  | variable, minimum at 270 K   |   |
| $\text{fossusp}$           | global mean organic part of sea particles  | 0.3  | <i>Wania and Mackay</i> , 1995  |
| $\text{regc}$              | regression coefficient from equation $K_{\text{oc}} = \text{regc} K_{\text{ow}}$ , where $K_{\text{oc}}$ is the Partitioning coefficient of organic carbon and water | 0.35 L/kg  | <i>Seth et al.</i> , 1999   |
| $\rho_{\text{oom}}$        | density of organic matter  | 2.5 kg/L   | <i>Seth et al.</i> , 1999   |
| $\text{sea}_{\text{part}}$ | volumefraction of particles in seawater  | $5 \cdot 10^{-8}$ for latitudes 90-81 degrees<br>$10^{-7}$ for latitudes 81-72 degrees<br>$5 \cdot 10^{-7}$ for latitudes 72-0 degrees | <i>Wania and Mackay</i> , 1995  |
| $v_{\text{gasW}}$          | transfer velocity on the interface atmosphere-water: air over water  | 72 m/d   | <i>Mackay and Paterson</i> , 1991   |
| $v_{\text{water}}$         | transfer velocity on the interface atmosphere-water: in water  | 0.72 m/d   |   |
| $A_{\text{water}}$         | Area of water  | variable   |   |
| $V_{\text{gas}}$           | Volume of gaseous phase  | variable   |   |
| $K_{\text{owmin}}$         | Octanol/water partitioning coefficient, where $T_w$ is used for calculation of temperature dependence  | depending on substance compare substance property sheets, See Chapter 3 and Annex B.   |   |
| $K_{\text{hmin}}$          | Henry's law constant, where $T_w$ is used for calculation of temperature dependence  |  |   |
| $K_h$                      | Henry's law constant   |  |   |

Calculation of  $\text{Phisusp}w$

$$\text{Phisusp}w = \frac{\text{fossusp} \cdot \text{regc} \cdot \rho_{\text{oom}} \cdot K_{\text{ow}} \cdot \text{seapart}}{(1 + \text{fossusp} \cdot \text{regc} \cdot \rho_{\text{oom}} \cdot K_{\text{ow}} \cdot \text{seapart})}$$

| Parameter                  | Description  | Numeric Value  | Reference                      |
|----------------------------|--|--|--------------------------------|
| $\text{Phisusp}w$          | waterparticle-bound fraction of substance  |  |                                |
| $\text{fossusp}$           | global mean organic part of sea particles  | 0.3  | <i>Wania and Mackay</i> , 1995 |
| $\text{regc}$              | regression coefficient from equation $K_{\text{oc}} = \text{regc} K_{\text{ow}}$ , where $K_{\text{oc}}$ is the partitioning coefficient of organic carbon and water | 0.35 L/kg  | <i>Seth et al.</i> , 1999      |
| $\rho_{\text{oom}}$        | density of organic matter  | 2.5 kg/L   | <i>Seth et al.</i> , 1999      |
| $\text{sea}_{\text{part}}$ | volumefraction of particles in seawater  | $5 \cdot 10^{-8}$ for latitudes 90-81 degrees<br>$10^{-7}$ for latitudes 81-72 degrees<br>$5 \cdot 10^{-7}$ for latitudes 72-0 degrees | <i>Wania and Mackay</i> , 1995 |
| $K_{\text{ow}}$            | Octanol/water partitioning coefficient   | depending on substance, compare substance property sheets, See Chapter 3 and Annex B.  |                                |

## G-CIEMS

Typical formulation as that uses two thin-film theory of intermedia diffusion. Air-side and water-side mass transfer coefficient are calculated as the ratio of molecular diffusivity and diffusion path length for air and water. Same molecular diffusivity and diffusion path length are assumed on all water surfaces.

(Note: Gaseous fluxes using diffusive transportation module in our model is applied to the data in the Input data table in this calculation.)

## DEHM-POP

The gaseous exchange between atmosphere and water is determined by a similar expression as for the gaseous exchange between atmosphere and soil:

$$F_{exc,o} = v_e(C_a - C_o / H_{w/a}),$$

where  $v_e$  is the exchange velocity,  $C_a$  is the concentration in the lowermost atmospheric layer,  $C_o$  is the concentration in the ocean, and  $H_{w/a}$  is the partitioning coefficient between water and air (the dimensionless Henry's law constant). The exchange velocity is dependent on the wind speed and it is derived using the two-film layer resistance method.

## SimpleBox

cited from [Brandes et al., 1996]

Values for the overall mass transfer coefficients for gas absorption and volatilization may be estimated using the classical two-film resistance model. In the case of transport across the air-water interface, the overall transfer coefficients follow from summation of the resistances at the water- and air sides of the interface. The following equations may be used:

$$GASABS_{water\ i[S]} = \frac{kaw_{air[S]} \cdot kaw_{water[S]}}{kaw_{air[S]} \cdot K_{air-water[S]} + kaw_{water[S]}} \cdot (1 - FRass_{aerosol[S]})$$

- with
- $GASABS_{water\ i[S]}$  - overall mass transfer coefficient for gas absorption across the air-water interface, referenced to air at scale S [ $m_{air} \cdot s^{-1}$ ] (D);
  - $kaw_{air[S]}$  - partial mass transfer coefficient at the air-side of the air-water interface at scale S [ $m_{air} \cdot s^{-1}$ ] (A);
  - $kaw_{water[S]}$  - partial mass transfer coefficient at the water-side of the air-water interface at scale S [ $m_{water} \cdot s^{-1}$ ] (A);
  - $K_{air-water[S]}$  - air-water equilibrium distribution constant at scale S [ $m_{water}^3 \cdot m_{air}^{-3}$ ] (A);
  - $FRass_{aerosol[S]}$  - fraction of the chemical in air that is associated with aerosol particles at scale S [-] (A).

And, since the quotient of the mass transfer coefficients for gas absorption and volatilization is equal to the volume-based intermedia partition coefficient:

$$VOLAT_{water\ i[S]} = \frac{GASABS_{water\ i[S]} \cdot K_{air-water[S]} \cdot FRdisslvd_{water\ i[S]}}{1 - FRass_{aerosol[S]}}$$

- with
- $VOLAT_{water\ i[S]}$  - overall mass transfer coefficient for volatilization across the air-water interface, referenced to water at scale S (D);
  - $GASABS_{water\ i[S]}$  - overall mass transfer coefficient for gas absorption across the air-water interface, referenced to air at scale S [ $m_{air} \cdot s^{-1}$ ] (D);
  - $FRass_{aerosol[S]}$  - fraction of the chemical in air that is associated with aerosol particles at scale S [-] (A);
  - $K_{air-water[S]}$  - air-water equilibrium distribution constant at scale S [ $m_{water}^3 \cdot m_{air}^{-3}$ ] (A);
  - $FRdisslvd_{water(i)[S]}$  - dissolved fraction of water column  $i$  at scale S [-] (A).

A value for the partial mass transfer coefficient at the air-side of the air-water interface may be derived from the equation [Schwarzenbach et al., 1993]:

$$kaw_{air} = 0.01 \cdot (0.3 + 0.2 \cdot WINDSPEED_{[S]}) \cdot \left( \frac{0.018}{MOL\ WEIGHT} \right)^{0.4355}$$

- with  $kaw_{air}$  - partial mass transfer coefficient at the air side of the air-water interface [ $m_{air} \cdot s^{-1}$ ] (A);

$WINDSPEED_{[S]}$  - average windspeed at 10 m above the surface at scale S [ $m \cdot s^{-1}$ ] (A);  
 $MOL\ WEIGHT$ : - molecular weight of the chemical [ $kg \cdot mol^{-1}$ ] (A);  
 0.018 - molecular weight of water (C).

For the partial mass transfer coefficient at the water side of the air-water interface, the equation of [Schwarzenbach *et al.*, 1993] may be used:

$$k_{aw_{water}} = 0.01 \cdot (0.004 + 0.00004 \cdot WINDSPEED_{[S]}) \cdot \left( \frac{0.032}{MOLWEIGHT} \right)^{0.4047}$$

with  $k_{aw_{water}}$  - partial mass transfer coefficient at the water-side of the air-water interface [ $m_{water} \cdot s^{-1}$ ] (A);  
 $WINDSPEED_{[S]}$  - average windspeed at 10 m above the surface at scale S [ $m \cdot s^{-1}$ ] (A);  
 $MOL\ WEIGHT$  - molecular weight of the chemical [ $kg \cdot mol^{-1}$ ] (A);

## CAM/POPs

The air concentration above water,  $C_G$ , can be solved as:

$$C_G(t) = C_W \cdot K_{AW} + (C_{GO} - C_W \cdot K_{AW}) \exp(-K_{TA} \cdot t / h)$$

where  $C_{GO}$  is the initial air concentration,  $C_W$  is the water concentration,  $h$  is the height (m),  $t$  is the time. The equation is used in air-water surface flux calculations.  $K_{AW}$  has been shown in the Section 3,  $K_{TA}$  overall air side mass transfer coefficient, (m/s).

$$K_{TA} = 1 / (1 / K_A + K_{AW} / K_W)$$

where  $K_A$  (air-side),  $K_W$  (water-side) are mass transfer velocity [Mackay *et al.*, 1983; Schwarzenbach *et al.*, 1993]:

$$K_A = 10^{-3} + 4.62 \cdot 10^{-4} \cdot (6.1 + 0.63 u_{10})^{0.5} u_{10} [SC_{pcb,air}]^{0.67} \quad (m/s)$$

$$K_W = [2.5 \cdot (0.5246 + 1.6256 \cdot 10^{-2} \cdot T + 4.9946 \cdot 10^{-4} \cdot T^2) + 0.3 u_{10}^2] \cdot (SC_{pcb,water} / 660)^{-1/2} \quad (cm/h)$$

where the temperature,  $T$ , is in  $^{\circ}C$ , and the surface wind velocity at reference height of 10m,  $u_{10}$ , is in m/s.  $SC_{pcb,air}$ ,  $SC_{pcb,water}$  are Schmidt numbers.

## MSCE-POP

For POP flux through the sea surface the following expression is used [Strukov, 2001].

$$F_z|_{z=0} = \alpha_1 (c_{ga} / K_{HR}(T) - c_d) ((1 - \alpha_2) D_{\mu} / \delta + \alpha_2 K_{HR} h_f),$$

where:  $\delta = \delta_0 \exp(-0.15 \cdot U_a)$ ,

$$\alpha_1 = 1.75 - 0.75 \exp(-0.18 \cdot U_a),$$

$$\alpha_2 = 1 - \exp(-0.01 \cdot U_a).$$

$c_{ga}$  and  $c_d$  - POP gas-phase and dissolved concentration in the surface atmosphere,  $ng/m^3$ ;

$K_{HR}(T)$  - Henry's law constant depending on temperature, dimensionless;

$D_{\mu} = 5.14 \cdot 10^{-10}$  - molecular diffusion coefficient in water,  $m^2/s$ ;

$\delta_0 = 4 \cdot 10^{-5}$  - surface molecular layer depth at zero wind speed, m;

$U_a$  - wind speed absolute value near the surface, m/s;

$h_f = 8 \cdot 10^{-3}$  - foam settling rate on the sea surface, m/s;

$\alpha_1$  - coefficient introduced for the description of surface sea area expansion due to wave disturbance;

$\alpha_2$  - describes the relative sea surface area covered with foam at strong wind.

More detailed description of these processes is given in [Strukov *et al.*, 2000].

## C.6. Gaseous exchange between atmosphere and vegetation

### EVN-BETR and UK-MODEL

#### *Air-Vegetation Diffusion*

The vegetation side vegetation-air transport velocity (Veg\_airMTC) is calculated according to Cousins et al. [2001].

$$D = 1/((1/(Veg\ Area \cdot Veg\_airMTC \cdot Z_{veg})) + (1/(Veg\ Area \cdot Air\_VegMTC \cdot Z_{air})))$$

where: Veg\_area - vegetation area =  $8.36 \cdot 10^{12} \text{ m}^2$ ;

Veg\_airMTC - vegetation side air-vegetation transport velocity = 10.8 m/h;

Air\_VegMTC - air side air-vegetation transport velocity = 9 m/h;

Z<sub>veg</sub> - fugacity capacity in vegetation = 462 mol/m<sup>3</sup> Pa.

#### *Air-Vegetation Rain Dissolution*

$$D = Veg\ Area \cdot Rain\ Rate \cdot Z_{air} \cdot Foliage\_rain$$

where Foliage\_rain - fraction of rain intercepted by foliage = 0.1.

### CliMoChem

cited from [Scheringer et al., 2003]

#### *Diffusion from atmosphere to vegetation*

$$\frac{dC_{gas}}{dt} = -(1 - Phi) \cdot v_{gasdiff} \cdot \frac{A_{veg}}{V_{gas}} \cdot C_{gas}$$

| Parameter     | Description   | Numeric value                         | Reference |
|---------------|---|---------------------------------------|-----------|
| $C_{gas}$     | concentration of substance in gaseous phase                         |                                       |           |
| $Phi$         | particle-bound fraction of the substance (see C.1)                  | between 0-1                           |           |
| $v_{gasdiff}$ | diffusion rate from atmosphere to vegetation                        | variable, depending on climatic zone* |           |
| $A_{veg}$     | Area of vegetation (identical with Area of vegetation-covered soil) | variable                              |           |
| $V_{gas}$     | Volume of gaseous phase   | variable                              |           |

\* - the model contains three types of vegetation. For each type, the diffusion rate ( $v_{gasdiff}$ ) is different (see table below). Depending on the composition of a climatic zone,  $v_{gasdiff}$  is calculated as follows:

$$v_{gasdiff}_i = fraction_{grass}_i \cdot v_{gasdiff}_{grass} + fraction_{dec}_i \cdot v_{gasdiff}_{dec} + fraction_{con}_i \cdot v_{gasdiff}_{con}$$

| Parameter             | Description  | Numeric value | Reference    |
|-----------------------|--|---------------|--------------|
| $v_{gasdiff}_i$       | deposition rate in climatic zone i                                   |               |              |
| $v_{gasdiff}_{grass}$ | deposition rate to grass   | 85.3 m/d      | Möller, 2002 |
| $v_{gasdiff}_{dec}$   | deposition rate to deciduous forest                                  | 2207.28 m/d   | Möller, 2002 |
| $v_{gasdiff}_{con}$   | deposition rate to coniferous forest                                 | 673.92 m/d    | Möller, 2002 |
| $fraction_{grass}_i$  | fraction of grass of total vegetation in climatic zone i             | variable      |              |
| $fraction_{dec}_i$    | fraction of deciduous forest of total vegetation in climatic zone i  | variable      |              |
| $fraction_{con}_i$    | fraction of coniferous forest of total vegetation in climatic zone i | variable      |              |

## Diffusion from vegetation to atmosphere

$$\frac{dC_{gas}}{dt} = \left( f_{lipid} \cdot \frac{K_{ow}}{K_h} \cdot \left( 1 - \frac{tsp}{\rho_{part}} + k_{partair} \cdot \rho_{part} \cdot \frac{tsp}{\rho_{part}} \right) \right)^{-1} \cdot v_{gasdiff} \cdot \frac{A_{veg}}{V_{gas}} \cdot C_{veg} \cdot vegvolfactor^2$$

| Parameter      | Description   | Numeric value   | Reference   |
|----------------|---|---|---|
| $C_{gas}$      | concentration of substance in gaseous phase                                       |   |   |
| $C_{veg}$      | concentration of substance in vegetation  |   |   |
| $f_{lipid}$    | fraction of lipids in vegetation  | variable, depending on climate zone <sup>a</sup>                                      |   |
| $tsp$          | totalsuspended particles  | $86 \cdot 10^{-6} \text{ g/m}^3$  | <i>Bennett et al., 2001</i> , only mentioned  |
| $\rho_{part}$  | density of aerosols   | $2 \cdot 10^6 \text{ g/m}^3$  | <a href="http://www.mpi-hd.mpg.de/dustgroup/~graps/earth/properties.html">http://www.mpi-hd.mpg.de/dustgroup/~graps/earth/properties.html</a> |
| $k_{partair}$  | $K_{partair} = 0.55 \lg(K_{ow}/K_h) - 2.23$ (compare with 1)                      |   | <i>Finizio et al., 1997</i>   |
| $v_{gasdiff}$  | diffusion rate from atmosphere to vegetation                                      | variable, depending on climatic zone <sup>b</sup>                                     |   |
| $A_{veg}$      | Area of vegetation (= Area of vegetation-covered soil)                            | variable  |   |
| $V_{gas}$      | Volume of gaseous phase   | variable  |   |
| $vegvolfactor$ | factor taking into account the different vegetation volumes for different seasons | variable, depending on the climatic zone and the season*                              |   |
| $K_{ow}$       | Octanol/water partitioning coefficient  | depending on substance, compare substance property sheets, See Chapter 3 and Annex B. |   |
| $K_h$          | Henry's law constant  |   |   |

\* - the model contains three types of vegetation. For each type, the fraction of lipid ( $f_{lipid}$ ) is different (see table below). Depending on the composition of a climatic zone,  $f_{lipid}$  is calculated as follows:

$$flipid_i = fractiongrass_i \cdot flipid_{grass} + fractiondec_i \cdot flipid_{dec} + fractioncon_i \cdot flipid_{con}$$

| Parameter         | Description  | Numeric value | Reference           |
|-------------------|--|---------------|---------------------|
| $flipid_i$        | fraction of lipids in vegetation in climatic zone i                  |               |                     |
| $flipid_{grass}$  | fraction of lipids in grass  | 0.02          | <i>Möller, 2002</i> |
| $flipid_{dec}$    | fraction of lipids in deciduous forest                               | 0.01          | <i>Möller, 2002</i> |
| $flipid_{con}$    | fraction of lipids in coniferous forest                              | 0.06          | <i>Möller, 2002</i> |
| $fractiongrass_i$ | fraction of grass of total vegetation in climatic zone i             | variable      |                     |
| $fractiondec_i$   | fraction of deciduous forest of total vegetation in climatic zone i  | variable      |                     |
| $fractioncon_i$   | fraction of coniferous forest of total vegetation in climatic zone i | variable      |                     |

<sup>b</sup> The model contains three types of vegetation. For each type, the diffusion rate ( $v_{gasdiff}$ ) is different (see table below). Depending on the composition of a climatic zone,  $v_{gasdiff}$  is calculated as follows:

$$v_{gasdiff}_i = fractiongrass_i \cdot v_{gasdiff}_{grass} + fractiondec_i \cdot v_{gasdiff}_{dec} + fractioncon_i \cdot v_{gasdiff}_{con}$$

| Parameter             | Description  | Numeric Value | Reference  |
|-----------------------|--|---------------|--|
| $v_{gasdiff}_i$       | deposition rate in climatic zone i                                   |               |  |
| $v_{gasdiff}_{grass}$ | deposition rate to grass   | 85.3 m/d      | <i>Horstmann and McLachlan, 1998; Möller, 2002</i> |
| $v_{gasdiff}_{dec}$   | deposition rate to deciduous forest                                  | 2207.28 m/d   |  |
| $v_{gasdiff}_{con}$   | deposition rate to coniferous forest                                 | 673.92 m/d    |  |
| $fractiongrass_i$     | fraction of grass of total vegetation in climatic zone i             | variable      |  |
| $fractiondec_i$       | fraction of deciduous forest of total vegetation in climatic zone i  | variable      |  |
| $fractioncon_i$       | fraction of coniferous forest of total vegetation in climatic zone i | variable      |  |

Because of increased stability of the atmosphere in the spring, fall and winterseason, the deposition rates  $v_{gasdiff}_{grass}$ ,  $v_{gasdiff}_{dec}$  and  $v_{gasdiff}_{con}$  are divided by 3 for the winterseason and by 2 for the spring and fall seasons [*Horstmann, and McLachlan, 1998*].

The winter value of the vegetation volume is set to 10% of the summer value, spring and fall values are interpolations between summer and winter value. The *vegvolfactor* is calculated weighing the volumes of the seasons with the spring volume (which is equal to the fall volume), resulting in the following values:

| season | <i>vegvolfactor</i> |
|--------|---------------------|
| spring | 1                   |
| summer | 1.82                |
| fall   | 1                   |
| winter | 0.182               |

Exception to this calculation is the coniferous vegetation volume which is the same for all the seasons, and the vegetation volume in the equator region which is assumed to be the same for all seasons.

Because the composition of vegetation varies for different climate zones, the *vegvolfactor* is weighed with the fractions of the respective vegetation types.

## G-CIEMS

Similar to air-soil processes, but different parameters values.

## DEHM-POP

Vegetation is not included in the model, and we have not made any calculations for this part of the inter-comparison.

## SimpleBox

cited from [Brandes et al., 1996]

Diffusive transport between air and vegetation by means of gas absorption and volatilization is described by:

$$\underline{DIFF_{air-veg\ i[S]} = XCH_{air-veg\ i[S]} \cdot C_{air[S]}}$$

with  $DIFF_{air-veg\ i[S]}$  - diffusive mass flow from air to vegetation *i* at scale *S* by gas absorption [ $\text{mol} \cdot \text{s}^{-1}$ ] (I);  
 $XCH_{air-veg\ i[S]}$  - transport coefficient for gas absorption by vegetation *i* at scale *S* [ $\text{m}_{air}^3 \cdot \text{s}^{-1}$ ] (I);  
 $C_{air[S]}$  total concentration in air (gas phase + aerosol phase + rain water phase) at scale *S* [ $\text{mol} \cdot \text{m}_{air}^{-3}$ ] (S).

$$\underline{XCH_{air-veg\ i[S]} = \text{GASABS}_{veg\ i[S]} \cdot \text{AREA}_{leaves\ i[S]}}$$

with  $XCH_{air-veg\ i[S]}$  - transport coefficient for gas absorption to vegetation *i* at scale *S* [ $\text{m}_{air}^3 \cdot \text{s}^{-1}$ ] (I);  
 $\text{GASABS}_{veg\ i[S]}$  - overall mass transfer coefficient for gas absorption across the air-vegetation interface, referenced to air at scale *S* [ $\text{m}_{air} \cdot \text{s}^{-1}$ ] (D);  
 $\text{AREA}_{leaves\ i[S]}$  - leaf surface area at scale *S* [-] (D).

$$\text{GASABS}_{veg\ i[S]} = (1 - \text{FRass}_{aerosol[S]}) \cdot g_{veg\ i[S]}$$

with  $\text{GASABS}_{veg\ i[S]}$  - overall mass transfer coefficient for gas absorption across the air-vegetation interface, referenced to air at scale *S* [ $\text{m}_{air} \cdot \text{s}^{-1}$ ] (D);  
 $\text{FRass}_{aerosol[S]}$  - fraction of the chemical in air that is associated with aerosol particles at scale *S* [-] (A);  
 $g_{veg\ i[S]}$  - conductance [ $\text{m} \cdot \text{s}^{-1}$ ] (D).

The conductance,  $g_{veg}$ , depends on the chemical properties, plant species and environmental conditions [Trapp and Matthies, 1995]:

$$\underline{g_{veg\ i[S]} = 0.001\ m \cdot s^{-1}}$$

with  $g_{veg\ i[S]}$  conductance [ $m \cdot s^{-1}$ ] (D)

may be taken as default value.

The volatilization mass flows are obtained from:

$$DIFF_{veg\ i-air[S]} = XCH_{veg\ i-air[S]} \cdot C_{veg\ i[S]}$$

with  $DIFF_{veg\ i-air[S]}$  - diffusive mass flow from vegetation i to air at scale S by volatilization [ $mol \cdot s^{-1}$ ] (I);  
 $XCH_{veg\ i-air[S]}$  - transport coefficient for volatilization from vegetation i at scale S [ $m_{veg}^3 \cdot s^{-1}$ ] (I);  
 $C_{veg\ i[S]}$  - dissolved concentration in vegetation i at scale S [ $mol \cdot m_{veg}^{-3}$ ] (S).

$$XCH_{veg\ i-air[S]} = VOLAT_{veg\ i[S]} \cdot AREA_{leaves\ i[S]}$$

with  $XCH_{veg\ i-air}$  - transport coefficient for volatilization from vegetation i at scale S [ $m_{veg}^3 \cdot s^{-1}$ ] (I);  
 $VOLAT_{veg\ i[S]}$  - overall mass transfer coefficient for volatilization across the vegetation-air interface, referenced to vegetation i at scale S [ $m_{water} \cdot s^{-1}$ ] (D);  
 $AREA_{leaves\ i[S]}$  - leaf surface area at scale S [-] (D).

$$VOLAT_{veg\ i[S]} = \frac{g_{veg\ i[S]}}{K_{leafi-air[S]}}$$

with  $VOLAT_{veg\ i[S]}$  - overall mass transfer coefficient for volatilization across the air-vegetation interface, referenced to vegetation at scale S [ $m_{air} \cdot s^{-1}$ ] (D);  
 $g_{veg\ i[S]}$  - conductance [ $m \cdot s^{-1}$ ] (D);  
 $K_{leafi-air[S]}$  - plant tissue-air partition coefficient at scale S [ $m^3 \cdot m^{-3}$ ] (A).

## CAM/POPs

Similar to air-soil processes.

## MSCE-POP

Three types of vegetation are distinguished in the model: coniferous forest, deciduous forest, and grass. Coefficients governing exchange processes between the atmosphere and vegetation are determined separately for each of the above vegetation types. Besides, we consider forest litter as an intermediate medium between vegetation and soil. The description of these media is placed in this section.

The equation describing atmosphere/vegetation exchange has the following form:

$$\frac{dC_V}{dt} = \frac{1}{R_{tot}} \cdot (C_a^g - C_V / K_{Va}),$$

where  $C_a^g$  - air concentration of a pollutant;  
 $C_V$  - concentration in the vegetation of a given type;  
 $K_{Va}$  - bioconcentration factor (BCF);  
 $R_{tot}$  - total resistance to the gaseous exchange given by the formula.

$$R_{tot} = R_a + a_V / k,$$

where  $R_a$  - aerodynamic resistance of turbulent atmospheric layer;  
 $k$  - mass transfer coefficient, m/s;  
 $a_V$  - specific surface area of vegetation,  $m^2/m^3$  (assumed value is 8000, see [Duyzer and van Oss, 1997]);

The total amount of the pollutant in vegetation of a given type in a certain grid cell is then expressed by the equation:

$$Q = C_V \frac{S \cdot LAI}{a_V},$$

where  $S$  - area covered by vegetation of a given type within a grid cell;  
 $LAI$  - particular leaf area index for the considered type of vegetation.

Parameterization of BCF. The bioconcentration factor is determined by the following equation [McLachlan and Horstmann, 1998]:

$$K_{Va} = mK_{OA}^n, \quad \text{C.1.}$$

where  $K_{OA}$  - partitioning coefficient between octanol and air;  
 $m, n$  - regression coefficients presented in Table C.5.

**Table C5.** Parameters of regression for equation C.1

|     | Grass<br>[Thomas et al., 1998] | Forest, [McLachlan and Horstmann, 1998] |           |
|-----|--------------------------------|---|-----------|
|     |                                | Coniferous                              | Deciduous |
| $m$ | 22.91                          | 38                                      | 14        |
| $n$ | 0.445                          | 0.69                                    | 0.76      |

While calculating BCF using eq. C.1 the temperature dependence of  $K_{OA}$  should be taken into account. In the model it is assumed that:

$$K_{oa} = K_{oa}^0 \exp \left[ a_K \left( \frac{1}{T} - \frac{1}{T_0} \right) \right],$$

where as earlier  $T_0 = 283.15$  K - reference temperature;  
 $K_{oa}^0$  -  $K_{oa}$  value at the reference temperature;  
 $a_K$  - coefficient of  $K_{oa}$  temperature dependence, K.

Parameterization of the mass transfer coefficient  $k$ . According to [Pekar et al., 1999], mass transfer coefficient is directly proportional to  $K_{oa}$  value. Hence, for the evaluation of temperature dependence of  $k$  the following formula can be used:

$$k = k_0 \exp \left[ a_K \left( \frac{1}{T} - \frac{1}{T_0} \right) \right],$$

where  $k_0$  is the  $k$  value at the reference temperature based on the data given in [McLachlan and Horstmann, 1998] for forests and in [Pekar et al., 1999] for grass.

For PCB-153:

$$K_{oa}^0 = 3.64 \cdot 10^{10} - K_{oa} \text{ value at the reference temperature};$$

$$a_K = 10811 \text{ } ^\circ\text{K} - \text{coefficient of } K_{oa} \text{ temperature dependence.}$$

## C.7. Degradation processes

### CliMoChem

#### Degradation in atmosphere

$$\frac{dC_{gas}}{dt} = -(1 - Phi) \cdot k_{gas} \cdot C_{gas}$$

| Parameter | Description  | Numeric value  | Reference |
|-----------|--|--|-----------|
| $C_{gas}$ | Concentration of substance in atmosphere           |  |           |
| $\Phi$    | particle-bound fraction of the substance (see C.1) | between 0-1  |           |
| $k_{gas}$ | first order degradation rate in the atmosphere     | depending on substance compare substance property sheets, See Chapter 3 and Annex B. |           |

For calculations with PCBs, the degradation in the atmosphere is described as follows:

$$\frac{dC_{gas}}{dt} = -k \cdot c_{OH} \cdot C_{gas}$$

| Parameter | Description   | Numeric value   | Reference                 |
|-----------|---|---|---------------------------|
| $C_{gas}$ | Concentration of substance in atmosphere                    |   |                           |
| $k_{gas}$ | second order degradation rate in the atmosphere in $cm^3/s$ | depending on substance compare substance property sheets, See Chapter 3 and Annex B |                           |
| $c_{OH}$  | concentration of OH-radicals in the atmosphere in $1/cm^3$  | depending on temperature, calculation see below                                     | <i>Beyer et al., 2002</i> |

compare substance property sheets, See Chapter 3 and Annex B

$$c_{OH} = (0.5 + (T - 273.15) \cdot 0.4) \cdot 10^5 \text{ for } T \geq 273.15K$$

$$c_{OH} = 5 \cdot 10^4 \text{ for } T \leq 273.15K$$

### ***Degradation in baresoil and vegetation-covered soil***

$$\frac{dC_i}{dt} = -k_{soil} \cdot C_i$$

| Parameter  | Description   | Numeric value   | Reference |
|------------|---|---|-----------|
| $C_i$      | Concentration of substance in i, i: baresoil, vegetation-covered soil |   |           |
| $k_{soil}$ | first order degradation rate in soil                                  | depending on substance compare substance property sheets, See Chapter 3 and Annex B |           |

### ***Degradation in vegetation***

$$\frac{dC_{veg}}{dt} = -k_{veg} \cdot C_{veg}$$

| Parameter | Description                              | Numeric value   | Reference |
|-----------|--|---|-----------|
| $C_{veg}$ | Concentration of substance in vegetation |   |           |
| $k_{veg}$ | first order degradation rate             | depending on substance compare substance property sheets, See Chapter 3 and Annex B |           |

### ***Degradation in water***

$$\frac{dC_{water}}{dt} = - \left( k_{water} + \frac{v_{partdep}}{h_{water}} \cdot \Phi_{susp} \right) \cdot C_{water}$$

| Parameter     | Description                                 | Numeric value   | Reference                                   |
|---------------|---|---|---|
| $C_{water}$   | Concentration of substance in water         |   |   |
| $k_{water}$   | first order degradation rate                | depending on substance compare substance property sheets, See Chapter 3 and Annex B |   |
| $v_{partdep}$ | velocity of particle deposition to deep sea | 1.23 m/d  | <i>Falkowski et al., 1998, Murray, 1992</i> |
| $h_{water}$   | height of water                             | 200 m   |   |
| $\Phi_{susp}$ | waterparticle-bound fraction of substance   | calculated  |   |

## SimpleBox

cited from [Brandes et al., 1996]

### Degradation in air

$$kdeg_{air[S]} = (1 - FRass_{aerosol[S]}) \cdot krad_{OH[S]}$$

- with  $kdeg_{air[S]}$  - pseudo first order transformation rate constant in air at scale S [ $s^{-1}$ ] (D);  
 $FRass_{aerosol[S]}$  - fraction of the chemical in air that is associated with aerosol particles at scale S [-] (A);  
 $krad_{OH[S]}$  - pseudo first order rate constant for reaction with OH-radicals at scale S [ $s^{-1}$ ] (A).

As a default for  $krad_{OH}$ , it may be considered that nearly all organic chemicals show some reactivity with OH-radicals. According to Peijnenburg (personal communication), a half life of 160 days, equivalent to:

$$krad_{OH[S]} = \frac{\ln 2}{160} d^{-1}$$

- with  $krad_{OH[S]}$  - pseudo first order rate constant for reaction with OH-radicals at scale S [ $d^{-1}$ ] (A);  
160 - maximum half-life for organic chemicals in air [d] may be taken as a minimum reactivity.

### Degradation in water

A value for  $kdeg_{water}$  may be obtained by means of the scaling procedure proposed by Struijs and Van den Berg [1995]. This procedure assumes that the pseudo first order rate constant for degradation in water is proportional to the concentration of bacteria in the water. The degradation rate is corrected by an empirical relationship which changes the degradation rate 50% per 10 degrees<sup>1</sup>. The rate constant for surface water may be deduced from the rate constant observed in laboratory tests at 20 °C by scaling:

$$kdeg_{water\ i[S]} = kdeg_{test} \cdot \left(1.072^{TEMPERATURE_{[S]} - 293}\right) \cdot \frac{BACT_{water}}{BACT_{test}} \cdot FRdisslv_{water\ i[S]}$$

- with  $kdeg_{water\ i[S]}$  - pseudo first order degradation rate constant in water i at scale S [ $s^{-1}$ ] (D);  
 $FRdisslv_{water(i)[S]}$  - dissolved fraction of water column i at scale S [-] (A);  
 $kdeg_{test}$  - pseudo first order degradation rate constant in laboratory test [ $s^{-1}$ ] (A);  
 $BACT_{water}$  - concentration of bacteria in the water compartment [ $cfu \cdot ml_{water}^{-1}$ ] (A);  
 $BACT_{test}$  - concentration of bacteria in the laboratory test water [ $cfu \cdot ml_{test\ water}^{-1}$ ] (A);  
 $TEMPERATURE_{[S]}$  - temperature at scale S [K] (A).

It is further assumed in this procedure that a pseudo first order degradation rate constant may be obtained by extrapolation from the results of standard screening tests for ready biodegradability in water:

$$kdeg_{test} = \frac{\ln 2}{5} d^{-1} \text{ if } PASS_{readytest} = y$$
$$kdeg_{test} = \frac{\ln 2}{1000} d^{-1} \text{ if } PASS_{readytest} = n$$

- with  $kdeg_{test}$  - pseudo first order degradation rate constant in laboratory test [ $d^{-1}$ ] (A);  
 $PASS_{readytest}$  - the result of a standard screening test; expressed as "y" if the chemical is "readily biodegradable" and "n" if the chemical is not "readily biodegradable".

For derivation of the degradation rate in water, the following default-values may be considered:

$$BACT_{test} = 4 \cdot 10^4 \text{ cfu} \cdot \text{ml}^{-1}$$

---

<sup>1</sup> : the degradation rates in the EUSES-system are not temperature dependent. For a simulation of EUSES with SimpleBox 2.0 the  $kdeg$ -values of EUSES must be entered.

with  $BACT_{test}$  - concentration of bacteria in the laboratory test water [ $\text{cfu} \cdot \text{ml}_{\text{test water}}^{-1}$ ] (A).

$$BACT_{water} = 4 \cdot 10^4 \text{ cfu} \cdot \text{ml}^{-1}$$

$BACT_{water}$  - concentration of bacteria in the water compartment [ $\text{cfu} \cdot \text{ml}_{\text{water}}^{-1}$ ] (A).

### Degradation in sediment

A value for  $kdeg_{sed}$  may be obtained by means of the scaling procedure proposed by *Struijs and Van den Berg* [1995]. The degradation rate is corrected by an empirical relationship which changes the degradation rate 50% per 10 degrees. As with degradation in water, it is assumed that the degradation rate is related to the degradation rate constant observed in standard tests for (aerobic) ready degradability in water. Degradation in sediment is treated as disappearance from the water phase of the sediment. The concentration of bacteria, present in the pore water or at the surface of the solid phase (or both), in the sediment compartment is expressed on a pore water volume basis:

$$kdeg_{sed\ i[S]} = kdeg_{test} \cdot (1.072^{TEMPERATURE_{[S]} - 293}) \cdot \frac{BACT_{sed\ i[S]}}{BACT_{test}} \cdot FRdisslvd_{sed\ i[S]}$$

with  $kdeg_{sed\ i[S]}$  - pseudo first order degradation rate constant in sediment [ $\text{s}^{-1}$ ] (D);  
 $kdeg_{test}$  - pseudo first order degradation rate constant in laboratory test [ $\text{s}^{-1}$ ] (A);  
 $BACT_{sed\ i[S]}$  - concentration of bacteria in sediment, expressed on a pore water basis [ $\text{cfu} \cdot \text{ml}_{\text{pore water}}^{-1}$ ] (A);  
 $BACT_{test}$  - concentration of bacteria in the laboratory test water [ $\text{cfu} \cdot \text{ml}_{\text{test water}}^{-1}$ ] (A);  
 $FRdisslvd_{sed\ i[S]}$  - fraction of the chemical in sediment, present in the pore water phase of the sediment [-];  
 $TEMPERATURE_{[S]}$  - temperature at scale S [K] (A).

For derivation of the degradation rate in sediment, a value for  $BACT_{sed}$  may be derived from:

$$BACT_{sed\ i[S]} = \frac{1.8 \cdot 10^9}{FRwater_{sed\ i[S]}}$$

with  $BACT_{sed\ i[S]}$  - concentration of bacteria in sediment i, expressed on a pore water basis at scale S [ $\text{cfu} \cdot \text{ml}_{\text{pore water}}^{-1}$ ] (A);  
 $1.8 \cdot 10^9$  - concentration of bacteria reported in aerobic sediment [ $\text{cfu} \cdot \text{cm}_{\text{sed}}^{-3}$ ];  
 $FRwater_{sed\ i[S]}$  - volume fraction of the water phase of the sediment i at scale S [-] (A).

It should be noted that this procedure to derive a degradation rate constant in sediment applies only to aerobic sediments and that generally only the top few millimeters of the sediment are aerobic.

### Degradation in soil

A value for  $kdeg_{soil}$  may be obtained by means of the scaling procedure proposed by *Struijs and Van den Berg* [1995], in analogy with the derivation of  $kdeg_{sed}$ . The degradation rate is corrected by an empirical relationship which changes the degradation rate 50% per 10 degrees.

$$kdeg_{soil\ i[S]} = \frac{kdeg_{water\ i[S]} \cdot (1.072^{TEMPERATURE_{[S]} - 293})}{FRdisslvd_{water\ i[S]}} \cdot \frac{BACT_{soil\ water}}{BACT_{water}} \cdot FRdisslvd_{soil\ i[S]}$$

with  $kdeg_{soil\ i[S]}$  - pseudo first order degradation rate constant in soil i at scale S [ $\text{s}^{-1}$ ] (D);  
 $kdeg_{water\ i[S]}$  - pseudo first order degradation rate constant in water i at scale S [ $\text{s}^{-1}$ ] (D);  
 $BACT_{soil}$  - concentration of bacteria in soil, expressed on a pore water basis [ $\text{cfu} \cdot \text{ml}_{\text{pore water}}^{-1}$ ] (A);  
 $FRdisslvd_{soil\ i[S]}$  - fraction of the chemical in soil i at scale S, present in the pore water phase [-];

|                               |   |
|-------------------------------|---|
| $FR_{diss}/v_{d,water\ i[S]}$ | - dissolved fraction of water column i at scale S [-] (A);                                |
| $BACT_{water}$                | - concentration of bacteria in the water compartment [ $cfu \cdot ml_{water}^{-1}$ ] (A); |
| $TEMPERATURE_{[S]}$           | - temperature at scale S [K] (A).   |

For derivation of the degradation rate in soil, a value for  $BACT_{soil}$  may be derived from *Struijs and Van den Berg* [1995]:

$$BACT_{soil} = \frac{10^6 / 1.4}{FR_{water\ soil\ i[S]}}$$

with  $BACT_{soil}$  - concentration of bacteria in soil, expressed on a pore water basis [ $cfu \cdot ml_{pore\ water}^{-1}$ ] (A);  
 $10^6$  - concentration of bacteria reported in aerobic soil [ $cfu \cdot g_{soil}$ ];  
1.4 - bulk density of soil [ $kg_{soil} \cdot m_{soil}^{-3}$ ] (A);  
 $FR_{water\ soil\ i[S]}$  - volume fraction water of soil i at scale S [-] (A).

It should be noted that this procedure for deriving a degradation rate constant in soil applies only to aerobic systems.

## MSCE-POP

### *Degradation in air*

The process of POP degradation in the atmosphere is viewed only as a reaction of a pollutant with hydroxyl radicals. In regional model version, this reaction is described by the equation of the first order:

$$\frac{dC}{dt} = -k_{air} \cdot C,$$

where  $C$  is the pollutant concentration in air (gaseous phase),  $ng/m^3$ ;  
 $k_{air}$  is the degradation rate constant for air,  $s^{-1}$ .

Three different values of degradation rate constant  $k_{air}$  are used for winter, spring/autumn and summer, respectively.

In hemispheric version, the degradation process in the atmosphere is described by the equation of the second order:

$$\frac{dC}{dt} = -k_{air} \cdot C \cdot [OH],$$

where  $C$  is the pollutant concentration in air (gaseous phase),  $ng/m^3$ ;  
 $[OH]$  is the concentration of OH radical,  $molec/cm^3$ ;  
 $k_{air}$  is the degradation rate constant for air,  $cm^3/(molec \cdot s)$ .

OH radical concentrations in the atmosphere vary substantially depending on many factors (latitude, cloudiness, day time, season, some atmospheric properties, etc.). At present, in the MSCE-POP model as a first approximation, OH radical concentrations have no diurnal variations and depend only on the season. At the latitude of  $45^{\circ}N$  mean diurnal OH-radical concentration in the surface layer of 2 km depth is  $2 \cdot 10^6$   $molec/cm^3$  in summer,  $0.8 \cdot 10^6$   $molec/cm^3$  in spring and autumn and  $0.09 \cdot 10^6$   $molec/cm^3$  in winter at mean annual concentration  $0.8 \cdot 10^6$   $molec/cm^3$  [Yu Lu and Khall, 1991]. To assess the influence of this assumption rough experimental calculations are made (see Annex A). Temporal and spatial variations of this parameter will be taken into account in the model in the near future.

Temperature dependence of rate constant of the gas-phase reaction with OH-radical is taken in the form of Arrhenius equation:

$$k_{air} = A \cdot \exp(-E_a / RT),$$

where  $A$  is the pre-exponential multiplier;  $cm^3/(molec \cdot s)$ ;

$E_a$  is the activation energy of interaction with OH-radical in air, J/mol;

$R$  is the universal gas constant, J/(mol · K);

$T$  is the ambient temperature, K.

Values of parameters  $A$  and  $E_a$  depend on pollutant properties.

This equation is applied for the gaseous phase of a pollutant only. Currently the process of degradation of a pollutant associated with particles is not included in the model due to lack of information on this topic.

### ***Degradation in soil***

The degradation process in soil is described as a first-order process by the equation:

$$\frac{dC}{dt} = -k_{soil} C,$$

where  $C$  is the pollutant concentration in soil, ng/m<sup>3</sup>;

$k_{soil}$  is the degradation rate constant for soil, s<sup>-1</sup>.

The degradation rate constant  $k_{soil}$  is a part of model parameterization for a given pollutant. It is assumed, as a first approximation, that doubling of the degradation rate constant occurs with each 10K temperature increase. This temperature dependence was adapted from [Lammel, et al., 2001].

### ***Degradation in vegetation***

There is very little data on degradation rates of considered chemicals in vegetation. For this reason, the degradation process in vegetation is not considered at present. A more detailed discussion of this question with rough estimation of degradation rates in vegetation for some POPs can be found in [Pekar et al., 1999]. On the basis of preliminary investigations, the degradation process in forest litter was introduced to the model as a first-order process with a degradation constant rate two times higher than that in soil.

### ***Degradation in seawater***

The degradation process in seawater is described as a first-order process by the equation:

$$dC/dT = -k_{sea} \cdot C$$

where  $C$  is the pollutant concentration in seawater, pg/l;

$k_{sea}$  is the degradation rate constant for seawater, s<sup>-1</sup>.

The degradation rate constant  $k_{sea}$  is a part of model parameterization for a given pollutant.

## COMPARISON OF RESULTS OF COMPUTATIONAL EXPERIMENTS FOR PCB-28

### D.1. Gas/particle partitioning:

#### D.1.1. Input data

Eleven sets of input data (different ambient temperatures in the range from – 12° C to 32° C) are proposed for modelling experiments with PCB-28.

*Table D.1. Input data for computation experiments with PCB-28 describing gas/particle partitioning*

|   | Exp. 1 | Exp.2 | Exp.3 | Exp. 4 | Exp. 5 | Exp. 6 | Exp. 7 | Exp. 8 | Exp. 9 | Exp. 10 | Exp. 11 |
|---|--------|-------|-------|--------|--------|--------|--------|--------|--------|---------|---------|
| Averaged ambient temperature, C                       | -12    | -5    | 0     | 6      | 10     | 15     | 20     | 25     | 25     | 26      | 32      |
| Total Suspended Matter, TSP, $\mu\text{g}/\text{m}^3$ | 30     | 30    | 30    | 30     | 30     | 30     | 30     | 51     | 29     | 49      | 66      |
| Organic content in the aerosol, %                     | 20     | 20    | 20    | 20     | 20     | 20     | 20     | 17     | 21     | 20      | 20      |

Output: PCB particulate fractions calculated for a range of temperatures (for PCB-28: from – 12°C to 32°C).

#### D.1.2. Comparison of the results

*Table D.2. Calculation results: fractions of particulate phase of PCB-28 calculated by models and statistical parameters used for evaluation*

| N  | Temperature (C) | EVN-BETR and UK-MODEL | DEHM-POP | MSCE-POP* |       | CliMoChem | SimpleBox** | $m_\varphi$ | $\sigma_\varphi$ |
|----|-----------------|-----------------------|----------|-----------|-------|-----------|-------------|-------------|------------------|
|    |                 |                       |          | 1         | 2     |           |             |             |                  |
| 1  | -12             | 0.190                 | 0.061    | 0.061     | 0.054 | 0.028     | 0.256       | 0.108       | 0.092            |
| 2  | -5              | 0.083                 | 0.025    | 0.025     | 0.023 | 0.017     | 0.123       | 0.049       | 0.044            |
| 3  | 0               | 0.045                 | 0.014    | 0.013     | 0.013 | 0.012     | 0.071       | 0.028       | 0.025            |
| 4  | 6               | 0.022                 | 0.007    | 0.006     | 0.007 | 0.008     | 0.036       | 0.014       | 0.012            |
| 5  | 10              | 0.014                 | 0.004    | 0.004     | 0.004 | 0.007     | 0.023       | 0.009       | 0.008            |
| 6  | 15              | 0.008                 | 0.002    | 0.002     | 0.002 | 0.005     | 0.014       | 0.006       | 0.005            |
| 7  | 20              | 0.004                 | 0.001    | 0.001     | 0.001 | 0.004     | 0.008       | 0.003       | 0.003            |
| 8  | 25              | 0.004                 | 0.001    | 0.001     | 0.001 | 0.005     | -           | 0.002       | 0.002            |
| 9  | 25              | 0.003                 | 0.001    | 0.001     | 0.001 | 0.003     | -           | 0.002       | 0.001            |
| 10 | 26              | 0.004                 | 0.001    | 0.001     | 0.001 | 0.004     | 0.004       | 0.003       | 0.002            |
| 11 | 32              | 0.003                 | 0.001    | 0.0004    | 0.001 | 0.004     | 0.002       | 0.002       | 0.001            |

\* - See process description of MSCE-POP model (MSCE-POP 1: current version; MSCE-POP 2: experimental version);

\*\* - Only 9 experiments for Simple Box.

The plot of dependence of  $\varphi$  on  $T$  calculated by participating models is presented in Fig. D.1.

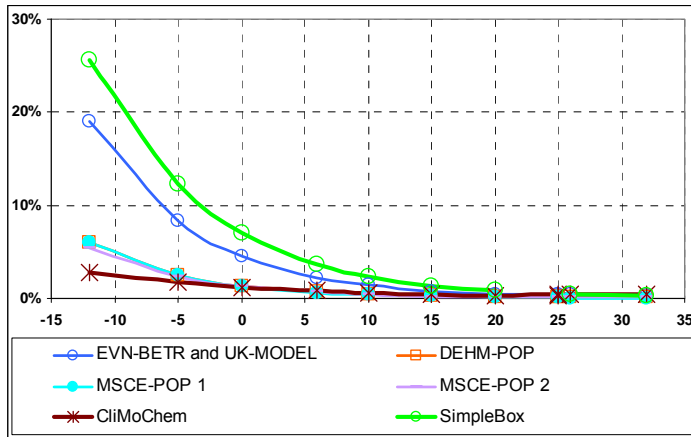


**Fig. D.1.** Fractions of PCB-28 particulate phase for different ambient temperatures (Calculation results of the participating models)

**Table D.3.** Coefficients of regression dependence between the models ( $\alpha / \beta$ )

|                       | DEHM-POP     | MSCE-POP 1    | MSCE-POP 2    | CliMoChem    | SimpleBox *    |
|-----------------------|--------------|---------------|---------------|--------------|----------------|
| EVN-BETR and UK-MODEL | 0.32/-0.0001 | 0.32/ -0.0004 | 0.28/ 0.00003 | 0.13 / 0.004 | 1.35 / 0.004   |
| DEHM-POP              | -            | 1.00/-0.0003  | 0.89 / 0.0002 | 0.42 / 0.004 | 4.25 / 0.005   |
| MSCE-POP 1            | -            | -             | 0.89 / 0.0004 | 0.42 / 0.004 | 4.22 / 0.007   |
| MSCE-POP 2            |              |               | -             | 0.47 / 0.004 | 4.76 / 0.004   |
| CliMoChem             |              |               | -             | -            | 10.05 / -0.040 |

\* - by 9 experiments only

**Table D.4.** Correlation coefficients

|                       | DEHM-POP | MSCE-POP 1 | MSCE-POP 2 | CliMoChem | SimpleBox * |
|-----------------------|----------|------------|------------|-----------|-------------|
| EVN-BETR and UK-MODEL | 1.00     | 1.00       | 1.00       | 0.98      | 1.00        |
| DEHM-POP              | -        | 1.00       | 1.00       | 0.98      | 1.00        |
| MSCE-POP 1            | -        | -          | 1.00       | 0.98      | 1.00        |
| MSCE-POP 2            | -        | -          | -          | 0.98      | 1.00        |
| CliMoChem             | -        | -          | -          | -         | 0.99        |

\* - by 9 experiments only

**Table D.5.** Residual square deviation ( $\sigma$ )

|                       | DEHM-POP | MSCE-POP 1 | MSCE-POP 2 | CliMoChem | SimpleBox * |
|-----------------------|----------|------------|------------|-----------|-------------|
| EVN-BETR and UK-MODEL | 0.001    | 0.002      | 0.001      | 0.004     | 0.013       |
| DEHM-POP              | -        | 0.001      | 0.001      | 0.005     | 0.018       |
| MSCE-POP 1            | -        | -          | 0.002      | 0.005     | 0.019       |
| MSCE-POP 2            | -        | -          | -          | 0.004     | 0.014       |
| CliMoChem             | -        | -          | -          | -         | 0.026       |

\* - by 9 experiments only

## D.2. Dry deposition of particulate phase

### D.2.1. Input data

The following four sets of input data are proposed for modelling experiments with PCB-28.

**Table D.6.** Input data for computation experiments with PCB-28 describing dry deposition of particulate phase

| N   | Experiment 1 | Experiment 2 | Experiment 3 | Experiment 4 |
|---|--------------|--------------|--------------|--------------|
| Type of underlying surfaces                               | Grass        | Forest       | Bare soil    | Seawater     |
| Mean wind velocity, m/sec                                 | 4            | 4            | 4            | 4            |
| Air concentration of particulate phase, ng/m <sup>3</sup> | 1            | 1            | 1            | 1            |

### D.2.2. Comparison of the results

See chapter 4.2.3. According to EVN-BETR and UK-MODEL, DEHM-POP, G-CIEMS, CAM/POPs, CliMoChem, SimpleBox and MSCE-POP parameterizations, these calculations were made for all considered PCB congeners together.

## D.3. Wet deposition

### D.3.1. Input data

Six sets of input data are proposed for modeling experiments with PCB-28.

*Table D.7. Input data for computation experiments with PCB-28 describing wet deposition*

| N   | Experiment 1 | Experiment 2 | Experiment 3 | Experiment 4 | Experiment 5 | Experiment 6 |
|---|--------------|--------------|--------------|--------------|--------------|--------------|
| Precipitation intensity, mm/hour                        | 1            | 1            | 1            | 10           | 10           | 10           |
| Precipitation height, m                                 | 1000         | 1000         | 1000         | 1000         | 1000         | 1000         |
| Average ambient temperature, °C                         | -1           | 3            | 10           | -1           | 3            | 10           |
| Air concentration, gaseous phase, pg/m <sup>3</sup>     | 7            | 14           | 225          | 7            | 14           | 225          |
| Air concentration, particulate phase, pg/m <sup>3</sup> | 3            | 5.3          | 0.2          | 3            | 5.3          | 0.2          |

**Output:** calculated wet deposition fluxes, ng/m<sup>2</sup>/hour and total (dissolved+particulate) concentrations of PCB in precipitation, pg/l.

### D.3.2. Comparison of the results

Since additional experiments on wet deposition (last three experiments) were made only by two participating models, statistical processing is performed for the calculation results of the first three experiments. It should be mentioned that results of Experiments 4, 5 and 6 calculated by MSCE-POP and SimpleBox show the same concentration in precipitation as in Experiments 1, 2, and 3, respectively. Fluxes between Experiments 1, 2, 3 and Experiments 4, 5, 6 differ ten times in accordance with the different values of precipitation intensity given (See Table D.7).

*Table D.8. Calculation results: total (dissolved + particulate) concentrations of PCB-28 in precipitation, pg/l and statistical parameters used for evaluation*

| N | Temperature (C) | EVN-BETR and UK model | MSCE-POP | CliMoChem | SimpleBox | $m_\phi$ | $\sigma_\phi$ |
|---|-----------------|-----------------------|----------|-----------|-----------|----------|---------------|
| 1 | -1              | 24                    | 456      | 1307      | 612       | 600      | 533           |
| 2 | 3               | 30                    | 803      | 2306      | 1077      | 1054     | 945           |
| 3 | 10              | 166                   | 99       | 423       | 202       | 222      | 140           |

*Table D.9 Calculation results: wet deposition flux of PCB-28, ng/m<sup>2</sup>/hour and statistical parameters used for evaluation*

| N | Temperature (C) | EVN-BETR and UK model | MSCE-POP | CliMoChem | SimpleBox | $m_\phi$ | $\sigma_\phi$ |
|---|-----------------|-----------------------|----------|-----------|-----------|----------|---------------|
| 1 | -1              | 0.024                 | 0.456    | 0.176     | 0.612     | 0.317    | 0.266         |
| 2 | 3               | 0.030                 | 0.803    | 0.311     | 1.077     | 0.555    | 0.472         |
| 3 | 10              | 0.166                 | 0.099    | 0.031     | 0.202     | 0.124    | 0.076         |

**Table D.10.** Correlation coefficients for concentration in precipitation

|                       | MSCE-POP | CliMoChem | SimpleBox |
|-----------------------|----------|-----------|-----------|
| EVN-BETR and UK model | -0.85    | -0.83     | -0.83     |
| MSCE-POP              | -        | 1.00      | 1.00      |
| CliMoChem             | -        | -         | 1.00      |

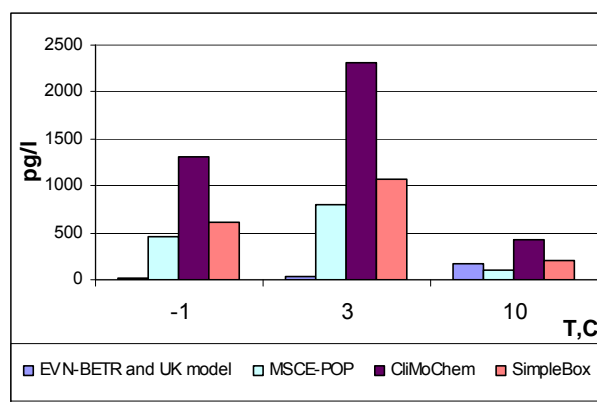


**Fig. D.2.** Concentration in precipitation calculated by different models for different values of ambient temperatures, pg/l

**Table D.11.** Coefficients of regression dependence between the models,  $\alpha / \beta$  for concentration in precipitation

|                                     | MSCE-POP       | CliMoChem       | SimpleBox      |
|-------------------------------------|----------------|-----------------|----------------|
| EVN-BETR and UK model               | -3.73 / 726.24 | -9.71 / 2057.25 | -4.51 / 960.96 |
| MSCE-POP                            | -              | 2.67 / 134.48   | 1.24 / 68.02   |
| CliMoChem                           | -              | -               | 0.46 / 5.50    |
| Mean concentration in precipitation | 452.67         | 1345.15         | 630.47         |

**Table D.12.** Residual square deviation ( $\sigma$ ) for concentration in precipitation

|                       | MSCE-POP | CliMoChem | SimpleBox |
|-----------------------|----------|-----------|-----------|
| EVN-BETR and UK model | 261.38   | 748.22    | 348.44    |
| MSCE-POP              |          | 57.76     | 27.82     |
| CliMoChem             |          |           | 0.98      |

## D.4. Gaseous exchange between the atmosphere and soil

### D.4.1. Input data

Four sets of input data are proposed for modelling experiments with PCB-28.

**Table D.13.** Input data for computation experiments with PCB-28 describing air/soil exchange

| N   | Experiment 1 | Experiment 2 | Experiment 3 | Experiment 4 |
|---|--------------|--------------|--------------|--------------|
| Average ambient temperature, °C                     | 10           | 10.9         | 12.9         | 13.9         |
| Air concentration, gaseous phase, pg/m <sup>3</sup> | 1.2          | 5.6          | 4.2          | 1.8          |
| Bulk soil density, kg/m <sup>3</sup>                | 1210         | 1080         | 890          | 1360         |
| Volumetric water content in soil, %                 | 20.6         | 41.4         | 26.4         | 16.8         |
| Volumetric air content in soil, %                   | 20           | 20           | 20           | 20           |
| Fraction of organic carbon in soil, %               | 7.1          | 17.7         | 12.3         | 4            |

**Output:** calculation of PCB-28 soil concentrations, ng/g and gaseous fluxes from and to soil and/or net gaseous flux to soil, ng/m<sup>2</sup>/d.

## D.4.2. Comparison of the results

1) Fig. D.3. illustrates air concentration trend used in calculations for Experiment 1.

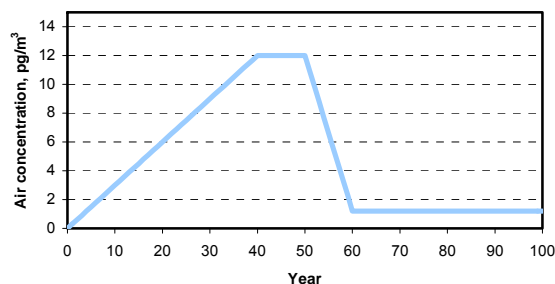


**Fig. D.3.** Air concentration trend used for calculations for MSCE-POP model (second version) for Experiment 1

**Table D.14.** Calculation results: soil concentrations of PCB-28 calculated by models and statistical parameters used for evaluation, ng/g

| N | Air conc, pg/m <sup>3</sup> | EVN-BETR and UK-MODEL | DEHM-POP | MSCE-POP* |        | CliMoChem | SimpleBox | m      | σ      |
|---|-----------------------------|-----------------------|----------|-----------|--------|-----------|-----------|--------|--------|
|   |                             |                       |          | 1         | 2      |           |           |        |        |
| 1 | 1.2                         | 0.0001                | 0.0184   | 0.0096    | 0.0513 | 0.0072    | 0.0001    | 0.0144 | 0.0193 |
| 2 | 5.6                         | 0.0005                | 0.1961   | 0.0761    | 0.4213 | 0.0549    | 0.0011    | 0.1250 | 0.1619 |
| 3 | 4.2                         | 0.0004                | 0.0890   | 0.0453    | 0.2411 | 0.0387    | 0.0006    | 0.0692 | 0.0904 |
| 4 | 1.8                         | 0.0001                | 0.0195   | 0.0071    | 0.0360 | 0.0037    | 0.0001    | 0.0111 | 0.0142 |

\* - MSCE-POP 1: steady-state calculations; MSCE-POP 2: calculations from dynamic model

**Table D.15.** Calculation results: net gaseous flux to soil, of PCB-28 calculated by models and statistical parameters used for evaluation, ng/m<sup>2</sup>/d

| N | Air conc, pg/m <sup>3</sup> | EVN-BETR and UK-MODEL | MSCE-POP  |           | CliMo Chem | SimpleBox | m *       | σ *      |
|---|-----------------------------|-----------------------|-----------|-----------|------------|-----------|-----------|----------|
|   |                             |                       | 1         | 2         |            |           |           |          |
| 1 | 1.2                         | 1.18E-03              | -2.90E-02 | -1.52E-01 | 0          | 7.15E-02  | -2.70E-02 | 9.33E-02 |
| 2 | 5.6                         | 5.18E-03              | -3.12E-02 | -6.17E-01 | 0          | 4.02E-01  | -6.01E-02 | 4.20E-01 |
| 3 | 4.2                         | 3.96E-03              | -9.64E-02 | -5.09E-01 | 0          | 2.52E-01  | -8.76E-02 | 3.17E-01 |
| 4 | 1.8                         | 1.73E-03              | -7.12E-02 | -2.05E-01 | 0          | 8.43E-02  | -4.75E-02 | 1.23E-01 |

\* - statistical parameters are calculated for models using steady-state and dynamic approaches.

**Table D.16.** Correlation coefficients for soil concentrations of PCB-28

|                       | DEHM-POP | MSCE-POP 1 | MSCE-POP 2 | CliMoChem | SimpleBox |
|-----------------------|----------|------------|------------|-----------|-----------|
| EVN-BETR and UK-MODEL | 0.93     | 0.97       | 0.97       | 0.99      | 0.97      |
| DEHM-POP              | -        | 0.99       | 0.99       | 0.96      | 0.99      |
| MSCE-POP 1            | -        | -          | 1.00       | 0.99      | 1.00      |
| MSCE-POP 2            | -        | -          | -          | 0.99      | 1.00      |
| CliMoChem             | -        | -          | -          | -         | 0.99      |

**Table D.17.** Correlation coefficients for net gaseous flux to soil of PCB-28\*

|                       | MSCE-POP 1 | MSCE-POP 2 | SimpleBox |
|-----------------------|------------|------------|-----------|
| EVN-BETR and UK-MODEL | -0.08      | -1.00      | 0.99      |
| MSCE-POP 1            | -          | 0.13       | 0.08      |
| MSCE-POP 2            | -          | -          | -0.98     |

\* - statistical parameters are calculated for models using steady-state and dynamic approaches.

**Table D.18.** Coefficients of regression dependence between the models ( $\alpha / \beta$ ) for soil concentrations

|                         | DEHM-POP       | MSCE-POP 1     | MSCE-POP 2     | CliMoChem      | SimpleBox        |
|-------------------------|----------------|----------------|----------------|----------------|------------------|
| EVN-BETR and UK-MODEL   | 398.33 / -0.03 | 163.59 / -0.01 | 902.92 / -0.06 | 126.57 / -0.01 | 2.26 / -0.0001   |
| DEHM-POP                | -              | 0.39 / 0.003   | 2.15 / 0.01    | 0.28 / 0.003   | 0.01 / 0.00004   |
| MSCE-POP 1              | -              | -              | 5.55 / -0.004  | 0.75 / 0.0001  | 0.01 / -0.000002 |
| MSCE-POP 2              | -              | -              | -              | 0.14 / 0.001   | 0.003 / 0.00001  |
| CliMoChem               | -              | -              | -              | -              | 0.02 / 0.000004  |
| Mean soil concentration | 0.0808         | 0.0345         | 0.1874         | 0.0261         | 0.0005           |

**Table D.19.** Coefficients of regression dependence between the models ( $\alpha / \beta$ ) for net gaseous flux to soil of PCB-28\*

|                       | MSCE-POP 1    | MSCE-POP 2      | SimpleBox     |
|-----------------------|---------------|-----------------|---------------|
| EVN-BETR and UK-MODEL | -1.38 / -0.05 | -120.50 / -0.01 | 82.07 / -0.05 |
| MSCE-POP 1            | -             | 0.90 / -0.32    | 0.38 / 0.22   |
| MSCE-POP 2            | -             | -               | -0.67 / -0.05 |
| Mean flux             | -0.06         | -0.37           | 0.20          |

\* - statistical parameters are calculated for models using steady-state and dynamic approaches.

**Table D.20.** Residual square deviation ( $\sigma$ ) for soil concentrations

|                       | DEHM-POP | MSCE-POP 1 | MSCE-POP 2 | CliMoChem | SimpleBox |
|-----------------------|----------|------------|------------|-----------|-----------|
| EVN-BETR and UK-MODEL | 0.055    | 0.013      | 0.081      | 0.005     | 0.0002    |
| DEHM-POP              | -        | 0.009      | 0.043      | 0.012     | 0.0001    |
| MSCE-POP 1            | -        | -          | 0.007      | 0.005     | 0.0000    |
| MSCE-POP 2            | -        | -          | -          | 0.006     | 0.00001   |
| CliMoChem             | -        | -          | -          | -         | 0.0001    |

**Table D.21.** Residual square deviation ( $\sigma$ ) for net gaseous flux to soil of PCB-28\*

|                       | MSCE-POP 1 | MSCE-POP 2 | SimpleBox |
|-----------------------|------------|------------|-----------|
| EVN-BETR and UK-MODEL | 0.06       | 0.03       | 0.04      |
| MSCE-POP 1            | -          | 0.39       | 0.27      |
| MSCE-POP 2            | -          | -          | 0.06      |

\* - statistical parameters are calculated for models using steady-state and dynamic approaches.

## 2) Accumulation/clearance dynamics of POPs in soil (optional):

Figs. D.4, D.5, and D.6 below show the results of the experiment obtained by MSCE-POP, EVN-BETR and UK model, and SimpleBox models, respectively.

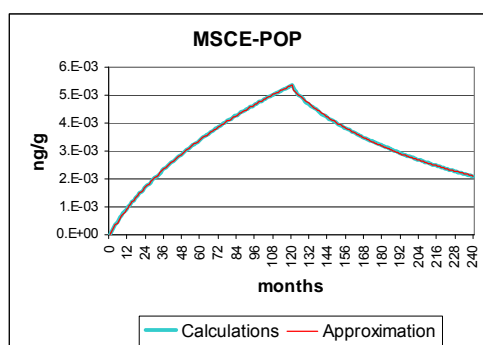


**Fig. D.4.** Long-term trends of accumulation and clearance obtained by MSCE-POP model

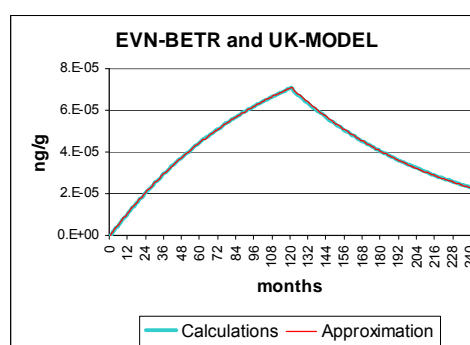


**Fig. D.5.** Long-term trends of accumulation and clearance obtained by EVN-BETR and UK-MODEL model

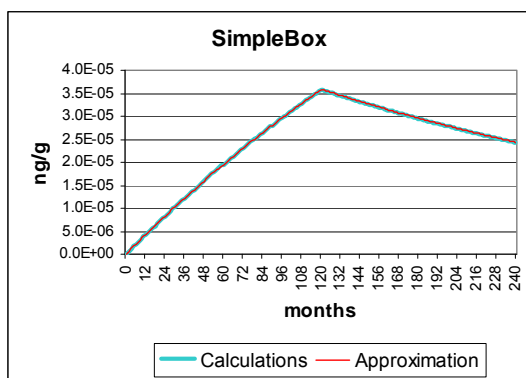


Fig. D.6. Long-term trends of accumulation and clearance obtained by SimpleBox model

Table D.22. Parameters of multi-exponential approximation

|                    |                   | EVN-BETR and UK model |          | SimpleBox |          | MSCE-POP |          |
|--------------------|-------------------|-----------------------|----------|-----------|----------|----------|----------|
|                    |                   | Slow                  | Fast     | Slow      | Fast     | Slow     | Fast     |
| Accumulation phase | Lambda            | 8.94E-03              | 8.94E-03 | 3.09E-03  | 3.09E-03 | 5.61E-03 | 5.00E-02 |
|                    | $t_{1/2}$ , years | 6.46                  | 6.46     | 18.68     | 18.68    | 10.30    | 1.16     |
| Clearance phase    | Lambda            | 9.38E-03              | 9.66E-03 | 3.24E-03  | 3.24E-03 | 5.38E-03 | 2.00E-02 |
|                    | $t_{1/2}$ , years | 6.16                  | 5.98     | 17.84     | 17.83    | 10.73    | 2.89     |

## D.5. Gaseous exchange between the atmosphere and water

### D.5.1. Input data

Four sets of input data are proposed for modelling experiments with PCB-28.

Table D.23. Input data for calculation experiments with PCB-28 describing air/water exchange.

|   | Experiment 1 | Experiment 2 | Experiment 3 | Experiment 4 |
|---|--------------|--------------|--------------|--------------|
| Average ambient temperature, °C                     | 23           | 23           | 10           | 13.9         |
| Air concentration, gaseous phase, pg/m <sup>3</sup> | 75           | 168          | 134.4        | 51           |
| Mean wind velocity, m/sec                           | 3            | 5.6          | 5            | 3.25         |

**Output:** calculation of PCB-28 water concentrations, pg/l and gaseous fluxes from and to water and/or net gaseous flux to water, ng/m<sup>2</sup>/d

### D.5.2. Comparison of the results

Table D.24. Calculation results: water concentrations of PCB-28 (pg/l) calculated by all participating models and statistical parameters used for evaluation

| N | EVN-BETR and UK-MODEL | DEHM-POP | CliMoChem | SimpleBox | MSCE-POP | $m$ | $\sigma$ |
|---|-----------------------|----------|-----------|-----------|----------|-----|----------|
| 1 | 4.74                  | 290.37   | 1024.85   | 19.61     | 7.46     | 269 | 439      |
| 2 | 10.43                 | 83.90    | 2295.67   | 54.87     | 16.77    | 492 | 1009     |
| 3 | 17.00                 | 67.16    | 4624.42   | 103.76    | 39.43    | 970 | 2043     |
| 4 | 5.32                  | 150.45   | 1340.76   | 26.06     | 10.72    | 307 | 581      |

**Table D.25.** Calculation results: statistical evaluation of PCB-28 water concentrations (pg/l) calculated by models having results of the same order

| N | EVN-BETR and UK-MODEL | DEHM-POP | SimpleBox | MSCE-POP | <i>m</i> | $\sigma$ |
|---|-----------------------|----------|-----------|----------|----------|----------|
| 1 | 4.74                  | 290.37   | 19.61     | 7.46     | 80.5     | 140.0    |
| 2 | 10.43                 | 83.90    | 54.87     | 16.77    | 41.5     | 34.4     |
| 3 | 17.00                 | 67.16    | 103.76    | 39.43    | 56.8     | 37.4     |
| 4 | 5.32                  | 150.45   | 26.06     | 10.72    | 48.1     | 68.8     |

**Table D.26.** Calculation results: Gaseous flux to water of PCB-28 (ng/m<sup>2</sup>/d) calculated by all participating models and statistical parameters used for evaluation

| N | EVN-BETR and UK-MODEL | CliMoChem | SimpleBox | MSCE-POP | <i>m</i> | $\sigma$ |
|---|-----------------------|-----------|-----------|----------|----------|----------|
| 1 | 4.29                  | 2.55      | 5.92      | 7.81     | 5.14     | 2.25     |
| 2 | 9.44                  | 5.71      | 26.28     | 21.08    | 15.63    | 9.66     |
| 3 | 15.82                 | 6.61      | 31.32     | 20.17    | 18.48    | 10.26    |
| 4 | 4.89                  | 2.28      | 6.64      | 6.75     | 5.14     | 2.09     |

**Table D.27.** Correlation coefficients for water concentrations

|                       | DEHM-POP | CliMoChem | SimpleBox | MSCE-POP |
|-----------------------|----------|-----------|-----------|----------|
| EVN-BETR and UK-MODEL | -0.78    | 0.99      | 1.00      | 0.98     |
| DEHM-POP              | -        | -0.75     | -0.77     | -0.72    |
| CliMoChem             | -        | -         | 1.00      | 1.00     |
| SimpleBox             | -        | -         | -         | 0.99     |

**Table D.28.** Correlation coefficients for gaseous flux to water

|                       | CliMoChem | SimpleBox | MSCE-POP |
|-----------------------|-----------|-----------|----------|
| EVN-BETR and UK-MODEL | 0.94      | 0.94      | 0.84     |
| CliMoChem             | -         | 1.00      | 0.98     |
| SimpleBox             | -         | -         | 0.98     |

**Table D.29.** Coefficients of regression dependence between the models ( $\alpha / \beta$ ) for water concentrations

|                             | DEHM-POP        | CliMoChem        | SimpleBox     | MSCE-POP      |
|-----------------------------|-----------------|------------------|---------------|---------------|
| EVN-BETR and UK-MODEL       | -13.93 / 278.54 | 283.18 / -332.68 | 6.72 / -11.90 | 2.47 / -4.60  |
| DEHM-POP                    | -               | -12.02 / 4099.41 | -0.29 / 94.35 | -0.10 / 33.77 |
| CliMoChem                   | -               | -                | 0.02 / -3.42  | 0.01 / -1.91  |
| SimpleBox                   | -               | -                | -             | 0.37 / -0.39  |
| Mean concentration in water | 147.97          | 2321.43          | 51.08         | 18.60         |

**Table D.30.** Coefficients of regression dependence between the models ( $\alpha / \beta$ ) for gaseous flux to water

|                            | CliMoChem   | SimpleBox    | MSCE-POP     |
|----------------------------|-------------|--------------|--------------|
| EVN-BETR and UK-MODEL      | 0.39 / 0.96 | 2.32 / -2.41 | 1.22 / 3.43  |
| CliMoChem                  | -           | 5.98 / -8.11 | 3.44 / -0.79 |
| SimpleBox                  | -           | -            | 0.57 / 3.91  |
| Mean gaseous flux to water | 4.29        | 17.54        | 13.95        |

**Table D.31.** Residual square deviation,  $\sigma$  for water concentrations

|                       | DEHM-POP | CliMoChem | SimpleBox | MSCE-POP |
|-----------------------|----------|-----------|-----------|----------|
| EVN-BETR and UK-MODEL | 109.81   | 392.84    | 4.25      | 5.32     |
| DEHM-POP              | -        | 1866.32   | 41.96     | 17.26    |
| CliMoChem             | -        | -         | 5.13      | 1.87     |
| SimpleBox             | -        | -         | -         | 3.79     |

**Table D.32.** Residual square deviation,  $\sigma$  for gaseous flux to water

|                       | CliMoChem | SimpleBox | MSCE-POP |
|-----------------------|-----------|-----------|----------|
| EVN-BETR and UK-MODEL | 1.33      | 7.93      | 7.21     |
| CliMoChem             | -         | 1.66      | 2.87     |
| SimpleBox             | -         | -         | 2.91     |

## D.6. Gaseous exchange between the atmosphere and vegetation

### D.6.1. Input data

Four sets of input data are proposed for modelling experiments with PCB-28.

**Table D.33.** Input data for calculation experiments with PCB-28 describing air/vegetation exchange

| N  | Experiment 1 | Experiment 2 | Experiment 3 | Experiment 4 |
|--|--------------|--------------|--------------|--------------|
| Type of vegetation compartment:                            | Grass        | Grass        | Grass        | Grass        |
| Average ambient temperature, °C                            | 5            | 25           | 11           | 18           |
| Air concentration, gaseous phase, $\mu\text{g}/\text{m}^3$ | 10           | 35           | 17           | 13           |
| Mean wind velocity, m/sec                                  | 4            | 4            | 4            | 4            |

**Output:** calculation of PCB-28 concentration in vegetation, ng/g dry weight and gaseous fluxes from and to vegetation and/or net gaseous flux to vegetation,  $\text{ng}/\text{m}^2/\text{d}$ ;

### D.6.2. Comparison of the results

**Table D.34.** Calculation results: concentrations of PCB-28 in vegetation calculated by models, ng/g d.w

| N | Air concentration, $\mu\text{g}/\text{m}^3$ | EVN-BETR and UK-MODEL | SimpleBox* | MSCE-POP |
|---|---|-----------------------|------------|----------|
| 1 | 10  | 0.010                 | 0.067      | 0.126    |
| 2 | 35  | 0.004                 | 0.057      | 0.150    |
| 3 | 17  | 0.008                 | 0.073      | 0.171    |
| 4 | 13  | 0.003                 | 0.034      | 0.089    |

\* - ng/g wet weight

**Table D.35.** Calculation results: net gaseous flux of PCB-28 to vegetation,  $\text{ng}/\text{m}^2/\text{d}$  calculated by models

| N | Air concentration, $\mu\text{g}/\text{m}^3$ | EVN-BETR and UK-MODEL | SimpleBox | MSCE-POP |
|---|---|-----------------------|-----------|----------|
| 1 | 10  | 0.09                  | 2.33      | 0.41     |
| 2 | 35  | 0.03                  | 3.42      | 0.48     |
| 3 | 17  | 0.07                  | 2.88      | 0.55     |
| 4 | 13  | 0.03                  | 1.61      | 0.29     |

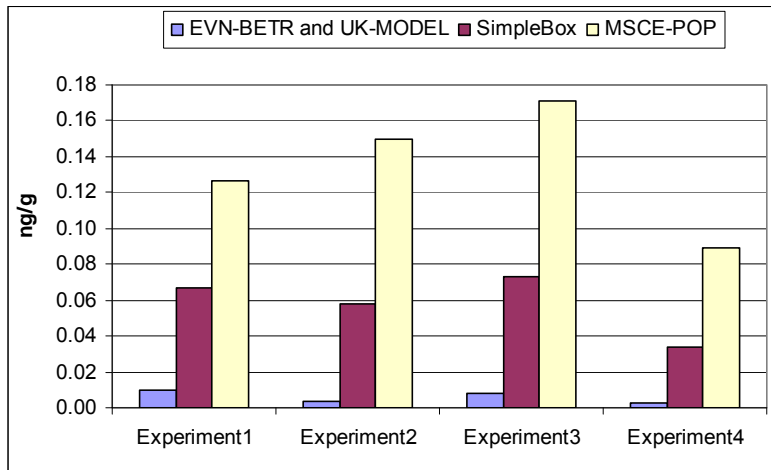


**Fig. D.7.** Comparison of concentration in vegetation calculated by different models, ng/g

**Table D.36.** Correlation coefficients for concentrations in vegetation

|                       | SimpleBox | MSCE-POP |
|-----------------------|-----------|----------|
| EVN-BETR and UK-MODEL | 0.81      | 0.42     |
| SimpleBox             | –         | 0.87     |

**Table D.37.** Correlation coefficients for net gaseous flux

|                       | SimpleBox | MSCE-POP |
|-----------------------|-----------|----------|
| EVN-BETR and UK-MODEL | -0.02     | 0.32     |
| SimpleBox             | –         | 0.86     |

**Table D.38.** Coefficients of regression dependence between the models ( $\alpha / \beta$ ) for concentrations in vegetation

|                       | SimpleBox    | MSCE-POP    |
|-----------------------|--------------|-------------|
| EVN-BETR and UK-MODEL | 3.98 / 0.033 | 4.25 / 0.11 |
| SimpleBox             | -            | 1.78 / 0.03 |

**Table D.39.** Coefficients of regression dependence between the models ( $\alpha / \beta$ ) for net gaseous flux

|          | SimpleBox   |
|----------|-------------|
| MSCE-POP | 0.12 / 0.11 |

## COMPARISON OF RESULTS OF COMPUTATIONAL EXPERIMENTS FOR PCB-180

### E.1. Gas/particle partitioning:

#### E.1.1. Input data

Twelve sets of input data (different ambient temperatures in the range from – 12° C to 25° C) are proposed for modelling experiments with PCB-180.

**Table E.1.** Input data for computation experiments with PCB-180 describing gas/particle partitioning.

| N   | Exp. 1 | Exp.2 | Exp.3 | Exp. 4 | Exp. 5 | Exp. 6 | Exp. 7 | Exp. 8 | Exp. 9 | Exp. 10 | Exp. 11 | Exp. 12 |
|---|--------|-------|-------|--------|--------|--------|--------|--------|--------|---------|---------|---------|
| Averaged ambient temperature, C                       | -12    | -5    | 0     | 3      | 5      | 8      | 10     | 12     | 15     | 17      | 20      | 25      |
| Total Suspended Matter, TSP, $\mu\text{g}/\text{m}^3$ | 30     | 30    | 35    | 31     | 18     | 25     | 30     | 30     | 40     | 33      | 34      | 29      |
| Organic content in the aerosol, %                     | 20     | 20    | 20    | 20     | 20     | 20     | 20     | 20     | 20     | 20      | 20      | 21      |

**Output:** PCB particulate fractions calculated for a range of temperatures (for PCB-180: from – 12°C to 25°C).

#### E.1.2. Comparison of the results

**Table E.2.** Calculation results: fractions of particulate phase of PCB-180 calculated by models and statistical parameters used for evaluation

| N  | Temperature (°C) | EVN-BETR and UK-MODEL | DEHM-POP | CAM/POPs* | MSCE-POP** |      | CliMoChem | SimpleBox*** | $m_\varphi$ | $\sigma_\varphi$ |
|----|------------------|-----------------------|----------|-----------|------------|------|-----------|--------------|-------------|------------------|
|    |                  |                       |          |           | 1          | 2    |           |              |             |                  |
| 1  | -12              | 0.98                  | 0.93     | 0.99      | 0.98       | 0.97 | 0.22      | 1.00         | 0.87        | 0.29             |
| 2  | -5               | 0.95                  | 0.84     | 0.97      | 0.94       | 0.92 | 0.14      | 0.99         | 0.82        | 0.30             |
| 3  | 0                | 0.92                  | 0.75     | 0.95      | 0.87       | 0.87 | 0.12      | –            | 0.75        | 0.32             |
| 4  | 3                | 0.86                  | 0.64     | 0.92      | 0.81       | 0.80 | 0.09      | –            | 0.69        | 0.31             |
| 5  | 5                | 0.73                  | 0.45     | 0.82      | 0.76       | 0.64 | 0.05      | –            | 0.57        | 0.29             |
| 6  | 8                | 0.71                  | 0.44     | 0.81      | 0.67       | 0.62 | 0.05      | –            | 0.55        | 0.27             |
| 7  | 10               | 0.69                  | 0.42     | 0.79      | 0.60       | 0.60 | 0.05      | 0.92         | 0.58        | 0.28             |
| 8  | 12               | 0.63                  | 0.36     | 0.74      | 0.53       | 0.54 | 0.05      | 0.90         | 0.47        | 0.24             |
| 9  | 15               | 0.60                  | 0.34     | 0.71      | 0.43       | 0.52 | 0.05      | –            | 0.44        | 0.23             |
| 10 | 17               | 0.49                  | 0.25     | 0.60      | 0.36       | 0.41 | 0.04      | –            | 0.36        | 0.20             |
| 11 | 20               | 0.40                  | 0.20     | 0.51      | 0.27       | 0.33 | 0.03      | –            | 0.29        | 0.17             |
| 12 | 25               | 0.23                  | 0.11     | 0.31      | 0.16       | 0.19 | 0.02      | –            | 0.17        | 0.10             |

\* - an additional input data of 12 size-bin structure is applied on the TSP in the experiment of CAM/POPs model;

\*\* - see process description of MSCE-POP model (MSCE-POP 1: current version; MSCE-POP 2: experimental version).

\*\*\* - only 4 experiments for SimpleBox

The plot of dependence of  $\varphi$  on  $T$  calculated by participating models is presented in Fig. E.1.

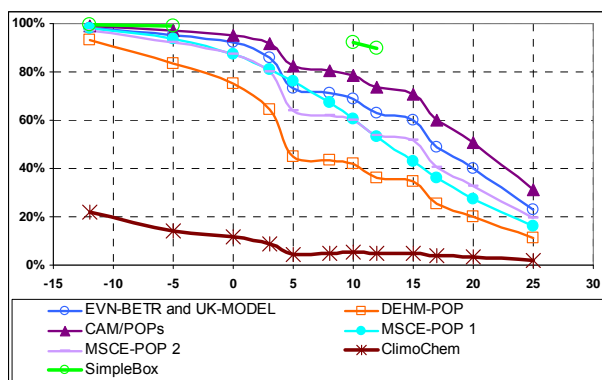


**Fig. E.1.** Fractions of PCB-180 particulate phase for different ambient temperatures (Calculation results of the participating models)

**Table E.3.** Coefficients of regression dependence between the models ( $\alpha / \beta$ )

|                       | DEHM-POP   | CAM/POPs  | MSCE-POP 1 | MSCE-POP 2 | CliMoChem    | SimpleBox * |
|-----------------------|------------|-----------|------------|------------|--------------|-------------|
| EVN-BETR and UK-MODEL | 1.08/-0.26 | 0.88/0.16 | 1.15/-0.17 | 1.04/-0.09 | 0.20 /-0.06  | 0.27 / 0.73 |
| DEHM-POP              | -          | 0.72/0.41 | 0.99/0.14  | 0.92/0.18  | 0.21 / -0.02 | 0.17 / 0.84 |
| CAM/POPs              | -          | -         | 1.28/-0.35 | 1.15/-0.26 | 0.21 / -0.09 | 0.38 / 0.62 |
| MSCE-POP 1            | -          | -         | -          | 0.88/0.07  | 0.17 / -0.03 | 0.21 / 0.79 |
| MSCE-POP 2            | -          | -         | -          | -          | 0.21/-0.05   | 0.22 / 0.78 |
| CliMoChem             | -          | -         | -          | -          | -            | 0.55 / 0.89 |

\* - by 4 experiments only

**Table E.4.** Correlation coefficients

|                       | DEHM-POP | CAM/POPs | MSCE-POP 1 | MSCE-POP 2 | CliMoChem | SimpleBox * |
|-----------------------|----------|----------|------------|------------|-----------|-------------|
| EVN-BETR and UK-MODEL | 0.96     | 0.99     | 0.98       | 0.99       | 0.81      | 1.00        |
| DEHM-POP              | -        | 0.92     | 0.96       | 0.98       | 0.93      | 0.99        |
| CAM/POPs              | -        | -        | 0.97       | 0.97       | 0.75      | 1.00        |
| MSCE-POP 1            | -        | -        | -          | 0.98       | 0.80      | 1.00        |
| MSCE-POP 2            | -        | -        | -          | -          | 0.86      | 1.00        |
| CliMoChem             | -        | -        | -          | -          | -         | 0.93        |

\* - by 4 experiments only

**Table E.5.** Residual square deviation ( $\sigma$ )

|                       | DEHM-POP | CAM/POPs | MSCE-POP 1 | MSCE-POP 2 | CliMoChem | SimpleBox *) |
|-----------------------|----------|----------|------------|------------|-----------|--------------|
| EVN-BETR and UK-MODEL | 0.248    | 0.080    | 0.159      | 0.089      | 0.114     | 0.004        |
| DEHM-POP              | -        | 0.268    | 0.264      | 0.145      | 0.072     | 0.011        |
| CAM/POPs              | -        | -        | 0.218      | 0.182      | 0.128     | 0.002        |
| MSCE-POP 1            | -        | -        | -          | 0.145      | 0.115     | 0.005        |
| MSCE-POP 2            | -        | -        | -          | -          | 0.099     | 0.006        |
| CliMoChem             | -        | -        | -          | -          | -         | 0.031        |

\* - by 4 experiments only

## E.2. Dry deposition of particulate phase

### E.2.1. Input data

The following four sets of input data are proposed for modelling experiments with PCB-180

**Table E.6.** Input data for computation experiments with PCB-180 describing dry deposition of particulate phase

| N   | Experiment 1 | Experiment 2 | Experiment 3 | Experiment 4 |
|---|--------------|--------------|--------------|--------------|
| Type of underlying surfaces                               | Grass        | Forest       | Bare soil    | Seawater     |
| Mean wind velocity, m/sec                                 | 4            | 4            | 4            | 4            |
| Air concentration of particulate phase, ng/m <sup>3</sup> | 1            | 1            | 1            | 1            |

### E.2.2. Comparison of the results

See chapter 4.2.3. According to EVN-BETR and UK-MODEL, DEHM-POP, G-CIEMS, CAM/POPs, CliMoChem, SimpleBox and MSCE-POP parameterizations, these calculations were made for all considered PCB congeners together.

## E.3. Wet deposition

### E.3.1. Input data

Eight sets of input data are proposed for modeling experiments with PCB-180.

**Table E.7.** Input data for computation experiments with PCB-180 describing wet deposition

| N   | Experiment 1 | Experiment 2 | Experiment 3 | Experiment 4 | Experiment 5 | Experiment 6 | Experiment 7 | Experiment 8 |
|---|--------------|--------------|--------------|--------------|--------------|--------------|--------------|--------------|
| Precipitation intensity, mm/hour                        | 1            | 1            | 1            | 1            | 10           | 10           | 10           | 10           |
| Precipitation height, m                                 | 1000         | 1000         | 1000         | 1000         | 1000         | 1000         | 1000         | 1000         |
| Average ambient temperature, °C                         | -1           | 3            | 10           | 15           | -1           | 3            | 10           | 15           |
| Air concentration, gaseous phase, pg/m <sup>3</sup>     | 5.5          | 2            | 25           | 4.5          | 5.5          | 2            | 25           | 4.5          |
| Air concentration, particulate phase, pg/m <sup>3</sup> | 4.3          | 1.3          | 1.5          | 0.5          | 4.3          | 1.3          | 1.5          | 0.5          |

**Output:** calculated wet deposition fluxes, ng/m<sup>2</sup>/hour and total (dissolved+particulate) concentrations of PCB in precipitation, pg/l.

### E.3.2. Comparison of the results

Since additional experiments on wet deposition (last four experiments) were made only by two participating models, statistical processing is performed for the calculation results of the first four experiments. It should be mentioned that results of Experiments 5, 6, 7 and 8 calculated by MSCE-POP and SimpleBox show the same concentration in precipitation as in Experiments 1, 2, 3 and 4, respectively. Fluxes between Experiments 1, 2, 3, 4 and Experiments 5, 6, 7, 8 differ ten times in accordance with the different values of precipitation intensity given (See Table E.7).

**Table E.8.** Calculation results: total (dissolved + particulate) concentrations of PCB-180 in precipitation (pg/l) and statistical parameters used for evaluation

| N | Temperature (C) | EVN-BETR and UK model | CAM/POPs* | MSCE-POP | CliMoChem | SimpleBox | $m_\varphi$ | $\sigma_\varphi$ |
|---|-----------------|-----------------------|-----------|----------|-----------|-----------|-------------|------------------|
| 1 | -1              | 138                   | 5720.22   | 663      | 1890      | 929       | 1868        | 2245             |
| 2 | 3               | 609                   | 1403.2    | 199      | 1200      | 277       | 738         | 542              |
| 3 | 10              | 3900                  | 9109.5    | 250      | 1283      | 410       | 2991        | 3720             |
| 4 | 15              | 570                   | 1048.27   | 78       | 411       | 113       | 444         | 396              |

\* - A typical 12 size-bin structure of Sulphate Aerosol as additional input data in this experiment.

**Table E.9.** Calculation results: wet deposition flux of PCB-180 (ng/m<sup>2</sup>/hour) and statistical parameters used for evaluation

| N | Temperature (C) | EVN-BETR and UK model | CAM/POPs* | MSCE-POP | CliMoChem | SimpleBox | $m_\varphi$ | $\sigma_\varphi$ |
|---|-----------------|-----------------------|-----------|----------|-----------|-----------|-------------|------------------|
| 1 | -1              | 0.138                 | 5.720     | 0.663    | 0.255     | 0.929     | 1.541       | 2.358            |
| 2 | 3               | 0.609                 | 1.403     | 0.199    | 0.077     | 0.277     | 0.513       | 0.535            |
| 3 | 10              | 3.900                 | 9.110     | 0.250    | 0.093     | 0.410     | 2.752       | 3.891            |
| 4 | 15              | 0.570                 | 1.048     | 0.078    | 0.030     | 0.113     | 0.368       | 0.438            |

\* - a typical 12 size-bin structure of Sulphate Aerosol as additional input data in this experiment.

**Table E.10.** Correlation coefficients for concentration in precipitation

|                       | CAM/POPs | MSCE-POP | CliMoChem | SimpleBox |
|-----------------------|----------|----------|-----------|-----------|
| EVN-BETR and UK model | 0.76     | -0.24    | -0.003    | -0.16     |
| CAM/POPs              | -        | 0.44     | 0.57      | 0.51      |
| MSCE-POP              | -        | -        | 0.91      | 1.00      |
| CliMoChem             | -        | -        | -         | 0.92      |

Отформатировано

Отформатировано

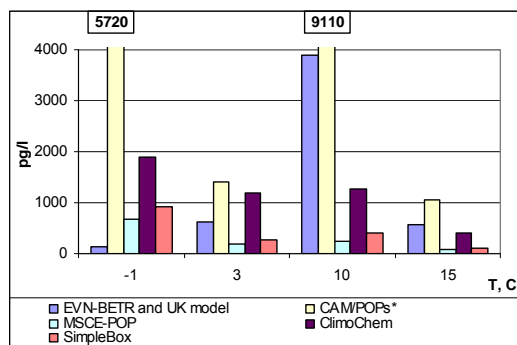


**Fig. E.2.** Concentration in precipitation calculated by different models for different values of ambient temperatures, pg/l

**Table E.11.** Coefficients of regression dependence between the models. ( $\alpha$  /  $\beta$ ) for concentration in precipitation

|                                     | CAM/POPs       | MSCE-POP       | CliMoChem        | SimpleBox      |
|-------------------------------------|----------------|----------------|------------------|----------------|
| EVN-BETR and UK model               | 1.67 / 2142.46 | -0.04 / 343.25 | -0.001 / 1197.41 | -0.03 / 474.41 |
| CAM/POPs                            | -              | 0.03 / 171.19  | 0.09 / 809.54    | 0.05 / 227.75  |
| MSCE-POP                            | -              | -              | 2.18 / 548.82    | 1.38 / 20.34   |
| CliMoChem                           | -              | -              | -                | 0.54 / -209.67 |
| Mean concentration in precipitation | 4320.3         | 297.5          | 1196.1           | 432.2          |

**Table E.12.** Residual square deviation ( $\sigma$ ) for concentration in precipitation

|                       | CAM/POPs | MSCE-POP | CliMoChem | SimpleBox |
|-----------------------|----------|----------|-----------|-----------|
| EVN-BETR and UK model | 4322.2   | 427.2    | 1051.5    | 603.6     |
| CAM/POPs              | -        | 395.0    | 867.6     | 524.5     |
| MSCE-POP              | -        | -        | 434.5     | 50.7      |
| CliMoChem             | -        | -        | -         | 235.4     |

## E.4. Gaseous exchange between the atmosphere and soil

### E.4.1. Input data

Four sets of input data are proposed for modelling experiments with PCB-180.

**Table E.13** Input data for computation experiments with PCB-180 describing air/soil exchange

| N  | Experiment 1 | Experiment 2 | Experiment 3 | Experiment 4 |
|--|--------------|--------------|--------------|--------------|
| Average ambient temperature, °C                          | 10           | 10.9         | 12.9         | 13.9         |
| Air concentration, gaseous phase, $\text{pg}/\text{m}^3$ | 0.3          | 1.3          | 2.4          | 0.7          |
| Bulk soil density, $\text{kg}/\text{m}^3$                | 1210         | 1080         | 890          | 1360         |
| Volumetric water content in soil, %                      | 20.6         | 41.4         | 26.4         | 16.8         |
| Volumetric air content in soil, %                        | 20           | 20           | 20           | 20           |
| Fraction of organic carbon in soil, %                    | 7.1          | 17.7         | 12.3         | 4            |

**Output:** calculation of PCB-180 soil concentrations,  $\text{ng}/\text{g}$  and gaseous fluxes from and to soil and/or net gaseous flux to soil,  $\text{ng}/\text{m}^2/\text{d}$ .

### E.4.2. Comparison of the results

1) Fig. E.3. illustrates air concentration trend used in calculations for Experiment 1.

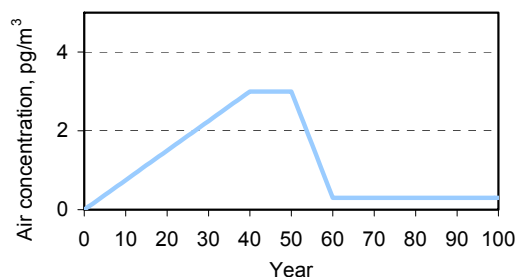


**Fig. E.3.** Air concentration trend used for calculations for MSCE-POP model (second version) for Experiment 1

**Table E.14.** Calculation results: soil concentrations of PCB-180 ( $\text{ng}/\text{g}$ ) calculated by models and statistical parameters used for evaluation

| N | Air conc $\text{pg}/\text{m}^3$ | EVN-BETR and UK-MODEL | DEHM-POP | CAM/POPs* | MSCE-POP** |       | CliMoChem | SimpleBox | m    | $\sigma$ |
|---|---------------------------------|-----------------------|----------|-----------|------------|-------|-----------|-----------|------|----------|
|   |                                 |                       |          |           | 1          | 2     |           |           |      |          |
| 1 | 0.3                             | 0.004                 | 0.355    | 0.638     | 0.013      | 0.075 | 0.068     | 0.0001    | 0.16 | 0.24     |
| 2 | 1.3                             | 0.019                 | 3.742    | 6.604     | 0.064      | 0.363 | 0.488     | 0.0003    | 1.61 | 2.58     |
| 3 | 2.4                             | 0.034                 | 4.808    | 7.203     | 0.139      | 0.792 | 0.855     | 0.0005    | 1.98 | 2.86     |
| 4 | 0.7                             | 0.006                 | 0.768    | 0.710     | 0.027      | 0.154 | 0.056     | 0.0001    | 0.25 | 0.34     |

\* - A typical 12 size-bin structure of Sulphate Aerosol as additional input data in this experiment;

\*\* - MSCE-POP 1: steady-state calculations; MSCE-POP 2: calculations from dynamic model.

**Table E.15.** Calculation results: net gaseous flux to soil of PCB-180 ( $\text{ng/m}^2/\text{d}$ ) calculated by models and statistical parameters used for evaluation

| N | Air conc<br>$\text{pg/m}^3$ | EVN-BETR and UK-MODEL | CAM/POPs | MSCE-POP** |           | CliMoChem | SimpleBox | $m^*$     | $\sigma^*$ |
|---|-----------------------------|-----------------------|----------|------------|-----------|-----------|-----------|-----------|------------|
|   |                             |                       |          | 1          | 2         |           |           |           |            |
| 1 | 0.3                         | 3.59E-04              | 3.51E-13 | 6.75E-03   | 3.62E-03  | 0         | 2.71E-02  | 7.563E-03 | 1.125E-02  |
| 2 | 1.3                         | 1.62E-03              | 3.27E-12 | 3.15E-02   | 2.50E-02  | 0         | 1.18E-01  | 3.513E-02 | 4.812E-02  |
| 3 | 2.4                         | 2.89E-03              | 3.84E-12 | 5.40E-02   | 2.94E-02  | 0         | 2.17E-01  | 6.058E-02 | 8.998E-02  |
| 4 | 0.7                         | 8.47E-04              | 3.94E-13 | 1.26E-02   | -4.37E-03 | 0         | 6.31E-02  | 1.442E-02 | 2.790E-02  |

\* - statistical parameters are calculated for models using steady-state and dynamic approaches.

**Table E.16.** Correlation coefficients for soil concentrations of PCB-180

|                       | DEHM-POP | CAM/POPs | MSCE-POP 1 | MSCE-POP 2 | CliMoChem | SimpleBox |
|-----------------------|----------|----------|------------|------------|-----------|-----------|
| EVN-BETR and UK-MODEL | 0.97     | 0.93     | 0.99       | 0.99       | 1.00      | 1.00      |
| DEHM-POP              | -        | 0.99     | 0.93       | 0.93       | 0.98      | 0.98      |
| CAM/POPs              | -        | -        | 0.87       | 0.87       | 0.94      | 0.94      |
| MSCE-POP 1            | -        | -        | -          | 1.00       | 0.98      | 0.98      |
| MSCE-POP 2            | -        | -        | -          | -          | 0.98      | 0.98      |
| CliMoChem             | -        | -        | -          | -          | -         | 1.00      |

**Table E.17.** Correlation coefficients for net gaseous flux to soil of PCB-180\*

|                       | CAM/POPs | MSCE-POP 1 | MSCE-POP 2 | SimpleBox |
|-----------------------|----------|------------|------------|-----------|
| EVN-BETR and UK-MODEL | 0.92     | 1.00       | 0.86       | 1.00      |
| CAM/POPs              | -        | 0.94       | 0.98       | 0.91      |
| MSCE-POP 1            | -        | -          | 0.90       | 1.00      |
| MSCE-POP 2            | -        | -          | -          | 0.85      |

\* - statistical parameters are calculated for models using steady-state and dynamic approaches.

**Table E.18.** Coefficients of regression dependence between the models ( $\alpha / \beta$ ) for soil concentrations

|                         | DEHM-POP        | CAM/POPs        | MSCE-POP 1    | MSCE-POP 2     | CliMoChem      | SimpleBox          |
|-------------------------|-----------------|-----------------|---------------|----------------|----------------|--------------------|
| EVN-BETR and UK-MODEL   | 152.07 / -0.007 | 239.01 / -0.023 | 4.00 / -0.003 | 22.80 / -0.017 | 27.29 / -0.068 | 0.02 / -0.00002    |
| DEHM-POP                | -               | 1.62 / -0.140   | 0.02 / 0.003  | 0.14 / 0.017   | 0.17 / -0.044  | 0.0001 / -0.000001 |
| CAM/POPs                | -               | -               | 0.01 / 0.009  | 0.08 / 0.053   | 0.10 / -0.013  | 0.0001 / 0.00002   |
| MSCE-POP 1              | -               | -               | -             | 5.70 / -0.0004 | 6.63 / -0.036  | 0.004 / 0.000003   |
| MSCE-POP 2              | -               | -               | -             | -              | 1.16 / -0.036  | 0.001 / 0.000003   |
| CliMoChem               | -               | -               | -             | -              | -              | 0.001 / 0.00003    |
| Mean soil concentration | 2.4184          | 3.7888          | 0.0608        | 0.3461         | 0.3668         | 0.0002             |

**Table E.19.** Coefficients of regression dependence between the models ( $\alpha / \beta$ ) for net gaseous flux to soil of PCB-180\*

|                       | CAM/POPs             | MSCE-POP 1       | MSCE-POP 2        | SimpleBox        |
|-----------------------|----------------------|------------------|-------------------|------------------|
| EVN-BETR and UK-MODEL | 1.54E-09 / -2.40E-13 | 19.26 / -0.001   | 12.69 / -0.005    | 74.82 / -0.001   |
| CAM/POPs              | -                    | 1.09E+10 / 0.005 | 8.62E+09 / -0.004 | 4.06E+10 / 0.026 |
| MSCE-POP 1            | -                    | -                | 0.69 / -0.005     | 3.85 / 0.005     |
| MSCE-POP 2            | -                    | -                | -                 | 4.29 / 0.049     |
| Mean flux             | 1.96E-12             | 2.62E-02         | 1.34E-02          | 1.06E-01         |

\* - statistical parameters are calculated for models using steady-state and dynamic approaches.

**Table E.20.** Residual square deviation ( $\sigma$ ) for soil concentrations

|                       | DEHM-POP | CAM/POPs | MSCE-POP 1 | MSCE-POP 2 | CiiMoChem | SimpleBox |
|-----------------------|----------|----------|------------|------------|-----------|-----------|
| EVN-BETR and UK-MODEL | 0.962    | 2.364    | 0.013      | 0.076      | 0.051     | 0.00002   |
| DEHM-POP              | -        | 0.926    | 0.036      | 0.206      | 0.145     | 0.0001    |
| CAM/POPs              | -        | -        | 0.048      | 0.276      | 0.218     | 0.0001    |
| MSCE-POP 1            | -        | -        | -          | 0.001      | 0.138     | 0.0001    |
| MSCE-POP 2            | -        | -        | -          | -          | 0.138     | 0.0001    |
| CiiMoChem             | -        | -        | -          | -          | -         | 0.00002   |

**Table E.21.** Residual square deviation ( $\sigma$ ) for net gaseous flux to soil of PCB-180\*

|                       | CAM/POPs | MSCE-POP 1 | MSCE-POP 2 | SimpleBox |
|-----------------------|----------|------------|------------|-----------|
| EVN-BETR and UK-MODEL | 1.27E-12 | 3.15E-03   | 1.45E-02   | 3.51E-03  |
| CAM/POPs              | -        | 1.22E-02   | 5.92E-03   | 5.94E-02  |
| MSCE-POP 1            | -        | -          | 1.25E-02   | 1.43E-02  |
| MSCE-POP 2            | -        | -          | -          | 7.55E-02  |

\* - statistical parameters are calculated for models using steady-state and dynamic approaches.

**2) Accumulation/clearance dynamics of POPs in soil (optional):**

Figs. E.4, E.5, E.6 and E.7 below show the results of the experiment obtained by CAM/POPs, MSCE-POP, EVN-BETR and UK model, and SimpleBox models, respectively.

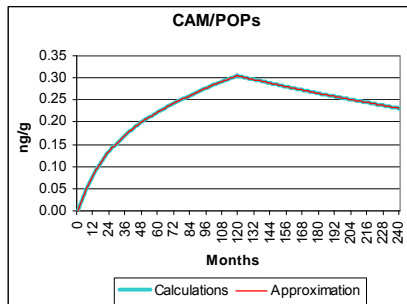


**Fig. E.4.** Long-term trends of accumulation and clearance obtained by CAM/POPs model

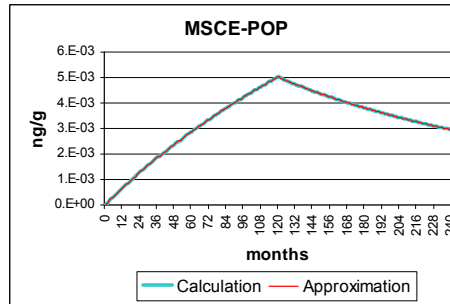


**Fig. E.5.** Long-term trends of accumulation and clearance obtained by MSCE-POP model

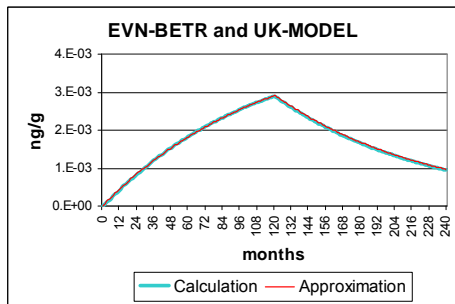


**Fig. E.6.** Long-term trends of accumulation and clearance obtained by EVN-BETR and UK-MODEL model

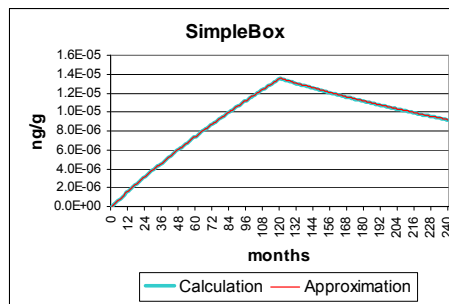


**Fig. E.7.** Long-term trends of accumulation and clearance obtained by SimpleBox model

**Table E.22.** Parameters of multi-exponential approximation

|                    |                   | EVN-BETR and UK model |          | CAM/POPs |          | SimpleBox |          | MSCE-POP |          |
|--------------------|-------------------|-----------------------|----------|----------|----------|-----------|----------|----------|----------|
|                    |                   | Slow                  | Fast     | Slow     | Fast     | Slow      | Fast     | Slow     | Fast     |
| Accumulation phase | Lambda            | 8.64E-03              | 8.64E-03 | 4.08E-03 | 5.11E-02 | 3.22E-03  | 3.22E-03 | 3.07E-03 | 1.73E-02 |
|                    | $t_{1/2}$ , years | 6.69                  | 6.69     | 14.15    | 1.13     | 17.93     | 17.94    | 18.81    | 3.35     |
| Clearance phase    | Lambda            | 9.16E-03              | 9.33E-03 | 1.89E-03 | 5.00E-03 | 3.25E-03  | 3.25E-03 | 3.28E-03 | 1.00E-02 |
|                    | $t_{1/2}$ , years | 6.31                  | 6.19     | 30.49    | 11.55    | 17.77     | 17.76    | 17.61    | 5.78     |

## E.5. Gaseous exchange between the atmosphere and water

### E.5.1. Input data

Four sets of input data are proposed for modelling experiments with PCB-180.

**Table E.23.** Input data for calculation experiments with PCB-180 describing air/water exchange

|   | Experiment 1 | Experiment 2 | Experiment 3 | Experiment 4 |
|---|--------------|--------------|--------------|--------------|
| Average ambient temperature, °C                     | 23           | 23           | 10           | 13.9         |
| Air concentration, gaseous phase, pg/m <sup>3</sup> | 3.3          | 3.4          | 4.1          | 14           |
| Mean wind velocity, m/sec                           | 3            | 5.6          | 5            | 3.25         |

**Output:** calculation of PCB-180 water concentrations, pg/l and gaseous fluxes from and to water and/or net gaseous flux to water, ng/m<sup>2</sup>/d;

### E.5.2. Comparison of the results

**Table E.24.** Calculation results: water concentrations of PCB-180 (pg/l) calculated by all participating models and statistical parameters used for evaluation

| N | EVN-BETR and UK-MODEL | CAM/POPs | DEHM-POP | CliMoChem | SimpleBox | MSCE-POP | $m$ | $\sigma$ |
|---|-----------------------|----------|----------|-----------|-----------|----------|-----|----------|
| 1 | 0.96                  | 1.70     | 2.24     | 744.91    | 2.10      | 0.89     | 125 | 303      |
| 2 | 0.96                  | 5.20     | 4.99     | 716.02    | 3.72      | 0.91     | 122 | 291      |
| 3 | 5.16                  | 23.10    | 0.45     | 2135.2    | 7.07      | 3.87     | 362 | 868      |
| 4 | 12.50                 | 50.00    | 0.47     | 5532.53   | 14.94     | 8.98     | 937 | 2252     |

**Table E.25.** Calculation results: statistical evaluation of PCB-180 water concentrations (pg/l) calculated by models having results of the same order

| N | EVN-BETR and UK-MODEL | CAM/POPs | DEHM-POP | SimpleBox | MSCE-POP | $m$  | $\sigma$ |
|---|-----------------------|----------|----------|-----------|----------|------|----------|
| 1 | 0.96                  | 1.70     | 2.24     | 2.10      | 0.89     | 1.6  | 0.6      |
| 2 | 0.96                  | 5.20     | 4.99     | 3.72      | 0.91     | 3.2  | 2.1      |
| 3 | 5.16                  | 23.10    | 0.45     | 7.07      | 3.87     | 7.9  | 8.8      |
| 4 | 12.50                 | 50.00    | 0.47     | 14.94     | 8.98     | 17.4 | 19.0     |

**Table E.26.** Calculation results: Gaseous flux to water of PCB-180 (ng/m<sup>2</sup>/d) calculated by all participating models and statistical parameters used for evaluation

| N | EVN-BETR and UK-MODEL | CAM/POPs | CliMoChem | SimpleBox | MSCE-POP | $m$ | $\sigma$ |
|---|-----------------------|----------|-----------|-----------|----------|-----|----------|
| 1 | 0.47                  | 0.32     | 0.13      | 0.63      | 0.43     | 0.4 | 0.2      |
| 2 | 0.47                  | 0.35     | 0.14      | 1.15      | 0.50     | 0.5 | 0.4      |
| 3 | 1.03                  | 0.29     | 0.22      | 1.57      | 0.67     | 0.8 | 0.6      |
| 4 | 3.47                  | 0.76     | 0.71      | 3.57      | 2.14     | 2.1 | 1.4      |

**Table E.27.** Correlation coefficients for water concentrations

|                       | CAM/POPs | DEHM-POP | CliMoChem | SimpleBox | MSCE-POP |
|-----------------------|----------|----------|-----------|-----------|----------|
| EVN-BETR and UK-MODEL | 1.00     | -0.71    | 1.00      | 0.99      | 1.00     |
| CAM/POPs              | -        | -0.70    | 0.99      | 1.00      | 1.00     |
| DEHM-POP              | -        | -        | -0.67     | -0.63     | -0.71    |
| CliMoChem             | -        | -        | -         | 0.99      | 1.00     |
| SimpleBox             | -        | -        | -         | -         | 0.99     |

**Table E.28.** Correlation coefficients for gaseous flux to water

|                       | CAM/POPs | CliMoChem | SimpleBox | MSCE-POP |
|-----------------------|----------|-----------|-----------|----------|
| EVN-BETR and UK-MODEL | 0.96     | 1.00      | 0.98      | 1.00     |
| CAM/POPs              | -        | 0.97      | 0.93      | 0.98     |
| CliMoChem             | -        | -         | 0.98      | 1.00     |
| SimpleBox             | -        | -         | -         | 0.98     |

**Table E.29.** Coefficients of regression dependence between the models ( $\alpha / \beta$ ) for water concentrations

|                             | CAM/POPs    | DEHM-POP     | CliMoChem         | SimpleBox     | MSCE-POP      |
|-----------------------------|-------------|--------------|-------------------|---------------|---------------|
| EVN-BETR and UK-MODEL       | 4.04 / 0.22 | -0.28 / 3.40 | 415.10 / 250.25   | 1.04 / 1.86   | 0.70 / 0.23   |
| CAM/POPs                    | -           | -0.07 / 3.40 | 101.38 / 254.67   | 0.26 / 1.81   | 0.17 / 0.22   |
| DEHM-POP                    | -           | -            | -713.26 / 3735.43 | -1.69 / 10.40 | -1.26 / 6.24  |
| CliMoChem                   | -           | -            | -                 | 0.002 / 1.26  | 0.002 / -0.16 |
| SimpleBox                   | -           | -            | -                 | -             | 0.66 / -0.95  |
| Mean concentration in water | 20.00       | 2.04         | 2282.16           | 6.96          | 3.66          |

**Table E.30.** Coefficients of regression dependence between the models ( $\alpha / \beta$ ) for gaseous flux to water

|                            | CAM/POPs    | CliMoChem    | SimpleBox    | MSCE-POP     |
|----------------------------|-------------|--------------|--------------|--------------|
| EVN-BETR and UK-MODEL      | 0.15 / 0.23 | 0.19 / 0.04  | 0.88 / 0.53  | 0.56 / 0.17  |
| CAM/POPs                   | -           | 1.21 / -0.22 | 5.42 / -0.60 | 3.57 / -0.60 |
| CliMoChem                  | -           | -            | 4.57 / 0.36  | 2.93 / 0.06  |
| SimpleBox                  | -           | -            | -            | 0.62 / -0.14 |
| Mean gaseous flux to water | 0.43        | 0.30         | 1.73         | 0.94         |

**Table E.31.** Residual square deviation,  $\sigma$  for water concentrations

|                       | CAM/POPs | DEHM-POP | CliMoChem | SimpleBox | MSCE-POP |
|-----------------------|----------|----------|-----------|-----------|----------|
| EVN-BETR and UK-MODEL | 3.41     | 2.62     | 297.58    | 1.16      | 0.03     |
| CAM/POPs              | -        | 2.64     | 601.54    | 0.94      | 0.56     |
| DEHM-POP              | -        | -        | 2900.80   | 7.65      | 4.65     |
| CliMoChem             | -        | -        | -         | 1.32      | 0.53     |
| SimpleBox             | -        | -        | -         | -         | 0.77     |

**Table E.32.** Residual square deviation,  $\sigma$  for gaseous flux to water

|                       | CAM/POPs | CliMoChem | SimpleBox | MSCE-POP |
|-----------------------|----------|-----------|-----------|----------|
| EVN-BETR and UK-MODEL | 0.11     | 0.02      | 0.40      | 0.10     |
| CAM/POPs              | -        | 0.12      | 0.80      | 0.30     |
| CliMoChem             | -        | -         | 0.41      | 0.05     |
| SimpleBox             | -        | -         | -         | 0.26     |

## E.6. Gaseous exchange between the atmosphere and vegetation

### E.6.1. Input data

Three sets of input data are proposed for modelling experiments with PCB-180.

**Table E.33.** Input data for calculation experiments with PCB-180 describing air/vegetation exchange

| N  | Experiment 1 | Experiment 2 | Experiment 3 | Experiment 4 |
|--|--------------|--------------|--------------|--------------|
| Type of vegetation compartment:                            | Grass        | Grass        | Grass        | Grass        |
| Average ambient temperature, °C                            | 5            | 25           | 11           | 20           |
| Air concentration, gaseous phase, $\mu\text{g}/\text{m}^3$ | 1            | 11           | 0.77         | 4            |
| Mean wind velocity, m/sec                                  | 4            | 4            | 4            | 4            |

**Output:** calculation of PCB-180 concentration in vegetation, ng/g dry weight and gaseous fluxes from and to vegetation and/or net gaseous flux to vegetation,  $\text{ng}/\text{m}^2/\text{d}$ ;

### E.6.2. Comparison of the results

**Table E.34.** Calculation results: concentrations of PCB-180 in vegetation calculated by models, ng/g d.w

| N | Air concentration, $\mu\text{g}/\text{m}^3$ | EVN-BETR and UK-MODEL | SimpleBox* | MSCE-POP |
|---|---|-----------------------|------------|----------|
| 1 | 1   | 0.120                 | 0.081      | 0.018    |
| 2 | 11  | 0.130                 | 0.458      | 0.192    |
| 3 | 0.77  | 0.061                 | 0.054      | 0.014    |
| 4 | 4   | 0.098                 | 0.207      | 0.070    |

\* - ng/g wet weight

**Table E.35.** Calculation results: net gaseous flux of PCB-180 to vegetation calculated by models,  $\text{ng}/\text{m}^2/\text{d}$

| N | Air concentration, $\mu\text{g}/\text{m}^3$ | EVN-BETR and UK-MODEL | SimpleBox | MSCE-POP |
|---|---|-----------------------|-----------|----------|
| 1 | 1   | -0.02                 | 2.85      | 0.06     |
| 2 | 11  | -0.06                 | 27.25     | 0.62     |
| 3 | 0.77  | -0.01                 | 2.12      | 0.04     |
| 4 | 4   | -0.04                 | 10.32     | 0.23     |

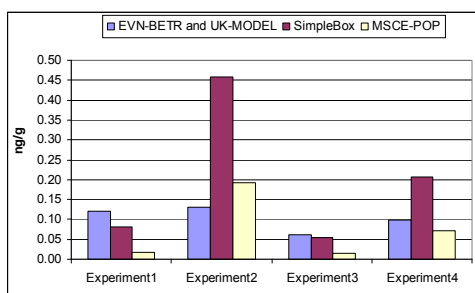


**Fig. E.8.** Comparison of concentration in vegetation calculated by different models, ng/g

**Table E.36.** Correlation coefficients for concentrations in vegetation

|                       | SimpleBox | MSCE-POP |
|-----------------------|-----------|----------|
| EVN-BETR and UK-MODEL | 0.65      | 0.63     |
| SimpleBox             | –         | 1.00     |

**Table E.37.** Correlation coefficients for net gaseous flux

|                       | SimpleBox | MSCE-POP |
|-----------------------|-----------|----------|
| EVN-BETR and UK-MODEL | -0.96     | -0.95    |
| SimpleBox             | –         | 1.00     |

**Table E.38.** Coefficients of regression dependence between the models ( $\alpha / \beta$ ) for concentrations in vegetation

|                       | SimpleBox  | MSCE-POP    |
|-----------------------|------------|-------------|
| EVN-BETR and UK-MODEL | 3.9 / -0.2 | 1.69 / -0.1 |
| SimpleBox             | -          | 0.45 / 0.02 |

**Table E.39.** Coefficients of regression dependence between the models ( $\alpha / \beta$ ) for net gaseous flux

|          | SimpleBox      |
|----------|----------------|
| MSCE-POP | 0.023 / -0.008 |